

Developing more sustainable aldehyde oxidation and reduction in water

Mingxin Liu

Thesis submitted to McGill University
in partial fulfillment of the requirement for the degree of

Doctor of Philosophy

Department of Chemistry
McGill University, Montréal

April, 2017

© Mingxin Liu, 2017

Abstract

Mingxin Liu

Supervisor: Prof. Dr. Chao-Jun Li

McGill University

This thesis focuses on the development of more sustainable aldehyde reduction and oxidation reactions in air and water, as an effort towards both minimizing the necessity of hazardous reductant/oxidant and organic solvent, and expanding the adaptability/application for such processes.

As the beginning of the thesis, chapter 1 will give a brief survey on historic aldehyde reduction and oxidation methods. The survey will mainly be conducted in a chronological manner. Both homogeneous and heterogeneous methods will be discussed. We will also separately discuss examples using relatively abundant metal, as it being part of the focus of our research interest.

At the ending of chapter 1, we will summarize both achievements as well as limitations of the current aldehyde reduction/oxidation reactions. Then we will move on to discuss our inspirations to develop an alternative catalyst to resolve the above-mentioned limitations in chapter 2. We will first talk about some of the important previous work, followed by our hypothesis on how our designed catalyst can provide good catalytic efficiency and substrate adaptability.

The chapter 3 will mainly talk about our silver(I)-catalyzed aldehyde reduction system. The reduction was achieved in a transfer hydrogenation manner with formate as naturally abundant reductant. Relatively more abundant silver catalyst serves as a more sustainable alternative compared to traditional catalysts such as ruthenium, iridium, etc. The reduction was conducted in air and water, thus eliminating the need for inert gas protection and air/moisture-tight operating, which is required by most of the previous systems. A satisfying substrate scope of this reduction was achieved with both aliphatic and aromatic aldehydes in good efficiency.

In the beginning of chapter 4, we will introduce how we were inspired by nature and classic examples to design our silver catalyst towards the oxidation of aldehyde. We will include the result and discussion regarding our catalytic Tollens' reaction – a widely adaptable silver-catalyzed aerobic oxidation of aldehyde in water, along with its optimization, scope investigation, and mechanism proposal.

The chapter 5 will focus on the attempt of using even more abundant metal than silver to conduct efficient aerobic aldehyde oxidation in water. Inspired by the classic Fehling's reaction, a similar aerobic oxidation of aldehyde catalyzed by copper in water, a catalytic Fehling's reaction was developed. High efficiency of oxidation was obtained with wide substrate adaptability. We will also present our efforts on investigating the mechanism of our catalytic Fehling's reaction.

Résumé

Cette thèse est centrée sur le développement de réactions de réduction plus environnementale des aldéhydes et de réactions d'oxydation dans l'air et dans l'eau, en minimisant la nécessité de réducteur et/ou oxydant dangereux, de solvant organique tout en élargissant l'application de tels procédés.

Initialement, le chapitre 1 donnera un bref aperçu des méthodes historiques de réduction et d'oxydation des aldéhydes. Cet aperçu se déroulera principalement de manière chronologique. Les méthodes homogènes et hétérogènes seront discutées. De plus, nous discuterons séparément des exemples utilisant un métal relativement abondant, puisque cela fait partie de l'intérêt de notre recherche.

En fin de chapitre 1, nous résumerons les réactions actuelles de réduction/oxydation des aldéhydes, ainsi que leurs limites. Ensuite, nous discuterons de nos inspirations pour développer un catalyseur alternatif afin de surmonter les limitations mentionnées dans le chapitre 2. D'abord, nous parlerons de certaines études antérieures et importantes, suivis de la présentation de notre hypothèse sur la façon dont notre catalyseur conçu peut fournir une bonne activité catalytique et s'adapter à une grande diversité de substrats.

Le chapitre 3 discutera principalement de notre système de réduction des aldéhydes, catalysé par l'argent (I). La réduction a été réalisée grâce à la technique de transfert d'hydrogène avec du formiate comme réducteur naturellement abondant. Le catalyseur d'argent relativement plus abondant sert d'alternative plus durable par rapport aux catalyseurs traditionnels tels que le ruthénium, l'iridium, etc. La réduction a été effectuée dans l'air et dans l'eau, éliminant ainsi la nécessité de protection de la réaction par des gaz inertes et évitant un fonctionnement étanche à l'air et à l'humidité, un prérequis pour la majorité des systèmes précédents. Cette réduction des aldéhydes a été réalisée de manière satisfaisante et efficace sur une grande variété de substrats comprenant des aldéhydes aliphatiques et aromatiques.

Au début du chapitre 4, nous présenterons comment nous nous sommes inspirés de la nature et des exemples traditionnels afin de concevoir notre catalyseur d'argent pour l'oxydation d'aldéhyde. Nous inclurons le résultat et la discussion concernant notre réaction catalytique de

Tollens - une oxydation aérobie d'aldéhyde catalysée par l'argent dans l'eau, son optimisation, notre étude sur son applicabilité à divers substrats et une proposition de mécanisme.

Le chapitre 5 se concentrera sur la tentative d'utiliser un métal encore plus abondant que l'argent pour mener une oxydation aérobie et efficace dans l'eau. Inspiré par la traditionnelle réaction de Fehling, une oxydation similaire aérobie d'aldéhyde catalysée par le cuivre dans l'eau, a été développée. Un rendement élevé de la réaction d'oxydation a été obtenu avec une large diversité de substrat. Nous présenterons également nos efforts pour étudier le mécanisme de notre réaction catalytique.

“Your bitter memories have time to change into sweet ones.”

Arthos, Comte de la Fère

The Three Musketeers

by Alexandre Dumas

for Xu, my beloved soul mate and my dear parents, Lan and Hong

Acknowledgments

I would first like to thank my PhD supervisor, Prof. Dr. Chao-Jun Li, for his generous help and kind advice throughout my entire PhD life at McGill. In countless times, it was him who accepted all the mistakes I made, and patiently guided me step by step till success. I could have done nothing in my academic life without the help from him. He is not only a mentor for research, but also a role model when it comes to everything I am about to face in the future. It was a priceless privilege to have chance to become part of his research team, and those memories will always be some of my best companions as I set sail into the unknowns.

I would also like to thank my other professors in McGill. To Prof. Nicolas Moitessier, Prof. Scott Bohle, Prof. Parisa Ariya, Prof. Audrey Moores, Prof. Laura Pavelka, Prof. Bruce Arndtsen, Prof. Theo van de Ven. Thank you all for giving me valuable guidance and all the amazing courses which I was lucky to learn. Special thanks go to Prof. Tomislav Frišćić, for the kind guidance I had from you before I begin my life in McGill, and Prof. James Gleason, for all the time and efforts you have made for me to help improve my skills in spectroscopy and scientific writing, which I will never forget. For the departmental and administrative staff, Ms. Chantal Marotte, Ms. Linda Del Paggio, Ms. Lina Alvarez, Ms. Sandra Aerssen, Ms. Jennifer Marleau, Ms. Alison McCaffrey, Ms. Karen Turner, Mr. Jean-Marc Gauthier, Mr. Mitchell Huot, Mr. Mathieu Bedard, Mr. Mike Daoust, Mr. Mario Perrone, Mr. Claude Perryman, Mr. Jean-Philippe Guay, Dr. Fred Morin, Dr. Robin Stein, Mr. Nadim, Saadé, and Dr. Thierry Maris (Université de Montréal), thank you all for all the support and assistance I have received throughout my PhD. Special thank goes to Ms. Jacqueline Farrell, for your time and efforts to proofread lots of my writings, and guidance in the CREATE program.

To my other professors in China, Prof. Lei Liu and Prof. Yongge Wei, my undergraduate supervisors in Tsinghua University, thank you so much for all the generous guidance I had from you. I am so sorry that I was too unsophisticated when I was an undergrad, that there were so many valuable words from you that I did not fully understand by that time. However, they all made more and more perfect sense as further and further I devoted myself into academia. I wish I could learn more from you once I was in your laboratory. My thanks also go to Prof. Meixiang Wang, Prof. Yong Ju, and Prof. Xi Zhang in Tsinghua University, Prof. Wei Wang, Prof. Yongqiang Tu, and

Prof. Yongmin Liang in Lanzhou University. Thank you so much for all the great inspirations I had from all of you, and thank you for always provide me help and support when I need.

To all my dear colleagues in the Li Lab, thank you so much for making an amazing PhD life even more amazing. Special thanks go to Dr. Feng Zhou, Dr. Zhenhua Jia, Dr. Camille Correia, Dr. Nicolas Uhlig, Dr. Huiying Zeng, Dr. Haining Wang, Pierre Querard, Dr. Inna Perepichka, Dr. Lu Li, Dr. Xiaobo Yang, Dr. Jiangsheng Li, and Dr. Zhongzhen Zhou. Thank you so much for being great partners and thank you for all the great helps and inspirations you gave me.

Finally, I owe all that I have achieved to my dear wife, Xu Zhang, for the unconditional love and being my soul mate since the day we met. While I am in McGill, pursuing my interests in study and research, you took over most of the financial burden of the whole family and doing incredibly hard works. *“She is one of the most hard-working wives in Montréal”* says the others. All these efforts were aimed solely to make my life in McGill more at ease. I am so lucky that I can share my life with you. And to my dearest parents, Lan Gao and Hong Liu, thank you so much for giving me all it takes to walk this world, and bear with all the failure and mistakes I occasionally made. I could never thank you enough for what you have given me.

Contributions and Publications

During my work, the following papers of original research were published, and therefore were discussed in this thesis:

- 1) “A silver-catalyzed transfer hydrogenation of aldehyde in air and water” **Liu, M.**; Zhou, F.; Jia, Z.; Li, C.-J. *Org. Chem. Front.* 2014, **1**, 161-166.
- 2) “Silver(I) as a widely applicable, homogeneous catalyst for aerobic oxidation of aldehydes toward carboxylic acids in water – ‘silver mirror’: From stoichiometric to catalytic” **Liu, M.**; Wang, H.; Zeng, H.; Li, C.-J. *Sci. Adv.* 2015, **1**, e1500020;
- 3) “Catalytic Fehling’s reaction: an efficient aerobic oxidation of aldehyde catalyzed by copper in water” **Liu, M.**; Li, C.-J. *Angew. Chem. Int. Ed.* 2016, **55**, 10806-10810.

For those works, I was in charge of designing and conducting most of the experiments, including but not limited to condition optimization, substrate scope investigation, mechanistic study (if applicable), etc. I also participated in all the necessary discussions within the team concerning the research project. For 2), I was also the initial discoverer of the transformation described in the paper and this thesis.

The following works to which I also contributed were published during my PhD study, but are not going to be discussed in this thesis:

- 4) “Highly efficient reduction of aldehydes with silanes in water catalyzed by silver” Jia, Z.; **Liu, M.**; Li, X.; Chan, A. S. C.; Li, C.-J. *Synlett* 2013, **24**, 2049-2056.
- 5) “Silver-catalyzed hydrogenation of aldehydes in water” Jia, Z.; Zhou, F.; **Liu, M.**; Li, X.; Chan, A. S. C.; Li, C.-J. *Angew. Chem. Int. Ed.* 2013, **52**, 11871-11874.

Those publications comprised the doctorate work of Dr. Zhenhua Jia. I contributed partially to the substrate investigation and majorly in the revisions of paper and additional experimental data in the peer-reviewing stage.

Table of Contents

Abstract	ii
Résumé	iv
Acknowledgments	viii
Contributions and Publications	x
Table of Contents	xi
List of Tables	xv
List of Figures	xvii
List of Schemes	xix
List of Abbreviation	xx
Chapter 1 – A brief survey for aldehyde reduction and oxidation	1
1.1 Aldehyde and its importance regarding reduction and oxidation	1
1.2 Reduction of aldehyde	2
1.2.1 The Meerwein-Ponndorf-Verley Reduction	2
1.2.2 Homogeneous catalyzed hydrogenation and transfer hydrogenation	3
1.2.2.1 Discovery and early attempts	3
1.2.2.2 The Noyori hydrogenation and transfer hydrogenation of aldehyde	10
1.2.2.3 Other hydrogenation and transfer hydrogenation system utilizing N-M ligand-metal bifunctional catalyst	13
1.2.2.4 The Shvo hydrogenation of aldehyde	16
1.2.2.5 Donor-acceptor reduction by nanoparticle	18
1.2.2.6 Hydrogenation and transfer hydrogenation catalyzed by abundant metal	19
1.2.2.7 Transfer hydrogenation in water	22
1.2.3 Heterogeneous catalyst for aldehyde hydrogenation	24
1.2.3.1 Heterogeneous Pt catalyst for aldehyde hydrogenation	25
1.2.3.2 Heterogeneous Pd catalyst for aldehyde hydrogenation	27
1.2.3.3 Heterogeneous Au catalyst for aldehyde hydrogenation	27

1.2.3.4 Heterogeneous Ru/Rh catalyst for aldehyde hydrogenation	27
1.2.3.5 Abundant metal as heterogeneous aldehyde hydrogenation catalyst	29
1.2.3.5.1 Cu catalyst	29
1.2.3.5.2 Ni catalyst	29
1.2.3.5.3 Co catalyst	30
1.3 Oxidation of aldehyde	31
1.3.1 Historic methods and challenges for aldehyde oxidation	31
1.3.2 Enzymatic oxidation of aldehyde	35
1.3.3 New oxidants for catalyzed aldehyde oxidation	35
1.3.4 Catalyzed aerobic oxidation of aldehyde.....	39
1.4 Conclusion	42
1.5 References	42
Chapter 2 – Designing a more sustainable aldehyde reduction	49
2.1 Initial discovery: silver-catalyzed A^3 / A^2 – coupling	49
2.2 Our hypothesis for developing aldehyde reduction using silver system	50
2.3 Proposed research	51
2.4 Conclusion	52
2.5 References	52
Chapter 3 – Silver(I)-catalyzed transfer hydrogenation of aldehyde in air and water	54
3.1 Objective	54
3.2 Results and discussion	54
3.2.1 Condition optimization	54
3.2.2 First scope investigation	57
3.2.3 Condition re-optimization	57
3.2.4 Final scope investigation	60
3.3 Conclusion and perspective	61
3.4 Contributions of authors	61
3.5 Experimental section	62
3.5.1 General information	62
3.5.2 General procedures	63

3.5.3 Identification of products	63
3.6 References	66
Chapter 4 – ‘Silver Mirror’ from stoichiometric to catalytic	67
4.1 Hypothesis and objective	67
4.2 Result and discussion	68
4.2.1 Condition optimization	68
4.2.2 First scope investigation	69
4.2.3 Re-optimization	70
4.2.4 Second scope optimization	73
4.2.5 Mechanism discussion	75
4.3 Conclusion and perspective	77
4.4 Contributions of authors	78
4.5 Experimental	78
4.5.1 General Information	78
4.5.2 General procedures	79
4.5.3 Identification of products	80
4.6 References	94
Chapter 5 – Catalytic Fehling, a copper-catalyzed aerobic oxidation of aldehyde in water	95
5.1 Background and hypothesis	95
5.2 Feasibility investigation	95
5.3 Result and discussion	97
5.3.1 Condition optimization	97
5.3.2 Scope investigation	98
5.3.3 Mechanism investigation	101
5.4 Conclusion and perspective	105
5.5 Contributions of authors	106
5.6 Experimental	106
5.6.1 General information	106
5.6.2 General procedures	107

5.6.3 Identification of products	109
5.6.4 X-ray single crystallography result	117
5.7 References	119
Chapter 6 – Contribution to fundamental knowledge	121
Appendix	I
NMR spectra of products described in chapter 1	I
NMR spectra of products described in chapter 2	XVII
NMR spectra of products described in chapter 3	LXXI

List of Tables

Table 1.1. Ru-catalyzed aldehyde hydrogenation in 1979	4
Table 1.2. Aldehyde hydrogenation in 1982 using electron-rich phosphine	5
Table 1.3. Reactivity comparison for mono- and bi-dentate phosphine	6
Table 1.4. Substrate scope of Rh-catalyzed hydrogenation in 1994	7
Table 1.5. Ir-catalyzed aldehyde hydrogenation in 1989	8
Table 1.6. Investigation over bi-dentate phosphine in efficiency and selectivity	9
Table 1.7. The Noyori catalyst for bulky substrates	13
Table 1.8. Ru-catalyzed transfer hydrogenation of aldehyde using pincer ligand	14
Table 1.9. Ru-catalyzed aldehyde hydrogenation in 2007	15
Table 1.10. Donor-acceptor hydrogenation pathway for AuNP	18
Table 1.11. Cu-catalyzed aldehyde hydrogenation in 2009	20
Table 1.12. The Morris hydrogenation/transfer hydrogenation of aldehyde/ketone	22
Table 1.13. Oxidation of aldehyde using oxone	36
Table 1.14. PCC catalyzed aldehyde oxidation using periodic acid	37
Table 1.15. Flavin-catalyzed bio-mimic oxidation of aldehyde	38
Table 1.16. Catalytic oxidation of hydrazine	39
Table 1.17. Ag ₂ O-CuO-catalyzed aldehyde aerobic oxidation	41
Table 3.1. First condition optimization	56
Table 3.2. First scope optimization	57
Table 3.3. Condition optimization for aliphatic aldehyde	58
Table 3.4. Final substrate scope	60
Table 4.1. First condition optimization	69

Table 4.2. First scope examination	70
Table 4.3. Re-optimization of condition	72
Table 4.4. Final scope investigation	76
Table 5.1. Optimization of reaction condition	99
Table 5.2. Scope investigation	100

List of Figures

Figure 1.1. Applications. Applications of alcohol/aldehyde/carboxylic acid	1
Figure 1.2. The Traditional and new MPV reduction	2
Figure 1.4. Ru-catalyzed aldehyde hydrogenation in 1979	3
Figure 1.5. The ideal catalyst for aldehyde hydrogenation according to Sanchez-Delgado's design	5
Figure 1.6. Aqueous phase Ru catalysis using cyclodextrin	7
Figure 1.7. Mechanism for the 1 st generation Noyori catalyst	11
Figure 1.8. The Noyori transfer hydrogenation catalyst in 1997	12
Figure 1.9. The 2 nd generation Noyori hydrogenation / transfer hydrogenation of aldehyde	12
Figure 1.10. Os catalyst designed from their corresponding Noyori's catalyst	15
Figure 1.11. Typical mechanism for the Shvo hydrogenation	17
Figure 1.12. Casey's catalyst for acidic hydrogenation of aldehyde	17
Figure 1.13. Mono-metallic intermediates for Casey's system in 2016	18
Figure 1.14. Early discovery of Fe-catalyzed hydrogenation and its limitation	19
Figure 1.15. Aldehyde hydrogenation catalyzed by the Knölker catalyst	21
Figure 1.16. Ogo's Ir-catalyzed transfer hydrogenation in water	23
Figure 1.17. Ni-Rh bi-metallic catalyst for hydrogenation in water	23
Figure 1.18. Xiao's a) 1 st generation and b) 2 nd generation catalyst for transfer hydrogenation in water	24
Figure 1.19. Principle and selectivity for heterogeneous carbonyl hydrogenation	25
Figure 1.20. Challenges for aldehyde oxidation	32

Figure 1.21. The Fehling and the Tollens reagent in aldehyde oxidation	33
Figure 1.22. The Jones reagent and its application in aldehyde oxidation	33
Figure 1.23. The Pinnick oxidation and its application in pharmaceutical synthesis	34
Figure 1.24. A typical mechanism for aldehyde oxidation using persistent radical system	35
Figure 1.25. Typical mechanism for previous aldehyde oxidation	36
Figure 1.26. Mechanism of autoxidation of aldehyde	40
Figure 1.27. Ru-catalyzed aerobic oxidation of aldehyde	40
Figure 1.28. Mechanism of AuNP-catalyzed aerobic oxidation of aldehyde	41
Figure 1.29. NHC-catalyzed aerobic oxidation of aromatic aldehyde	42
Figure 2.1. Ag-catalyzed A^3/A^2 -coupling reaction in water	49
Figure 2.2. Our hypothesized silver-catalyzed aldehyde reduction mechanism	50
Figure 2.3. Our proposed silver-catalyzed aldehyde reduction	51
Figure 3.1. Developments of our silver-catalyzed reduction system	54
Figure 4.1. Our design for silver-catalyzed oxidation of aldehyde	67
Figure 4.2. Proposed mechanism for our aerobic oxidation	77
Figure 5.1. Our proposed catalytic Fehling's reaction	95
Figure 5.2. Applications of Cu(I)/Cu(II)/O ₂ relay	96
Figure 5.3. A typical Cu-catalyzed alcohol oxidation with hydrogen extractor (R ₂ NO in this case)	97
Figure 5.4. Comparison of silver and copper in our catalysis	98
Figure 5.5. Mechanism investigation	103
Figure 5.6. Proposed mechanism of our catalytic Fehling's reaction	105

List of Schemes

Scheme 1.1. Selectivity for C=C over C=O	6
Scheme 1.2. Example of natural product reduction using Pt/Et₃N system	16
Scheme 1.3. Nitrous oxide oxidation of aldehyde	38
Scheme 4.1. Aerobic oxidation of natural products	75
Scheme 4.2. Gram-scale oxidation test	75
Scheme 4.3. Detection of hydrogen generated in our aerobic oxidation	75
Scheme 5.1. Gram-scale experiment result	101

List of Abbreviations

MPV reduction	Meerwein-Ponndorf-Verley reduction
OPP oxidation	Oppenauer oxidation
Et	ethyl
Ph	phenyl
<i>i</i> -Pr	isopropyl
β -H	β -hydride
Ac	acetyl
<i>t</i> -Bu	tert-butyl
Me	methyl
DiPFc	1,1'-bis(diisopropylphosphino)ferrocene
BINAP	2,2'-bis(diphenylphosphino)-1,1'-binaphthyl
NA(T)H	Noyori's asymmetric (transfer) hydrogenation
Ts	4-toluenesulfonyl
gen	generation
ee	enantiomeric excess
DMSO	dimethyl sulfoxide
TON	turn-over number
Ms	methanesulfonyl
Ar	aromatic group
Cp	cyclopentadienyl (anion)
Tf	trifluoromethanesulfonyl
TMS	trimethylsilyl
NP	nanoparticle
SPO	Secondary phosphine oxide
Cp*	Pentamethylcyclopentadienyl (anion)
PEG	poly(ethylene glycol)
SET	single electron transfer
Boc	tert-butyloxycarbonyl
TEMPO	(2,2,6,6-tetramethylpiperidin-1-yl)oxyl

DMF	N,N-dimethylformamide
PCC	pyridinium chloroperchromate
Cy	cyclohexyl
Nu	nucleophile
LUMO	lowest unoccupied molecular orbital
NMR	nuclear-magnetic resonance
dppf	1,1'-bis(diphenylphosphino)ferrocene
XPhos	2-dicyclohexylphosphino-2',4',6'-triisopropylbiphenyl
RuPhos	2-dicyclohexylphosphino-2',6'-diisopropoxybiphenyl
SPhos	2-dicyclohexylphosphino-2',6'-dimethoxybiphenyl
DavePhos	2-dicyclohexylphosphino-2'-N,N-dimethylaminobiphenyl
NHC	N-heterocyclic carbene
IMes	1,3-bis(2,4,6-trimethylphenyl)imidazol-2-ylidene
DIPEA	diisopropylethylamine
N.D.	not detected
BrettPhos	2-(Dicyclohexylphosphino)3,6-dimethoxy-2',4',6'-triisopropyl-1,1'-biphenyl
TLC	thin-layer chromatography
DCM	dichloro methane / methylene chloride
ALDH	aldehyde dehydrogenase
NAD ⁺	nicotinamide adenine dinucleotide
bipy / bpy	2,2'-bipyridyl
IPr	1,3-bis(2,6-diisopropylphenyl)imidazol-2-ylidene
SIMes	1,3-bis(2,4,6-trimethylphenyl)-4,5-dihydro-imidazol-2-ylidene
SIPr	1,3-bis(2,6-diisopropylphenyl)-4,5-dihydro-imidazol-2-ylidene

Chapter 1 – A brief survey for aldehyde reduction and oxidation

1.1 Aldehyde and its importance regarding reduction and oxidation

Oxidation and reduction are 2 fundamental reactions in chemistry. Every day, there are mass quantities of chemical products manufactured by those reactions. Among them, oxidation/reduction between alcohol/aldehyde/carboxylic acid series are among the most important and demanding oxidation/reduction reactions [1]. Being in the center of this series, aldehyde is regarded as one of the most important chemical products. The global production of aldehyde is under a constant increase. Only counting hydroformylation process, aldehydes are produced in over 10-million-ton scale annually [2]. This is majorly due to the potential for aldehyde to be either readily oxidized into the corresponding carboxylic acids or reduced into the corresponding alcohols, which are extremely useful in vast number of daily products (Figure 1.1). Historically, the industry oxidation/reduction processes rely heavily on the use of stoichiometric hazardous reagents such as NaBH_4 , LiAlH_4 , $\text{K}_2\text{Cr}_2\text{O}_7$, KMnO_4 , etc. [3], and sometimes in harsh reaction conditions. The synthesis of those materials, practice of such processes, and extrusion of remaining waste all contributed a major part to the great pollution problem in early ages of industry revolution [4].

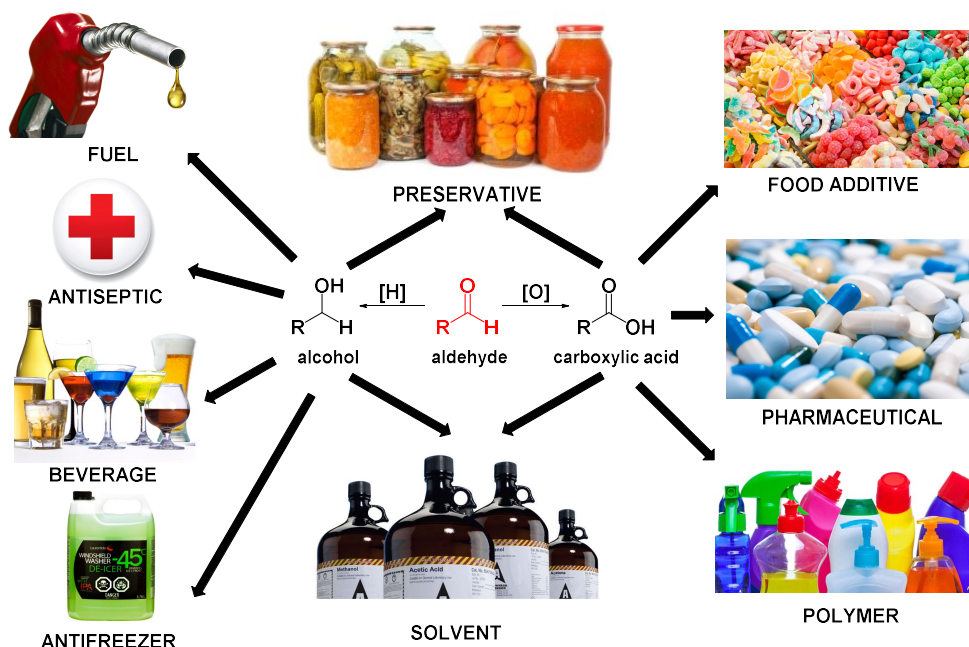


Figure 1.1 Applications of alcohol/aldehyde/carboxylic acid

1.2 Reduction of aldehyde

1.2.1 Meerwein-Ponndorf-Verley Reduction

Realizing such problems, chemists started to seek methods that can give efficient desired transformation, at the same time minimizing the environmental impact. Among them, one particularly notable example is the Meerwein-Ponndorf-Verley (MPV) reduction (or the Oppenauer OPP oxidation for its reverse process) (Figure 1.2a) [5]. The hydride was transferred from the hydrogen source, which usually represented by isopropyl alcohol, to the target aldehyde via a 6 member-ring transition state, catalyzed by Lewis acidic aluminum alkoxide. The downside of the MPV reduction, however, is the requirement of high aluminum alkoxide catalyst load, which generates large quantities of waste.

In 1990, Joo reported the use of Ru catalyst to conduct the MPV reduction, in attempt to reduce the required catalyst load [6]. Compared to 20 mol% to 50 mol% catalyst loads in certain cases, the new Ru catalyst only requires 1 mol% catalyst load, showing the enhanced stability of the catalytic cycle by Ru. The reduction mechanism is generally similar to the 6-member ring transition state of the classic MPV reduction (Figure 1.2b). Although only aromatic and unsaturated aldehyde was reported in the substrate scope, the reported reaction shows good functional tolerance.

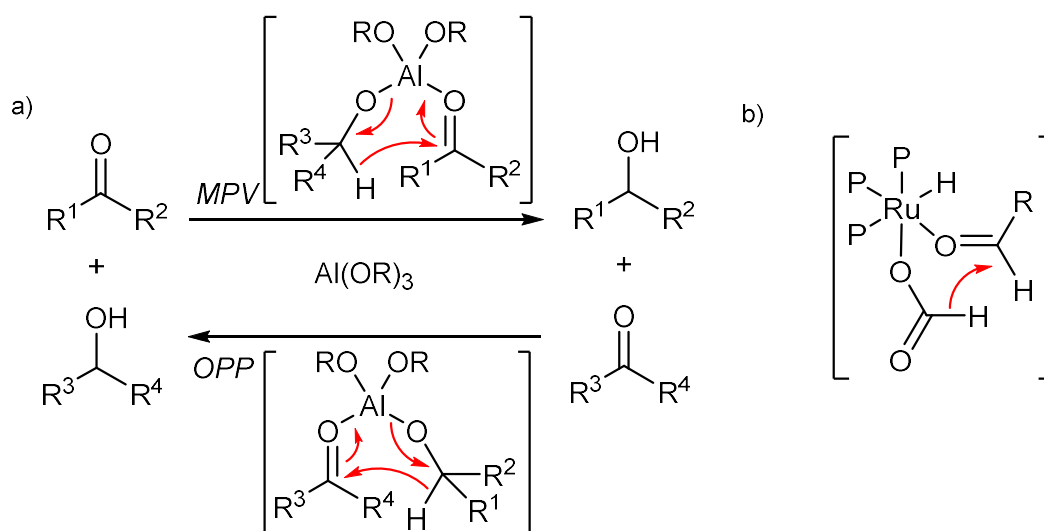


Figure 1.2 The Traditional and new MPV reduction

However, despite wide application of the MPV reduction and its derivatives, such reduction usually give low atom-economy, as stoichiometric amount of ketone waste is often generated. Alternative method with higher atom-economy for aldehyde reduction is also necessary, especially when it comes to certain case that require low environmental impact.

1.2.2 Homogeneous catalyzed hydrogenation and transfer hydrogenation

1.2.2.1 Discovery and early attempts

Alongside the development of the MPV transfer hydrogenation, the direct hydrogenation was also considered a highly desirable approach to achieve reduction of compounds, especially due to its great atom economy. As early as 19th century, people started to realize that certain metals, such as Pt or Ni, are capable of directly activating hydrogen gas to do reduction of various compounds [7]. Importantly, those reduction reactions in most cases give very clean reduction and generate very little amount of side-reactions and wastes, which is very difficult to achieve using other reducing reagents. With such discoveries, development of methods to achieve hydrogenation of aldehyde is imminent.

In 1975, a homogeneous Rh-catalyzed hydrogenation of aldehyde was developed [8]. The catalyst was composed of single molecule containing only one Rh atom. Although only 2 substrates, cinnamaldehyde and croton aldehyde, was reported, the reported transformation achieved the first selective hydrogenation of C=O instead of C=C, reducing cinnamaldehyde into the corresponding unsaturated alcohol. It was demonstrated that the addition of amine affects the above-mentioned selectivity greatly (Figure 1.3).

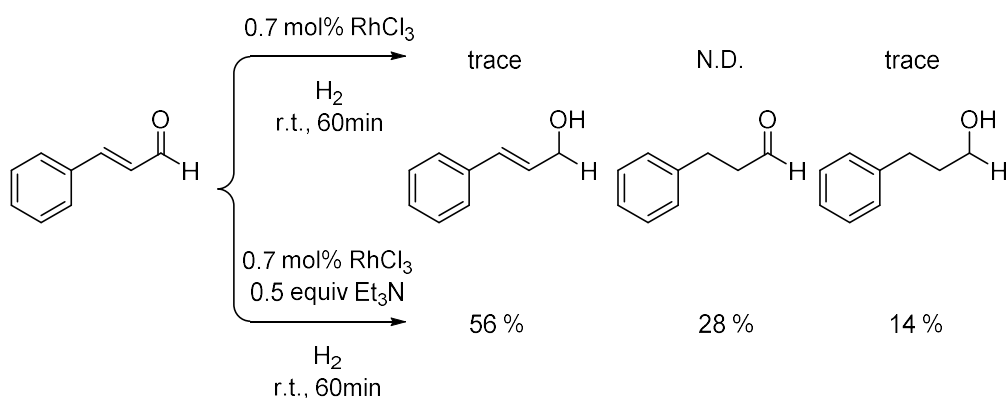
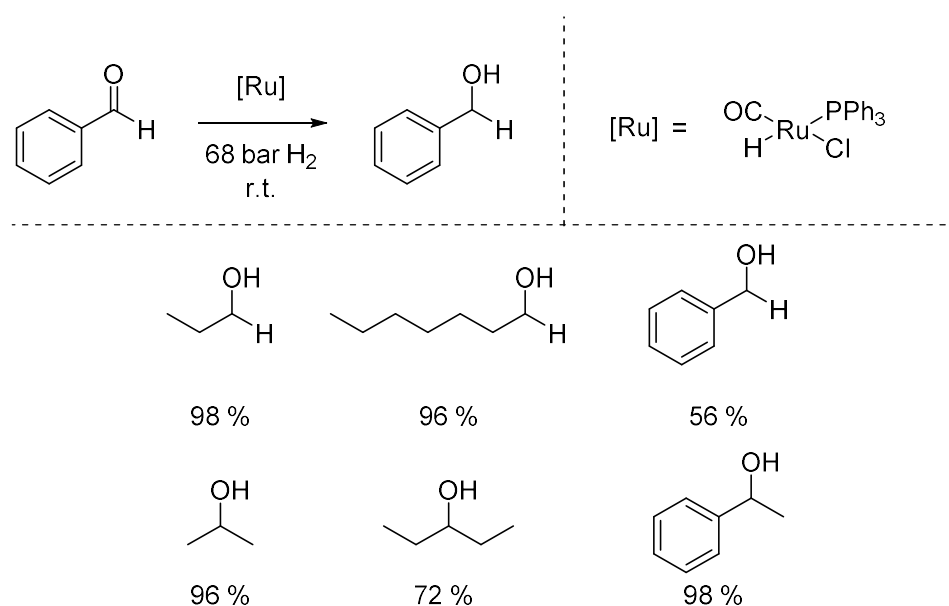


Figure 1.3 Homogeneous Rh-catalyzed hydrogenation in 1975 and the effect of amine

Four years later in 1979, Ru catalyst was also developed for aldehyde hydrogenation [9]. In such case, triphenylphosphine was applied as ligand to efficiently boost the catalyst activity and stability. It was also demonstrated that CO ligand can also increase the catalyst activity. Despite that a hazardous pressure of hydrogen was required (68 bar), there are still 6 substrates reported to be efficiently reduced to the corresponding alcohol (Table 1.1). The substrate scope includes both aliphatic and aromatic compounds, both aldehydes and ketones. Ever since this report, ligands tuning became the focus for designing hydrogenation catalyst.

Table 1.1. Ru-catalyzed aldehyde hydrogenation in 1979



Though efforts have been made towards aldehyde hydrogenation, however, mechanistic study was never conducted regarding how the hydrogen is transferred from bi-molecular gas to the aldehyde and become the α -hydrogen of the corresponding alcohol. In 1981, Grey and Pez synthesized anionic Ru and Ir hydride complexes and demonstrated that those anionic hydride complexes represent important intermediates in Ru and Ir-catalyzed hydrogenation of aldehyde [10]. Although the possibility for oxidative addition of metal catalyst, which is common for olefin hydrogenation, was not excluded, the author hypothesized that the mechanism of aldehyde hydrogenation is more likely to undergo bi-molecular hydrogen heterolysis into hydride and proton (Figure 1.4). It was also demonstrated that decarbonylation is a major side reaction in aldehyde

hydrogenation. It also serves as the main reason for catalyst poisoning due to the generation of metal carbonyl. Notably, such problem was generally not observed in ketone hydrogenation.

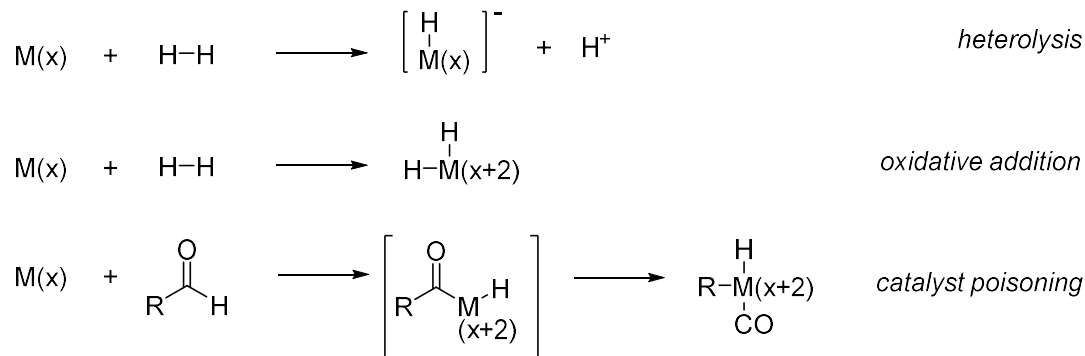
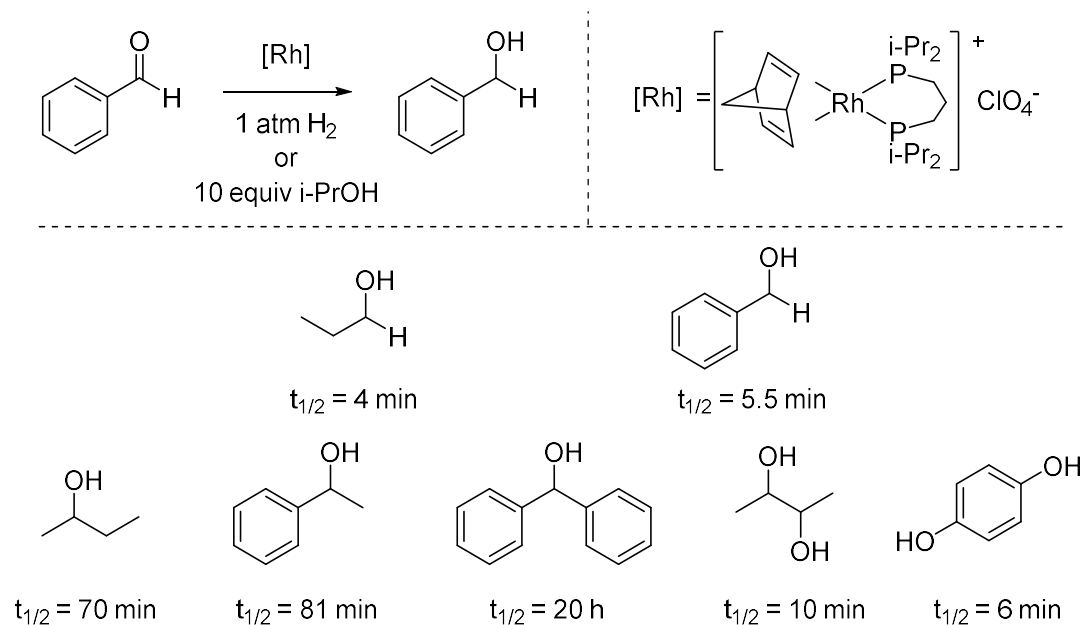


Figure 1.4. Two potential pathways for hydrogen activation and catalyst poisoning

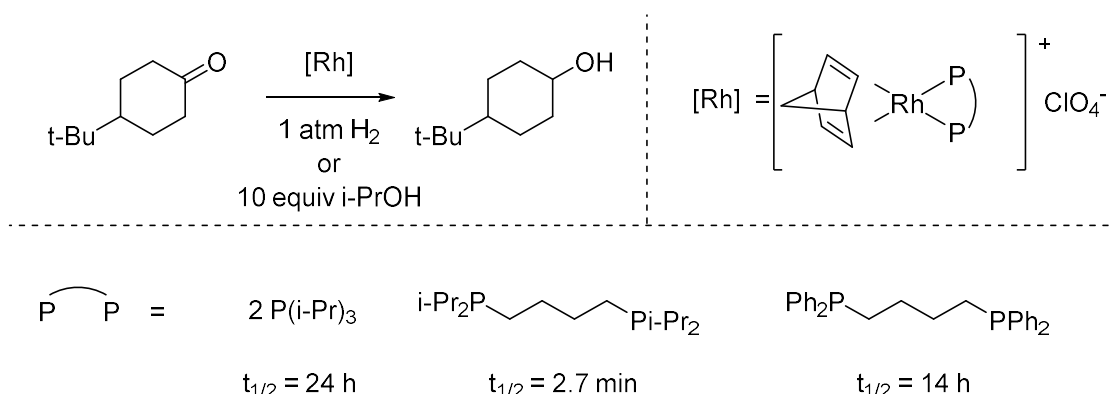
Since then, many efforts have been made to design more efficient catalyst for aldehyde hydrogenation. It was not difficult for chemists to realize that the aldehyde hydrogenation catalyst activity can be further increased by even more electron-rich ligands, as such process facilitates potential oxidative addition towards hydrogen at the same time inhibit the undesired decarbonylation. In 1982, Tani and Otsuka demonstrated that the use of fully alkylated phosphine,

Table 1.2. Aldehyde hydrogenation in 1982 using electron-rich phosphine



which is generally much more electron-rich than previous arylated phosphine, increased the efficiency of catalyzed aldehyde hydrogenation in almost every substrate examined (Table 1.2) [11]. The experiments also shown that the catalyst's increase in electron density significantly inhibited the undesired decarbonylation as well as the β -H elimination, which resulted in the re-oxidation of the reduction product. It was also shown that bidentate diphosphine ligands generally functions more efficiently than monodentate ligands (Table 1.3).

Table 1.3. Reactivity comparison for mono- and bi-dentate phosphine

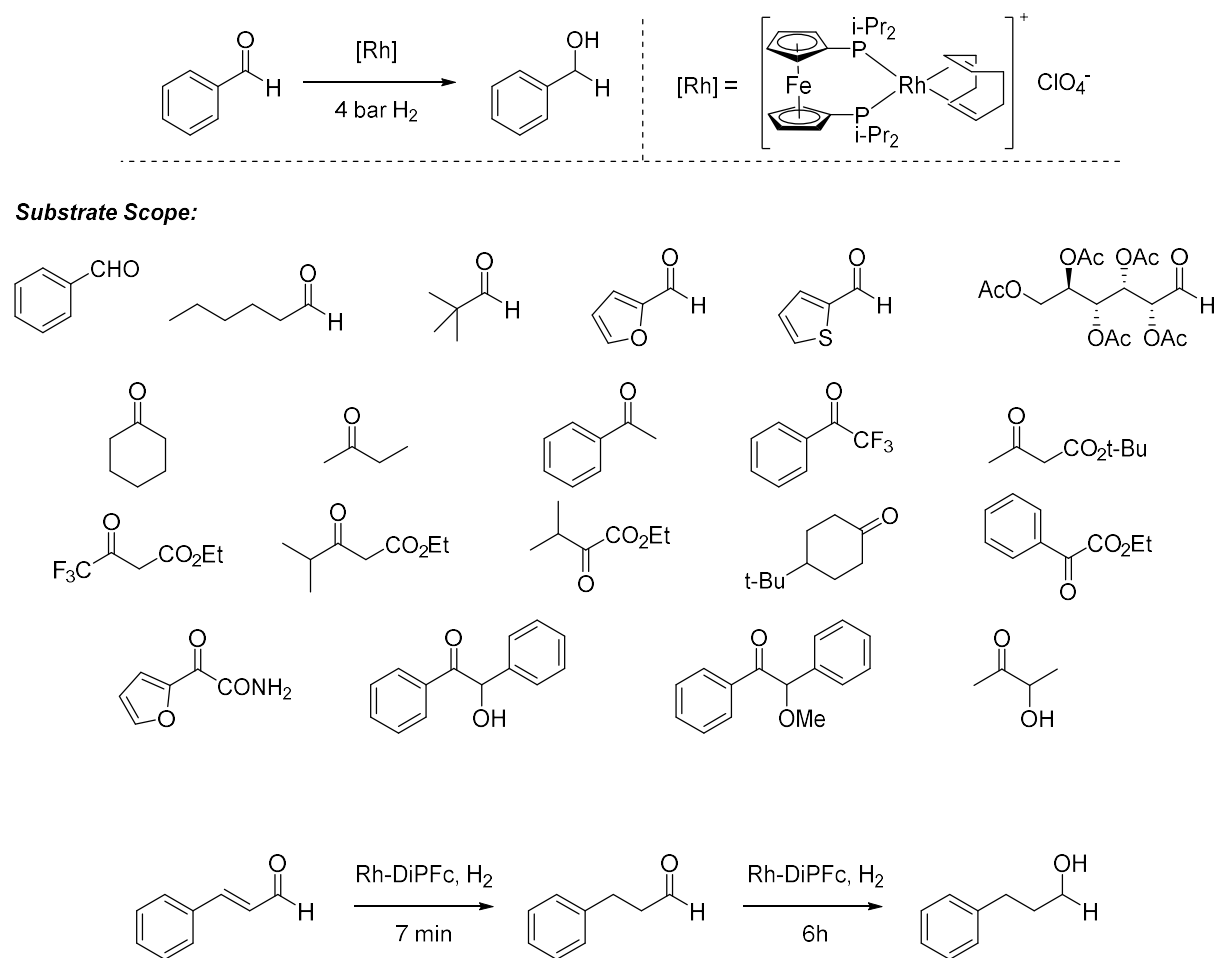


Similar result was also obtained in 1994, when Burk demonstrated a powerful Rh hydrogenation catalyst [12]. Very electron-rich bidentate 1,1'-bis(diisopropylphosphino)ferrocene was shown to also be the key to achieve high efficiency and low H₂ pressure. Many substrates, including aliphatic, aromatic and even protected carbohydrate carbonyl compounds were claimed to be successfully reduced to the corresponding alcohol (Table 1.4). However, it was also observed that for unsaturated aldehydes, the undesired C=C hydrogenation was facilitated rather than C=O hydrogenation (Scheme 1.1).

In 1986, Sanchez-Delgado concluded that 3 factors were necessary when designing efficient aldehyde hydrogenation catalyst [13]: 1) at least one empty coordination site for substrate coordination; 2) the ability for metal to afford a stable pair of oxidation state $x/x+2$; 3) one CO ligand to minimize the undesired decarbonylation, since such process was observed when catalyst contains only hydride and phosphine ligand, which possibly promote the initial oxidative addition of aldehyde C-H (Figure 1.5). The author also made an enhancement for the current catalyst by switching the anion to carboxylate. The author hypothesized that the bidentate carboxylate is very labile and its carbonyl coordination to the metal can dissociate to open empty coordination site for

substrate. It was also demonstrated that more electron-poor carboxylate facilitates the desired transformation, which is consistent with the author's hypothesis.

Table 1.4. Substrate scope of Rh-catalyzed hydrogenation in 1994



Scheme 1.1. Selectivity for C=C over C=O

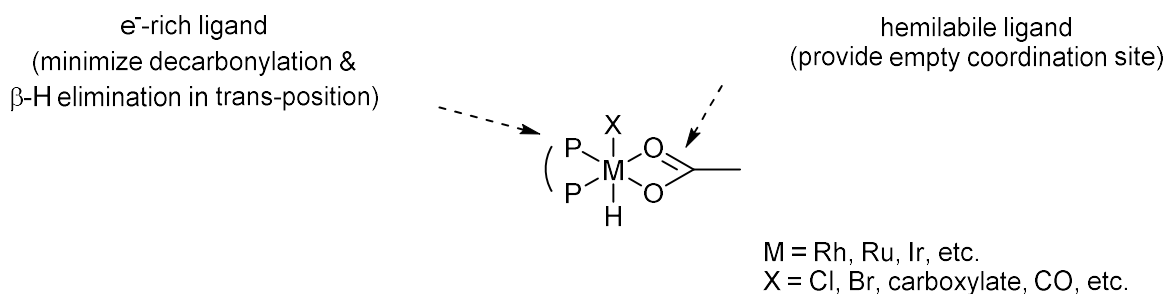
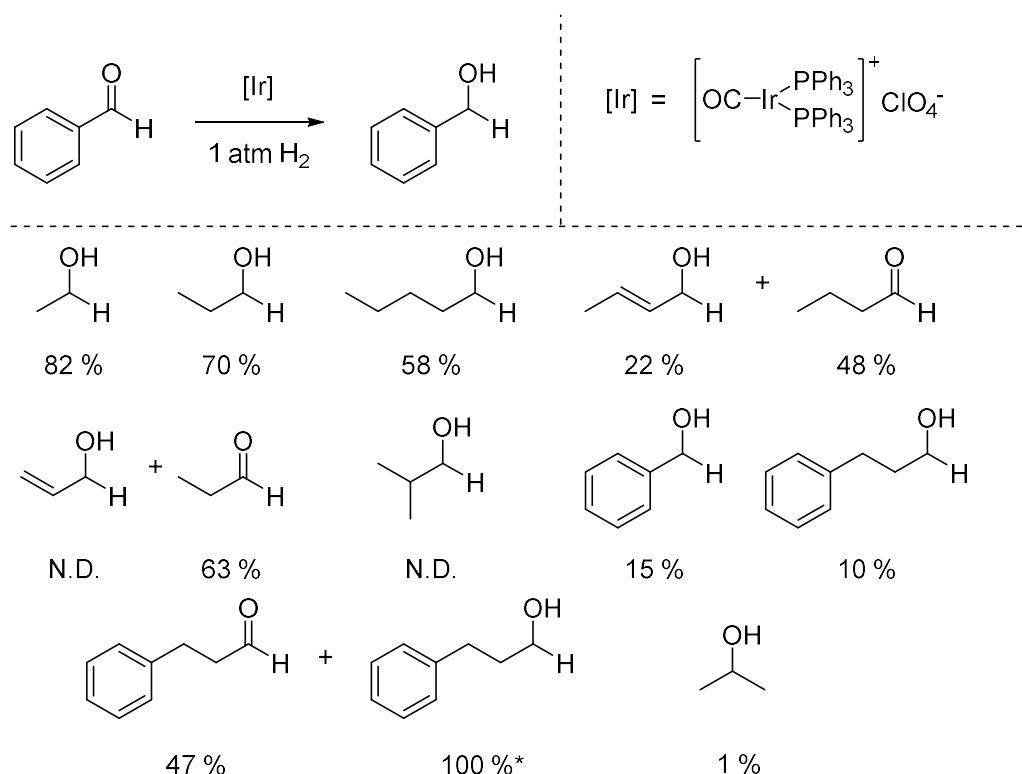


Figure 1.5 The ideal catalyst for aldehyde hydrogenation according to Sanchez-Delgado's design

As relatively limited examples were reported for Ir as aldehyde hydrogenation catalyst, in 1989, a $[\text{Ir}(\text{CO})(\text{PPh}_3)_2]\text{ClO}_4$ catalyst was developed to conduct aldehyde hydrogenation in room temperature under atmospheric hydrogen [14]. However, the substrate is relatively limited, for bulkier *iso*-butanal did not react in the reported condition (Table 1.5). Aromatic-containing aldehydes also showed inferior reactivity. For unsaturated aldehydes, the reported catalyst seemed to prefer C=C hydrogenation rather than C=O, as C=C reduction was mainly observed.

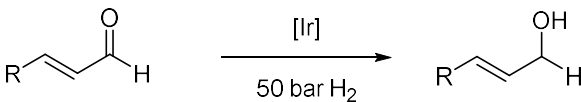
Table 1.5. Ir-catalyzed aldehyde hydrogenation in 1989

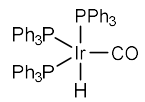
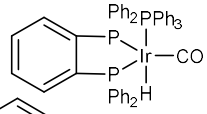
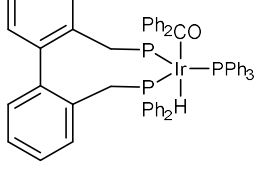
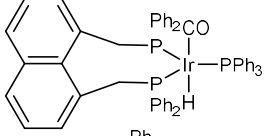
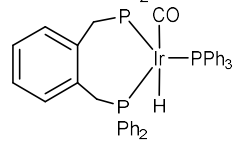
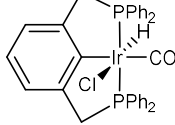


* After increase the pressure of H_2 to 3 bar

In 2002, Ir catalyst containing bidentate phosphine was developed for aldehyde hydrogenation catalyst [15]. The experiment depicted in the research shown that the bidentate phosphine functions more efficiently compared to 2 similar monodentate phosphine ligands. It was also shown that Ir exhibits even better selectivity of C=O rather than C=C (Table 1.6), which contrasts with previous reports where Ir usually shown inferior catalyst activity when compared to Ru or Rh.

Table 1.6. Investigation over bi-dentate phosphine in efficiency and selectivity



[Ir]	Citral		Cinnamaldehyde	
	Conversion	Selectivity	Conversion	Selectivity
	3 %	71 %	11 %	35 %
	8 %	61 %	27 %	19 %
	12 %	92 %	45 %	13 %
	19 %	96 %	21 %	77 %
	59 %	96 %	58 %	9 %
	14 %	43 %	52 %	1 %

One of the biggest disadvantage for homogeneous catalysis compared to heterogeneous is the difficulty in clean and facile isolation of product. In 2001, the group of Monflier described an interesting solution, where a water-soluble phosphine was used as ligand and cyclodextrin as phase transfer catalyst [16]. The Ru catalyst was successfully conducted in an organic/water biphasic reaction system. The hydrogenation took place in water phase and the alcohol product was enriched in the organic phase (Figure 1.6). Such report not only partially addressed the isolation problem for homogeneous catalysis, but also shown the potential to easily modify the reactivity of

aldehyde hydrogenation catalyst just by tuning the ligand, implying the great potential of ligand in modern catalysis.

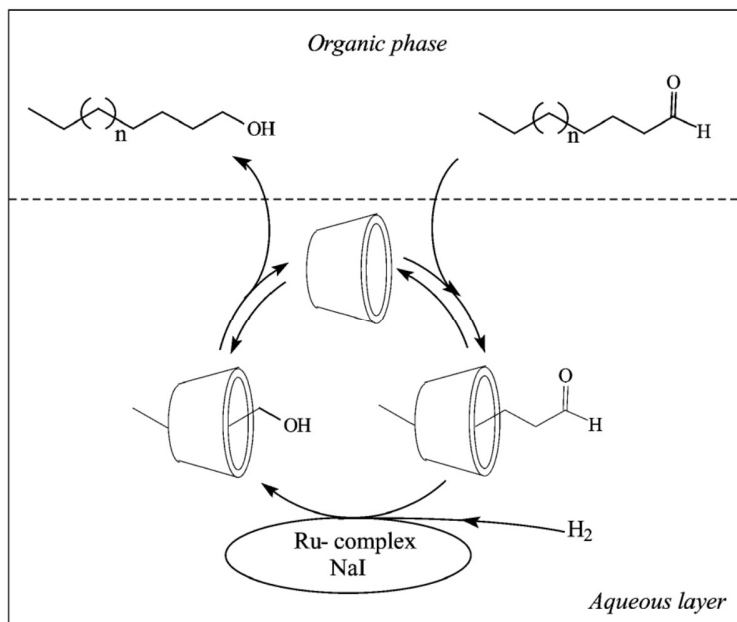


Figure 1.6 Aqueous phase Ru catalysis using cyclodextrin

1.2.2.2 The Noyori hydrogenation and transfer hydrogenation of aldehyde

Inspired by the demonstrated potential for bidentate diphosphine ligand in catalytic aldehyde hydrogenation, in 1987, Noyori and co-workers reported the use of a Ru catalyst chelated by a specialized phosphine to carry out carbonyl hydrogenation [17]. By introducing BINAP as a chiral ligand, high-efficiency asymmetric hydrogenation of carbonyl compound was achieved for the first time. The catalyst was shown to functioned via the hydrogen heterolysis mechanism, rather than the oxidative addition mechanism (Figure 1.7). This work is considered the precursor of the later known name reaction Noyori Asymmetric Hydrogenation/Transfer hydrogenation (NAH or NATH). Though significant, however, such system only functions with activated ketone, in most cases, β -ketocarboxylic derivatives. Aldehyde was not active towards the reduction.

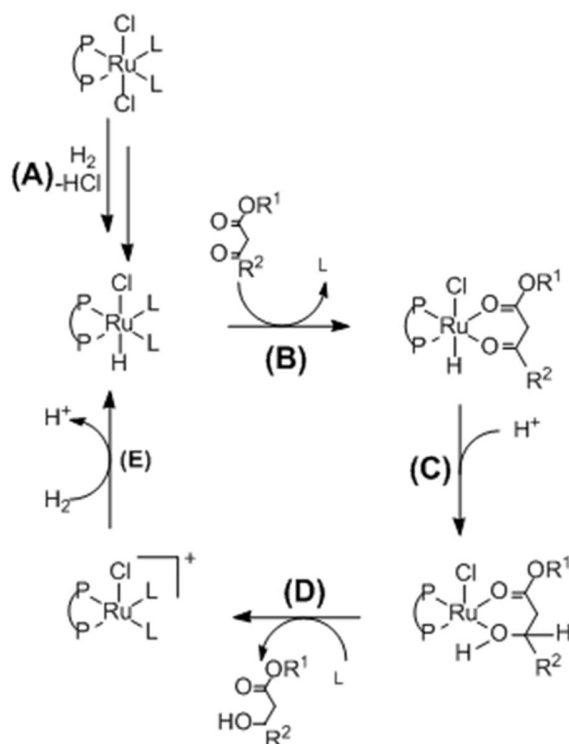


Figure 1.7. Mechanism for the 1st generation Noyori catalyst

As early as the report in 1975 [8], chemists started to realize that the presence of amine in the catalyst system can greatly enhance the aldehyde hydrogenation efficiency. Although the mechanism behind this phenomenon was not fully investigated at the time, this effect was later demonstrated to be of great potential. In 1997, Noyori demonstrated the use of asymmetric diamine, rather than diphosphine, as ligand and achieved asymmetric transfer hydrogenation using alternative alcohol as hydrogen source [18]. It was hypothesized that the hydrogen heterolysis involves both the Ru and the nitrogen ligand. The hydride coordinated to the Ru and become a covalent ligand, the anionic nitrogen captured the proton and become a dative ligand. No oxidation state change was observed throughout the whole process (Figure 1.8). Although the hydride transfer between different substrate is reversible and cannot go to completion, the discovery of this nitrogen-assisted activation of hydrogen set the stage for the development of the next generation Noyori catalyst. Notably, it was later demonstrated that this catalyst is also capable of conducting direct hydrogenation of aldehyde and ketone, giving satisfying efficiency.

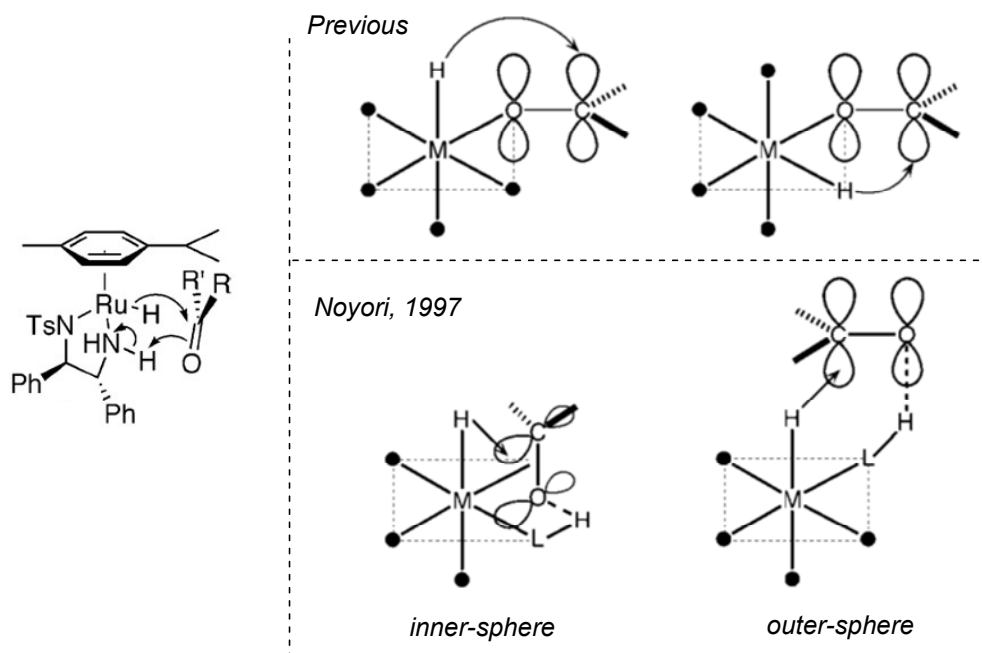


Figure 1.8. The Noyori transfer hydrogenation catalyst in 1997

In 2001, the milestone work by Noyori greatly expanded the efficiency and versatility of hydrogenation and transfer hydrogenation processes [19]. At the same time, the enantioselectivity of the previous Noyori catalyst was also preserved. The efficient catalytic activity and good functional tolerance of the Noyori catalyst for carbonyl reduction relies heavily on the diamine bi-dentate ligand. [20] The mechanism of Noyori system is shown in Figure 1.9. A donor-acceptor [21] H-Ru-N-H complex generated by heterolysis of hydrogen gas with Ru-N is mainly responsible for the high efficiency activation of carbonyl via a 6-member ring transition state.

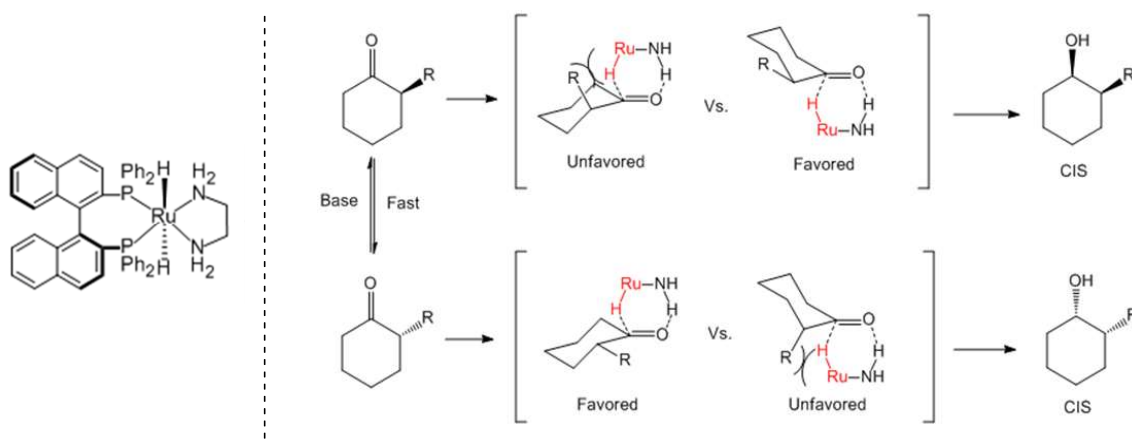
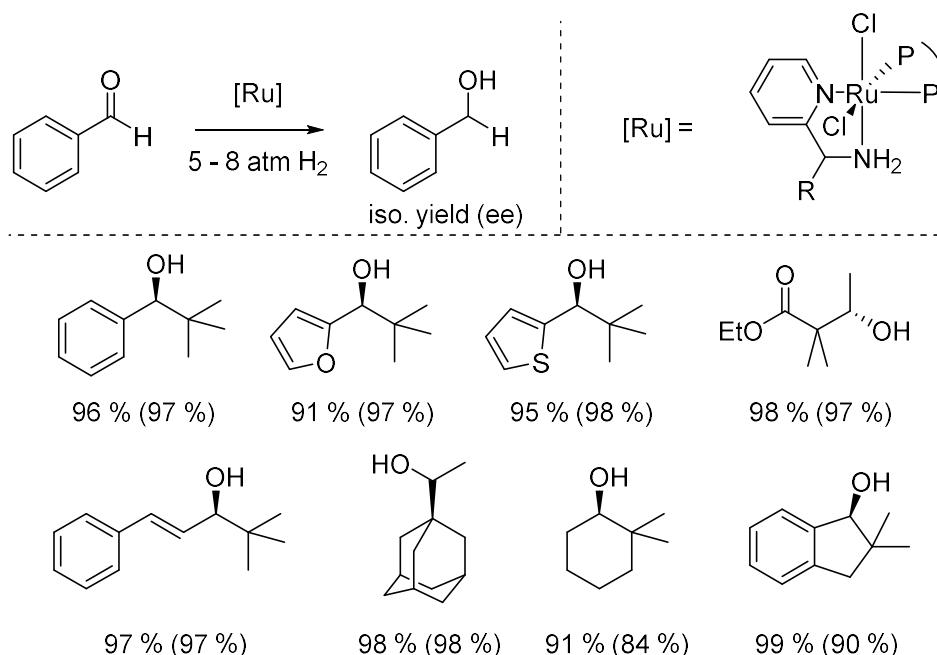


Figure 1.9 The 2nd generation Noyori hydrogenation / transfer hydrogenation of aldehyde

Sterically hindered substrates have been a long-persisting issue for methodology studies. For Noyori system, tert-butyl carbonyl compound shows much inferior reactivity in both yield and ee. In 2005, Noyori and Ohkuma demonstrated that this problem can be solved by switching the symmetric diamine into an asymmetric amine/pyridine hybrid ligand, α -picolylamine [22]. This modification potentially allows a wider empty coordination site for bulkier substrates. As a result, excellent efficiency was obtained for bulky aldehydes/ketones (Table 1.7).

Table 1.7. The Noyori catalyst for bulky substrates



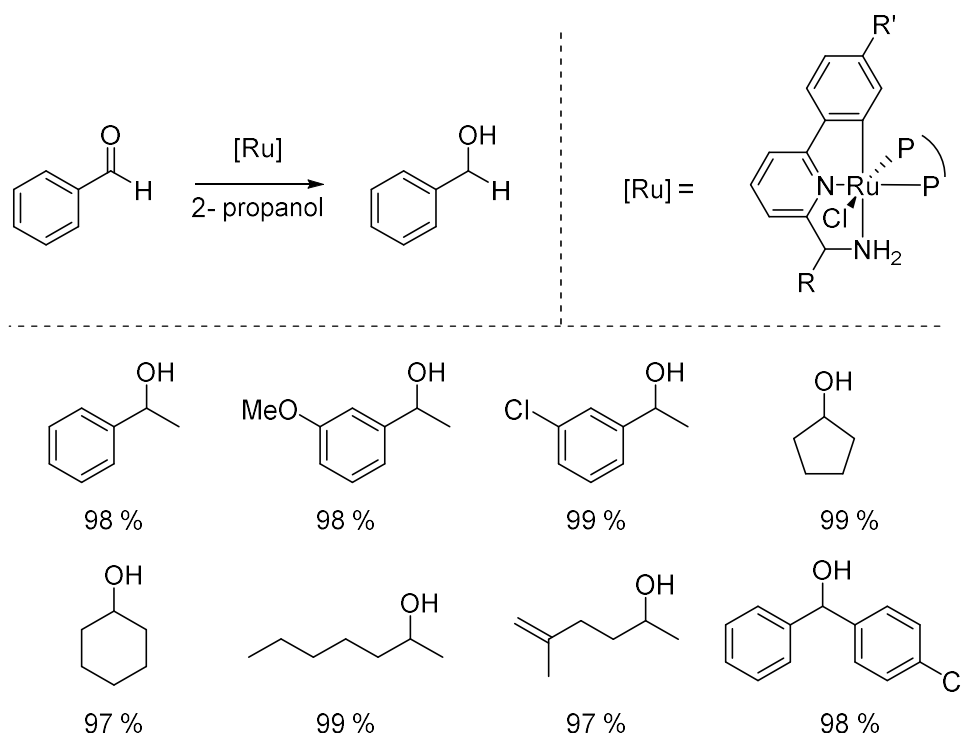
1.2.2.3 Other hydrogenation and transfer hydrogenation system utilizing N-M ligand-metal bifunctional catalysis

Since the Noyori reaction is widely practiced, countless works were introduced to improve the Noyori ligand-metal donor-acceptor catalyst. Those developed systems generally consist an electron-rich phosphine donor to facilitate metal hydride interaction, and a bifunctional nitrogen donor to capture the proton.

As ‘Pincer’ terdentate ligand, which usually contains a non-labile anionic covalent donor and up to 3 labile dative donors, has received intensive research interest especially in the 1990s [23], however, they have not yet been applied to the Noyori system. In 2005, Baratta first reported the use of a C, N, N,-tridentate pincer ligand in Ru hydrogenation and transfer hydrogenation system.

The design of this pincer ligand was inspired by the above-mentioned asymmetric amine/pyridine hybrid ligand, which was also applied in the Noyori system for hydrogenation of bulkier substrate. By adding a covalent C donor to the amine/pyridine, the new tridentate ligand gave impressive efficiency and selectivity over substrates (Table 1.8). It was also demonstrated that the same catalyst also functions efficiently with transfer hydrogenation from 2°-alcohol.

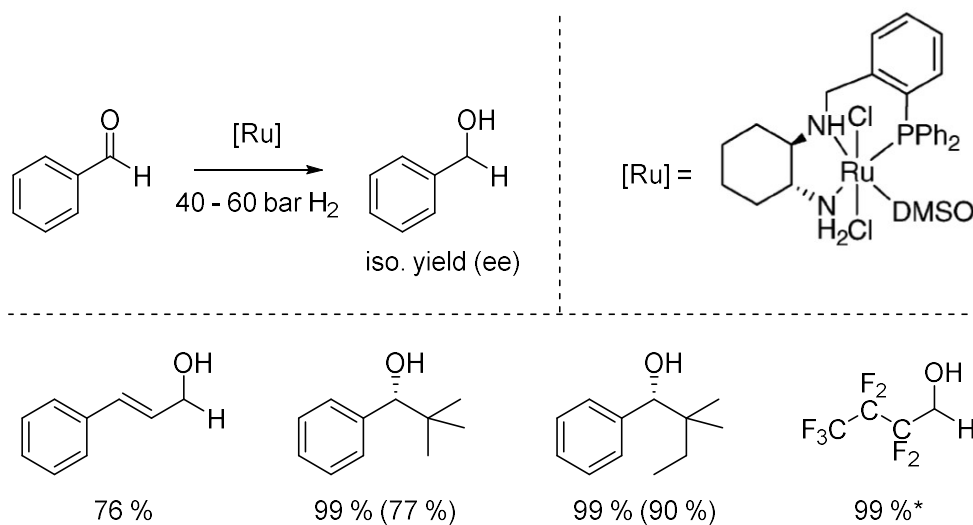
Table 1.8. Ru-catalyzed transfer hydrogenation of aldehyde using pincer ligand



As the asymmetric Noyori catalyst often involves 2 chiral ligands, which is difficult to prepare, in 2007, a P, N, N- tridentate ligand was developed to replace such requirement [24]. The sole ligand contains all the required donors for the Noyori catalyst, at the same time the enantioselectivity of the traditional catalyst was greatly preserved. Compared to preparation of 2 chiral ligands at the same time, the cost for synthesizing this new catalyst was also significantly reduced. The catalyst complex was identified and shown good catalyst efficiency. However, high-pressure hydrogen gas is required to obtain efficient transformation. In addition, the reported hydrogenation shown limitations in selectivity by also reducing ester group (Table 1.9).

To further improve the activity of the existing hydrogenation and transfer hydrogenation catalyst, it is not difficult for chemists to realize that Os, which is just one slot down to Ru in the periodic

Table 1.9. Ru-catalyzed aldehyde hydrogenation in 2007



* Reducing from the corresponding methyl ester

table, forms stronger metal-ligand coordination to generally soft ligands used in the Noyori catalyst. Such effect can potentially increase the catalyst stability and allows greater TON. In 2008-2009, Baratta demonstrated the use of Os to replace Ru in the Noyori catalyst (Figure 1.10) [25-27]. As

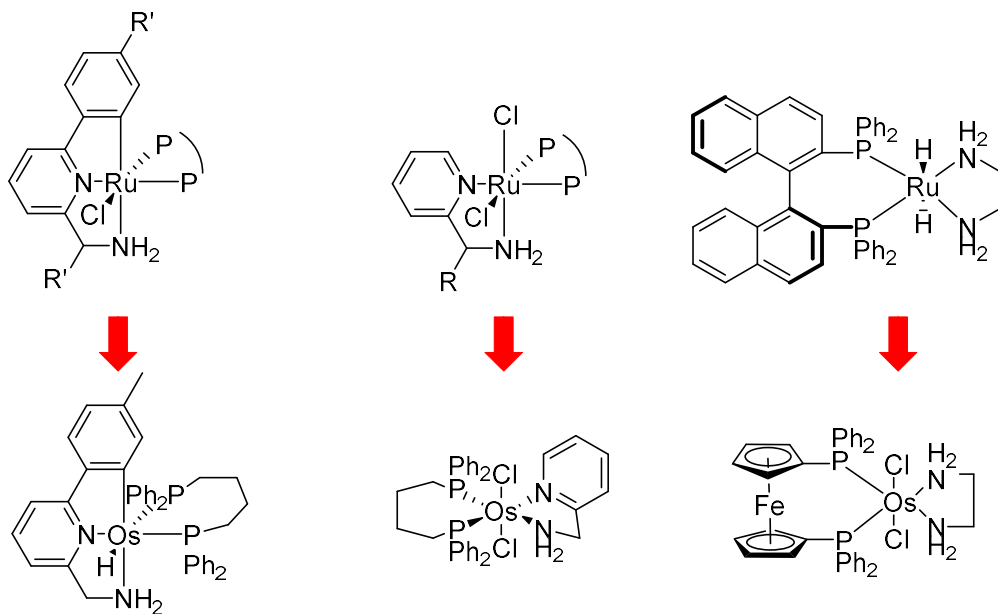
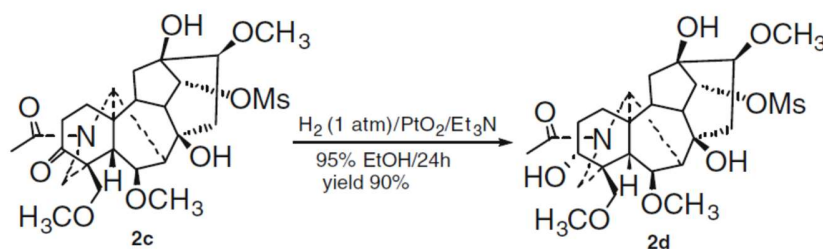


Figure 1.10. Os catalyst designed from their corresponding Noyori's Ru catalyst

they have designed, enhancement in catalyst efficiency and enantioselectivity was observed in all cases, which allows those catalysts to be extremely active for both hydrogenation and transfer hydrogenation of both aldehydes and ketones. However, as Os being an expensive and usually toxic metal, Ru catalysts remain the most widely-applied choice. Nevertheless, the development of Os catalyst opened an alternative solution for more efficient hydrogenation and transfer hydrogenation requiring better enantioselectivity.

Another potentially active metal for hydrogenation and transfer hydrogenation of aldehyde is Pt. Historically, Pt was the first metal to show hydrogenation activity [7]. It was also widely applied in heterogeneous hydrogenation of carbonyl compound (will be discussed in heterogeneous section). Nevertheless, Pt was never used as homogeneous carbonyl hydrogenation catalyst. Although the mechanistic reason behind this disagreement remains uninvestigated, in 2009, Wang reported the use of a simple PtO₂-triethyl amine system to conduct hydrogenation of aldehyde [28]. No additional phosphine or chiral amine ligand was necessary, the simple metal oxide shows remarkable hydrogenation efficiency and selectivity by reducing many natural products. Many of those natural products contain multiple carbonyl groups, surprisingly, only one of them was reduced into the desired enantiomeric pure alcohol (Scheme 1.2). Despite mechanistic study was absent, it was presumably agreed that the Et₃N functions similar to the N-M ligand-metal bifunctional catalyst in the Noyori system. This study shows great potential to explore Pt as hydrogenation catalyst.



Scheme 1.2. Example of natural product reduction using Pt/Et₃N system

1.2.2.4 The Shvo hydrogenation of aldehyde

As early as 1986, one year earlier than Noyori's discovery of Ru-BINAP and Ru-diamine system, Shvo had developed an alternative ligand-metal bifunctional catalyst for the donor-acceptor reduction of aldehyde [29], which is composed of a cyclopentadienone-Ru-carbonyl catalyst

complex. It was suggested that this catalyst system also functions via ligand-metal bifunctional pathway. The heterolysis of hydrogen was accomplished by Ru and the carbonyl of cyclopentadienone, generating the corresponding Ru-H and hydroxycyclopentadiene complex, which can efficiently undergo donor-acceptor hydrogenation of aldehyde (Figure 1.11).

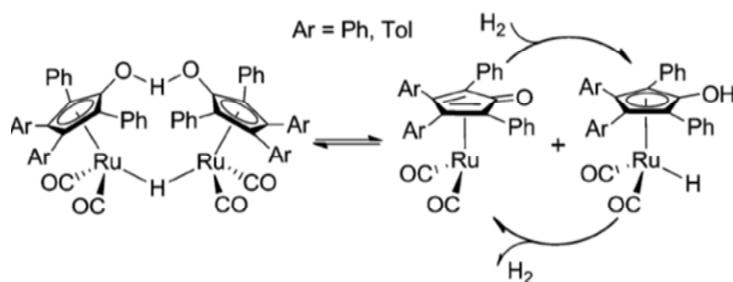


Figure 1.11. Typical mechanism for the Shvo hydrogenation

Since the discovery of the Shvo catalyst, many mechanistic studies were conducted [30]. Similar to the Noyori system, the hydrogenation of the Shvo catalyst also involves the donor-accepter 6-member ring intermediate. It was also shown that the dimerization of catalyst poses the main factor that inhibits the catalytic cycle and limits the efficiency of the Shvo catalyst. To overcome this barrier, the first solution was proposed by Casey in 2002 [31]. In his study, the cyclopentadienone ligand in the Shvo catalyst was replaced by Cp-NHPh (Figure 1.12). It was shown that the bulky -NHPh was efficient in preventing catalyst dimerization, however, the new Shvo catalyst requires the addition of strong acid (TfOH) to stabilize the ammonium intermediate.

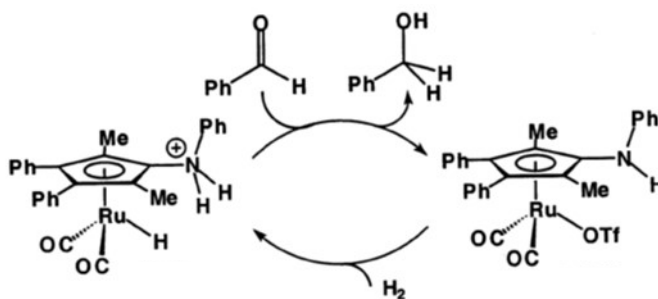


Figure 1.12. Casey's catalyst for acidic hydrogenation of aldehyde

A better solution was proposed by Casey 4 years later [32]. It was later discovered that the substituent on the Cp ring can greatly inhibit the dimerization. In his study, the most efficient

hydrogenation was obtained with [2,5-(SiMe₃)₂-3,4-(CH₂OCH₂)(η⁵-C₄COH)]Ru(CO)₂H [33], where a bulky -TMS group significantly improves the stability of catalytic cycle (Figure 1.13). Both hydrogenation and transfer hydrogenation were efficiently obtained with satisfying substrate scope.

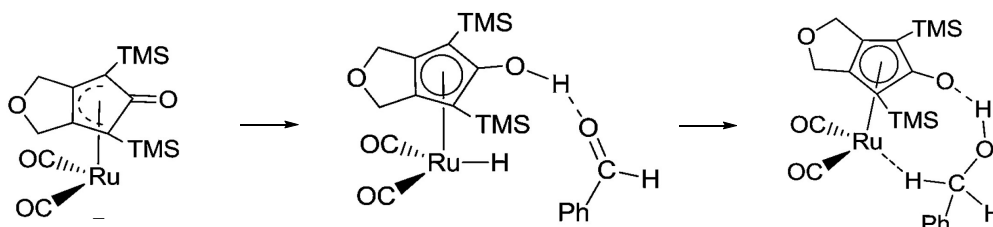
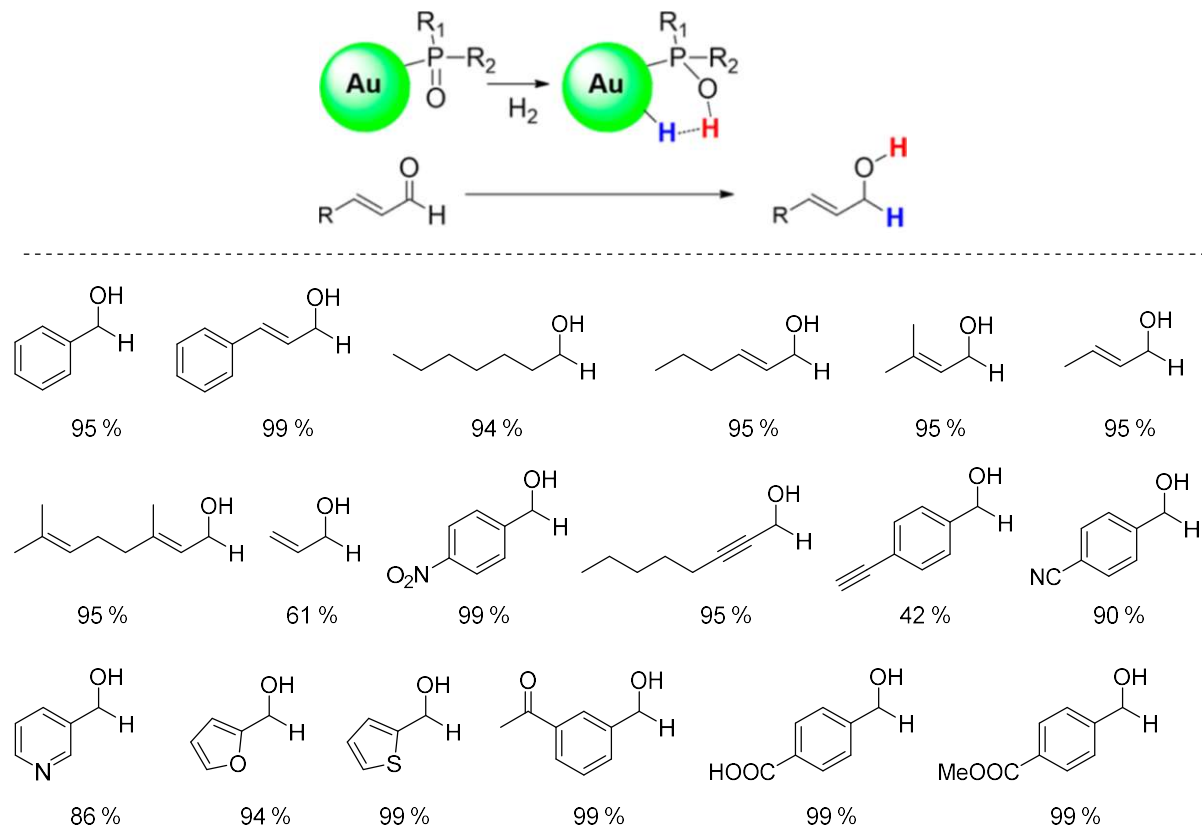


Figure 1.13 Mono-metallic intermediates for Casey's system in 2016

1.2.2.5 Donor-acceptor reduction by nanoparticle

As the noble metal catalyst in the previously described system usually cannot be reused, efforts have been made towards catalyst recycling for hydrogenation and transfer hydrogenation. Notably, **Table 1.10. Donor-acceptor hydrogenation pathway for AuNP**



in 2014, van Leeuwen group reported a Gold-nanoparticle-(AuNP)-secondary phosphine oxide(SPO) system and achieved efficient aldehyde hydrogenation and recyclability of catalyst (Table 1.10) [34]. The catalyst functions through a similar donor-acceptor mechanism, in which the hydride coordinates to the AuNP and the SPO captures proton. Although the recyclability of the catalyst still needs improvement (only 4 cycles), this work demonstrated that the application of the ligand-metal donor-acceptor system can also be applied towards mesoscopic system.

1.2.2.6 Hydrogenation and transfer hydrogenation catalyzed by abundant metal

Historically, among all the effort towards aldehyde hydrogenation, noble metals were predominantly used as catalyst, such as Pt, Ru, Rh, Ir, etc., for their great affinity towards hydrogen. The use of abundant metal as hydrogenation catalyst is extremely scarce. However, in fact, abundant metals such as Fe are among the earliest developed aldehyde hydrogenation catalysts [35]. However, since the migratory insertion of substrate carbonyl in the Fe-H is generally slow, the application of such catalyst was greatly limited (Figure 1.14).

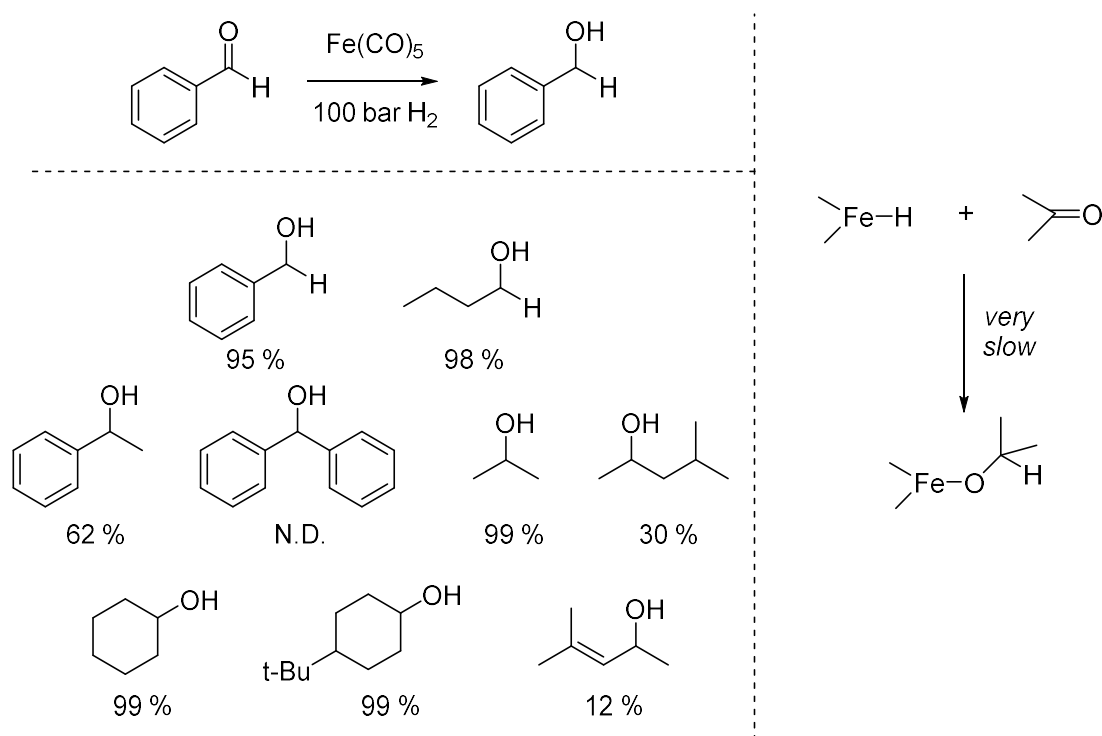
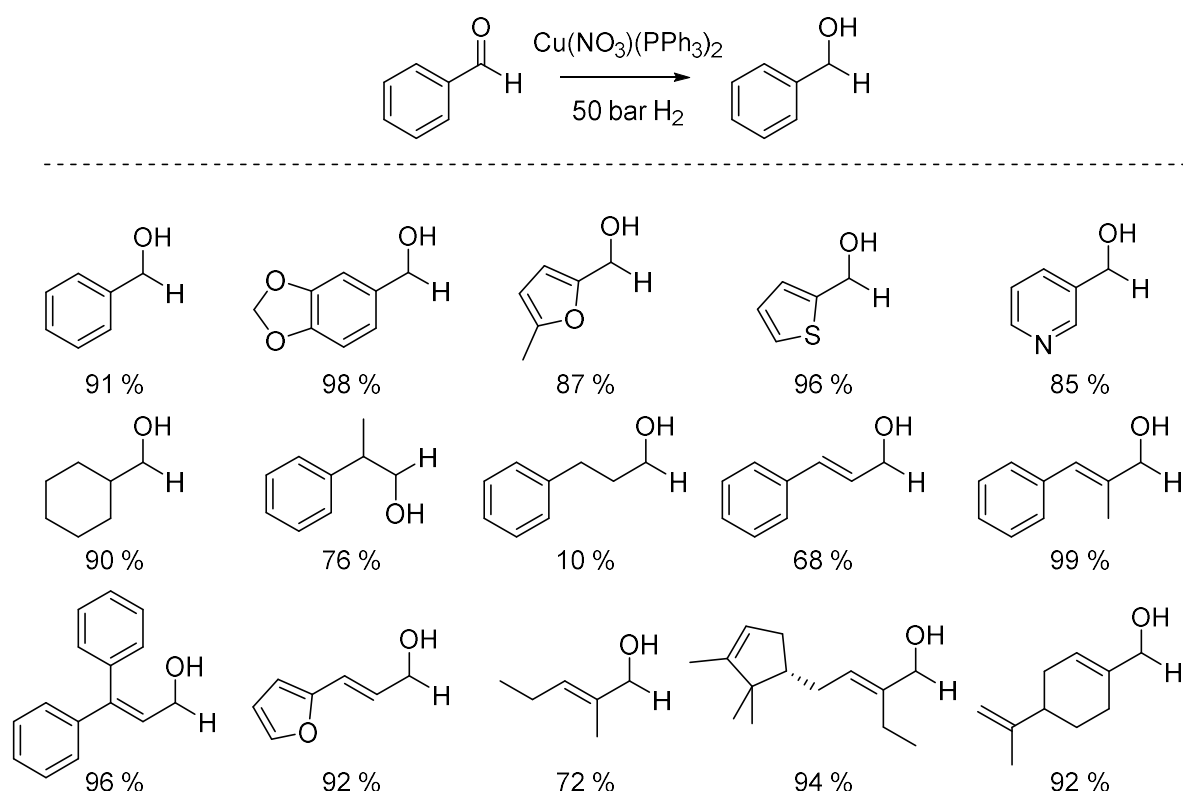


Figure 1.14. Early discovery of Fe-catalyzed hydrogenation and its limitation

In 2009, a copper catalyst bearing triphenylphosphine ligand and nitrate anion was developed [36]. Although great hydrogen pressure is required (5.0 MPa), the catalyst achieve impressive substrate scope with both aromatic and aliphatic aldehydes (Table 1.11). Notably, the catalyst shown exceptional selectivity where in an unsaturated aldehyde, only carbonyl was reduced into the corresponding alcohol. No reduction or isomerization of the C=C was observed.

Table 1.11. Cu-catalyzed aldehyde hydrogenation in 2009



As Noyori and Shvo introduced the more efficient donor-accepter catalyst for aldehyde hydrogenation, the use of abundant metal in such system had attracted considerable interests. In 1999, a new Shvo's catalyst uses Fe instead of traditional Ru (later known as the Knölker catalyst) was developed [37]. Impressive substrate scope was achieved using very low load of Fe catalyst (Figure 1.15). Computational study also demonstrated that the Knölker-type catalyst shows better tolerance of bulky substrate [38].

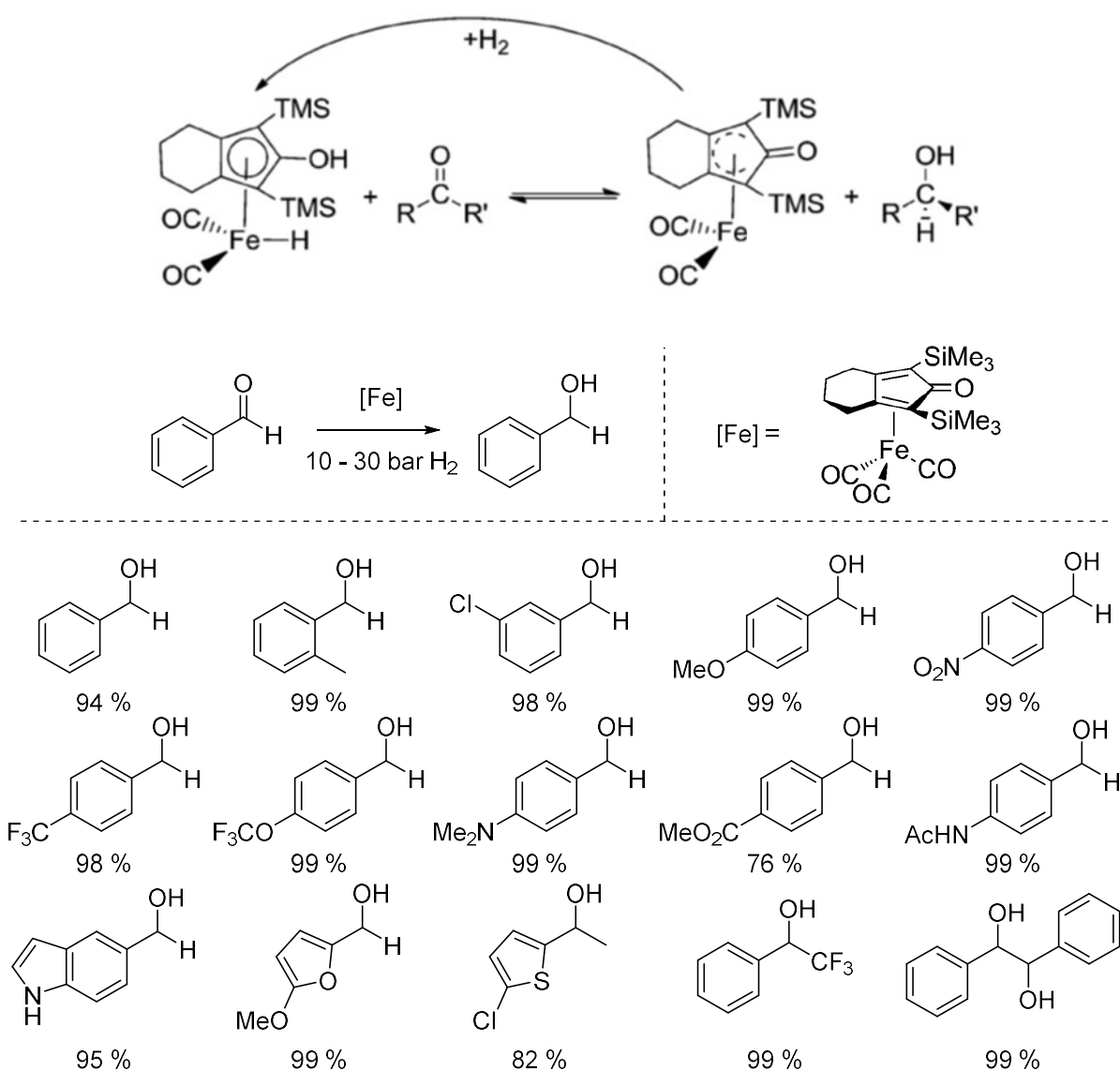
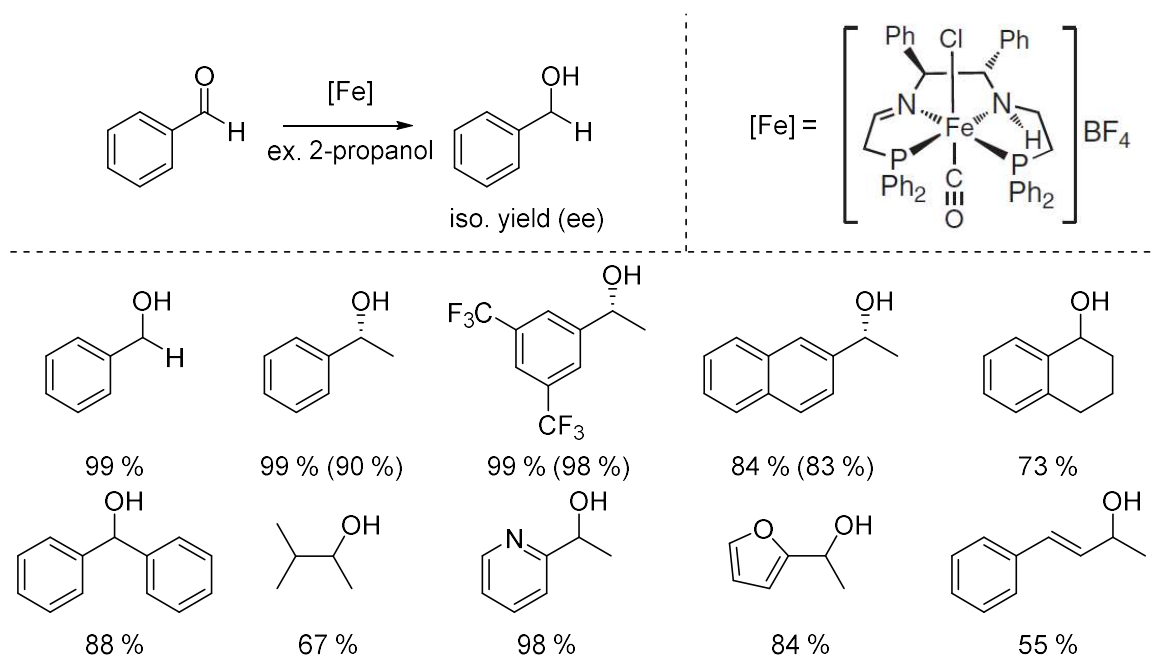


Figure 1.15. Aldehyde hydrogenation catalyzed by the Knölker catalyst

Another particularly notable example comes from a great Canadian Chemist [39]. The Morris hydrogenation/transfer hydrogenation of aldehyde/ketone using a pincer-type iron catalyst achieved good efficiency and adaptability, with very low load of Fe. The catalyst also functions via ligand-metal donor-acceptor model to achieve high efficiency (Table 1.12). Wide substrate scope was achieved with good enantioselectivity for ketones.

Table 1.12. The Morris hydrogenation/transfer hydrogenation of aldehyde/ketone



1.2.2.7 Transfer hydrogenation in water

Although using abundant metal, those above-mentioned methods generally require the use of an excess of organic solvent, which has become one of the most important environmental challenges for all pharmaceutical industry nowadays. [40]

Some great efforts for aldehyde reduction were also made using water as the sole solvent and transfer hydrogenation from alternative hydrogen source. Those methods possess great potential especially in small scale aldehyde reduction, e.g. in pharmaceutical chemistry, for eliminating the need of organic solvent, pressure-withstanding equipment and spark-sensitive environment, which are generally required in direct hydrogenation. In 1999, Ogo reported a bi-metallic $[\text{Cp}^*\text{IrOH}]_2$ catalyst and achieved the first transfer hydrogenation of aldehyde in water [41]. The hydride was extracted and give a stable Ir-H-Ir bridging intermediate (Figure 1.16). However, only water-soluble aldehydes were reported in the substrate, which significantly limits the application of the Ogo system. In addition, the hydroxyl-Ir bi-metallic intermediate is less stable, which result in very high catalyst load (10 mol%).

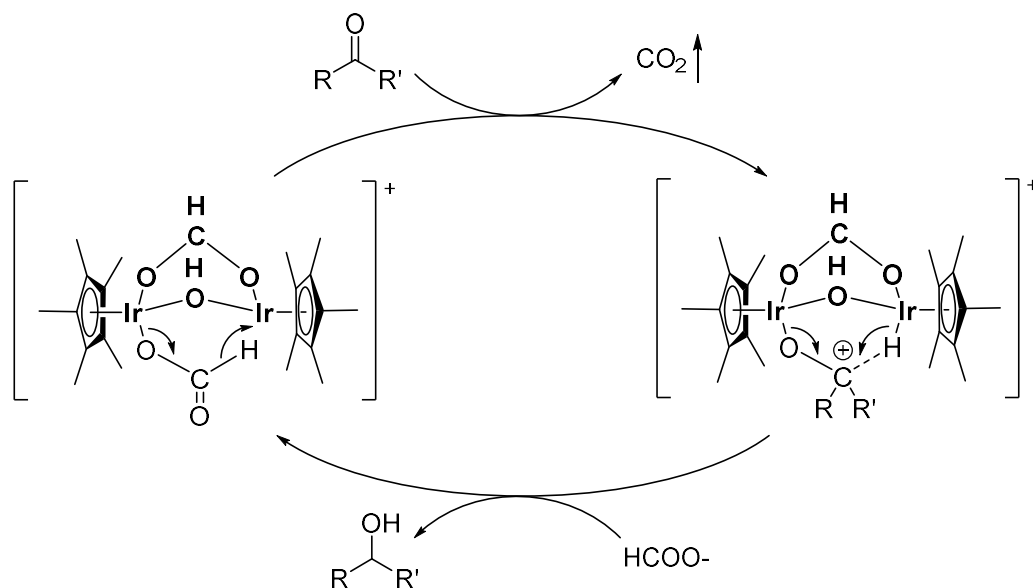


Figure 1.16. Ogo's Ir-catalyzed transfer hydrogenation in water

Inspired by the hydrogenase enzyme in nature, which involves a Ni-Fe bi-metallic catalyst center, in 2012, a similar Ni-Rh bridging system was also reported for direct hydrogenation in water [42]. Although more abundant Ni was used, the system cannot evade the bimetallic Ni-H-Rh intermediate. As a result, only 5 substrates were reported to underwent the desired transformation (Figure 1.17), which greatly limits the application of this method. However, the success of a bio-mimic catalyst still indicates interesting potential for further application with this catalyst.

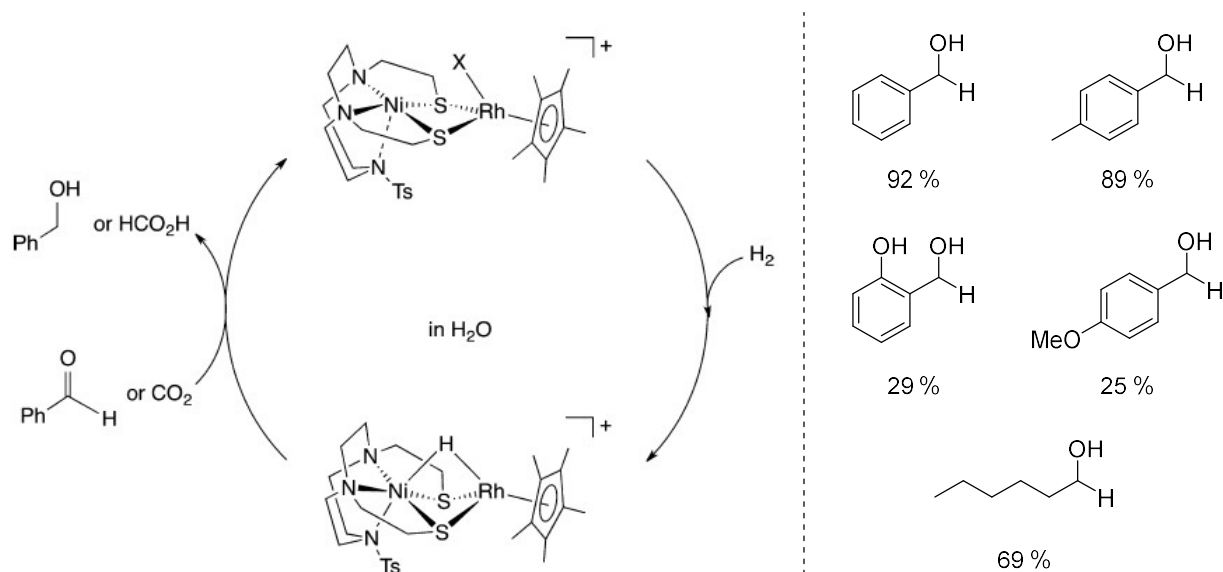


Figure 1.17. Ni-Rh bi-metallic catalyst for hydrogenation in water

Compared to the classic Noyori catalyst, by simply switching to a water-soluble Noyori diamine, aqueous transfer hydrogenation of aldehyde was also efficiently achieved by Xiao [43]. Those reported methods gave good catalyst efficiency and satisfying scope of substrates. Less than 1 mol% catalyst load was required for the system. Another catalyst for transfer hydrogenation in water was later developed by Xiao using an N, C-acetophenone imine ligand [44], which is similar to the α -picolylamine ligand in the 2nd generation Noyori catalyst. The reported transfer hydrogenation gave impressive efficiency (Figure 1.18).

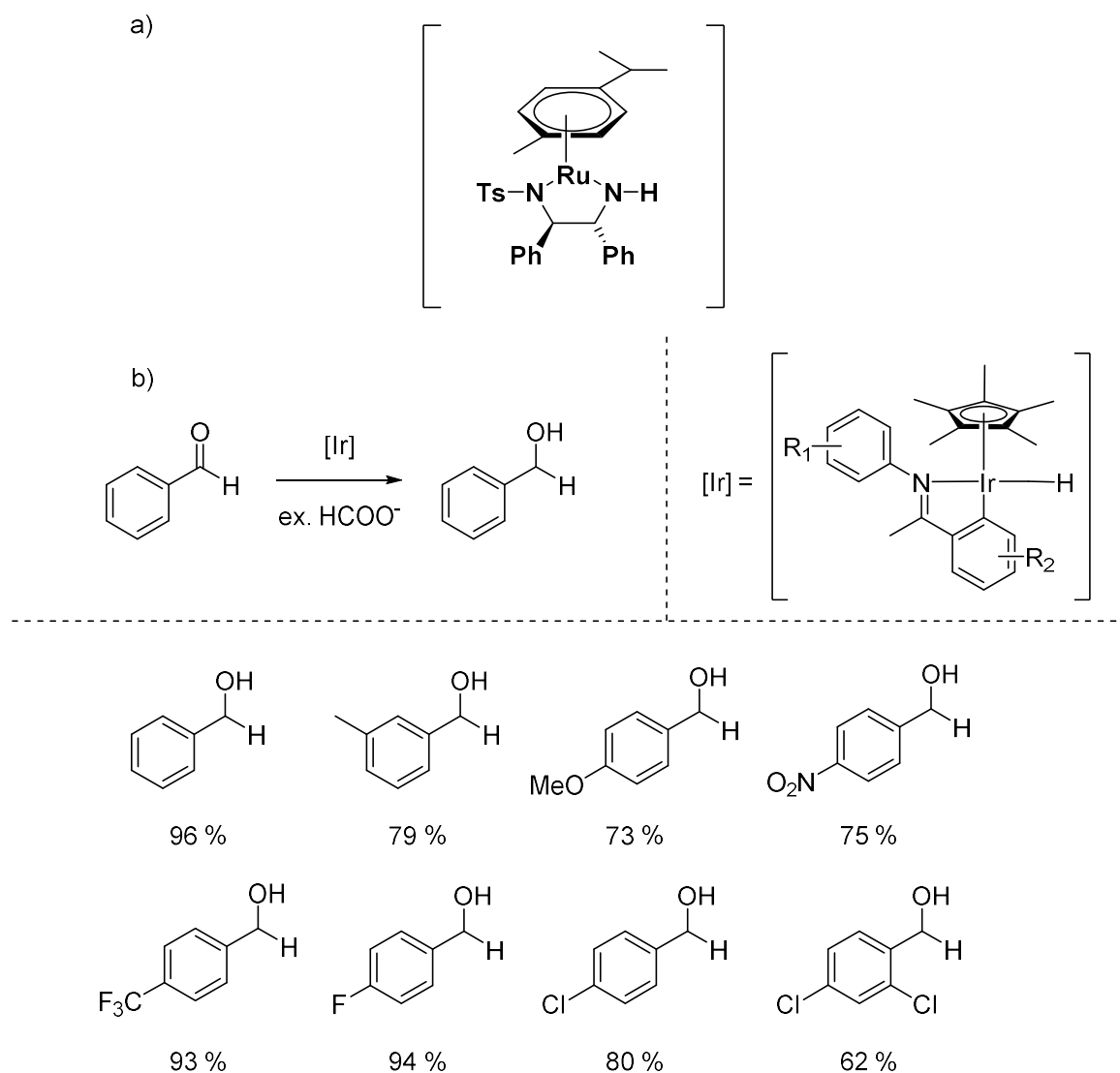


Figure 1.18. Xiao's a) 1st generation and b) 2nd generation catalyst for transfer hydrogenation in water

1.2.3 Heterogeneous catalyst for aldehyde hydrogenation

Heterogeneous catalysts receive more attention from industry and larger-scale production, as good catalyst recyclability was obtained and usually fixed instead of various product was required to manufacture. In early times, heterogeneous catalytic hydrogenation of carbonyl compounds poses a great challenge, as selectivity over C=C to C=O was difficult to obtain. The mechanism rationalization of such selectivity remained unclear for decades until 21st century, as the development of microscopic instruments. It was demonstrated than the choice over catalyst, support and even geometry of the catalyst and hydrogen absorption all contributed to the selectivity over the desired hydrogenation (Figure 1.19) [45]. Generally, 1) an activated carbonyl (e.g. by Lewis acid), 2) the steric proximity for hydride to attack carbonyl, plus 3) partial poisoning of catalyst to minimize undesired C=C hydrogenation will lead to efficient hydrogenation of the desired carbonyl.

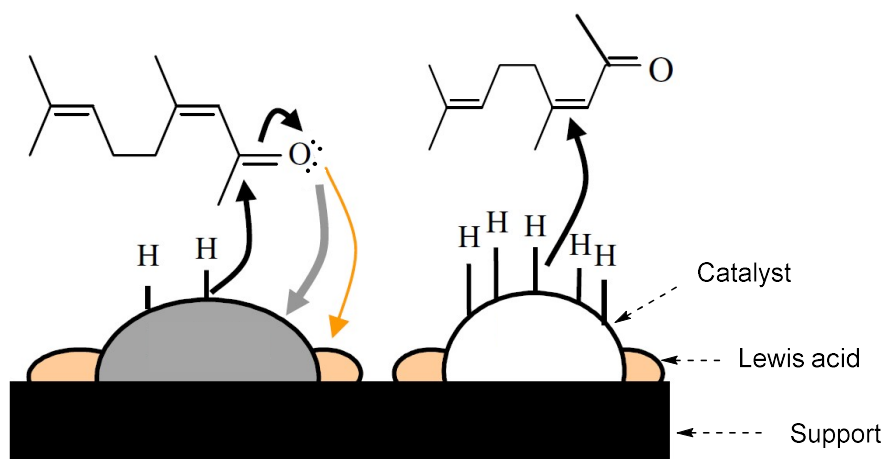


Figure 1.19. Principle and selectivity for heterogeneous carbonyl hydrogenation

1.2.3.1 Heterogeneous Pt catalyst for aldehyde hydrogenation

Pt was the first metal discovered for hydrogenation chemistry [7]. In early times, as other factors were difficult to manipulate due to limitations of techniques, support was chosen to be the focus for catalyst tuning towards better C=O hydrogenation. In 1995, Pt catalyst was synthesized with silica or alumina support (Pt@silica or Pt@alumina) for selective hydrogenation of acrolein to product unsaturated alcohol [46]. However, as gaseous phase reaction was necessary, substrate was limited to volatile aldehydes. Alternatively, Pt@clay was also developed to examine the

selectivity in hydrogenating cinnamaldehyde, crotonaldehyde and citral in room temperature [47]. Despite significant selectivity obtained, the desired product was still produced in lower yield and in mixture, especially for crotonaldehyde and citral.

As new techniques were proven of concept in many research areas, more in-depth tuning of hydrogenation catalyst was enabled. In 2000, ultra-sonication of the catalyst prior to reaction was demonstrated to enhance the hydrogenation efficiency [48]. Good selectivity of C=O over C=C was obtained especially in lower H₂ pressure. However, as H₂ pressure decreasing, reaction efficiency as well as yield of product was also diminishing.

As the development of modern electronic microscopy, in 2008, Pt nanoparticle supported on carbon (PtNP@C) was synthesized and successfully introduced into hydrogenation of aldehyde [49]. It was demonstrated that the shape, size, and surface of the NP all contributed to the selectivity and efficiency of Pt-catalyzed hydrogenation of aldehyde. It was demonstrated that the hexagonal Pt nanocrystal shows better selectivity of C=O over C=C for crotonaldehyde and cinnamaldehyde. The corresponding unsaturated alcohol was obtained. It was also demonstrated that the catalyst activity was strongly dependent on the surface of exposed unsaturated Pt, which in this study was only observed in crystal corner and edges.

In 2011, it was demonstrated that the use of a second metal along with Pt can potentially enhance the catalytic hydrogenation selectivity and efficiency [50]. A series of M-Pt bi-metallic nanocrystals was generated and examined towards the hydrogenation of cinnamaldehyde. It was hypothesized that the second metal functions via 1) blocking unselective low coordination metal and 2) optimizing the surface electronics of Pt. The best result was obtained with Co-Pt bi-metallic nanocrystal and shown good selectivity over the desired cinnamyl alcohol.

As people realize that the blocking of low coordination metal site can be beneficial to the selective hydrogenation, another possible solution was to only enable the reaction to occur in microscopically confined space. The steric constraint in the reaction space could potentially inhibit undesired C=C coordination. In 2013, such confined reaction space was successfully generated using well-defined zeolite as template [51]. Within the nanochannels across zeolite, PtNP was deposited along with Lewis acid to further facilitate C=O activation. As designed, molecules with terminus C=O, represented by aldehydes, shows exceptional selectivity for the desired hydrogenation.

In 2014, the above-mentioned system was further enhanced with synthesis of PtNP dispersed in hyperbranched polystyrene [52]. In addition to the steric constraint enhancement, in this report, hydrophilic ammonium salt was decorated on the surface of hydrophobic polystyrene. The decoration was well-controlled so that the reaction environment within polystyrene nanochannel remained hydrophobic. The catalyst achieved great selectivity and efficiency, especially with water as solvent, for the hydrophobic substrates were 'forced' by repelling from hydrophilic solvent and polystyrene surface into the hydrophobic nanochannel. This mechanism was demonstrated to be very successful, as very bulky substrates, which are difficult to react in other systems, also gave excellent yield of the corresponding alcohol.

1.2.3.2 Heterogeneous Pd catalyst for aldehyde hydrogenation

One slot upper than Pt on the periodic table, Pd is extremely widely used for C=C hydrogenation. However, C=O hydrogenation of Pd was extremely limited. In 1994, Sautet concluded from experimental and computational studies that the reason behind such poor C=O affinity is due to weaker electronic repulsion between C=C and Pd, which presented in $5s^04d^{10}$ electron configuration. [53] Therefore, the C=C is greatly favored over C=O in Pd-catalyzed hydrogenation. However, certain examples of Pd-catalyzed hydrogenation of C=O also presents [54], as Lewis acid doping (FeCl_2 in this case) activated the C=O. Still, low selectivity and efficiency was obtained.

1.2.3.3 Heterogeneous Au catalyst for aldehyde hydrogenation

In addition to the example described in 1.2.2.4 where AuNP-phosphine oxide was used as a powerful catalyst for hydrogenation of aldehyde, in 2009, Volpe studied the hydrogenation of unsaturated aldehyde catalyzed by AuNP [55]. It was demonstrated that AuNP functioned more efficiently on iron oxide support. The catalytic efficiency does not relate to the redox property of the iron oxide. Interestingly, the size of AuNP does not play an important role in catalytic hydrogenation. However, the morphology affected the selectivity of C=O over C=C greatly, possibly due to the presence of Au ion that activates the carbonyl.

1.2.3.4 Heterogeneous Ru/Rh catalyst for aldehyde hydrogenation

The development of heterogeneous Ru/Rh catalyst focuses heavily on methods to efficiently recycle their homogeneous counterpart, as excellent efficiency and selectivity have already obtained with them.

The pioneering work for homogeneous Ru/Rh recycling was done by Grosselin in 1991 [56]. An aqueous/organic bi-phase reaction mixture was proposed. The Ru/Rh was immobilized in the aqueous phase with the help of water-soluble sulfonated phosphine ligand. This proof-of-concept study was generally successful, as the substrate/product can be easily extracted into the organic phase to recycle the aqueous catalyst. This approach was widely accepted especially for smaller-scale synthesis, for example pharmaceutical and cosmetic industry where reactions were mostly carried out in small-scale solution, and continue to be used even nowadays. Recently in 2011, this system was improved by Melean and co-workers to give better selectivity of C=O hydrogenation over C=C [57].

Despite being significant, the problem for the biphasic recycling system is obvious, as hydrophobic substrates are generally difficult to enter the aqueous catalyst phase. This issue become particularly problematic for aldehydes with larger molecular mass. In 1993, Fache compared the catalyst efficiency and recyclability between biphasic system and the stationary system using SiO₂ [58], in which homogeneous Ru or Ir catalyst was immobilized on solid phase, which poses a great advantage for this system due to its simple synthesizing step. It was demonstrated that in this case Ir functions more efficiently and easier to recover. However, two problems prevail, as 1) the reaction can only be conducted in non-polar solvent, as severe leaching was observed in polar solvent; 2) product and catalyst are difficult to isolate, even in non-polar media, as poisonous absorption of various organic compounds by SiO₂.

Realizing such problem, the development of alternative support was desirable for heterogeneous Ru/Rh catalysts. In 1993, Galvano and co-workers uses active carbon as heterogenization support for Ru catalyst and successfully conducted aldehyde hydrogenation [59]. A bi-metallic Ru-Sn catalyst was also examined on active carbon support. It was demonstrated that increasing Sn/Ru ratio leads to less exposure of Ru. At the same time, addition of Sn²⁺ facilitates the desired hydrogenation, as Lewis acidic Sn²⁺ activates carbonyl into cationic form.

In 1997, Kaneda described the use of polystyrene as support to immobilize Rh catalyst for hydrogenation [60]. Rh₆(CO)₁₆ cluster was used as active catalyst and afforded [Rh₆(CO)₁₅H]⁻ as

intermediate. It was advantageous for the use of metal carbonyl clusters as catalyst as they are very easy to prepare, even possible to do direct carbonylation inside mines [61]. It was also suggested that the basicity and hydrophilicity of support all contributed to the efficiency of catalyst.

Based on the previous result, in 2008, CO₂ saturated poly(ethylene glycol) (PEG/CO₂) was developed as a new generation catalyst support [62]. Due to the easy synthesizing steps for catalyst, eco-friendly nature and great mechanical feature of the support, it was widely accepted into various industry. Compared to polystyrene, PEG is much more hydrophilic, therefore good efficiency and functional tolerance was observed for the hydrogenation. Great selectivity of C=O over C=C was also observed for unsaturated substrates.

1.2.3.5 Abundant metal as heterogeneous aldehyde hydrogenation catalyst

1.2.3.5.1 Cu catalyst

Cu are among the earliest developed heterogeneous hydrogenation catalyst for aldehyde. In 1980, the pioneer work by Jenck and Germain using copper chromite as catalyst achieved hydrogenation of aldehyde, ketone and olefin in various conditions [63]. In contrast with noble metal catalyst system, the olefin was the least reactive compared to aldehyde or ketone in this report. Despite the decarbonylation and other potential side-reactions, this system was widely adapted especially in polymer, fine chemical, and farm industries for decades.

However, the use of chromite poses significant environmental hazard. In 1988, an alternative Cu catalyst with SiO₂ support was developed [64]. The hydrogenation was able to proceed in less than 2 atm of hydrogen pressure. The deuterium isotope experiment confirmed that the 2 added hydrogen in alcohol are both from the hydrogen gas. Though the condition was very promising, the reaction happens in gaseous phase, thus very limited product was reported to be successfully reduced. The catalyst was also able to catalyze reduction of ester in the same condition, therefore limits its functional tolerance.

1.2.3.5.2 Ni catalyst

In late 20th century, started by the development of previous-mentioned copper chromite system for aldehyde hydrogenation, the aldehyde industry received a blooming period. With copper chromite hydrogenation, especially when coupled with hydroformylation process, various industry products

were readily manufactured in facile steps. However, as chromium leaching and pollution become a more and more serious issue, alternative transfer hydrogenation catalysts need to be immediately developed. Ni, as one of the earliest developed and very important hydrogenation catalyst [65], has attracted considerable attention from the chemistry society. Fe-doped Ni-B alloy was developed as hydrogenation catalyst in 2003 for furfural industry [66]. It was suggested that the aldehyde C=O was coordinated at electron deficient Fe or Fe³⁺, the Ni, however, receives considerable electron enrichment and weakens the C=O bond by donating electron to the C=O antibonding orbital. However, this catalyst system requires careful control over Fe-dopant during the catalyst synthesis. A higher Fe-dopant resulted in inactivation of the Ni, as many active sites will be covered; a lower Fe-dopant resulted in undesirable side-reaction, as remaining Fe become too active.

Another developed system for aldehyde hydrogenation is the Ni-Mo/Al₂O₃ catalyst. This catalyst was extensively applied previously for hydrodesulfurization and hydrogenitrogenation of fossil fuel [67]. Many reports were dedicated to enable better understanding of catalyst character [68-72]. Generally, reduced Ni-Mo catalyst performs better than NiMoS sulfurized catalyst. S or CO represent major poisoning reagent for the catalyst. Despite the draw-backs, efficient hydrogenation and good functional tolerance was achieved.

Despite the significance of Ni-Mo catalyst, the hydrogenation catalyzed by such catalyst generally requires high hydrogen pressure (around 70 bar). Furthermore, long-chain aldehyde reduction is generally inactive. In 2016, a Cu/Ni/Cr system was developed [73]. The catalyst possesses a high surface area from its porous structure. Long-chain nonyl aldehyde was used as model compound and achieved efficient hydrogenation at 180°C and 25 bar of hydrogen. Despite deactivation of catalyst after many catalytic cycles, majorly by the formation of carbonaceous fouling film inside the porous catalyst, the regeneration of catalyst can be done by aerobic oxidation by low-concentration oxygen within nitrogen flow.

1.2.3.5.3 Co catalyst

As early as 1969, selective hydrogenation of unsaturated aldehyde into the corresponding unsaturated alcohol was reported by Co [74]. Later kinetic investigation shown that Co possess better selectivity for aldehyde hydrogenation compared to Ni [75]. With Raney-Co catalyst, 2-

methyl-2-pentenal was first successfully reduced to the corresponding unsaturated alcohol. Promising selectivity over unsaturated alcohol was observed, however, demands enhancement.

As chemist realized the function of proper support over heterogeneous catalyst, various support, including silica [76] and alumina [77] were developed for Co-catalyzed aldehyde hydrogenation. It was determined that the size and shape of Co particle dispensed on the support play critical role on the application of the reported catalyst to various substrates. As a result, over 70 % selectivity of C=O over C=C was observed for supported Co-catalyzed hydrogenation of unsaturated aldehyde.

The bi-metallic hydrogenation catalyst was also developed, in 2015, as a supported Co-Cu catalyst [78]. This catalyst shows important reactivity over furfural, which is an important bio-renewable material and can be easily obtained in farm crops. Over 80 % selectivity was obtained in generating the corresponding furfuryl alcohol, which is a crucial substrate in polymer industry. Milder reaction condition (170°C, 20 bar H₂) was enough to achieve such selectivity. Indicating very promising potential for Co as aldehyde hydrogenation catalyst.

1.3 Oxidation of aldehyde

1.3.1 Historic methods and challenges for aldehyde oxidation

As established in 1.1, oxidation of aldehyde composes the other important counterpart to the interest of the organic chemistry community. [79] Although it seems autoxidation of aldehyde in air can be significant, however, high yields of the corresponding carboxylic acids are very hard to achieve, as mixtures of products were often obtained with autoxidation and other common oxidants. In fact, oxidation of aldehyde poses a highly challenging task for chemists. Kinetically, the interaction between electrophilic aldehyde and also-electrophilic oxidant is difficult. (Figure 1.20, left) Furthermore, the well-established single electron transfer (SET) mechanism for alcohol oxidations [80] is impractical for aldehydes, as the sp²-hybridized radical-cation intermediate generated from aldehyde is much more unstable than the sp³-intermediate from alcohol. (Figure 1.20, right)

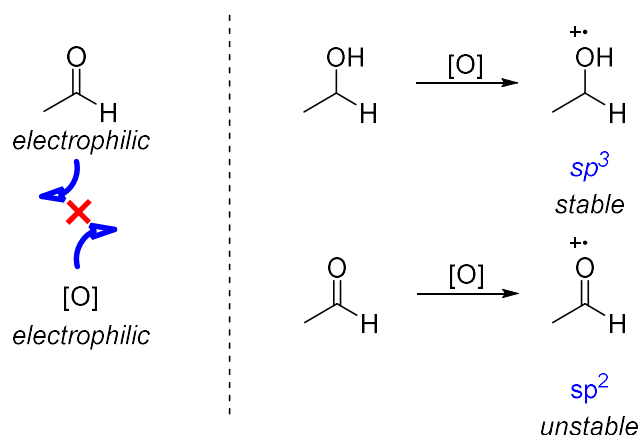


Figure 1.20. Challenges for aldehyde oxidation

Historically, the most important aldehyde oxidation methods are the Fehling oxidation [81] and the Tollens oxidation [82]. Using metallic oxidants such as Cu(II) or Ag(I), remarkably efficient aldehyde oxidation was readily achieved in very short reaction time. Both the reactions use water as the sole solvent and mild reaction temperature (warm water bath). After reaction, it was demonstrated that almost every type of aldehyde, aromatic, aliphatic, unsaturated, and even aldose such as glucose and fructose, are efficiently oxidized into the corresponding carboxylic acid (aldonic acid). This versatility made the Fehling and the Tollen oxidation among the most important aldehyde oxidation method in the history, especially for titration analysis and the production of aldonic acid, which is extremely difficult to achieve using other methods (Figure 1.21). The mechanism for those reactions are still controversial nowadays [83]. One hypothesis suggests the aldehyde was first hydrated in to the corresponding gem-diol and deprotonated in basic aqueous, then the Ag(I)/Cu(II) coordinated to the deprotonated gem-diol and extract one electron in SET, generating the gem-diol radical, which was further extracted of one electron and give the carboxylic acid. Another hypothesis involves the formation of Ag(I)/Cu(II)-OH intermediate. The aldehyde was activated by the metal and the anionic -OH give nucleophilic attack into the activated carbonyl. The generation of the tetrahedral intermediate was followed by β -H elimination. Since the Ag(I)/Cu(II)-H was not stable without additional ligand, the metal hydride collapse into lower valency metal and proton.

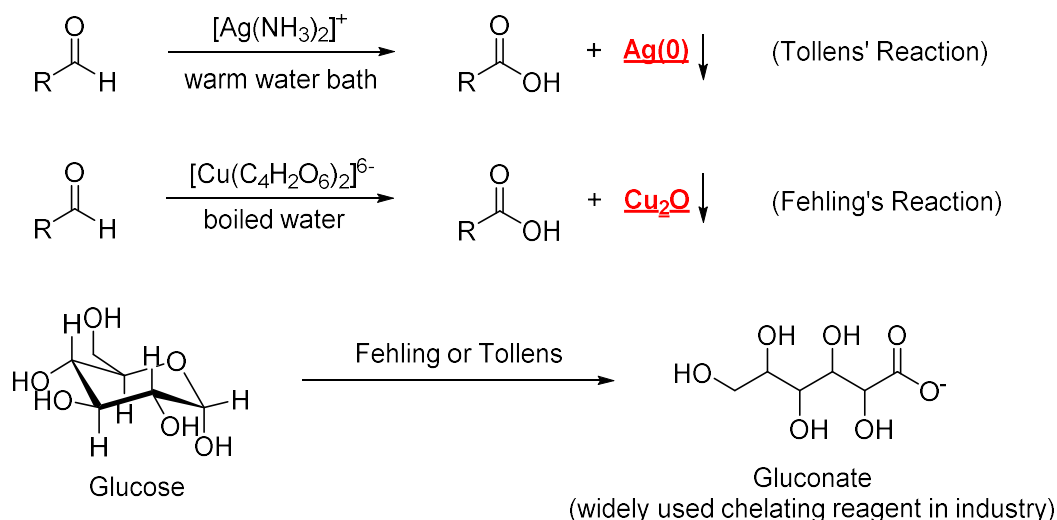


Figure 1.21. The Fehling and the Tollens reagent in aldehyde oxidation

Another notable example of important historic aldehyde oxidation is the Jones oxidation [84]. Although mainly used for alcohol oxidation, the Jones reagent has made significant contribution in the oxidation of aldehyde due to good functional tolerance and selectivity. The mechanism of the Jones oxidation involves the initial formation of alcohol perchromate ester (general formula $\text{CrO}_3(\text{OCH}_2\text{R})^-$). The ester then collapses with Cr(VI) obtained 2 electrons and become Cr(IV) , releasing the carboxylic acid. Even nowadays, the Jones' oxidation of aldehyde is still of great application. Very recently, in Hao's total synthesis of Perforanoid A [85], Jones' reagent played a key role for selectively oxidizing specific acetal into the corresponding ester (Figure 1.22).

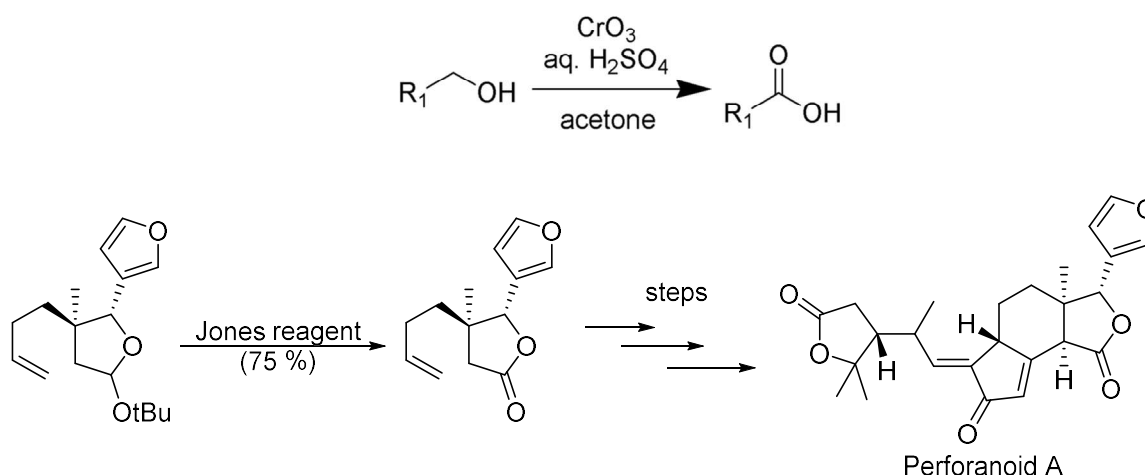


Figure 1.22. The Jones reagent and its application in aldehyde oxidation

Although achieving great utility and efficiency, the stoichiometric metallic wastes generated in those above-mentioned methods are particularly hazardous and difficult to process. As more and more restrictions were added regarding metal waste generation, the development of new aldehyde oxidation method without generation of metallic waste is eagerly demanded by academia and industry. In 1973, Lindgren first demonstrated the use of chlorite (ClO_2^-) as oxidant towards oxidation of aldehyde [86]. Though very limited substrate scope was obtained, the scope includes both aliphatic and aromatic aldehyde. Later in 1981, Pinnick demonstrated the oxidation of unsaturated aldehyde in same system [87]. The above-mentioned system was later recognized as the Pinnick oxidation. As one of the most widely applied aldehyde oxidation method even nowadays, many products in chemical industry, especially pharmaceuticals, was synthesized via this method (Figure 1.23) [88]. Despite the great utility achieved by the Pinnick oxidation, certain problems still remain. Since the oxidation generates stoichiometric amount of sodium hypochlorite (HOCl), which consumes the ClO_2^- oxidant and inhibits the desired transformation, scavenger was generally required to eliminate HOCl . The most commonly used scavenger was 2-methyl-2-butene, which was added stoichiometrically in almost every practice. Furthermore, some aldehydes show unsatisfying reactivity. For example, aliphatic conjugated $\text{C}=\text{C}$, unprotected amine/pyrrole and thioether containing aldehyde are easily oxidized in Pinnick oxidation condition.

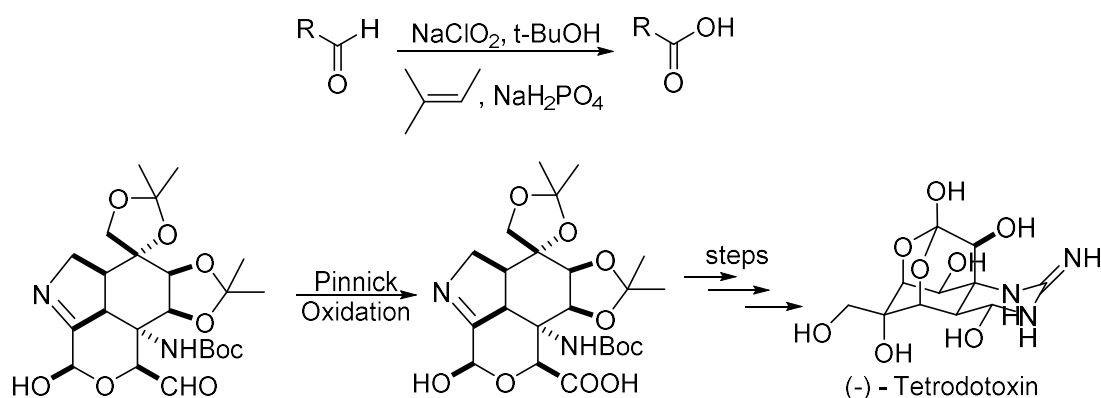


Figure 1.23. The Pinnick oxidation and its application in pharmaceutical synthesis

As early as 1979, Evans and co-workers have studied the effect of anion towards aldehyde oxidation using electrochemistry with different electrodes. [89] The result showed that the addition of OH^- to the aldehyde can dramatically boost its tendency towards oxidation. The generated gem-diol have a great oxidation potential shift. (which can be as great as 3.6 V) Indicating the potential

to conduct aldehyde oxidation using this alternative approach. The persistent radical (TEMPO, bicyclic-nitroxyl, etc.) /NO_x-catalyzed method, which was often used for alcohol oxidation [90], has been directly applied to the oxidation of gem-diol of the corresponding aldehyde (Figure 1.24) [91]. However, with those persistent radicals, which are generally volatile and reactive, poor functional-tolerance was also obtained.

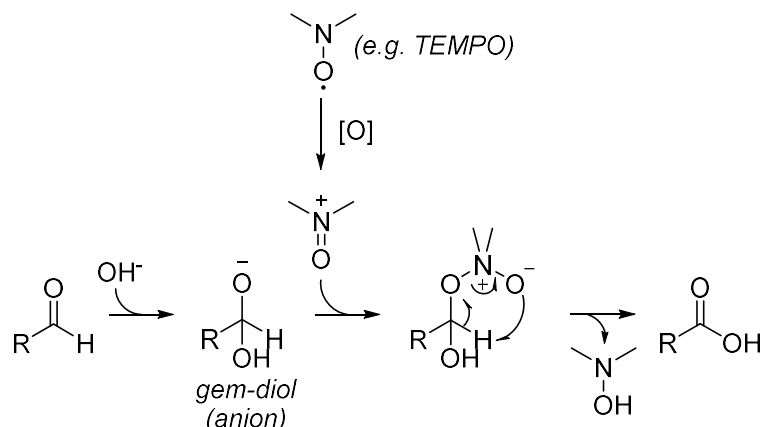


Figure 1.24. A typical mechanism for aldehyde oxidation using persistent radical system

1.3.2 Enzymatic oxidation of aldehyde

Despite the challenges and difficulties in developing aldehyde oxidation method, such process also widely exists in nature and even human body [92]. Those biochemical oxidations of aldehyde *in vivo* are generally catalyzed by fine-engineered enzyme from nature, using water as the sole solvent in mild temperature (in most cases 37 °C). Dissolved oxygen is either directly used from water, or consumed through biochemical oxidative cascade. Although most natural enzymes exhibit specificity towards substrate, many functionalized enzymes were isolated and investigated to catalyst different aldehydes oxidation. Only with human dehydrogenase family in our liver cell, the combined substrate scope has already covered almost all common aldehydes, including aliphatic, aromatic and unsaturated aldehydes [93]. Those processes are well adapted in some of the specific synthesizing processes. However, it is usually difficult for many industries to carry on *in vivo* or bio-mimic reactions due to the lack of equipment, etc. Furthermore, the enzyme specificity usually demands the industry to obtain many of those specific enzymes, and many of them require different storage and reaction conditions.

1.3.3 New oxidants for catalyzed aldehyde oxidation

Generally, due to the difficulty described in 1.3.1, up till now, methods which can carry out efficient and widely applicable oxidation of aldehyde is very limited. In attempts to solve these problems, at first, chemists are looking forward to alternative oxidants that does not require or generate undesirable materials. Those oxidants generally consist of high-valency or electron-deficient center, and anionic oxygen to increase the affinity towards the already-electrophilic carbonyl (Figure 1.25). The mechanism of those aldehyde oxidation is generally initiated by anionic oxygen attack of the carbonyl to generate the tetrahedral intermediate, then the tetrahedron collapses and electron was extracted by the electron deficient oxidant to generate the desired product.

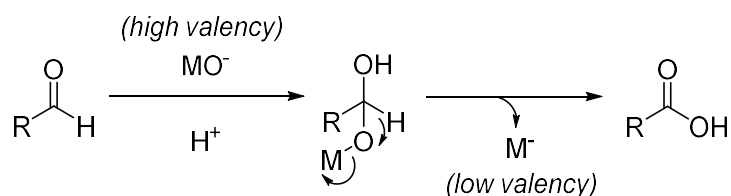
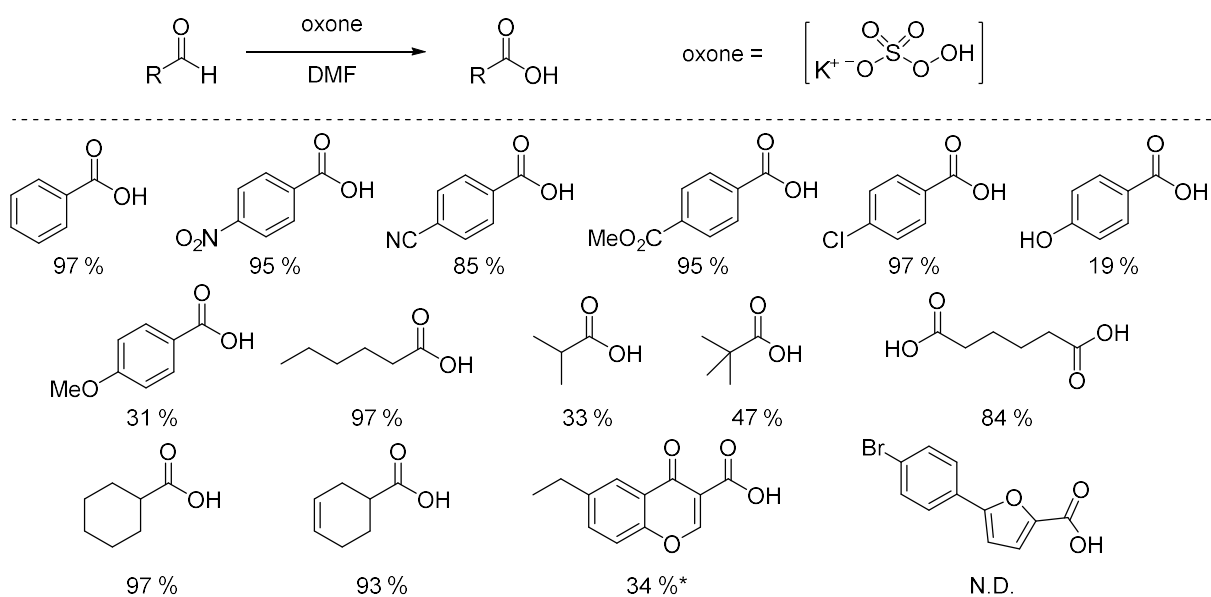


Figure 1.25. Typical mechanism for previous aldehyde oxidation

Among those catalysts, potassium hydropersulfate (oxone) shown great potential for its structural stability and cost-effectiveness. In 2003, Borhan systematically studied the use of oxone towards

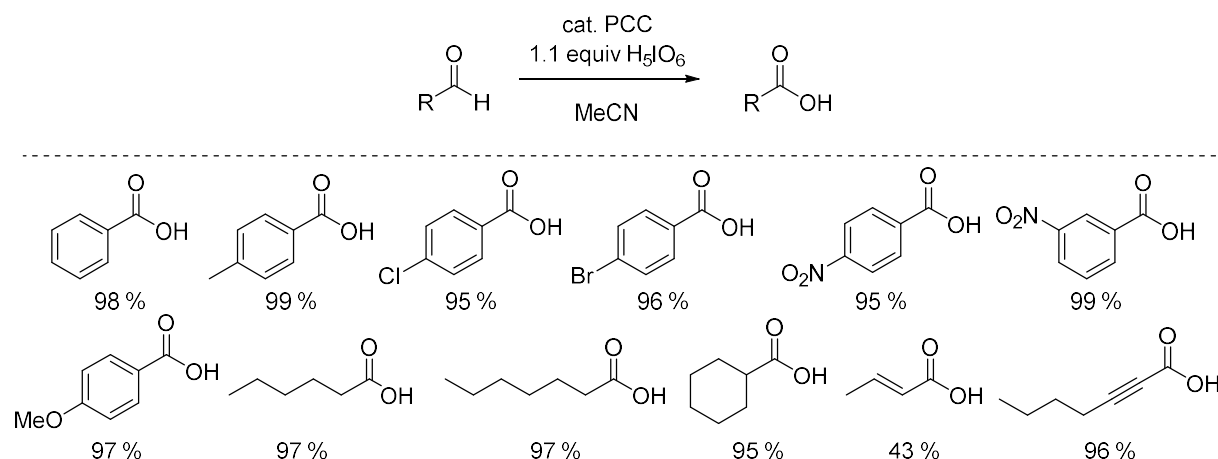
Table 1.13. Oxidation of aldehyde using oxone



oxidation of aldehyde (Table 1.13) [94]. The oxidation shown good efficiency and functional tolerance in mild reaction condition (50°C, DMF, 3h). Furthermore, the oxidation can also afford the desired ester by switching solvent to the corresponding alcohol. However, the oxone oxidation is not effective for unsaturated aldehyde and hydroxyl/alkoxyl containing substrates. Bulky tert-pentanal and even less bulky *iso*-butanal was not reactive either.

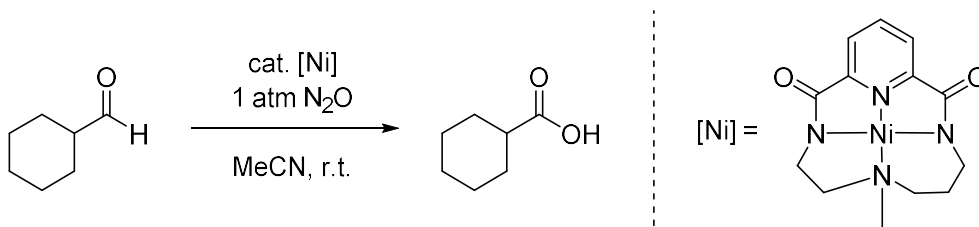
Another effort towards the development of alternative oxidant was introduced in 2005. While pyridinium chloroperchromate (PCC) was developed as a highly efficient alcohol oxidation reagent, Hunsen developed the combined use of catalytic PCC and stoichiometric periodate as efficient oxidation of aldehyde [95], which generates the active oxidant chlorochromatoperiodate *in situ* (Table 1.14). A satisfying substrate scope was achieved. However, excessive amount of periodate oxidant was required, which potentially result in side reactions such as C-C cleavage [96].

Table 1.14. PCC catalyzed aldehyde oxidation using periodic acid



To circumvent the undesired side-reaction caused by excessive oxidant, one solution is to use gaseous oxidant that can be introduced slowly in a controlled manner. As ozonolysis with alkene into the corresponding aldehyde/ketone is well established [97], it is natural to assume that ozone can also oxidize aldehyde into the corresponding carboxylic acid. In 2008, Johnson summarized the ozone oxidation of aldehyde attempts [98]. While achieving significant result, however, poor functional tolerance was obtained due to the harsh oxidation by ozone. In 2016, nitrous oxide was examined as a milder alternative for ozone to oxidize aldehyde [99]. It was demonstrated that nitrous oxide oxidation of cyclohexanecarboxyaldehyde was very efficient under atmospheric

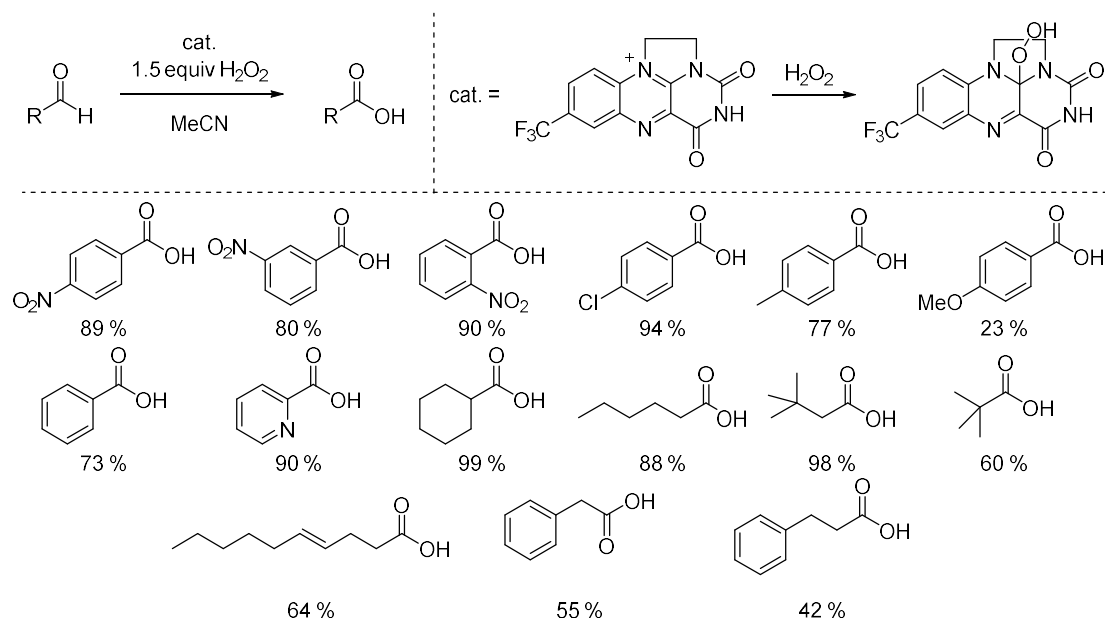
pressure and room temperature (Scheme 1.3). Although decarbonylation side-reaction was also observed, the use of nitrous oxide still poses an interesting potential.



Scheme 1.3. Nitrous oxide oxidation of aldehyde

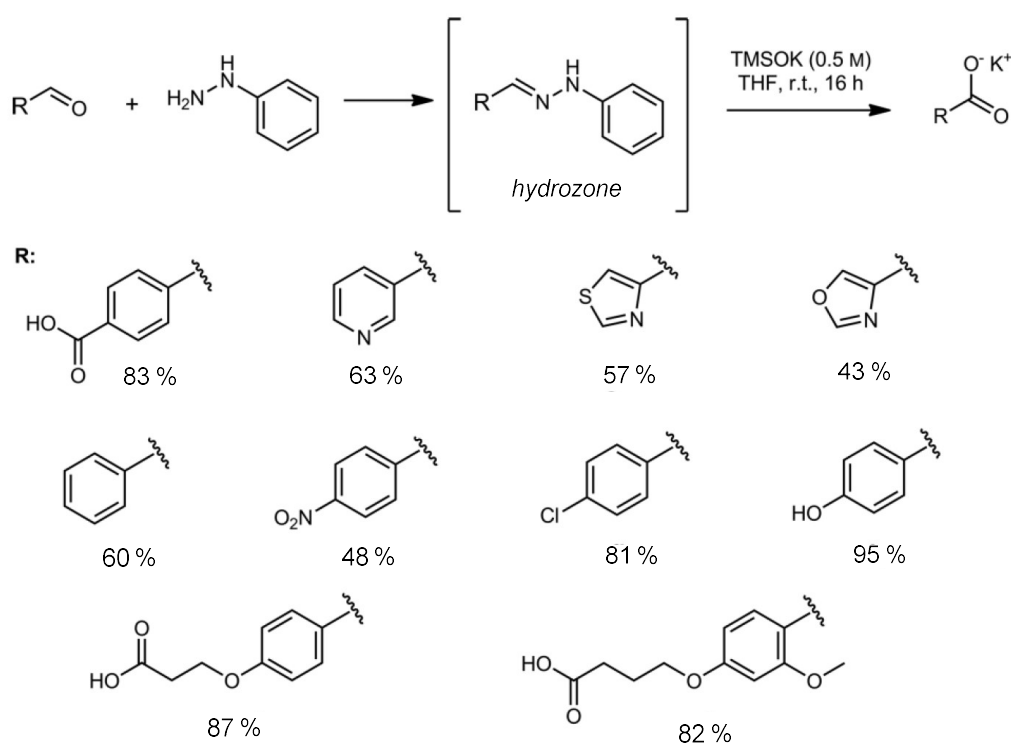
Another possible solution is the use of milder oxidant in aldehyde oxidation. Peroxide ($\text{OOH}^-/\text{O}_2^{2-}$) is more desirable for its cost-effectiveness and high atom economy. Inspired by the mechanism of a common bioluminescence, flavin, which undergoes catalytic nucleophilic addition of peroxide to the fatty aldehyde followed by the collapse of tetrahedral intermediate to eject fatty acid and a photon, a flavin-catalyzed bio-mimic oxidation of aldehyde was reported by Carbery using hydrogen peroxide in 2012 [100]. Impressive substrate scope was obtained, even bulky tart-pentalanal gave a satisfying yield (60 %). However, unsaturated aldehydes were not reactive (Table 1.15).

Table 1.15. Flavin-catalyzed bio-mimic oxidation of aldehyde



In 2017, Hlavac noticed that hydrazine, under certain circumstances, can oxidize aldehyde into the corresponding carboxylic acid by cleavage of C-N bond and the ejection of nitrogen gas [101]. He later further developed the system using resin linker and presynthesized hydrazone [102]. A series of aromatic aldehydes successfully underwent the desired transformation (Table 1.16). Despite the scope of substrate was limited to aromatic aldehyde, this approach still shows interesting potential by 1) avoiding the use of transition metal catalyst; 2) using resin support that can be easily cleaved, facilitating the purification of product.

Table 1.16. Catalytic oxidation of hydrazone



1.3.4 Catalyzed aerobic oxidation of aldehyde

Aerobic oxidation of aldehyde is probably one of the most exciting approach towards carboxylic acid, as no hazardous oxidant was used and the highest atom economy was achieved. Despite the promising outcome, this area of research has received very limited attention. The autoxidation of aldehyde by aerobic oxygen is generally significant, however, giving incomplete conversion and mixture of products. The mechanism for the autoxidation has been thoroughly studied (Figure 1.26) [103]. The process involves hydrogen extraction by oxygen radical, generating a peracid, which

oxidizes another aldehyde similarly to Baeyer-Villiger mechanism to generate 2 carboxylic acids. The process involves the generation of 1) a carbonyl radical and 2) a peracid. Both species are very reactive and causes many side reactions, which potentially contributed to the low efficiency of autoxidation and many attempts of catalytic aerobic oxidation of aldehyde.

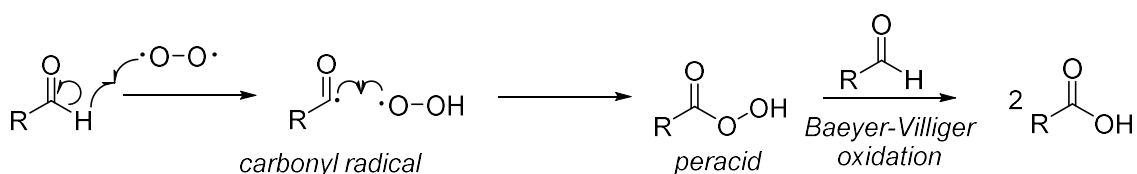


Figure 1.26. Mechanism of autoxidation of aldehyde

In 2009, Tada reported the synthesis of a SiO₂ supported Ru-*p*-cymene catalyst for aerobic oxidation of aldehyde [104]. A labile *p*-cymene ligand was designed to generate empty coordination site for oxygen (Figure 1.27). The catalyst shows good recyclability, and ability to catalyze the aerobic oxidation of a variety of substrates. However, the catalyst is also shown to catalyze epoxidation of alkene, thus greatly limits the substrate scope of this method.

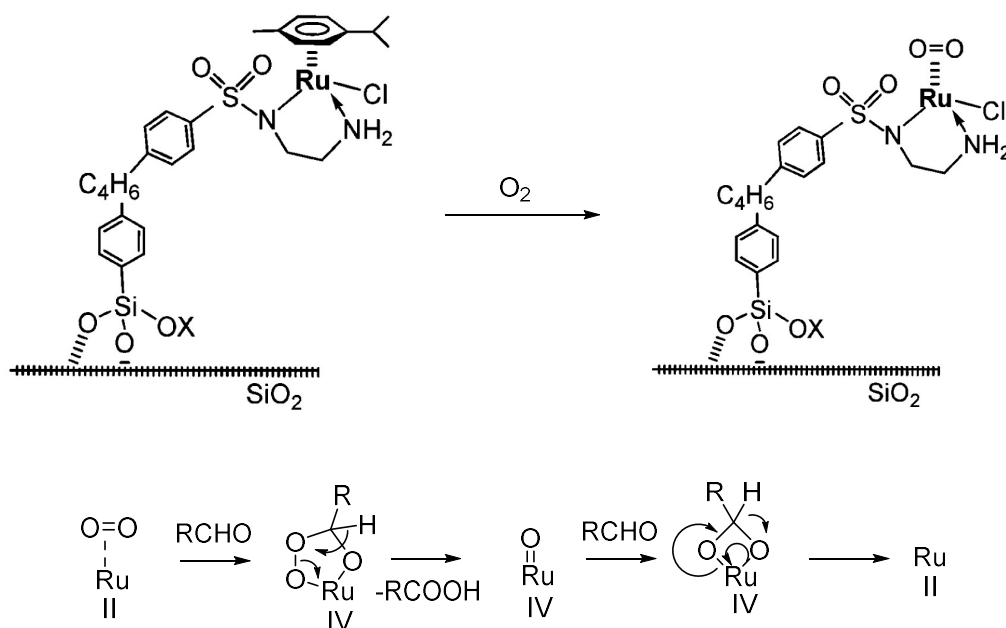


Figure 1.27. Ru-catalyzed aerobic oxidation of aldehyde

In 2009, Chechik and co-workers reported the aerobic oxidation of aldehyde using simple oxygen and gold-nanoparticles as catalyst. [105] Although significant, those oxidations did not avoid the

generation of the above-mentioned unstable sp^2 -hybridized carbonyl radical and the peracid (Figure 1.28), which resulted in low reaction efficiency and limited scope of substrates.

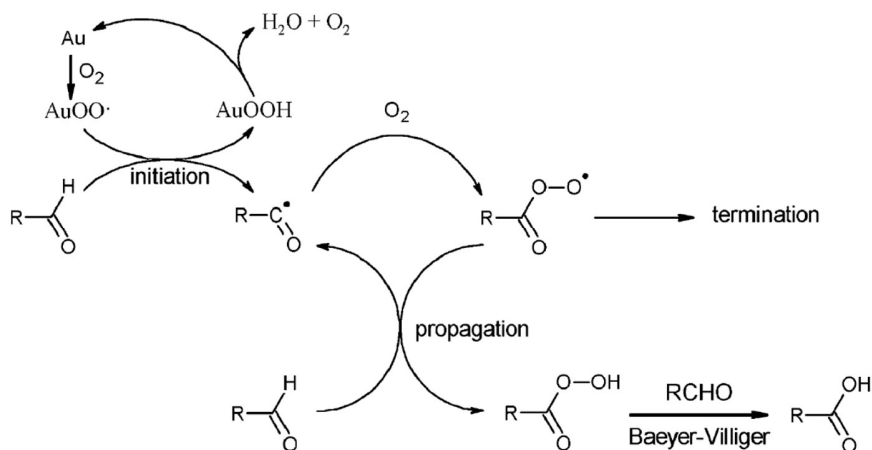
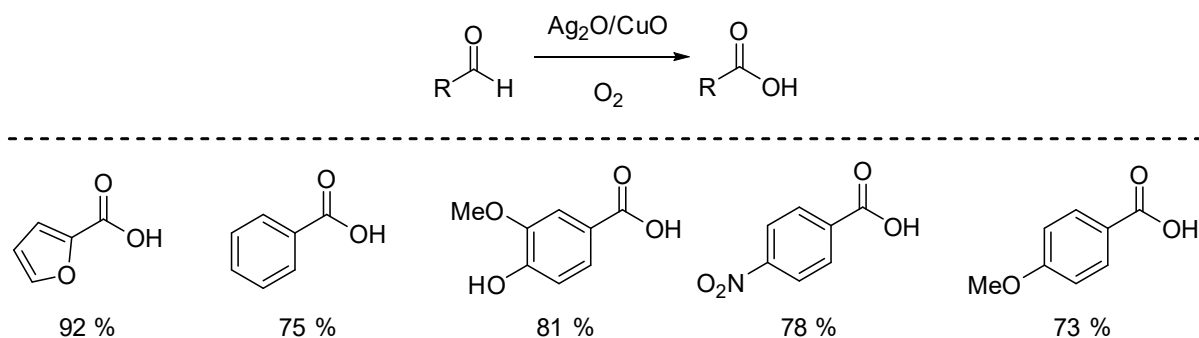


Figure 1.28. Mechanism of AuNP-catalyzed aerobic oxidation of aldehyde

In 2008, aerobic oxidation of aldehyde using heterogeneous Ag_2O/CuO catalyst in water was reported [106]. A few examples of substrate were reported to be efficiently oxidized (Table 1.17). However, in addition to the requirement of high catalyst load, limited substrate scope and side reactions were also obtained.

Table 1.17. Ag_2O/CuO -catalyzed aldehyde aerobic oxidation



In 2009, N-Heterocyclic Carbene was developed as aerobic oxidation organocatalyst. [107] Significantly different from the previous aerobic oxidation mechanism, the oxidation proceeds via the nucleophilic attack of the carbene to generate the Breslow intermediate, which was further hydrolyzed to build the carboxylic group (Figure 1.29). Oxygen was then involved to restore aromaticity of the system. However, the activation of oxygen was driven by the restoring of

aromaticity, therefore substrate was limited to aromatic aldehyde. Furthermore, this method cannot evade the requirement of organic solvents, which are necessary to be kept in air-free and dry environment.

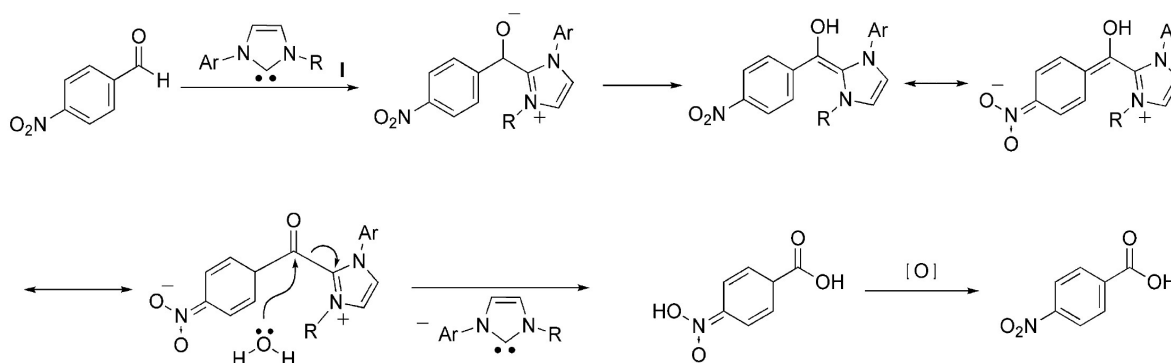


Figure 1.29. NHC-catalyzed aerobic oxidation of aromatic aldehyde

1.4 Conclusion

In this chapter, a brief survey over historic development of aldehyde reduction/oxidation was given. With precise designing over the catalyst, especially over various functionalized ligand for homogeneous catalysis or specific doping/geometry/support for heterogeneous catalysis, the desired selectivity and efficiency of the aldehyde reduction can be achieved via multiple methods. However, improvements are also desirable, as either organic solvent or scarce noble metal is still necessary. Furthermore, the development of innovative aldehyde oxidation with improved selectivity and adaptability, remains highly challenging. The development of those reactions will not only facilitate the transformation process of aldehyde into various everyday products, but will also likely to initiate the discovery of unprecedented aldehyde reduction/oxidation mechanisms, which can enable further innovative transformations and contribute to fundamental chemistry knowledge.

1.5 References

- [1] Moody, T. S.; Mix, S.; Brown, G.; Beecher, D. Ketone and aldehyde reduction. In *Science of Synthesis, Biocatalysis in Organic Synthesis*; Faber, K.; Fessner, W.-D.; Turner, N. J., Ed.; Georg Thieme Verlag: Stuttgart, Vol. 2; p 421-458.

- [2] a) Pino, P.; Botteghi, C. *Org. Synth.* 1977, **57**, 11; b) Ojima, I.; Tsai, C.-Y.; Tzamarioudaki, M.; Bonafoux, D. *Org. React.* 2000, **56**, 1.
- [3] a) Zanka, A. *Chem. Pharm. Bull.* 2003, **51**, 888–889; b) Babu, B. R.; Balasubramaniam, K. K. *Org. Prep. Proc. Int.* 1994, **26**, 123–125; c) Dalcanele, E.; Montanari, F. *J. Org. Chem.* 1986, **51**, 567–569; d) Bal, B. S.; Childers Jr., W. E.; Pinnick, H. W. *Tetrahedron* 1981, **37**, 2091–2096; e) Bayle, J. P.; Perez, F.; Courtieu, J. *Bull. Soc. Chim. Fr.* 1990, **4**, 565–567; f) Kumaraswamy, G.; Jena, N.; Sastry, M. N. V.; Kumar, B. A. *Org. Prep. Proc. Int.* 2004, **36**, 341–345; g) Kamal, A.; Reddy, B. S. N.; Reddy, G. S. K.; Ramesh, G. *Bioorg. Med. Chem. Lett.* 2002, **12**, 1933–1935; h) Gupta, K. K. S.; Dey, S.; Gupta, S. S.; Adhikari, M.; Banerjee, A. *Tetrahedron* 1990, **46**, 2431–2444; i) Hurd, C. D.; Garrett, J. W.; Osborne, E. N. *J. Am. Chem. Soc.* 1933, **55**, 1082–1084; j) Salehi, P.; Firouzabadi, H.; Farrokhi, A.; Gholizadeh, M. *Synthesis* 2001, **15**, 2273–2276; k) Chaubey, G. S.; Das, S.; Mahanti, M. K. *Bull. Chem. Soc. Jpn.* 2002, **75**, 2215–2220; l) Balasubramanian, K.; Prathiba, V. *Indian J. Chem. Sect. B* 1986, **25**, 326–327; m) Chaubey, G. S.; Kharsyntiew, B.; Mahanti, M. K. *J. Phys. Org. Chem.* 2004, **17**, 83–87; n) Takemoto, T.; Yasuda, K.; Ley, S. V. *Synlett.* 2001, 1555–1556 o) Zhivich, A. B.; Myznikov, Y. E.; Koldobskii, G. V.; Ostrovskii, V. A. *Russ. J. Gen. Chem.* 1988, **58**, 1701–1708; p) Juršić, B. *Can. J. Chem.* 1989, **67**, 1381–1383; q) Heaney, H.; Newbold, A. J. *Tetrahedron Lett.* 2001, **42**, 6607–6609; r) Sato, K.; Hyodo, M.; Takagi, J.; Aoki, M.; Noyori, R. *Tetrahedron Lett.* 2000, **41**, 1439–1442.
- [4] Mason, N.; Hughes, P.; MacMllan, R. *Introduction to environmental physics* (CRC, 2001), pp. 112–13.
- [5] a) Meerwein, H.; Schmidt, R. *Liebigs. Ann.* 1925, **444**, 221–238; b) Pondorf, W. *Angew. Chem.* 1926, **39**, 138–143; c) Verley, A. *Bull. Soc. Chim. Fr.* 1925, **37**, 537.
- [6] Benyei, A.; Joo, F.; *J. Mol. Catal.* 1990, **58**, 151–163.
- [7] Halpern, J. *Advan. Catalysis* 1959, **11**, 301.
- [8] Meguro, S.-I.; Mizoroki, T.; Ozaki, A. *Chem. Lett.* 1975, 943–946.
- [9] Sanchez-Delgado, R. A.; de Ochoa, O. L. *J. Mol. Catal.* 1979, **6**, 303–305.
- [10] Grey, R. A.; Pez, G. P.; Wallo, A. *J. Am. Chem. Soc.* 1981, **103**, 7536–7542.
- [11] Tani, K.; Suwa, K.; Tanigawa, E.; Yoshida, T.; Okano, T.; Otsuka, S. *Chem. Lett.* 1982, 261–264.
- [12] Burk, M. J.; Harper, T. G. P.; Lee, J. R.; Kalberg, C. *Tetrahedron Lett.* 1994, **35**, 4963–4966.
- [13] Sanchez-Delgado, R. A.; Valencia, N.; Marquez-Silva, R.-L.; Andriollo, A.; Medina, M. *Inorg. Chem.* 1986, **25**, 1106–1111.
- [14] Chin, C. S.; Park, S. C.; Shin, J. H. *Polyhedron* 1989, **8**, 121–122.

- [15] Li, R.-X.; Li, X.-J.; Wong, N.-B.; Tin, K. C.; Zhou, Z.-Y.; Mak, T. C. W. *J. Mol. Catal. A: Chem.* 2002, **178**, 181-190.
- [16] Tilloy, S.; Bricout, H.; Monflier, E. *Green Chem.* 2002, **4**, 188-193
- [17] Noyori, R.; Ohkuma, T.; Kitamura, M. *J. Am. Chem. Soc.* 1987, **109**, 5856-5858.
- [18] Haack, K.-J.; Hashiguchi, S.; Fujii, A.; Ikariya, T.; Noyori, R. *Angew. Chem. Int. Ed. Engl.* 1997, **36**, 285-288.
- [19] Noyori, R.; Ohkuma, T. *Angew. Chem. Int. Ed.* 2001, **40**, 40-73.
- [20] Kitamura, M.; Nakatsuka, H. *Chem. Commun.* 2011, **47**, 842-846
- [21] Noyori, R.; Kitamura, M. *Angew. Chem. Int. Ed. Engl.* 1991, **30**, 49-69
- [22] Ohkuma, T.; Sandoval, C. A.; Srinivasan, R.; Lin, Q.; Wei, Y.; Muniz, K.; Noyori, R. *J. Am. Chem. Soc.* 2005, **127**, 8288-8289.
- [23] Baratta, W.; Chelucci, G.; Gladiali, S.; Siega, K.; Toniutti, M.; Zanette, M.; Zangrando, E.; Rigo, P. *Angew. Chem. Int. Ed.* 2005, **44**, 6214-6219.
- [24] Clarke, M. L.; Diaz-Valenzuela, M. B.; Slawin, A. M. Z. *Organometallics* 2007, **26**, 16-19.
- [25] Baratta, W.; Ballico, M.; Chelucci, G.; Siega, K.; Rigo, P. *Angew. Chem. Int. Ed.* 2008, **47**, 4362-4365.
- [26] Baratta, W.; Ballico, M.; Del Zotto, A.; Siega, K.; Magnolia, S.; Rigo, P. *Chem. Eur. J.* 2008, **14**, 2557-2563.
- [27] Baratta, W.; Barbato, C.; Magnolia, S.; Siega, K.; Rigo, P. *Chem. Eur. J.* 2010, **16**, 3201-3206.
- [28] Gao, F.; Chen, Q.-H.; Wang, F.-P. *Tetrahedron Lett.* 2009, **50**, 5270-5273.
- [29] Shvo, Y.; Czarkie, D.; Rahamim, Y. *J. Am. Chem. Soc.* 1986, **108**, 7400-7402.
- [30] a) Samec, L. S. M.; Backvall, J.-E.; Andersson, P. G.; Brant, P. *Chem. Soc. Rev.* 2006, **35**, 237-248; b) Clapham, S. E.; Hadzovic, A.; Morris, R. H. *Coord. Chem. Rev.* 2004, **248**, 2201-2237; c) Csjernyk, G.; Ell, A.-H.; Fadini, L.; Pugin, B.; Backvall, J.-E. *J. Org. Chem.* 2002, **67**, 1657-1662; d) Casey, C. P.; Bikzhanova, G. A.; Cui, Q.; Guzei, I. A. *J. Am. Chem. Soc.* 2005, **127**, 14062-14071; e) Johnson, J. B.; Backvall, J.-E. *J. Org. Chem.* 2003, **68**, 7681-7684; f) Casey, C. P.; Guan, H. *J. Am. Chem. Soc.* 2007, **129**, 5816-5817.
- [31] Casey, C. P.; Vos, T. E.; Singer, S. W.; Guzei, I. A. *Organometallics* 2002, **21**, 5038-5046.
- [32] Casey, C. P.; Strotman, N. A.; Beetner, S. E.; Johnson, J. B.; Priebe, D. C.; Vos, T. E.; Khodavandi, B.; Guzei, I. A. *Organometallics* 2006, **25**, 1230-1235.
- [33] Lu, X.; Liu, Q.; Wang, X.; Cheng, R.; Zhang, M.; Sun, X. *RSC Adv.* 2015, **5**, 2827-2836.

- [34] a) Cano, I.; Chapman, A. M.; Urakawa, A.; van Leeuwen, P. W. N. M. *J. Am. Chem. Soc.* 2014, **136**, 2520-2528; b) Li, G.; Abroshan, H.; Chen, Y.; Jin, R.; Kim, H. J. *J. Am. Chem. Soc.* 2015, **137**, 14295-14304.
- [35] Marko, L.; Palagyi, J. *Transition Met. Chem.* 1983, **8**, 207-209.
- [36] Shimizu, H.; Sayo, N.; Saito, T. *Synlett* 2009, 1295-1298.
- [37] Knolker, H.-J.; Baum, E.; Goesmann, H.; Klauss, R. *Angew. Chem. Int. Ed.* 1999, **38**, 2064-2066.
- [38] Fleischer, S.; Zhou, S.; Junge, K.; Beller, M. *Angew. Chem. Int. Ed.* 2013, **52**, 5120-5124.
- [39] Zuo, W.; Lough, A. J.; Li, Y. F.; Morris, R. H. *Science* 2013, **342**, 1080-1083.
- [40] Sheldon, R. A.; Arends, I.; Hanefeld, U. "Green Chemistry and Catalysis", Wiley-VCH, Weinheim, 2007.
- [41] Ogo, S.; Makihara, N.; Watanabe, Y. *Organometallics* 1999, **18**, 5470-5474.
- [42] Kure, B.; Taniguchi, A.; Nakajima, T.; Tanase, T. *Organometallics* 2012, **31**, 4792-4800.
- [43] Wu, X.; Li, X.; King, F.; Xiao, J. *Chem. Commun.* 2005, 4447-4449.
- [44] Wei, Y.; Xue, D.; Lei, Q.; Wang, C.; Xiao, J. *Green Chem.* 2013, **15**, 629-634.
- [45] Vicente, A.; Lafaye, G.; Especel, C.; Marecot, P.; Williams, C. T. *J. Catal.* 2011, **283**, 133-142.
- [46] Marinelli, T. B. L. W.; Ponc, V. *J. Catal.* 1995, **156**, 51-59.
- [47] Szollosi, G.; Kun, I.; Torok, B.; Bartok, M. *Chemoselective hydrogenation of the C=O group in unsaturated aldehydes over clay-supported platinum catalysts*, in *Porous Materials in Environmentally Friendly Processes Vol. 125*, Ed. Kiricsi, I.; Pal-Borbely, G.; Nagy, J. B.; Karge, H. G. Elsevier Science B. V., 1999.
- [48] Szollosi, G.; Kun, I.; Torok, B.; Bartok, M. *Ultrason. Sonochem.* 2000, **7**, 173-176.
- [49] Serrano-Ruiz, J. C.; Lopez-Cudero, A.; Solla-Gullon, J.; Sepulveda-Escribano, A.; Aldaz, A.; Rodriguez-Reinoso, F. *J. Catal.* 2008, **253**, 159-166.
- [50] Oduro, W. O.; Cailuo, N.; Yu, K. M. K.; Yang, H.; Tsang, S. C. *Phys. Chem. Chem. Phys.* 2011, **13**, 2590-2602.
- [51] Concepcion, P.; Perez, Y.; Hernandez-Garrido, J. C.; Fajardo, M.; Calvino, J. J.; Corma, A. *Phys. Chem. Chem. Phys.* 2013, **15**, 12048-12055.
- [52] Chaiyanurakkul, A.; Gao, L.; Nishikata, T.; Kojima, K.; Nagashima, H. *Chem. Lett.* 2014, **43**, 1233-1235.
- [53] Delbecq, F.; Sautet, P. *J. Catal.* 1995, **152**, 217-236.
- [54] Aramendia, M. A.; Jimenez, V. B. C.; Marinas, J. M.; Porras, A.; Urbano, F. J. *J. Catal.* 1997, **172**, 46-54.

- [55] Lenz, J.; Campo, B. C.; Alvarez, M.; Volpe, M. A. *J. Catal.* 2009, **267**, 50-56.
- [56] Grosselin, J. M.; Mercier, C.; Allmang, G.; Grass, F. *Organometallics* 1991, **10**, 2126-2133.
- [57] Melean, L. G.; Rodriguez, M.; Gonzalez, A.; Gonzalez, B.; Rosales, M.; Baricelli, P. J. *Catal. Lett.* 2011, **141**, 709-716.
- [58] Fache, E.; Mercier, C.; Pagnier, N. *J. Mol. Catal.* 1993, **78**, 117-131.
- [59] Galvano, S.; Donato, A.; Pietropaolo, G. N. R.; Capannelli, G. *J. Mol. Catal.* 1993, **78**, 227-236.
- [60] Mizugaki, T.; Ebitani, K.; Kaneda, K. *Appl. Surf. Sci.* 1997, **121/122**, 360-365.
- [61] Mond, L.; Langer, C.; Quincke, F. *J. Chem. Soc. Trans.* 1890, **57**, 749-753.
- [62] Liu, R.; Cheng, H.; Wang, Q.; Wu, C.; Ming, J.; Xi, C.; Yu, Y.; Cai, S.; Zhao, F.; Arai, M. *Green Chem.* 2008, **10**, 1082-1086.
- [63] a) Jenck, J.; Germain, J. E. *J. Catal.* 1980, **65**, 133-140; b) Jenck, J.; Germain, J. E. *J. Catal.* 1980, **65**, 141-149.
- [64] Agarwal, A. K.; Wainwright, M. S.; Trimm, D. L.; Cant, N. W. *J. Mol. Catal.* 1988, **45**, 247-254.
- [65] Rideal, E. K. (1942). "Paul Sabatier. 1859-1941". Obituary Notices of Fellows of the Royal Society. 4 (11): 63–26
- [66] Li, H.; Luo, H.; Zhuang, L.; Dai, W.; Qiao, M. *J. Mol. Catal. A: Chem.* 2003, **203**, 267-275.
- [67] a) Schuit, G. C. A.; Gates, B.C.; *AIChE J.* 1973, **19**, 417; b) Grange, P. *Catal. Rev.-Sci. Eng.* 1980, **21**, 135; c) Topsoe, H.; Clausen, B.S. *Catal. Rev.-Sci. Eng.* 1984, **26**, 395; d) Prins, R.; de Beer, V. H. J.; Somorjai, G. A. *Catal. Rev.-Sci. Eng.* 1989, **31**, 1; e) Chianelli, R. R.; Daage, M.; Ledoux, M. J. *Adv. Catal.* 1994, **40**, 177. f) Topsoe, H.; Clausen, B. S.; Massoth, F. in *Hydrotreating Catalysis, Science and Technology Vol. 11*, Ed. Anderson, J. R.; Boudart, M. B., Springer, Berlin, 1996. g) Whitehurst, D. D.; Isoda, T.; Mochida, I. *Adv. Catal.* 1998, **42**, 345.
- [68] Wang, X.; Ozkan, U. S. *J. Catal.* 2004, **227**, 492-501.
- [69] Wang, X.; Ozkan, U. S. *J. Mol. Catal.* 2005, **232**, 101-112.
- [70] Wang, X.; Ozkan, U. S. *Appl. Catal.* 2005, **286**, 111-119.
- [71] Wang, X.; Saleh, R. Y.; Ozkan, U. S. *J. Catal.* 2005, **231**, 20-32.
- [72] Wang, X.; Ozkan, U. S. *J. Phys. Chem.* 2005, **109**, 1882-1890.

- [73] Reinsdorf, A.; Korth, W.; Jess, A.; Terock, M.; Klasovsky, F.; Franke, R. *ChemCatChem* 2016, **8**, 3592-3599.
- [74] Hotta, K.; Kubomatsu, T. *Bull. Chem. Soc. Jpn.* 1969, **42**, 1447-1449.
- [75] Hotta, K.; Kubomatsu, T. *Bull. Chem. Soc. Jpn.* 1972, **45**, 3118-3121.
- [76] Nitta, Y.; Ueno, K.; Imanaka, T. *Appl. Catal.* 1989, **56**, 9-22.
- [77] Ando, C.; Kurokawa, H.; Miura, H. *Appl. Catal. A: Gen.* 1999, **185**, L181-L183.
- [78] Srivastava, S.; Mohanty, P.; Parikh, J. K.; Dalai, A. K.; Amritphale, S. S.; Khare, A. K. *Chin. J. Catal.* 2015, **36**, 933-942.
- [79] Johnston, E. V.; Backvall, J.-E. *Oxidation of Carbonyl Compounds*, in *Modern Oxidation Methods*, 2nd Edition, ed. Backvall, J.-E., Wiley-VCH, New York, January 2011. pp 353-355.
- [80] Rahimi, A.; Azarpira, A.; Kim, H.; Ralph, J.; Stahl, S. S. *J. Am. Chem. Soc.* 2013, **135**, 6415-6418.
- [81] Fehling, H. *Ann. Chem. Pharm.* 1849, **72**, 106-113.
- [82] Oshitna, K.; Tollens, B. *Ber. Dtsch. Chem. Ges.* 1901, **34**, 1425.
- [83] Benet, W. E.; Lewis, G. S.; Yang, L. Z.; Hugn, D. E. P. *J. Chem. Res.* 2011, 675-677.
- [84] Heilbron, I. M.; Jones, E. R. H.; Sondheimer, F. *J. Chem. Soc.* 1949, 604
- [85] Lv, C.; Yan, X.; Tu, Q.; Di, Y.; Yuan, C.; Fang, X.; Ben-David, Y.; Xia, L.; Gong, J.; Shen, Y.; Yang, Z.; Hao, X. *Angew. Chem. Int. Ed.* 2016, **55**, 7539-7543.
- [86] Lindgren, B. O.; Nilsson, T. *Acta Chem. Scand.* 1973, **27**, 888.
- [87] Bal, B. S.; Childers Jr., W. E.; Pinnick, H. W. *Tetrahedron* 1981, **37**, 2091-2096.
- [88] Machara, T.; Motoyama, K.; Toma, T.; Yokoshima, S.; Fukuyama, T. *Angew. Chem. Int. Ed.* 2017, **56**, 1549-1552.
- [89] van Effen, R. M.; Evans, D. H. *J. Electroanal. Chem.* 1979, **103**, 383-397.
- [90] a) Liu, R.; Liang, X.; Dong, C.; Hu, X. *J. Am. Chem. Soc.* 2004, **126**, 4112. b) Liu, R.; Dong, C.; Liang, X.; Wang, X.; Hu, X. *J. Org. Chem.* 2005, **70**, 729. c) Xie, Y.; Mo, W.; Xu, D.; Shen, Z.; Sun, N.; Hu, B.; Hu, X. *J. Org. Chem.* 2007, **72**, 4288. d) Wang, X.; Liu, R.; Jin, Y.; Liang, X. *Chem. Eur. J.* 2008, **14**, 2679. e) Tao, J.; Lu, Q.; Chu, C.; Liu, R.; Liang, X. *Synthesis* 2010, 3974. f) He, X.; Shen, Z.; Mo, W.; Sun, N.; Hu, B.; Hu, X. *Adv. Synth. Catal.* 2009, **351**, 89. g) Miao, C.-X.; He, L.-N.; Wang, J.-L.; Wu, F. *J. Org. Chem.* 2010, **75**, 257. h) Kuang, Y.; Rokubuichi, H.; Nabae, Y.; Hayakawa, T.; Kakimoto, M.-A. *Adv. Synth. Catal.* 2010, **352**, 2635.

- i) Shibuya, M.; Osada, Y.; Sasano, Y.; Tomizawa, M.; Iwabuchi, Y. *J. Am. Chem. Soc.* 2011, **133**, 6497. j) Lauber, M. B.; Stahl, S. S. *ACS Catal.* 2013, **3**, 2612.
- [91] Anelli, P. L.; Biffi, C.; Montanari, F.; Quici, S. *J. Org. Chem.* 1987, **52**, 2559.
- [92] Sladek, N. E. *J. Biochem. Mol. Toxicol.* 2003, **17**, 6-23.
- [93] Yoshida, A.; Rzhetsky, A.; Hsu, L. C.; Chang, C. *Eur. J. Biochem.* 1998, **251**, 549-557.
- [94] Travis, B. R.; Sivakumar, M.; Hollist, G. O.; Barhan, B. *Org. Lett.* 2003, **5**, 1031-1034.
- [95] Hunsen, M. *Synthesis*, 2005, 2487-2490.
- [96] Malaprade, L. *Bull. Soc. Chim. Fr.* 1934, **3**, 833.
- [97] Harries, C.; Langheld, K. *Liebigs Ann. Chem.* 1905, **343**, 311.
- [98] Voukides, A. C.; Konrad, K. M.; Johnson, R. P. *J. Org. Chem.* 2009, **74**, 2108-2113.
- [99] Corona, T.; Anna Company *Dalton Trans.* 2016, **45**, 14530-14533.
- [100] Murray, A. T.; Matton, P.; Fairhurst, N. W. G.; John, M. P.; Carbery, D. R. *Org. Lett.* 2012, **14**, 3656-3659.
- [101] Okorochonkov, S.; Burglova, K.; Popa, I.; Hlavac, J. *Org. Lett.* 2015, **17**, 180-183.
- [102] Burglova, K.; Okorochonkov, S.; Budesinsky, M.; Hlavac, J. *Eur. J. Org. Chem.* 2017, 389-396.
- [103] Marteau, C.; Ruyffelaere, F.; Aubry, J.-M.; Penverne, C.; Favier, D.; Nardello-Rataj, V. *Tetrahedron* 2013, **69**, 2268-2275.
- [104] Tada, M.; Muratsugu, S.; Kinoshita, M.; Sasaki, T.; Iwasawa, Y. *J. Am. Chem. Soc.* 2010, **132**, 713-724.
- [105] Conte, M.; Miyamura, H.; Kobayashi, S.; Chechik, V. *Chem. Commun.* 2010, **46**, 145-147.
- [106] Tian, Q.; Shi, D.; Sha, Y. *Molecules* 2008, **13**, 948-957.
- [107] Yoshida, M.; Katagiri, Y.; Zhu, W.-B.; Shishido, K. *Org. Biomol. Chem.* 2009, **7**, 4062-4066.

Chapter 2 – Designing a more sustainable aldehyde reduction

2.1 Initial discovery: silver-catalyzed A^3/A^2 – coupling

As established in chapter 1, although current methodology development already enables fine-control over the reaction selectivity and efficiency, the main problem for aldehyde reduction nowadays is the requirement of scarce noble metals or organic solvents. We therefore set our research focus onto the development of more sustainable and efficiency aldehyde reduction method.

In the past years, our group has developed a series of transition metal catalysts that can efficiently catalyze the Aldehyde/Alkyne/Amine-(A^3)-coupling reaction in water (Figure 2.1a) [1], which involves the activation of aldehyde by amine into iminium to accept nucleophilic attack from alkyne. In 2003, our group developed the first silver-catalyzed A^3 -coupling in water [2]. The catalyst shown impressive efficiency. With as little as 1.5 mol% of Ag load, a variety of substrate was successfully coupled. Notably, the couplings of aliphatic aldehydes were particularly efficient [3]. Such efficiency cannot be achieved by other A^3 -coupling catalysts such as Au or Cu [1], whose substrate scopes were generally limited to aromatic aldehydes.

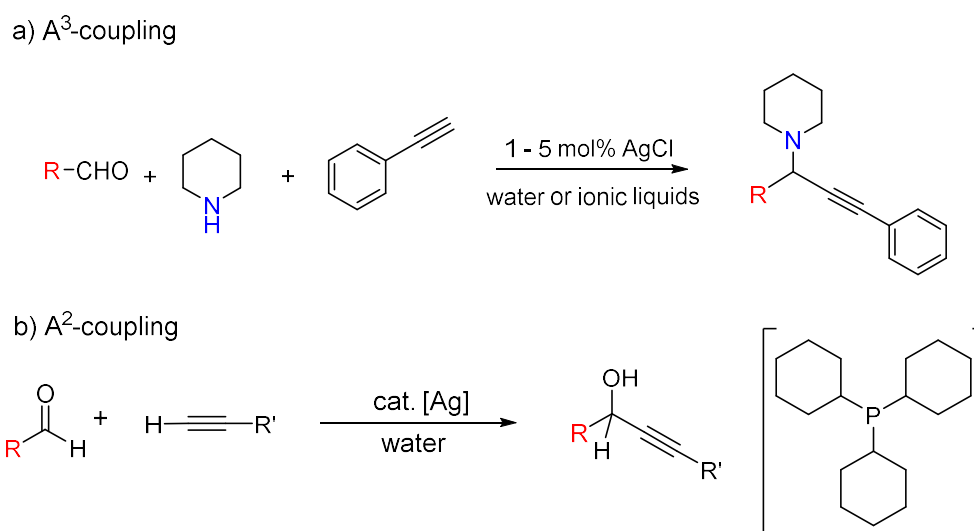


Figure 2.1. Ag-catalyzed A^3/A^2 -coupling reaction in water

With demonstrated exceptional catalytic activity by silver(I), our group began to further explore the potential for Ag as catalyst. Two years later in 2005, our group discovered that after the catalyst was further stabilized by phosphine ligand, the silver-catalyzed A^3 -coupling became extremely

efficient. The necessary step required by previous A^3 -coupling catalyst, which is the activation of aldehyde by 2°-amine to generate iminium, was generally unnecessary when 5 mol% Cy_3PAgCl was applied as catalyst (Figure 2.1b) [4]. The therefore established aldehyde/alkyne (A^2)-coupling achieves very good efficiency, both aliphatic and aromatic aldehydes successfully underwent the coupling without amine activation. As far as we are concerned, Ag is the only catalyst that capable of efficiently catalyzing such transformation.

2.2 Our hypothesis for developing aldehyde reduction using silver system

Impressed by the silver-catalyzed A^3/A^2 -coupling reaction, we were interested in the further development of other potential silver catalyst. In the previous methodology development, silver reagents are, in most cases, applied stoichiometrically or as Lewis acid. Examples using silver as catalyst are relatively limited [5]. To fully explorer the potential for silver as powerful catalyst for carbonyl chemistry, we hypothesized that silver possesses the potential to also serve as efficient catalyst for aldehyde reduction catalyst (Figure 2.2).

After examining the proposed mechanism of the previous transformations, we suggested that the high efficiency of silver catalyst came from 3 factors: 1) strong Ag^+ Lewis acidity; 2) weak Ag-Nu coordination; 3) long Ag-Nu bond length.

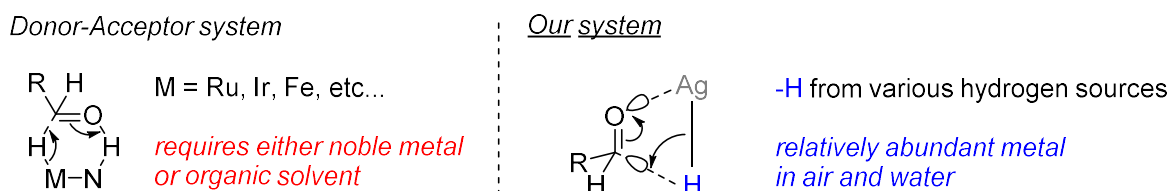


Figure 2.2. Our hypothesized silver-catalyzed aldehyde reduction mechanism

It has been well-established that carbonyl group can be activated by Lewis acid to generate stronger partial positive charge on C=O carbon [6]. The carbonyl group is relatively ‘inert’ if no such activation was applied. Ag^+ possess +1 positive charge, which enables its Lewis acidity. Furthermore, the 4d shell of Ag^+ cannot effectively shield the electrostatic force from positive charged nucleus, as shown by the electrochemical series in which silver is almost at the bottom ($E^0(Ag^+/Ag) = +0.799$ V) [7]. Though the charge is distributed due to larger ionic radius, many excellent reports have indicated Ag^+ as a powerful Lewis acid for organic catalysis [8].

Although enables strong Lewis acidity from its weak shielding, the $4d^{10}$ shell of Ag^+ is in an energetically stable state. Among all group 11 elements in the periodic table (Cu, Ag, Au), Ag possesses the greatest 2nd ionization energy [9], which indicates that in most cases silver can only afford +1 oxidation state. Such low charge is difficult to maintain a strong coordination between ligands and Ag^+ center. In most organometallic complexes, although exhibits very unsaturated $14e^-$ state, silver shows only linear 2-coordination geometry [10]. The ligand coordinated to Ag^+ is therefore relatively labile [11]. This is particular advantageous for nucleophiles, as most of their nucleophilicity were preserved even after coordination to Ag^+ , which results in powerful nucleophilic attack catalyzed by Ag.

As mentioned before, Ag^+ possess a relatively large ionic radius (around 1.29 Å) [12]. The Ag-Nu bonds were therefore relatively long (Ag-C: 2.1 Å, Ag-H: 1.7 Å) [13]. Compared to shorter C=O length (1.16 Å) [14], when Ag-Nu aligns with C=O, Ag-Nu shows good alignment with the LUMO of C=O (Figure 2.2 right) [15]. Nu attack on carbonyl can thus be enhanced with Ag catalyst. When Nu is represented by hydride, reduction of aldehyde can therefore be established.

2.3 Proposed research

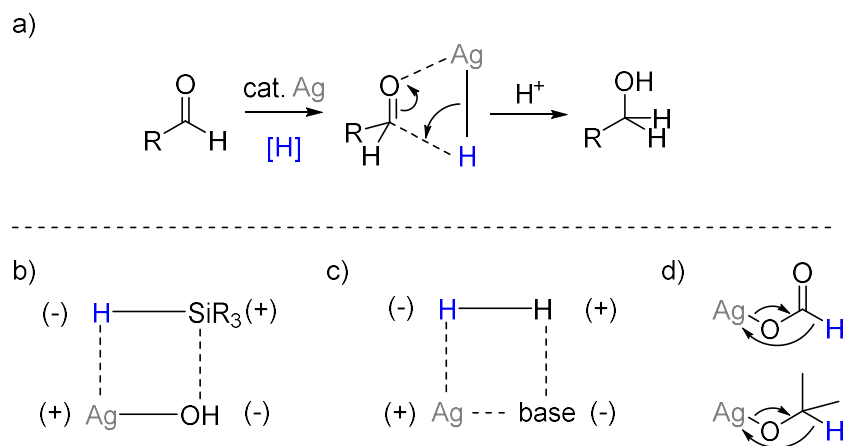


Figure 2.3. Our proposed silver-catalyzed aldehyde reduction

Based on our previous assumption and the demonstrated excellent efficiency for Ag towards carbonyl chemistry, we suggest the silver catalyzed hydrogenation/transfer hydrogenation from Ag-H intermediate can serve as a potential choice to efficiently reduce aldehyde into the corresponding alcohol (Figure 2.3a). In 2006, Stradiotto described the extraction of hydride from silane by silver (Figure 2.3b) [16]. The activation of molecular hydrogen was long reported by

Halpern (Figure 2.3c) [17]. Also, transfer hydrogenation by formate/2-propanol was suggested by many reports (Figure 2.3d) [18]. We then propose to use silane, hydrogen gas, and formate/2-propanol as hydrogen sources, to examine the potential for Ag as aldehyde reduction catalyst.

2.4 Conclusion

In the designing table, we have summarized the previous notable reports on silver as a powerful catalyst for carbonyl chemistry. A plausible mechanism was proposed for the efficiency of silver-catalyzed nucleophilic addition. Such mechanism inspires us of the potential for using silver as aldehyde reduction catalyst. Further development to fulfill our hypothesis is imminent.

2.5 References

- [1] Wei, C.; Li, Z.; Li, C.-J. *Synlett* 2004, **9**, 1472-1483.
- [2] Wei, C.; Li, Z.; Li, C.-J. *Org. Lett.* 2003, **5**, 4473-4475.
- [3] Li, Z.; Wei, C.; Chen, L.; Varma, R. S.; Li, C. J. *Tetrahedron Lett.* 2004, **45**, 2443.
- [4] a) Yao, X.; Li, C.-J. *Org. Lett.* 2005, **7**, 4395; b) Yu, M.; Skouta, R.; Zhou, L.; Jiang, H.-F.; Yao, X.; Li, C.-J. *J. Org. Chem.* 2009, **74**, 3378; c) Deng, G.-J.; Li, C.-J. *Synlett* 2008, 1571; d) Jia, Z. Li, X.; Chan, A. S. C.; Li, C.-J. *Synlett* 2012, **23**, 2758; e) Fu, X.-P.; Liu, L.; Wang, D.; Chen, Y.-J.; Li, C.-J. *Green Chem.* 2011, **13**, 549.
- [5] For example, a) Pellisier, H. *Chem. Rev.* 2016, **116**, 14868-14917; b) Sekine, K.; Yamada, T. *Chem. Soc. Rev.* 2016, **45**, 4524-4532.
- [6] Ouellette, R.J. and Rawn, J.D. "Organic Chemistry" 1st Ed. Prentice-Hall, Inc., 1996: New Jersey.
- [7] Vanyšek, Petr (2012). "Electrochemical Series". In Haynes, William M. Handbook of Chemistry and Physics: 93rd Edition. Chemical Rubber Company. pp. 5–80.
- [8] For example, a) Patmore, N. J.; Hague, C.; Cotgreave, J. H.; Mahon, M. F.; Frost, C. G.; Weller, A. S. *Chem. Eur. J.* 2002, **8**, 2088-2098; b) Firouzbadi, H.; Mohammadpoor-Baltork, I. *Synth. Commun.* 1994, **24**, 1065-1077.
- [9] Walker, N. R.; Wright, R. R.; Barran, P. E.; Murrell, J. N.; Stace, A. J. *J. Am. Chem. Soc.* 2001, **123**, 4223-4227.
- [10] Fackler, J. P.; Liu, C. W. *Sci. Synth.* 2004, **3**, 663-690.
- [11] Wang, H. M. J.; Lin, I. J. B. *Organometallics* 1998, **17**, 972-975.

- [12] Shannon, R. D. *Acta. Cryst.* 1976, **A32**, 751-767.
- [13] a) Dias, H. V. R.; Lovely, C. J. *Chem. Rev.* 2008, **108**, 3223-3238; b) Jordan, A. J.; Lalic, G.; Sadighi, J. P. *Chem. Rev.* 2016, **116**, 8318-8372.
- [14] R.T.Sanderson, *Chemical Bonds and Bond Energy*, 1976
- [15] Anh, N. T.; Elsenstein, O. *Tetrahedron Lett.* 1976, 155.
- [16] Wile, B. M.; Stradiotto, M. *Chem. Commun.* 2006, 4104-4106.
- [17] For a summary of Halpern's work, see: a) Beck, M. T.; Gimesi, I.; Farkas, J. *Nature* 1963, **197**, 73.
- [18] a) Bartoszewicz, A.; Nanna, A.; Belen, M.-M. *Chem. Eur. J.* 2013, **19**, 7274-7302; b) Liu, Z.; Sadler, P. J. *Acc. Chem. Res.* 2014, **47**, 1174-1185; c) Zhang, L.; Meggers, E. *Acc. Chem. Res.* 2017, **50**, 320-330.

Chapter 3 – Silver(I)-catalyzed transfer hydrogenation of aldehyde in air and water

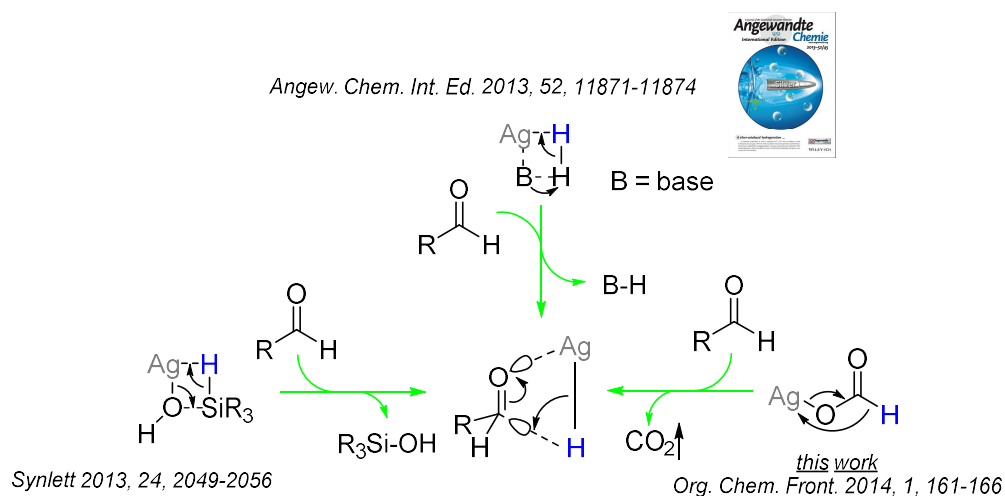


Figure 3.1 Developments of our silver-catalyzed reduction system

3.1 Objective

Inspired by the excellent catalytic efficiency of silver towards aldehyde, our group has demonstrated the potential of using hydride from various hydrogen sources as the nucleophile in our silver(I) system, via a key silver(I)-hydride intermediate [1], towards the development of aldehyde reduction. We have introduced silver-catalyzed reduction of aldehyde using silane [2] or hydrogen gas [3] as hydrogen source in water (Figure 3.1). Those methods achieved impressive substrate scope under mild reaction conditions. However, the shortcomings of these methods are the requirements of either silane, which is highly flammable and provides less atom economy [4], or hazardous hydrogen pressure (40 bar), which also involves pressure-resisting equipment and potential hazardous, as stoichiometric reductant. To address these challenges, transfer hydrogenation using non-toxic and inexpensive reagent as hydrogen source can serve as an appealing solution, as many reports have demonstrated such potential [5].

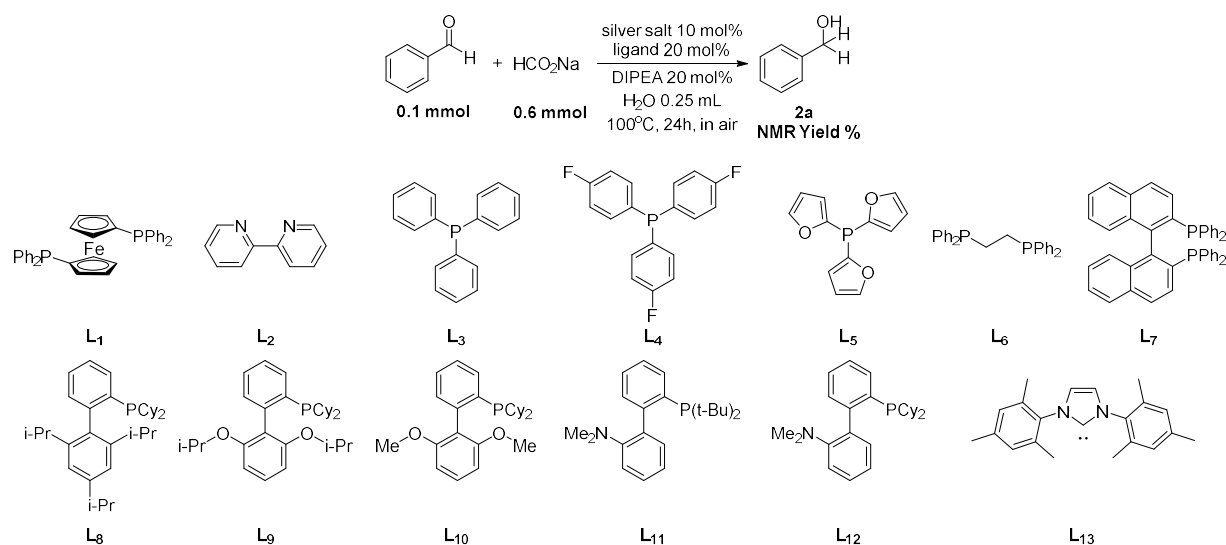
3.2 Results and discussion

3.2.1 Condition optimization

Isopropyl alcohol and formate have been widely applied as very good hydrogen source for transfer hydrogenation [6]. To begin our investigation, we attempted to use these two reagents as reductants under our previous transfer hydrogenation conditions (Table 3.1) [2], with pre-mixed AgPF₆ salt

and 1,1'-bis(diphenylphosphino)ferrocene (dppf) ligand as catalyst at 100 °C in water. Surprisingly, although in low yield, the reaction with sodium formate gave the desired product successfully (entry 1). We then focused our research into optimization of reaction conditions. Keeping the same ligand, when silver salt anion was switched from PF₆⁻ to F⁻, the yield slightly increased (entry 2). Although the increase was not significant, considering the better air- and moisture-stability of AgF compared to AgPF₆, we decided to use AgF for the optimization. Further switching the anion to Cl⁻, Br⁻, and I⁻ shut down the reaction (entries 3, 4, 5), indicating the necessity for weak coordinating anion. Similar yield was obtained with AgOTf (entry 6). Keeping AgF as the salt, switching dppf ligand to other common ligands such as 2,2'-bipyridyl (L₂) and triphenylphosphine (L₃) resulted in the elimination of product again (entries 7, 8). However, when slightly different tris(4-fluorophenyl)phosphine (L₄) was used, the yield increased to 6 % (entry 9). This result probably implied that hemilabile ligand, with one strong coordinating atom and another weak coordinating atom, can be beneficial to this reaction. Similar hemilabile ligand tris(2-furyl)phosphine (L₅) diminished the product (entry 10). Other chelating ligand such as diphos (L₆) and binap (L₇) also resulted in the elimination of product (entries 11, 12). For electron-rich Buchwald-type ligand, XPhos (L₈) did not give desired product (entry 13), while hemilabile ligand RuPhos (L₉) gave an astonishing 61 % yield (entry 14). Using less bulky SPhos (L₁₀) gave a further increased 66 % yield (entry 15). *t*-BuDavePhos (L₁₁) gave 50 % yield while DavePhos (L₁₂) gave an almost quantitative yield (entries 16, 17). N-Heterocyclic Carbene ligand IMes (L₁₃) did not give the desired product (entry 18). Keeping the optimized ligand, switching the salt from AgF to AgPF₆ gave a decreased 38 % yield (entry 19). AgCl, AgBr, and AgI gave decreasing yields of 85 %, 11 %, and 0 %, respectively (entries 20, 21, 22). Salt or ligand alone were proven to be unable to catalyze the reaction (entries 23, 24). When the reaction was performed without DIPEA as base, yield dropped to 33 % (entry 25). Neat reaction without solvent gave 26 % yield (entry 26). Switching solvent to ethanol, acetonitrile, acetone and DMF, the yield decreased to 80 %, 9 %, 0 % and 0 %, respectively (entries 27, 28, 29, 30). These results indicate the necessity of protonic solvent to this reaction.

Table 3.1 First condition optimization



Entry	Silver Salt	Ligand	NMR Yield ^a	Entry	Silver Salt	Ligand	NMR Yield ^a
1	AgPF ₆	L ₁	2 %	16	AgF	L ₁₁	50 %
2	AgF	L ₁	3 %	17	AgF	L ₁₂	>99 % (92 %) ^b
3	AgCl	L ₁	N.D.	18	AgF	L ₁₃	N.D.
4	AgBr	L ₁	N.D.	19	AgPF ₆	L ₁₂	38 %
5	AgI	L ₁	N.D.	20	AgCl	L ₁₂	85 %
6	AgOTf	L ₁	3 %	21	AgBr	L ₁₂	11 %
7	AgF	L ₂	N.D.	22	AgI	L ₁₂	N.D.
8	AgF	L ₃	N.D.	23	//	L ₁₂	N.D.
9	AgF	L ₄	6 %	24	AgF	//	N.D.
10	AgF	L ₅	N.D.	25	AgF	L ₁₂	33 % ^c
11	AgF	L ₆	N.D.	26	AgF	L ₁₂	26 % ^d
12	AgF	L ₇	N.D.	27	AgF	L ₁₂	80 % ^e
13	AgF	L ₈	N.D.	28	AgF	L ₁₂	9 % ^f
14	AgF	L ₉	61 %	29	AgF	L ₁₂	N.D. ^g
15	AgF	L ₁₀	66 %	30	AgF	L ₁₂	N.D. ^h

^a ¹H NMR yields were determined by using mesitylene as the internal standard;

^b Isolated Yield;

^c Reaction was performed without base.

^d Reaction was carried out without solvent

^e Reaction was carried out in Ethanol

^f Reaction was carried out in Acetonitrile

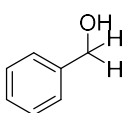
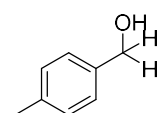
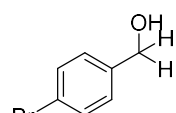
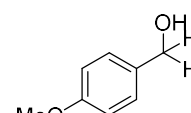
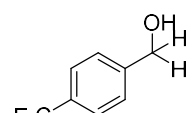
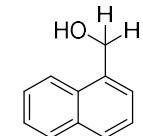
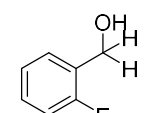
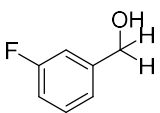
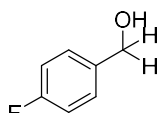
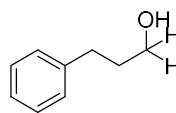
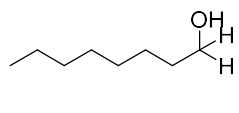
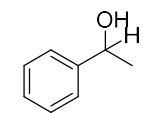
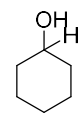
^g Reaction was carried out in Acetone

^h Reaction was carried out in N,N-dimethylformamide

3.2.2 First scope investigation

With the optimized conditions in hand, we then move on to test the substrate scope tolerance of this chemistry (Table 3.2). With nearly quantitative NMR yield, benzaldehyde gave 92 % isolated yield of benzoic acid (**2a**) after chromatography purifying. 4-tolualdehyde (**2b**) gave a similar 91 % isolated yield. 4-bromobenzaldehyde (**2c**) gave 95 % yield, indicating good tolerance of bromo-substitution. Electron-rich 4-anisaldehyde (**2d**) gave a slightly reduced 83 % yield, possibly due to undesired coordination of the methoxy- to silver. Electron-poor 4-trifluoromethyl-benzaldehyde (**2e**) gave 60 % yield, possibly due to poor affinity for electron-poor carbonyl towards Lewis-acidic silver. 1-naphthaldehyde (**2f**) gave an excellent 90 % yield. However, when substrate was switched to fluorine-substituted benzaldehyde, regardless of *ortho*- (**2g**), *meta*- (**2h**), or *para*- (**2i**) substitution, the yield decreased dramatically, with **2i** slightly better than **2g** than **2h**. Aliphatic aldehydes such as hydrocinnamaldehyde (**2j**) and octanal (**2k**), along with ketones such as acetophenone (**2l**) and cyclohexanone (**2r**), did not give any desired product. Since aliphatic aldehydes plays particularly important roles in chemistry society, further optimization of this reaction is desirable in order to expand its reactivity.

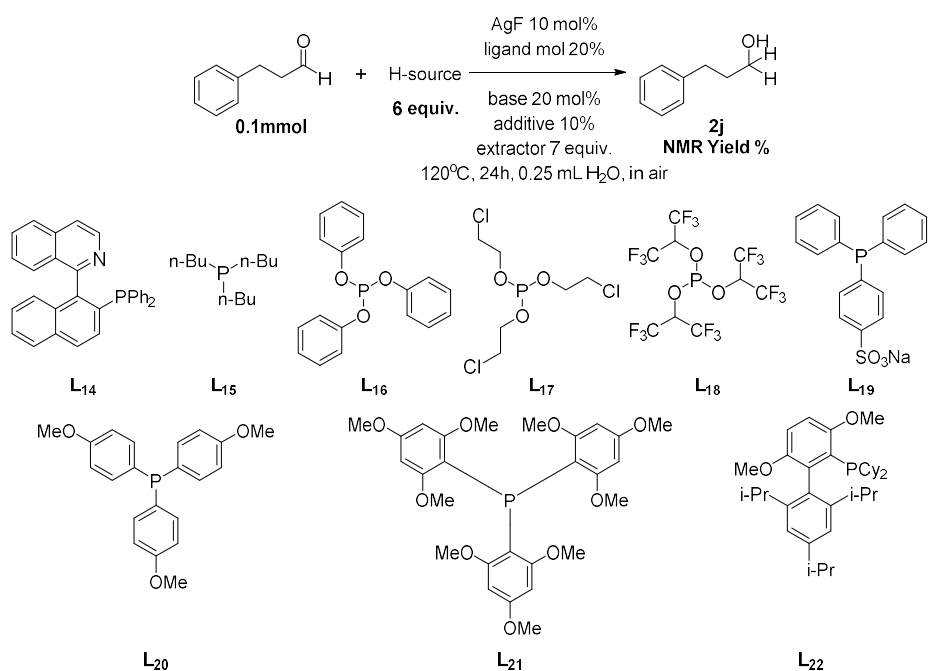
Table 3.2 First scope optimization

$ \begin{array}{c} \text{R}-\text{C}_6\text{H}_4-\text{CHO} + \text{HCO}_2\text{Na} \xrightarrow[\text{H}_2\text{O } 0.25 \text{ mL}]{[\text{AgF} + 2 \text{L}_{12}] \text{ 10 mol\%}, \text{DIPEA } 20 \text{ mol\%}} \text{R}-\text{C}_6\text{H}_4-\text{CH(OH)}_2 \\ \text{0.5 mmol} \qquad \qquad \text{3.0 mmol} \qquad \qquad \qquad \qquad \qquad \qquad \qquad \qquad \qquad \qquad \qquad \qquad \qquad \qquad \qquad \text{isolated yield \%} \\ \text{100}^\circ\text{C, 24h, in air} \end{array} $						
						
2a 92 %	2b 91 %	2c 95 %	2d 83 %	2e 60 %	2f 90 %	2g 26 %*
						
2h 9 %*	2i 33 %*	2j < 3 %*	2k N.D.	2l N.D.	2r N.D.	

* NMR yield, not isolated

3.2.3 Condition re-optimization

Table 3.3 Condition optimization for aliphatic aldehyde



Entry	H-Source	base	Ligand	additive	extractor	NMR Yield
1	HCO ₂ Na	DIPEA	L ₁₂	//	//	3 % ^a
2	HCO ₂ H	//	L ₁₂	//	//	n.d. ^a
3	HCO ₂ H·DIPEA	DIPEA	L ₁₂	//	//	6 % ^a
4	HCO ₂ H·DIPEA	CsF	L ₁₂	//	//	7 % ^a
5	HCO ₂ H·DIPEA	CsF	L ₁₂	LiF	//	n.d. ^a
6	HCO ₂ H·DIPEA	CsF	L ₁₂	//	//	11 %
7	HCO ₂ H·NH ₃	CsF	L ₁₂	//	//	n.d.
8	HCO ₂ H·1/2TMEDA	CsF	L ₁₂	//	//	n.d.
9	HCO ₂ H·1/2DABCO	CsF	L ₁₂	//	//	n.d.
10	HCO ₂ H·DBU	CsF	L ₁₂	//	//	10 %
11	HCO ₂ H·DIPEA	CsF	L ₁	//	//	n.d.
12	HCO ₂ H·DIPEA	CsF	L ₂	//	//	n.d.
13	HCO ₂ H·DIPEA	CsF	L ₄	//	//	n.d.
14	HCO ₂ H·DIPEA	CsF	L ₅	//	//	n.d.
15	HCO ₂ H·DIPEA	CsF	L ₇	//	//	n.d.
16	HCO ₂ H·DIPEA	CsF	L ₁₄	//	//	n.d.


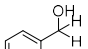
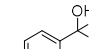
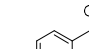
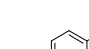

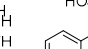
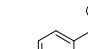
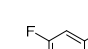
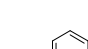
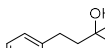
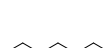
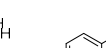
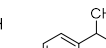
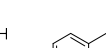

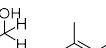
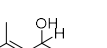
<i>Entry</i>	<i>H-Source</i>	<i>base</i>	<i>Ligand</i>	<i>additive</i>	<i>extractor</i>	<i>NMR Yield</i>
17	HCO ₂ H•DIPEA	CsF	L ₈	//	//	trace
18	HCO ₂ H•DIPEA	CsF	L ₁₃	//	//	n.d.
19	HCO ₂ H•DIPEA	CsF	L ₁₅	//	//	n.d.
20	HCO ₂ H•DIPEA	CsF	L ₁₆	//	//	trace
21	HCO ₂ H•DIPEA	CsF	L ₁₇	//	//	n.d.
22	HCO ₂ H•DIPEA	CsF	L ₁₈	//	//	n.d.
23	HCO ₂ H•DIPEA	CsF	L ₁₉	//	//	n.d.
24	HCO ₂ H•DIPEA	CsF	L ₂₀	//	//	n.d.
25	HCO ₂ H•DIPEA	CsF	L ₂₁	//	//	n.d.
26	HCO ₂ H•DIPEA	CsF	L ₂₂	//	//	21 %
27	HCO ₂ H•DIPEA	CsF	L ₁₀	//	//	15 %
28	HCO ₂ H•DIPEA	CsF	L ₁₀	//	DIPEA	30 %
29	HCO ₂ H•DIPEA	CsF	L ₁₀	//	PhCl	30 %
30	HCO ₂ H•DIPEA	CsF	L ₁₀	TfOH	PhCl	55 %
31	HCO ₂ H•DIPEA	CsF	L ₁₀	Benzoic Acid	PhCl	12 %
32	HCO ₂ H•DIPEA	CsF	L ₁₀	CF ₃ CO ₂ H	PhCl	11 %
33	HCO ₂ H•DIPEA	CsF	L ₁₀	TfOH	PhCl	75 % ^b
34	HCO ₂ H•DIPEA	CsF	L ₂₂	TfOH	PhCl	99 %
35	HCO ₂ H•DIPEA	//	L ₁₀	TfOH	PhCl	42 %

We used hydrocinnamaldehyde (**2j**) as the standard substrate, formate as hydrogen source, to examine various reaction condition towards successful transfer hydrogenation of aliphatic aldehyde (Table 3.3). Considering the weaker tolerance of base for aliphatic aldehydes compared to aromatic aldehydes due to side reactions, for example, aldol condensation, we first tried switching sodium formate into formates in less basic form. Acidic formic acid did not give the desired product (entry 2). By pre-mixing aqueous formic acid and DIPEA, we obtained a homogeneous neutral solution. (HCOOH•DIPEA) Using this solution as hydrogen source instead of sodium formate increased the yield to 6 %. (entry 3) Keeping this hydrogen source, considering the benefit of fluorine anion in the previous condition optimization, switching the extra 20 mol% base DIPEA into CsF gave 7 % yield (entry 4). Further increasing the fluorine anion by addition of LiF resulted in the elimination of product (entry 5). Increasing the reaction temperature to 120°C also increased the yield to 11 % (entry 6). We then tried to generate the neutral formate salt using

formic acid and ammonia, TMEDA, DABCO and DBU (entries 7, 8, 9, 10), but none of them surpasses the yield given by DIPEA. We then tried to examine various ligands from a much wider selection, including electron-rich ligands from previous condition optimization, electron poor phosphites, and other phosphine ligands. However, most of the candidates failed to give a better yield (entries 11-25). At the same time the Buchwald-type ligand BrettPhos (L_{22}) and SPhos (L_{10}) increased the yield to 21 % and 15 % (entries 26, 27) respectively. Coincidentally, from an experimental error, we discovered that adding excessive amount of DIPEA increased the yield to 30 % (entry 28), which potentially functioned by generating a bi-phasic reaction mixture. The equilibrium was therefore pushed forward by enriching alcohol product in organic phase. Switching the excessive extractor from DIPEA to chlorobenzene did not affect the yield (entry 29); however, we still accept the more cost-effective and non-basic chlorobenzene rather than DIPEA as extractor. We then found that using non-distilled cinnamaldehyde rather than re-distilled benzaldehyde increased the reaction yield, implying the benefit of adding extra acid into the reaction. We examined the addition of extra trifluoromethane sulfonic acid (TfOH), benzoic acid or trifluoroacetic acid into reaction mixture (entries 30, 31, 32); among them, TfOH increased the yield to 55 %. Keeping all the other reaction condition unchanged, increasing the water amount raised the yield to 75 % (entry 33), while same reaction using L_{22} gave almost quantitative yield (entry 34). The yield also decreased to 42 % if CsF was absent from the reaction mixture (entry 35).

3.2.4 Final scope investigation

Table 3.4 Final substrate scope

		iso. Yield %							
									
2a	2b	2c	2d	2e	2f	2g	2h	2i	
> 99 %*	> 99 %*	> 99 %*	51 %*	90 %*	> 99 %*	91 %*	96 %*	98 %*	
									
2j	2k	2l	2m	2n	2o	2p	2q		
73 %	76 %	N.D.	43 %*	82 %	< 5 %*	< 3 %*	< 3 %*		

* NMR yield, not isolated

We then examined the re-optimized conditions with a much wider scope of substrates, including different aliphatic/aromatic/unsaturated aldehydes, towards successful transfer hydrogenation to give their corresponding alcohol (Table 3.4). For convenience, we only calculated NMR yield using internal standard for aldehydes which were already successfully reduced efficiently with the previous condition. Benzaldehyde (**2a**), 4-tolualdehyde (**2b**), and 4-bromobenzaldehyde (**2c**) all gave quantitative NMR yield. 4-anisaldehyde (**2d**), while giving 83 % isolated yield with the previous conditions, only gave 51 % NMR yield. At the same time 4-trifluoromethylbenzaldehyde (**2e**) gave an excellent 90 % NMR yield, while only 60 % was obtained with the previous conditions. These results indicate that the new conditions might function better with more electron-poor substrates compared to the previous conditions. 1-naphthaldehyde (**2f**) gave also quantitative NMR yield. The yield of mono-fluoro-substituted benzaldehyde, regardless of *ortho*- (**2g**), meta- (**2h**), and para- (**2i**) substitution, all gave excellent isolated yields. Aliphatic hydrocinnamaldehyde (**2j**) gave a good 73 % isolated yield. Octanal (**2k**) also gave a good 76 % isolated yield. Acetophenone (**2l**) still gave quantitative starting material recovery, indicating good selectivity of our method towards aldehydes rather than ketones. α -phenylpropionaldehyde (**2m**) gave a reduced 43 % isolated yield, probably due to stronger enolization. Unsaturated aldehyde cinnamaldehyde (**2n**) also gave a good 82 % isolated yield, while substrates with non-conjugated C=C bond, such as perillaldehyde (**2o**), citral (**2p**), and 2,6,6-trimethyl-1-cyclohexene-1-acetaldehyde (**2q**) gave poor yields. These results are possibly due to the catalyst's better affinity towards more electron-rich C=C coordination.

3.3 Conclusion and perspective

In conclusion, we have developed the first example of homogeneous silver(I)-catalyzed transfer hydrogenation of aldehyde. Designed from our silver(I)-catalyzed hydride nucleophilic addition mechanism, under two different sets of reaction conditions, great substrate adaptability was achieved including both aromatic aldehydes and aliphatic aldehydes. The reaction uses environmentally benign water as solvent. Inert atmosphere was not necessary in the reduction procedures. Relatively abundant silver was used as the sole catalyst. The successful development of such system potentially represents an unprecedented catalyst system for achieving hydrogenation/transfer hydrogenation of aldehyde. The potential future works include transfer hydrogenation/direct hydrogenation of other substrates, such as ketone, imine, etc. The use of

chiral ligand on silver(I) catalyst is also plausible to further enable asymmetric transfer hydrogenation/direct hydrogenation of those substrates. Some of the above-mentioned works have already underway in our lab.

3.4 Contributions of authors

The inspiration of this research came from previous work by Dr. Zhenhua Jia. During the development of this reaction, the designing of all the experiments described in this chapter was the result of discussion between Prof. Chao-Jun Li and me. I was also in charge of carrying out all those experiments (including but not limited to all the condition optimization and all the substrate scope investigation), with technical help from Dr. Feng Zhou, and operating the NMR spectrometer for all the necessary acquisitions. The manuscript was prepared by me too, with revisions from Prof. Chao-Jun Li and Dr. Zhenhua Jia.

3.5 Experimental Section

3.5.1 General Information

All transfer hydrogenation reactions were carried out under air. All manipulation and purification procedures were carried out with reagent-grade solvents. Analytical thin-layer chromatography (TLC) was performed using E. Merck silica gel 60 F₂₅₄ precoated plates (0.25 mm). Flash chromatography was performed with Biotage Isolera One Flash Purification System, using Biotage SNAP Ultra 25g prepared column. Nuclear magnetic resonance (NMR) spectra were recorded on Varian MERCURY plus-300 spectrometer (¹H 300 MHz, ¹³C 75 MHz) or a Varian MERCURY plus-400 spectrometer (¹H 400 MHz, ¹³C 100 MHz). Chemical shifts for ¹H NMR spectra are reported in parts per million (ppm) from tetramethylsilane with the solvent resonance as the internal standard (CDCl₃: δ 7.26 ppm). Chemical shifts for ¹³C NMR spectra are reported in parts per million (ppm) from tetramethylsilane with the solvent as the internal standard (CDCl₃: δ 77.0 ppm). Data are reported as following: chemical shift, multiplicity (s = singlet, d = doublet, dd = doublet of doublets, t = triplet, q = quartet, m = multiplet, br = broad signal), and integration.

3.5.2 General Procedures

(Synthesis of AgF-DavePhos complex; all the other complexes used in the study were prepared in the same way). To an oven-dried reaction vessel, charged with silver (I) fluoride

(12.6 mg, 0.1 mmol, 1 equiv) and 2-dicyclohexylphosphino-2'-(N,N-dimethylamino)biphenyl (DavePhos, 78.7 mg, 0.2 mmol, 2 equiv), is flushed with argon 3 times. 2.5 mL of dry, air-free methylene chloride (DCM) is added into the vessel. The vessel is then sealed and stirred at room temperature. After stirring overnight (12 h), the mixture is stripped of solvent and the resulting solid is kept under vacuum for 1 h before ready to use.

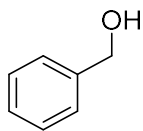
(General procedures for the reduction of aromatic aldehydes). To a stirred solution of sodium formate (81.6 mg, 1.2 mmol, 6 equiv) in 0.5 mL distilled H₂O in air, pre-formed AgF-DavePhos complex (9.1 mg, 0.02 mmol, 0.1 equiv) is added, along with benzaldehyde (20.5 μ L, 0.2 mmol, 1 equiv) and diisopropylethylamine (DIPEA, 7 μ L, 0.04 mmol, 0.2 equiv). The vessel is then sealed and stirred at 100°C for 24h. Then, the reaction mixture is cooled to room temperature, extracted with methylene chloride, and the organic phase is washed with brine. The organic phase is then stripped of solvent and the oily crude product is collected. Further purification can be carried out with flash chromatography to give the product in 19.5 mg (92% yield).

(General procedures for the reduction of aliphatic aldehydes). To a stirred vial of 2 mL H₂O in air, formic acid (45 μ L, 1.2 mmol, 6 equiv) and diisopropylethylamine (DIPEA, 209 μ L, 1.2 mmol, 6 equiv) are added. The mixture is kept stirring until the whole solution is transparent and clear. All the solution is then transferred into a reaction vessel which is charged with pre-formed AgF-SPhos complex (9.5 mg, 0.02 mmol, 0.1 equiv) and cesium fluoride (6.2 mg, 0.04 mmol, 0.2 equiv) in air. Hydrocinnamaldehyde (26.4 μ L, 0.2 mmol, 1 equiv), trifluoromethanesulfonic acid (1.8 μ L, 0.02 mmol, 0.1 equiv) and chlorobenzene (142 μ L, 1.4 mmol, 7 equiv) are then added and the reaction vessel is sealed. The vessel is stirred at 120°C for 24h before cooled down to room temperature. The mixture is extracted with methylene chloride and the resulting organic phase is washed with brine. The solution is then concentrated and subject to flash chromatography to give the desired product in 19.0 mg (71% yield.)

3.5.3 Identification of Products

All compounds are literature known and the data reported herein are consistent with the literature reports.

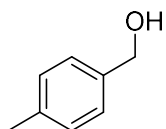
Compound 2a:



$^1\text{H-NMR}$ (ppm): 7.38 (m, 5H), 7.30 (m, 1H), 4.70 (s, 2H), 1.62 (br, 1H).

$^{13}\text{C-NMR}$ (ppm): 140.8, 128.5, 127.7, 127.0, 65.3.

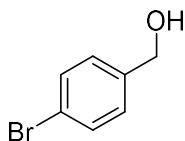
Compound 2b:



$^1\text{H-NMR}$ (ppm): 7.27 (m, 2H), 7.18 (m, 2H), 4.65 (s, 2H), 2.36 (s, 3H), 1.63 (br, 1H).

$^{13}\text{C-NMR}$ (ppm): 137.9, 137.4, 129.3, 127.2, 65.2, 21.1.

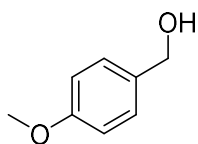
Compound 2c:



$^1\text{H-NMR}$ (ppm): 7.48 (m, 2H), 7.23 (m, 2H), 4.64 (s, 2H), 1.86 (br, 1H).

$^{13}\text{C-NMR}$ (ppm): 139.7, 131.7, 128.6, 121.4, 64.5.

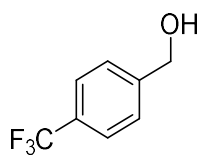
Compound 2d:



$^1\text{H-NMR}$ (ppm): 7.29 (m, 2H), 6.89 (m, 2H), 4.63 (s, 2H), 3.81 (s, 3H), 1.59 (br, 1H).

$^{13}\text{C-NMR}$ (ppm): 133.1, 129.4, 128.5, 113.9, 65.1, 55.3.

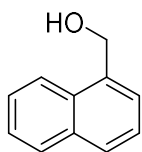
Compound 2e:



$^1\text{H-NMR}$ (ppm): 7.62(d, $J=8.19\text{Hz}$, 2H); 7.50 (d, $J=8.19\text{Hz}$, 2H); 4.78(s, 2H), 1.67 (br, 1H).

$^{13}\text{C-NMR}$ (ppm): 144.6, 130.5, 126.8, 125.4(q, $J_{\text{F-C}}=4.02\text{Hz}$), 122.3, 64.5.

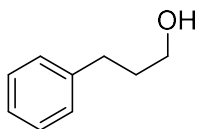
Compound 2f:



$^1\text{H-NMR}$ (ppm): 8.07 (m, 1H), 7.89 (m, 1H), 7.80 (m, 1H), 7.53 (m, 2H), 7.46 (m, 2H), 5.06(s, 2H), 2.49 (br, 1H).

$^{13}\text{C-NMR}$ (ppm): 136.3, 133.7, 131.2, 128.6, 128.5, 126.3, 125.8, 125.4, 125.3, 123.6, 63.4.

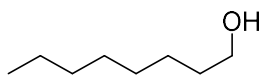
Compound 2j:



$^1\text{H-NMR}$ (ppm): 7.29 (m, 2H), 7.20 (m, 3H), 3.68 (t, $J=6.44\text{Hz}$, 2H), 2.72 (t, $J=6.41\text{ Hz}$, 2H), 1.90 (m, 2H), 1.64 (br, 1H).

$^{13}\text{C-NMR}$ (ppm): 141.8, 128.4 (2 peaks), 125.9, 62.3, 34.2, 32.1.

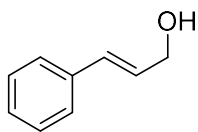
Compound 2k:



$^1\text{H-NMR}$ (ppm): 3.64 (t, $J=6.73\text{Hz}$, 2H), 1.55 (q, $J=6.73\text{Hz}$, 2H), 1.49 (br, 1H), 1.41-1.20 (m, 10H), 0.88 (m, 3H).

$^{13}\text{C-NMR}$ (ppm): 63.1, 32.8, 31.8, 29.3 (2 peaks), 25.6, 22.7, 14.1.

Compound 2n:



¹H-NMR (ppm): 7.43-7.19 (m, 5H), 6.62 (d, J=16.09Hz, 1H), 6.36 (dt, J= 16.09, 5.56Hz, 1H), 4.32 (d, J=5.56 Hz, 2H), 1.72 (br, 1H).

¹³C-NMR (ppm): 136.6, 131.1, 128.6, 127.7, 126.4, 63.7.

3.6 References

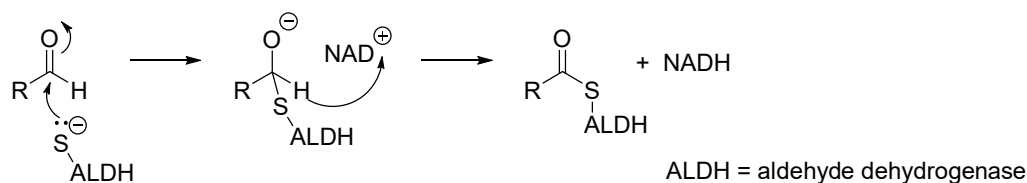
- [1] Jordan, A. J.; Lalic, G.; Sadighi, J. P. *Chem. Rev.* 2016, **116**, 8318-8372
- [2] Jia, Z.; Liu, M.; Li, X.; Chan, A. S. C.; Li, C.-J. *Synlett* 2013, **24**, 2049-2056.
- [3] Jia, Z.; Zhou, F.; Liu, M.; Li, X.; Chan, A. S. C.; Li, C.-J. *Angew. Chem. Int. Ed.*, 2013, **52**, 11871-11874.
- [4] Trost, B. M. *Angew. Chem., Int. Ed. Engl.* 1995, **34**, 259.
- [5] For a survey over recent transfer hydrogenation, see: He, Y.-M.; Fan, Q.-H. *ChemCatChem* 2015, **7**, 398-400
- [6] a) Bartoszewicz, A.; Nanna, A.; Belen, M.-M. *Chem. Eur. J.* 2013, **19**, 7274-7302; b) Liu, Z.; Sadler, P. J. *Acc. Chem. Res.* 2014, **47**, 1174-1185; c) Zhang, L.; Meggers, E. *Acc. Chem. Res.* 2017, **50**, 320-330.

Chapter 4 – ‘Silver Mirror’ from stoichiometric to catalytic

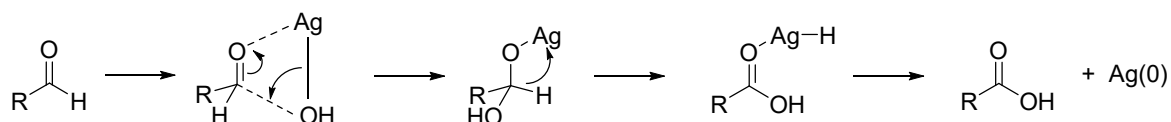
4.1 Hypothesis and objective

As established in chapter 1, oxidation of aldehyde represents the important counterpart of our research interest. Impressed by the high-efficiency of our previous developed silver(I)-catalyzed nucleophilic attack system towards carbonyl compounds [1], especially towards aldehydes activation, we started to question the feasibility of the silver(I) system to efficiently conduct desired aldehyde oxidation using this system. Our first inspiration came within our own human body – the nature’s oxidation of aldehyde catalyzed by aldehyde dehydrogenase (ALDH) in liver cell (Figure 4.1a) [2]. The oxidation was initiated by a nucleophilic attack from the thiol-anion of cysteine residue in ALDH, followed by the aldehyde hydride extracted by NAD^+ . It came to our notice that it could be very efficient to utilize our silver(I) system to deliver this initial nucleophilic

a) Biological oxidation of aldehyde (key step)



b) The classic Tollens reaction



c) Our hypothesis

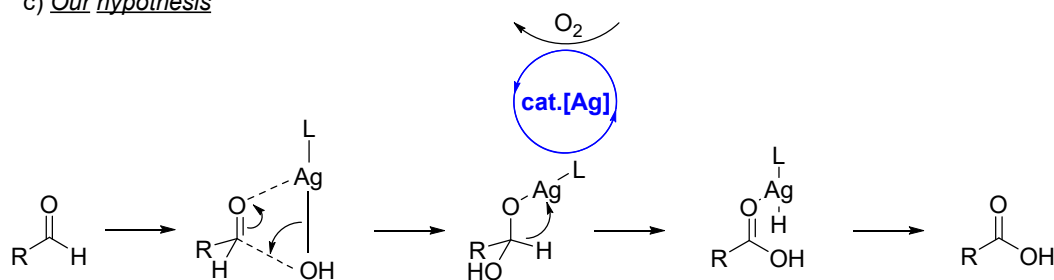


Figure 4.1. Our design for silver-catalyzed oxidation of aldehyde

attack. However, β -hydride elimination is rare in silver chemistry. It then came to our delight that the well-known Tollens oxidation (the ‘silver mirror’ test) also proceeds via a similar nucleophilic

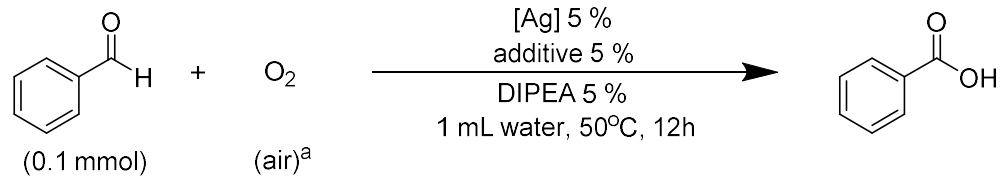
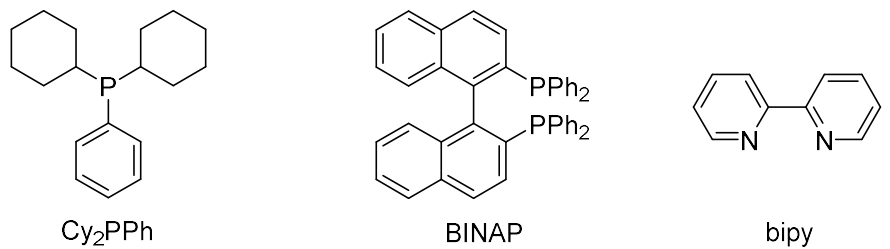
attack/ β -hydride elimination mechanism (Figure 4.1b) [3]. Such β -hydride elimination was possibly facilitated by electron lone pair on the neighbouring gem-diol anion [4]. These suggestions enable great potential for silver(I) to serve as a powerful catalyst towards oxidation of aldehyde, only by the introduction of oxygen to re-oxidize the Ag(0) generated in the Tollens oxidation back to Ag(I), and use ligand to stabilize the catalyst from precipitation (Figure 4.1c).

4.2 Results and discussion

4.2.1 Condition optimization

We then started our research using silver fluoride salt, pre-mixed with an electron-rich dicyclohexylphenylphosphine (Cy₂PPh) ligand in order to facilitate its interaction with molecular oxygen, as catalyst. 5 mol% DIPEA was added as base with water for its activity in the heterolysis of diatomic gas molecule (Table 4.1) [5]. The reaction vessel was directly sealed in air without flushing to enable the oxidation of benzaldehyde by oxygen sealed in the reaction vessel. After stirring at 50°C overnight, to our surprise, no oxidation occurred and there was no benzoic acid detected (entry 1). However, we were very delighted to find that the addition of a sodium salt, sodium formate, (NaCO₂H) gave 11 % yield of the benzoic acid with no benzyl alcohol detected (entry 2). Oxygen was also found to be responsible as oxidant as only less than 3 % yield was obtained when reaction vessel was flushed with argon (entry 3). Other sodium salt, for example, sodium fluoride (NaF), sodium chloride (NaCl), sodium bromide (NaBr), and sodium tetrafluoroborate (NaBF₄) was also examined (entry 4-7). NaF and NaBF₄ both gave 20 % yield with the later consume slightly more starting material. Keeping the fluoride anion, switching the counter-ion of the additional salt was ineffective, as all the other salt additive such as lithium fluoride (LiF), potassium fluoride (KF), magnesium fluoride (MgF₂), and aluminum fluoride (AlF₃) all gave complete starting material recovery (entry 8-11). Various catalyst ligands were also examined. The bidentate BINAP gave 21 % yield (entry 12). 2,2'-bipyridyl (bipy) gave 22 % yield (entry 13). Surprisingly, keeping bipy as ligand, switching AgF with AgPF₆ gave quantitative oxidation of benzaldehyde to the corresponding benzoic acid (entry 14). This yield boost can be explained as non-coordinative anion PF₆⁻ opens empty coordination site on silver to facilitate substrate binding. When then reaction was repeated using pure atmospheric oxygen instead of air, quantitative yield of benzoic acid was isolated (entry 15). The reaction is inefficient without the catalyst as only trace amount of benzoic acid was detected (entry 16).

Table 4.1. First condition optimization

<div style="display: flex; align-items: center; justify-content: center;"> <div style="text-align: center;">  <p>(0.1 mmol) (air)^a</p> </div> <div style="margin: 0 20px;"> $\xrightarrow[\text{1 mL water, 50}^\circ\text{C, 12h}]{\text{[Ag] 5 \% , additive 5 \% , DIPEA 5 \%}}$ </div> <div style="text-align: center;">  <p>Cy₂PPh BINAP bipy</p> </div> </div>				
Entry	[Ag]	additive	Starting Material Conversion	NMR Yield ^b
1	AgF/Cy ₂ PPh	—	0 %	0 %
2	AgF/Cy ₂ PPh	NaCO ₂ H	19 %	11 %
3 ^c	AgF/Cy ₂ PPh	NaCO ₂ H	5 %	< 3 %
4	AgF/Cy ₂ PPh	NaF	27 %	20 %
5	AgF/Cy ₂ PPh	NaCl	0 %	0 %
6	AgF/Cy ₂ PPh	NaBr	0 %	0 %
7	AgF/Cy ₂ PPh	NaBF ₄	30 %	20 %
8	AgF/Cy ₂ PPh	LiF	0 %	0 %
9	AgF/Cy ₂ PPh	KF	0 %	0 %
10	AgF/Cy ₂ PPh	MgF ₂	0 %	0 %
11	AgF/Cy ₂ PPh	AlF ₃	0 %	0 %
12	AgF/BINAP	NaF	31 %	21 %
13	AgF/bipy	NaF	30 %	22 %
14	AgPF ₆ /bipy	NaF	100 %	> 99 %
15 ^d	AgPF ₆ /bipy	NaF	100 %	> 99% ^e
16 ^d	—	NaF	trace	trace

^a All reactions were carried out in sealed 10 mL reaction vessels filled with atmospheric air or pure oxygen

^b ¹H-NMR Yield was determined using 1,3,5-mesitylene as an internal standard

^c Reaction was carried out under atmospheric argon

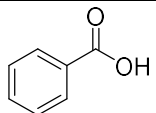
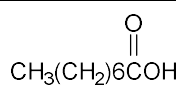
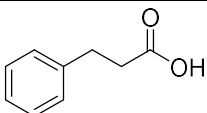
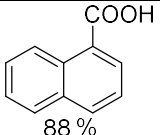
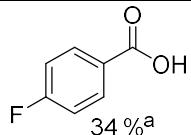
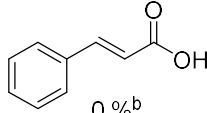
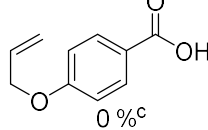
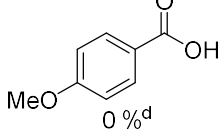
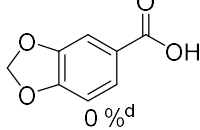
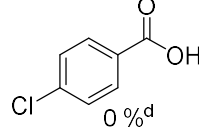
^d Reactions were carried out under atmospheric pure oxygen

^e Isolated Yield

4.2.2 First scope investigation

We then examined this condition with a handful of aldehyde substrates (Table 4.2). Other than benzaldehyde which gave quantitative isolated yield, aliphatic aldehyde octanal also gave quantitative isolated yield. Hydrocinnamaldehyde gave good 86 % isolated yield as well. 1-naphthaldehyde gave 88 % isolated yield. However, as we started to examine the tolerance of various other functional group substitution, we found *ortho*-fluorobenzaldehyde gave a reduced 34 % yield as 60 % starting material was converted. *Ortho*-chlorobenzaldehyde gave all starting material recovered. Cinnamaldehyde did not give the desired product while all the starting material was converted. 4-allyloxybenzaldehyde also did not give the desired product while 71 % starting material was converted. These results indicate the poor tolerance of our catalyst towards C=C bond, possibly due to catalyst's preference over more electron-rich C=C rather than more electron-poor C=O. 4-anisaldehyde also gave all starting material recovered, possibly due to relatively strong coordination of the oxygen atom. Similar piperonal also resulted in all starting material recovery.

Table 4.2. First scope examination

$ \begin{array}{c} \text{R}-\text{CHO} + \text{O}_2 \xrightarrow[\text{12h, 50}^\circ\text{C}]{\text{AgPF}_6/\text{bipy 5 \%}, \text{NaF 5 \%}, \text{DIPEA 5 \%}, \text{1 mL H}_2\text{O}} \text{R}-\text{COOH} \\ \text{0.1 mmol} \quad \quad \quad \text{1 bar} \quad \quad \quad \text{(Iso. Yield)} \end{array} $				
				
>99 %	>99 %	86 %	88 %	34 % ^a
				
0 % ^b	0 % ^c	0 % ^d	0 % ^d	0 % ^d

^a 60 % of starting material was converted

^b Starting material all converted

^c 71 % of starting material was converted

^d Starting material all recovered

4.2.3 Re-optimization of condition

To further optimize the functional tolerance of our oxidation, considering our previously obtained data in Table 4.1, the possible reasons could be the instability of catalyst, since stronger-coordinating heteroatoms and C=C bond eliminates the formation of desired product. To tackle

this problem, 2 strategies were proposed: 1) use electron-poor ligand to increase the oxidation potential of the catalyst; 2) use stronger-coordinating ligand to increase the stability of the catalyst. Piperonal was used as standard substrate for our optimization. To extract the product and push the equilibrium forward, 1 equiv. of NaOH was also added to transform the acid product into carboxylate form (Table 4.3). Under this condition, previous AgPF₆/bipy catalyst still gave all starting material recovered (entry 1). We first examine our above-proposed strategy one using electron-poor tris(1,1,1,3,3,3-hexafluoro-2-propyl)phosphite as ligand, premixing with AgPF₆ to generate the catalyst. As expected, the yield increased to 21 % (entry 2). However, on the other hand, 50 % starting material was consumed and we observed the loss of formaldehyde acetal substitution on piperonal. This probably indicates a milder oxidation is necessary. We then examined strategy two using stronger-coordinating trifurylphosphine. The yield also increased to a good 66 % with 80 % starting material consumption (entry 3). When examined even stronger-coordinating N-Heterocyclic Carbene (NHC) ligand 1,3-bis(2,6-diisopropylphenyl)imidazol-2-ylidene (IPr), which was generated by pre-mixing its imidazolium precursor with DBU as base, along with AgPF₆ added, the generated catalyst gave only 5 % yield (entry 4). Considering it is our first time trying to employ NHC ligand and our protocol might be inaccurate, we examined again a well-studied NHC-silver complex, IPr-Ag-Cl [6], generated by directly mixing IPr imidazolium chloride with silver oxide (Ag₂O). To our delight, almost quantitative yield of piperonylic acid was obtained (entry 5). At the same time, the post-experiment work-up was extremely facile and effective: just by washing the aqueous reaction mixture with minor organic solvent, such as dichloromethane or diethyl ether, then acidifying with hydrochloric acid (HCl) and extracting by diethyl ether, analytical-pure grade of product can be obtained very easily. Chromatography was generally unnecessary. Then, the attempt of reducing base load of this reaction resulted in decreased yield of product (entry 6). When Ag₂O alone was directly introduced to the reaction, only trace amount of product was obtained (entry 7). Using only free-carbene ligand also resulted in elimination of product (entry 8). AgCl alone was not effective either (entry 9). When we switched the reaction atmosphere with argon, we still can obtain 66 % yield with 69 % starting material consumed (entry 10). The reaction cannot be shut down unless we also degas the water solvent (entry 11). Considering most silver salt are light-sensitive, we conducted the reaction in dark and the same nearly-quantitative yield was obtained (entry 12).

Table 4.3. Re-optimization of condition

<div style="display: flex; align-items: center; justify-content: center;"> <div style="text-align: center;"> <p>0.1 mmol 1 bar</p> </div> <div style="margin: 0 20px;">+</div> <div style="text-align: center;"> O_2 1 bar </div> <div style="margin-left: 20px;"> $\xrightarrow{\text{AgX 5 \%}, \text{Ligand 5 \%}^a, \text{1 eq. NaOH}, \text{1 mL H}_2\text{O}, \text{50}^\circ\text{C}, \text{12h}}$ </div> <div style="text-align: center;"> <p>$[(CF_3)_2CHO]_3P$ trifurylphosphine IPr</p> </div> </div>				
Entry	AgX	Ligand	Starting Material Conversion	NMR Yield ^b
1	AgPF ₆	bipy	0 %	0 %
2	AgPF ₆	$[(CF_3)_2CHO]_3P$	50 %	21 %
3	AgPF ₆	trifurylphosphine	81 %	66 %
4	AgPF ₆ ^c	IPr ^d	9 %	5 %
5	Ag ₂ O ^e	IPr ^f	99 %	99 %
6 ^g	Ag ₂ O	IPr	50 %	50 %
7	Ag ₂ O	—	< 3 %	trace
8	—	IPr ^h	0 %	0 %
9	AgCl	—	0 %	0 %
10 ⁱ	Ag ₂ O	IPr	69 %	66 %
11 ^j	Ag ₂ O	IPr	7 %	5 %
12 ^k	Ag ₂ O	IPr	99 %	99 %

^a Silver(I) salt and the corresponding ligand were premixed in CH₂Cl₂ under inert gas at room temperature for 12h to generate the catalyst.

^b NMR yields were determined using 1,3,5-mesitylene as an internal standard.

^{c,d} This catalyst can be generated via mixing 5 mol % AgPF₆, 5 mol % imidazolium chloride corresponding to the NHC catalyst, and 5 mol % DBU in CH₂Cl₂ under inert gas at room temperature for 12h.

^{e,f} This catalyst can be generated via mixing 5 mol % Ag₂O with 5 mol % imidazolium chloride corresponding to the NHC catalyst. The mixture was stirred in acetonitrile under argon for 12h. The AgOH precipitate can either be filtered or left in the solution. The result is unaffected. The actual catalyst load is still 5 mol % due to half amount of silver being precipitated via AgOH.

^g This reaction is conducted with 0.5 eq. of NaOH.

^h This controlled experiment is conducted by mixing imidazolium chloride with DBU

ⁱ This reaction is done under argon with normal water

^j This reaction is done under argon with degassed water

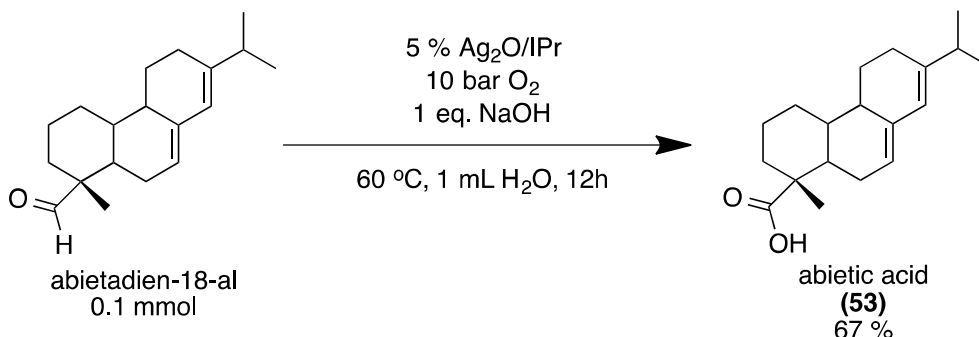
^k This reaction is done in dark

4.2.4 Second scope investigation

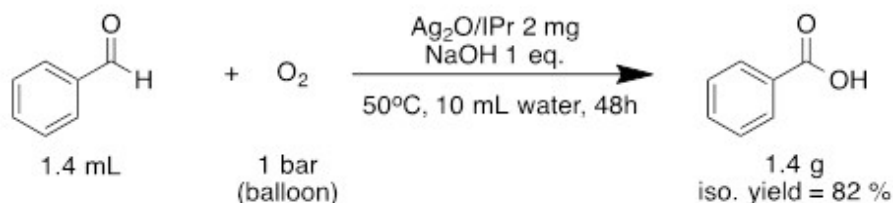
Inspired by the highly-efficient optimized condition in hand, along with the facile work-ups, we collected almost all the aldehydes in our inventory and examined the functional tolerance of our new condition (Table 4.4). Benzaldehyde gave quantitative yield of benzoic acid (**3a**). 4-tolualdehyde also gave quantitative yield of 4-toluic acid (**3b**). 1-indancarboxyaldehyde gave nearly quantitative yield of 1-indancarboxylic acid (**3c**). 1-naphthaldehyde gave quantitative yield of 1-naphthalic acid (**3d**). Piperonal gave nearly quantitative yield of piperonylic acid (**3e**). Other electron-rich aromatic aldehyde such as 4-anisaldehyde gave quantitative yield of 4-anisic acid (**3f**). 2-anisaldehyde gave a slightly reduced 97 % yield of 2-anisic acid (**3g**), possibly due to coordination of methoxy- group. At the same time 2,5-dimethoxybenzaldehyde gave quantitative yield of 2,5-dimethoxybenzoic acid (**3h**). 3,4,5-trimethoxybenzaldehyde also gave quantitative yield of eudesmic acid (**3i**). The purification of 4-pentoxybenzaldehyde and 4-hexoxybenzaldehyde require flash chromatography due to strong emulsifying during the extraction, possibly resulted in the slightly reduced 94 % and 90 % yield of 4-pentoxybenzoic acid (**3j**) and 4-hexoxybenzoic acid (**3k**), respectively. 4-allyloxybenzaldehyde gave quantitative yield of 4-allyloxybenzoic acid (**3l**), leaving the C=C bond intact and no Claisen Rearrangement observed. However, 4-benzyloxybenzaldehyde gave a reduced 65 % yield of 4-benzyloxybenzoic acid (**3m**), possibly due to hydrolysis of the ether since benzyloxy- is a better leaving group. 5-bromo-2,4-dimethoxybenzaldehyde also gave a reduced 77 % yield of 5-bromo-2,4-dimethoxybenzoic acid (**3n**). 5-bromobenzo[1,3]dioxole-4-carboxyaldehyde gave 72 % yield of 5-bromobenzo[1,3]dioxole-4-carboxylic acid (**3o**) either. Suspecting the possible influence of the halogen substitution, we examined 2-fluorobenzaldehyde and 4-fluorobenzaldehyde and gave the corresponding 2-fluorobenzoic acid (**3p**) and 4-fluorobenzoic acid (**3q**) in quantitative yield, indicating good tolerance of fluoro- substitution. 2-chlorobenzaldehyde, 3-chlorobenzaldehyde, 2,3-dichlorobenzaldehyde, 3,4-dichlorobenzaldehyde, and 2,6-dichlorobenzaldehyde all gave quantitative yield of the corresponding 2-chlorobenzoic acid (**3r**), 4-chlorobenzoic acid (**3s**), 2,3-dichlorobenzoic acid (**3t**), 3,4-dichlorobenzoic acid (**3u**), 2,6-dichlorobenzoic acid (**3v**), indicating very good tolerance of chloro-substitution either. 2-bromo-5-fluorobenzaldehyde also gave quantitative yield of 2-bromo-5-fluorobenzoic acid (**3w**), implying good tolerance of bromo-substitution either. A group of electron-deficient aromatic aldehyde was also examined. 4-cyanobenzaldehyde gave quantitative yield of 4-cyanobenzoic acid (**3x**). Terephthaldehyde gave

quantitative oxidation and complete selectivity towards 4-formylbenzoic acid (**3y**) under current condition, possibly due to the deprotonation of product and separation with the hydrophobic catalyst. However, when we increased the base load to 2 equiv., oxidation of both the formyl group was observed and approx. 30 % NMR yield was obtained. 4-acetylbenzaldehyde gave quantitative yield of 4-acetylbenzoic acid (**3z**). 4-acetaminobenzaldehyde gave quantitative yield as well (**3A**). 4-(hydroxymethyl)-benzaldehyde gave quantitative yield of 4-(hydroxymethyl)-benzaldehyde (**3B**), indicating good tolerance for alcohol hydroxyl- group. 4-quinolinecarboxyaldehyde gave a reduced 57 % yield of 4-quinolinecarboxylic acid (**3C**), possibly due to strong coordination of the nitrogen atom. Other heterocyclic aromatic aldehydes such as 2-furaldehyde and 2-thiophenecarboxyaldehyde gave quantitative and 60 % yield of 2-furic acid (**3D**) and 2-thiophenecarboxylic acid (**3E**), respectively. Nitro- substituted benaldehydes including 4-, 3-, and 2,4-disubstituted substrate all gave quantitative yield of the corresponding 4-nitrobenzoic acid (**3F**), 3-nitrobenzoic acid (**3G**), and 2,4-dinitrobenzoic acid (**3H**). 4-trifluoromethylbenzaldehyde also gave quantitative yield of 4-trifluoromethylbenzoic acid (**3I**). Aliphatic aldehydes were then examined. Hexanal, heptanal, octanal, and decanal all gave quantitative yield of hexanoic acid (**3J**), heptanoic acid (**3K**), octanoic acid (**3L**), and decanoic acid (**3M**), respectively. Branched chain aldehyde, including 2-methylbutanal, 2-methylpentanal, 2-ethylbutanal, and 2-ethylhexanal, resulted in quantitative yield of the corresponding 2-methylbutanoic acid (**3N**), 2-methylpentanoic acid (**3O**), 2-ethylbutanoic acid (**3P**), and 2-ethylhexanoic acid (**3Q**). 3,3-dimethylacrolein gave 3,3-dimethylacrylic acid (**3R**) in 77 % yield. Citronellal gave citronellic acid (**3S**) in 60 % yield. Citral gave geranic acid (**3T**) in 86 % yield. Cinnamaldehyde gave the corresponding cinnamic acid (**3U**) in quantitative yield. 2-methylcinnamaldehyde also gave 2-methylcinnamic acid (**3V**) in quantitative yield. Hydrocinnamaldehyde gave quantitative yield of hydrocinnamic acid (**3W**). 2-phenylpropionaldehyde gave quantitative yield of 2-phenylpropionic acid (**3X**). 4-nitrocinnamaldehyde gave an excellent 91 % yield of 4-nitrocinnamic acid (**3Y**). Natural product perillaldehyde gave quantitative oxidation of perillic acid (**3Z**). A much more complex natural product derivative, abietadien-18-al, with multiple unsaturated fuse-ring and a sterically hindered 3°-formyl group, was also succeeded in oxidizing to the corresponding abietic acid in 67 % yield with increased temperature and elevated oxygen pressure (Scheme 4.1), indicating the potential applicability of this method towards modern synthesis. Gram-scale oxidation was also successful

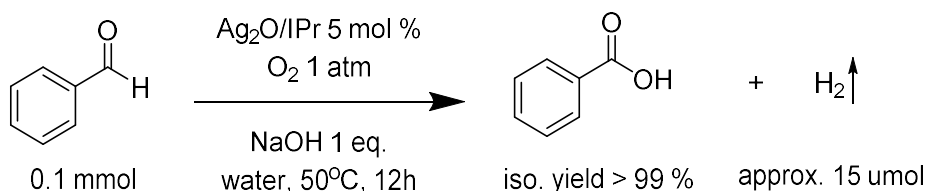
with only 2 mg of catalyst (360 ppm load) giving 82 % isolated yield when oxidizing 1.4 mL benzaldehyde (Scheme 4.2), indicating the potential applicability of this method in industrial scale.



Scheme 4.1. Aerobic oxidation of natural product



Scheme 4.2. Gram-scale oxidation test

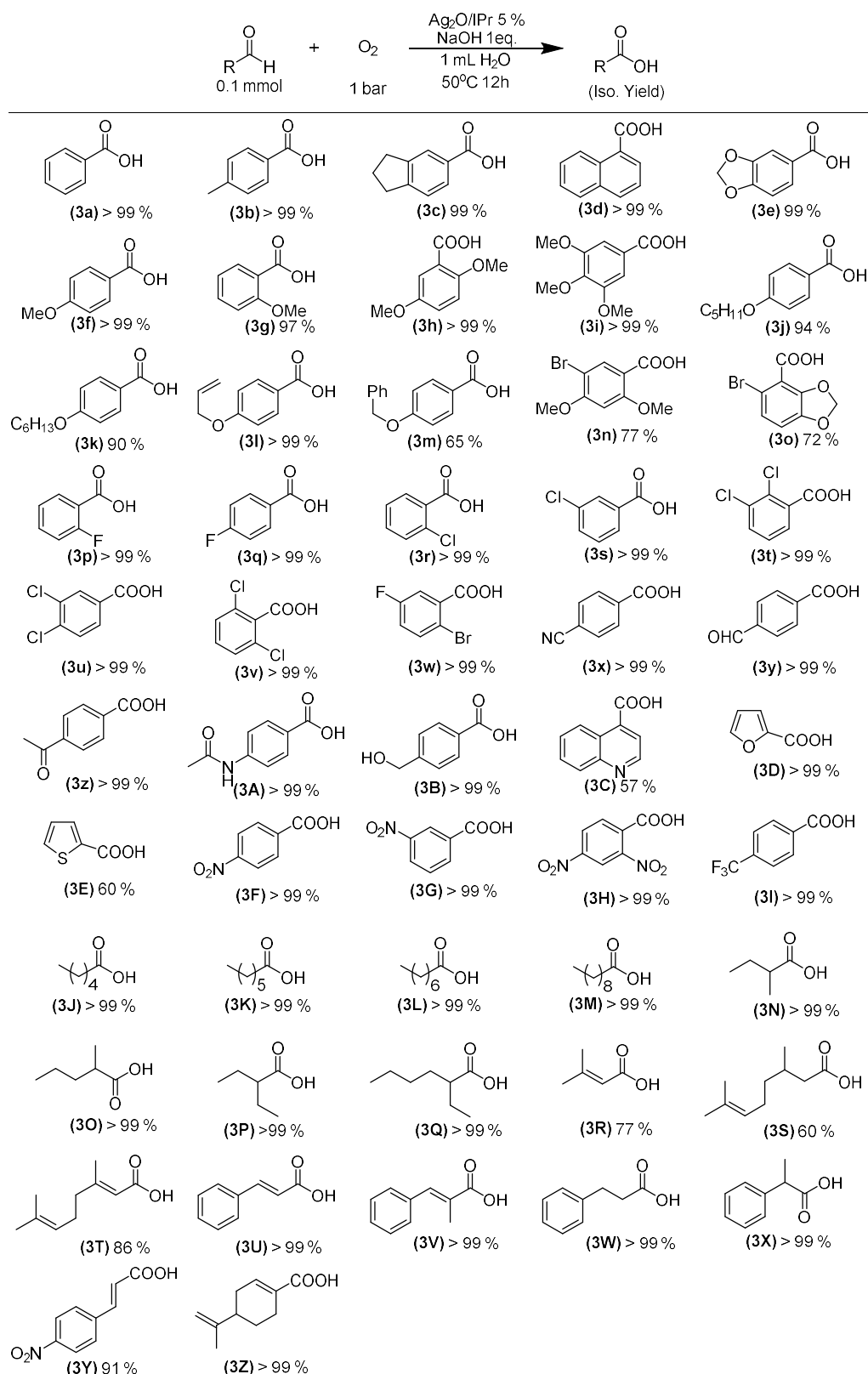


Scheme 4.3. Detection of hydrogen generated in our aerobic oxidation

4.2.5 Mechanism discussion

Lastly, we were interested in the mechanism behind this transformation. Our first proposal is that the oxidation proceeds through aldehyde C-H activation, which was suggested by some previous examples. [7] We then intended to examine the post-reaction atmosphere in the vessel, since decarbonylation was known for most transition-metals in catalysis involving such intermediate. Surprisingly, we did not observe the presence of carbon monoxide, (CO) instead a considerable amount of hydrogen was observed, (~10 μ L in 0.1 mmol scale reaction, see Scheme 4.3) which

Table 4.4. Final scope investigation



this area of research: 1) eliminating the need of stoichiometric oxidant; 2) reliability and widely-adapted substrate scope; 3) abandoning the need of chromatography in most purification. In our new method, atmospheric oxygen served as the sole oxidant, generating only water after oxidation. Over 50 examples of substrates with different structure and functionality were efficiently transformed into the corresponding carboxylic acid in excellent to quantitative yield, including complex nature product and gram-scale reaction. With extremely easy post-reaction work-ups, analytical pure grade products were obtained generally without the need of chromatography. This indicates that this method can be readily applicable outside laboratory and in industrial scale. Nowadays, among organic methodology researches, although many innovative results were published every day, most real-life industries are still applying very basic and traditional methods to do synthesis. In this way, our method could serve as an appealing solution to these problems. In the future, the efficiency for silver catalyst to activate molecular oxygen could potentially inspires silver-catalyzed aerobic oxidation of other substrates. For example, aerobic oxidative cleavage of 1,2-diol, which serves as another important method to install carboxylate group in the molecule, can be interesting. The above-mentioned work has already underway in our lab.

4.4 Contributions of authors

The initial discovery of this reaction was done by me. All the experiments depicted in this chapter, including but not limited to condition optimization, substrate scope investigation, and mechanism study, was carried out by me, with advices from Prof. Chao-Jun Li. Dr. Haining Wang did the computational study regarding the mechanism. Dr. Huiying Zeng contributed in repeating the oxidation of octanal and benzaldehyde under the optimized reaction condition and the gram-scale oxidation of benzaldehyde. Identifications of the products was mainly done by me using NMR spectrometer, with technical help from Dr. Huiying Zeng. The manuscript was prepared by me, with revisions from Prof. Chao-Jun Li, Dr. Haining Wang, and Dr. Huiying Zeng.

4.5 Experimental

4.5.1 General information

Unless otherwise noted, all oxidations were carried out in Biotage Microwave Reaction Vials size 2-5 mL equipped with a magnetic stir bar unless otherwise noticed. All reactions were in sealed closed system, no open-vial reaction is involved. No microwave is involved during the whole

investigation. All manipulation and purification procedures were carried out with reagent-grade solvents. Aldehydes which are in liquid form under normal conditions were redistilled under reduced pressure. abietadien-18-al was synthesized from abietic acid purchased from Sigma-Aldrich (purity ~ 75%) according to the previously reported method [8]. Pressurized oxidation was carried out using Biotage Endeavor Catalyst Screening System. Analytical thin-layer chromatography (TLC) was performed using E. Merck silica gel 60 F₂₅₄ precoated plates (0.25 mm). Flash chromatography was performed with Biotage Isolera One Flash Purification System, using Biotage SNAP Ultra 25g prepared column. Nuclear magnetic resonance (NMR) spectra were recorded on Varian MERCURY plus-300 spectrometer (¹H 300 MHz, ¹³C 75 MHz) or a Bruker Ascend 500 spectrometer (¹H 500 MHz, ¹³C 125 MHz). Chemical shifts for ¹H NMR spectra are reported in parts per million (ppm) from tetramethylsilane with the solvent resonance as the internal standard (CDCl₃: δ 7.26 ppm, DMSO: δ 2.46 ppm). Chemical shifts for ¹³C NMR spectra are reported in parts per million (ppm) from tetramethylsilane with the solvent as the internal standard (CDCl₃: δ 77.0 ppm, DMSO: δ 40.0 ppm). Data are reported as following: chemical shift, multiplicity (s = singlet, d = doublet, dd = doublet of doublets, t = triplet, q = quartet, m = multiplet, br = broad signal), and integration.

4.5.2 General procedures

(General procedures for the catalyst generation). An oven-dried reaction vessel, charged with 25.3 mg silver (I) hexafluorophosphate (0.1 mmol, 1 equiv.) and 15.6 mg 2,2'-bipyridine (bipy, 0.1 mmol, 1 equiv.), is flushed with argon 3 times. 2.5 mL of dry, air-free methylene chloride (DCM) is added into the vessel. The vessel is then sealed and stirred at room temperature overnight (12 h). The mixture can then be stripped of solvent with rotary evaporator in atmosphere and the resulting solid should be kept at a desiccator if not intend to use at once.

(Procedures for the synthesise of silver(I)-NHC catalyst). An oven-dried reaction vessel, charged with 23.2 mg silver (I) oxide (0.1 mmol, 1 equiv.; 2 equiv. of silver(I)) and 42.5 mg 1,3-bis(2,6-diisopropylphenyl)imidazolium chloride (IPr in imidazolium form, 0.1 mmol, 1 equiv), is flushed with argon 3 times. 3 mL of dry, air-free acetonitrile is added into the vessel. The vessel is then sealed and stirred at room temperature overnight (12 h). The reaction mixture can then be filtered or avoid so, the catalyst efficiency is unaffected. The mixture can then be stripped of

solvent with rotary evaporator in atmosphere and the resulting solid should be kept at a desiccator if not intend to use at once.

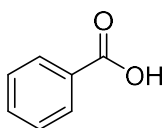
(General procedures for the oxidation of aldehydes using silver(I)-bipy catalyst). A reaction vessel, charged with 2.1 mg silver(I)-bipy catalyst (0.005 mmol, 5 mol %) and 2.1 mg sodium fluoride (0.005 mmol, 5 mol %), is gently flushed with oxygen of ordinary purity with a balloon or gas valve. After this, 1 mL of distilled water is added to the vessel, followed by the addition of 0.8 μ L of N,N-diisopropylethylamine (DIPEA, 0.005 mmol, 5 mol %). The reaction mixture is then warmed up to 50°C before the aldehyde (0.1 mmol, 1equiv.) can be added. The reaction vessel is then sealed and kept at 50°C for 12 h. After this, the pH of the reaction mixture is adjusted to 12 with 0.1M NaOH. The reaction mixture is then washed with methylene chloride (DCM) three times with a total DCM volume of 10 mL and the pH of the aqueous phase is adjusted to 2 with 0.1M HCl. The aqueous is then extracted with ethyl ether 3 times with a total ether volume of 10 mL and the combined organic phase is dried over anhydrous sodium sulfate and evaporated to obtain the carboxylic acid product.

(General procedures for the oxidation of aldehydes using silver(I)-NHC catalyst). A reaction vessel, charged with 2 mg silver(I)-IPr catalyst (0.005 mmol, 5 mol %; if the AgCl precipitate has not been removed during the catalyst generation, 3.4 mg catalyst should be used.), is gently flushed with oxygen of ordinary purity with a balloon or gas valve. After this, 1 mL of distilled water with 4 mg NaOH (1 equiv.) dissolved inside is added to the vessel, followed by the addition of aldehydes (0.1 mmol, 1 equiv.). The reaction vessel is then sealed and kept in a 50°C oil bath for 12 h. After this, the reaction mixture is washed with methylene chloride (DCM) three times with a total DCM volume of 10 mL and the pH of the aqueous phase is adjusted to 2 with 0.1M HCl. The aqueous is then extracted with ethyl ether 3 times with a total ether volume of 10 mL and the combined organic phase is dried over anhydrous sodium sulfate and evaporated to obtain the carboxylic acid product. Flash chromatography is generally not required but can be performed in order to obtain an even higher purity level.

4.5.3 Identification of products.

All compounds are literature known and the data reported herein are consistent with the literature reports.

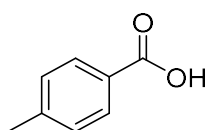
Compound 3a:



$^1\text{H-NMR}$ (ppm): 8.14 (m, 5H), 7.63 (tt, $^3\text{J}=7.32\text{Hz}$, $^4\text{J}=2.05\text{Hz}$, 1H), 7.49 (t, $^3\text{J}=7.32\text{Hz}$, 2H)

$^{13}\text{C-NMR}$ (ppm): 172.7, 133.8, 130.2, 129.3, 128.5

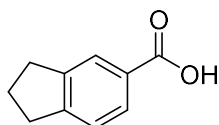
Compound 3b:



$^1\text{H-NMR}$ (ppm): 12.77 (br, 1H), 7.82 (d, $^3\text{J}=8.19\text{Hz}$, 2H), 7.28 (d, $^3\text{J}=8.19\text{Hz}$, 2H), 2.35 (s, 3H)

$^{13}\text{C-NMR}$ (ppm): 167.7, 143.5, 129.8, 129.6, 128.5, 21.6

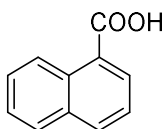
Compound 3c:



$^1\text{H-NMR}$ (ppm): 7.96 (s, 1H), 7.92 (d, $^3\text{J}=7.90\text{Hz}$, 1H), 7.30 (d, $^3\text{J}=7.90$, 1H), 2.97 (t, $^3\text{J}=7.61\text{Hz}$, 4H), 2.13 (m, $^3\text{J}=7.61\text{Hz}$, 2H)

$^{13}\text{C-NMR}$ (ppm): 172.5, 151.1, 144.7, 128.6, 127.3, 126.1, 124.3, 33.1, 32.5, 25.4

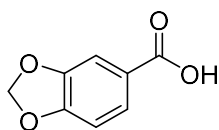
Compound 3d:



$^1\text{H-NMR}$ (ppm): 9.10 (d, $^3\text{J}=8.78\text{Hz}$, 1H), 8.44 (dd, $^3\text{J}=7.32\text{Hz}$, $^4\text{J}=1.46\text{Hz}$, 1H), 8.11 (d, $^3\text{J}=7.90\text{Hz}$, 1H), 7.93 (d, $^3\text{J}=7.90\text{Hz}$, 1H), 7.68 (m, 1H), 7.57 (m, 2H)

$^{13}\text{C-NMR}$ (ppm): 173.2, 134.7, 133.9, 131.9, 131.6, 128.7, 128.1, 126.3, 125.9, 125.5, 124.5

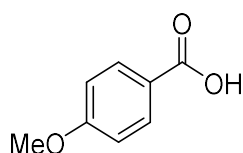
Compound 3e:



$^1\text{H-NMR}$ (ppm): 12.63 (br, 1H), 7.55 (dd, $^3J=8.24\text{Hz}$, $^4J=1.83\text{Hz}$, 1H), 7.36 (d, $^4J=1.83\text{Hz}$, 1H), 7.00 (d, $^3J=8.24\text{Hz}$, 1H), 6.12 (s, 3H)

$^{13}\text{C-NMR}$ (ppm): 167.1, 151.6, 147.9, 125.4, 125.1, 109.2, 108.5, 102.4

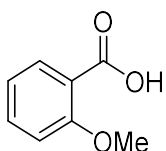
Compound 3f:



$^1\text{H-NMR}$ (ppm): 12.60 (br, 1H), 7.88 (dt, $^3J=9.07\text{Hz}$, $^4J=2.05\text{Hz}$, 2H), 7.00 (dt, $^3J=9.07\text{Hz}$, $^4J=2.05\text{Hz}$, 2H), 3.80 (s, 3H)

$^{13}\text{C-NMR}$ (ppm): 167.4, 163.3, 131.8, 123.4, 114.3, 55.9

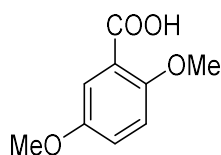
Compound 3g:



$^1\text{H-NMR}$ (ppm): 7.61 (dd, $^3J=7.90\text{Hz}$, $^4J=2.05\text{Hz}$, 1H), 7.48 (m, 1H), 7.10 (d, $^3J=8.49\text{Hz}$, 1H), 6.97 (dt, $^3J=7.32\text{Hz}$, $^4J=0.88\text{Hz}$, 1H), 3.79 (s, 3H)

$^{13}\text{C-NMR}$ (ppm): 167.8, 158.5, 133.5, 131.0, 121.7, 120.4, 112.9, 56.1

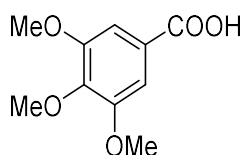
Compound 3h:



$^1\text{H-NMR}$ (ppm): 12.55 (br, 1H), 7.14 (m, 1H), 7.05 (m, 2H), 3.74 (s, 3H), 3.71 (s, 3H)

^{13}C -NMR (ppm): 167.5, 153.0, 152.6, 122.4, 118.8, 115.7, 114.6, 56.8, 56.0

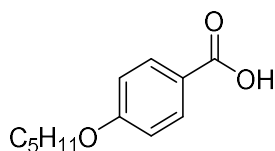
Compound 3i:



^1H -NMR (ppm): 7.21 (s, 2H), 3.80 (s, 6H), 3.70 (s, 3H)

^{13}C -NMR (ppm): 167.4, 153.1, 141.8, 126.4, 107.0, 60.6, 56.4

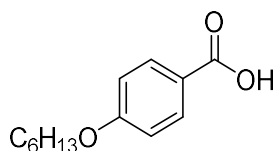
Compound 3j:



^1H -NMR (ppm): 8.06 (dt, $^3J=9.07\text{Hz}$, $^4J=2.05\text{Hz}$, 2H), 6.94 (dt, $^3J=9.07\text{Hz}$, $^4J=2.05\text{Hz}$, 2H), 4.02 (t, $^3J=6.44\text{Hz}$, 2H), 1.82 (m, $^3J=7.61\text{Hz}$, $^3J=6.44\text{Hz}$, 2H), 1.43 (m, 4H), 0.94 (t, $^3J=7.02\text{Hz}$, 3H)

^{13}C -NMR (ppm): 171.8, 163.7, 132.3, 121.3, 114.2, 68.3, 28.8, 28.1, 22.4, 14.0

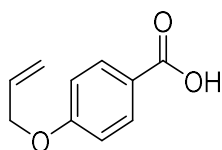
Compound 3k:



^1H -NMR (ppm): 8.05 (dt, $^3J=8.78\text{Hz}$, $^4J=1.76\text{Hz}$, 2H), 6.93 (dt, $^3J=8.78\text{Hz}$, $^4J=1.76\text{Hz}$, 2H), 4.02 (t, 6.73Hz, 2H), 1.81 (m, $^3J=7.90\text{Hz}$, $^3J=6.73\text{Hz}$, 2H), 1.47 (m, 2H), 1.35 (m, 4H), 0.91 (m, 3H)

^{13}C -NMR (ppm): 171.1, 163.7, 132.3, 121.3, 114.2, 68.3, 31.5, 29.0, 25.6, 22.6, 14.0

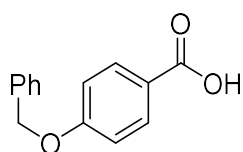
Compound 3l:



$^1\text{H-NMR}$ (ppm): 12.59 (br, 1H), 7.86 (dt, $^3J=9.07\text{Hz}$, $^4J=2.05\text{Hz}$, 2H), 7.00 (dt, $^3J=9.07\text{Hz}$, $^4J=2.05\text{Hz}$, 2H), 6.02 (m, 1H), 5.32 (m, $J=17.26\text{Hz}$, $J=10.53$, 2H), 4.62 (dt, $^3J=5.27\text{Hz}$, $^4J=1.46\text{Hz}$, 2H)

$^{13}\text{C-NMR}$ (ppm): 167.4, 162.2, 133.6, 131.8, 123.5, 118.3, 114.9, 68.8

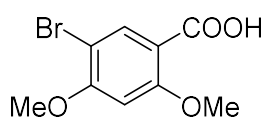
Compound 3m:



$^1\text{H-NMR}$ (ppm): 12.61 (br, 1H), 7.86 (d, $^3J=9.07\text{Hz}$, 2H), 7.38 (m, 5H), 7.08 (d, $^3J=9.07\text{Hz}$, 2H), 5.16 (s, 2H)

$^{13}\text{C-NMR}$ (ppm): 162.4, 137.0, 131.8, 128.9, 128.4, 128.2, 115.1, 69.9

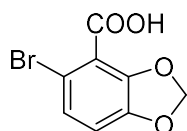
Compound 3n:



$^1\text{H-NMR}$ (ppm): 12.47 (br, 1H), 7.83 (s, 1H), 6.76 (s, 1H), 3.93 (s, 3H), 3.86 (s, 3H)

$^{13}\text{C-NMR}$ (ppm): 165.8, 160.8, 159.7, 135.5, 100.6, 98.5, 57.1, 56.7

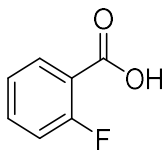
Compound 3o:



$^1\text{H-NMR}$ (ppm): 13.69 (br, 1H), 7.10 (d, $^3J=8.19\text{Hz}$, 1H), 6.94 (d, $^3J=8.19\text{Hz}$, 1H), 6.12 (s, 2H)

$^{13}\text{C-NMR}$ (ppm): 165.1, 147.8, 146.7, 126.0, 118.3, 111.1, 109.7, 103.1

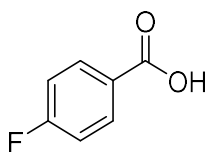
Compound 3p:



$^1\text{H-NMR}$ (ppm): 13.21 (br, 1H), 7.84 (m, 1H), 7.53 (m, 1H), 7.20 (m, 2H)

$^{13}\text{C-NMR}$ (ppm): 165.5, 163.3 159.9 ($^1\text{J}_{\text{C-F}}=256.91\text{Hz}$), 134.9 134.8 ($^3\text{J}_{\text{C-F}}=8.62\text{Hz}$), 132.3 132.30 ($^4\text{J}_{\text{C-F}}=1.15\text{Hz}$), 124.7 124.6 ($^3\text{J}_{\text{C-F}}=3.45\text{Hz}$), 119.8 119.7 ($^2\text{J}_{\text{C-F}}=10.35\text{Hz}$), 117.3, 117.0 ($^2\text{J}_{\text{C-F}}=22.41\text{Hz}$)

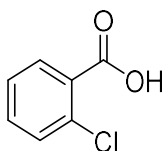
Compound 3q:



$^1\text{H-NMR}$ (ppm): 13.04 (br, 1H), 7.98 (m, $^3\text{J}=9.07\text{Hz}$, $^3\text{J}_{\text{H-F}}=5.56\text{Hz}$, 2H), 7.30 (m, $^3\text{J}=9.07$, 2H)

$^{13}\text{C-NMR}$ (ppm): 167.0 163.7 ($^1\text{J}_{\text{C-F}}=250.59\text{Hz}$), 166.8, 132.6 132.5 ($^3\text{J}_{\text{C-F}}=9.20\text{Hz}$), 127.8 127.8 ($^4\text{J}_{\text{C-F}}=2.87\text{Hz}$), 116.2 115.9 ($^2\text{J}=22.41\text{Hz}$)

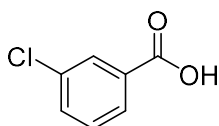
Compound 3r:



$^1\text{H-NMR}$ (ppm): 13.36 (br, 1H), 7.76 (m, 1H), 7.52 (m, 2H), 7.42 (m, 1H)

$^{13}\text{C-NMR}$ (ppm): 167.2, 133.0, 132.0, 131.9, 131.2, 131.1, 127.7

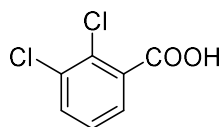
Compound 3s:



$^1\text{H-NMR}$ (ppm): 13.31 (br, 1H), 7.88 (m, 2H), 7.69 (m, 1H), 7.52 (t, $^3\text{J}=7.90\text{Hz}$, 1H)

^{13}C -NMR (ppm): 166.5, 133.8, 133.3, 133.2, 131.1, 129.3, 128.4

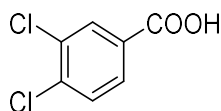
Compound 3t:



^1H -NMR (ppm): 13.63 (br, 1H), 7.78 (dd, $^3J=8.19\text{Hz}$, $^4J=1.46\text{Hz}$, 1H), 7.68 (dd, $^3J=7.90\text{Hz}$, $^4J=1.46\text{Hz}$, 1H), 7.43 (t, $^3J=8.19\text{Hz}$, $^3J=7.90\text{Hz}$, 1H)

^{13}C -NMR (ppm): 166.8, 135.0, 133.3, 133.1, 129.6, 129.2, 128.9

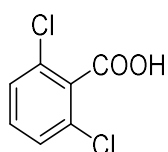
Compound 3u:



^1H -NMR (ppm): 13.45 (br, 1H), 8.04 (d, $^4J=2.05\text{Hz}$, 1H), 7.86 (dd, $^3J=8.19\text{Hz}$, $^4J=2.05\text{Hz}$, 1H), 7.76 (d, $^3J=8.19\text{Hz}$, 1H)

^{13}C -NMR (ppm): 165.9, 136.2, 132.0, 131.9, 131.5, 131.4, 129.8

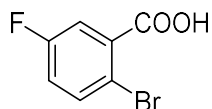
Compound 3v:



^1H -NMR (ppm): 14.00 (br, 1H), 7.52 (m, 3H)

^{13}C -NMR (ppm): 165.8, 131.9, 130.4, 128.7 (2 signals)

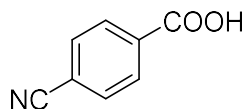
Compound 3w:



^1H -NMR (ppm): 13.66 (br, 1H), 7.74 (dd, $^3J=8.78\text{Hz}$, $^4J_{\text{H-F}}=4.97$, 1H), 7.57 (dd, $^3J_{\text{H-F}}=8.78\text{Hz}$, $^4J=3.22\text{Hz}$, 1H), 7.32 (dt, $^3J=^3J_{\text{H-F}}=8.78\text{Hz}$, $^4J=3.22\text{Hz}$, 1H)

^{13}C -NMR (ppm): 166.7, 163.0 159.7 ($^1\text{J}_{\text{C-F}}=246.56\text{Hz}$), 136.1 136.0 ($^3\text{J}_{\text{C-F}}=8.05\text{Hz}$, 2C), 120.3 120.0 ($^2\text{J}_{\text{C-F}}=22.91\text{Hz}$), 118.0 117.7 ($^2\text{J}_{\text{C-F}}=22.91\text{Hz}$), 115.0 115.0 ($^4\text{J}_{\text{C-F}}=2.87\text{Hz}$)

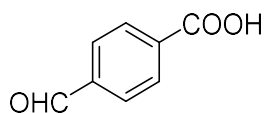
Compound 3x:



^1H -NMR (ppm): 13.46 (br, 1H), 8.06 (d, $^3\text{J}=8.49\text{Hz}$, 2H), 7.96 (d, $^3\text{J}=8.49\text{Hz}$, 2H)

^{13}C -NMR (ppm): 166.5, 135.3, 133.1, 130.4, 118.6, 115.5

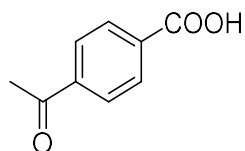
Compound 3y:



^1H -NMR (ppm): 13.37 (br, 1H), 10.09 (s, 1H), 8.12 (d, $^3\text{J}=8.49\text{Hz}$, 2H), 8.00 (d, $^3\text{J}=8.49\text{Hz}$, 2H)

^{13}C -NMR (ppm): 193.4, 167.0, 139.3, 136.1, 130.4, 130.0

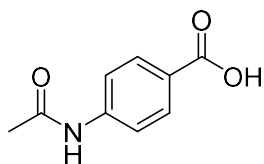
Compound 3z:



^1H -NMR (ppm): 13.28 (br, 1H), 8.03 (m, 4H), 2.61 (s, 3H)

^{13}C -NMR (ppm): 198.1, 167.1, 140.3, 134.9, 130.0, 128.8, 27.4

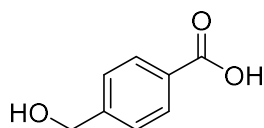
Compound 3A:



^1H -NMR (ppm): 12.64 (br, 1H), 10.12 (s, 1H), 7.86 (d, $^3\text{J}=8.78\text{Hz}$, 2H), 7.66 (d, $^3\text{J}=8.78\text{Hz}$, 2H), 2.06 (s, 3H)

^{13}C -NMR (ppm): 169.3, 167.4, 143.8, 130.8, 125.3, 118.6, 24.6

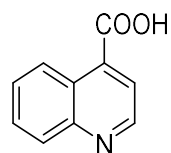
Compound 3B:



^1H -NMR (ppm): 12.81 (br, 1H), 7.88 (d, $^3J=8.19\text{Hz}$, 2H), 7.40 (d, $^3J=8.19\text{Hz}$, 2H), 5.32 (br, 1H), 4.55 (s, 2H)

^{13}C -NMR (ppm): 167.7, 148.2, 141.3, 129.6, 126.7, 126.6, 62.9

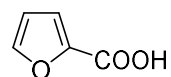
Compound 3C:



^1H -NMR (ppm): 9.04 (d, $^3J=4.39\text{Hz}$, 1H), 8.68 (dd, $^3J=8.49\text{Hz}$, $^4J=0.88\text{Hz}$, 1H), 8.10 (dd, $^3J=8.49\text{Hz}$, $^4J=0.88\text{Hz}$, 1H), 7.92 (d, $^3J=4.39\text{Hz}$, 1H), 7.83 (dt, $^3J=8.49\text{Hz}$, $^4J=1.46\text{Hz}$, 1H), 7.72 (m, 1H)

^{13}C -NMR (ppm): 168.0, 150.8, 148.7, 130.3, 130.0, 128.5, 126.0, 124.8, 122.4

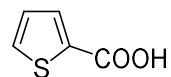
Compound 3D:



^1H -NMR (ppm): 7.65 (m, 1H), 7.34 (dd, $^3J=3.51\text{Hz}$, $^4J=0.88\text{Hz}$, 1H), 6.56 (dd, $^3J=3.51\text{Hz}$, $^4J=1.76\text{Hz}$, 1H)

^{13}C -NMR (ppm): 163.1, 147.4, 143.8, 120.1, 112.3

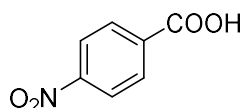
Compound 3E:



$^1\text{H-NMR}$ (ppm): 7.91 (dd, $^3J=3.80\text{Hz}$, $^4J=1.17\text{Hz}$, 1H), 7.66 (dd, $^3J=4.97\text{Hz}$, $^4J=1.15\text{Hz}$, 1H), 7.15 (dd, $^3J=3.80\text{Hz}$, $^3J=4.97$, 1H)

$^{13}\text{C-NMR}$ (ppm): 167.4, 135.0, 134.0, 132.8, 128.1

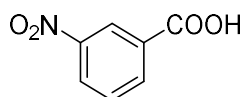
Compound 3F:



$^1\text{H-NMR}$ (ppm): 13.56, 8.30 (d, $^3J=9.07\text{Hz}$, 2H), 8.15 (d, $^3J=9.07\text{Hz}$, 2H),

$^{13}\text{C-NMR}$ (ppm): 166.2, 150.5, 136.9, 131.1, 124.2

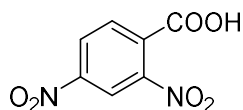
Compound 3G:



$^1\text{H-NMR}$ (ppm): 8.59 (m, 1H), 8.44 (m, 1H), 8.32 (m, 1H), 7.79 (t, $^3J=8.19\text{Hz}$, $^3J=7.90\text{Hz}$, 1H)

$^{13}\text{C-NMR}$ (ppm): 166.0, 148.3, 135.8, 132.9, 131.0, 127.8, 124.1

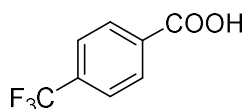
Compound 3H:



$^1\text{H-NMR}$ (ppm): 8.76 (d, $^4J=2.34\text{Hz}$, 1H), 8.56 (dd, $^3J=8.49\text{Hz}$, $^4J=2.34\text{Hz}$, 1H), 8.10 (d, $^3J=8.49\text{Hz}$, 1H)

$^{13}\text{C-NMR}$ (ppm): 165.3, 149.2, 148.4, 133.0, 131.9, 128.4, 120.0

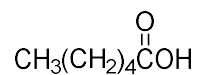
Compound 3I:



$^1\text{H-NMR}$ (ppm): 13.5 (br, 1H), 8.1 (d, $^3J=7.90\text{Hz}$, 2H), 7.8 (d, $^3J=7.90\text{Hz}$, 2H)

^{13}C -NMR (ppm): 167.4, 135.8, 133.7 (q, $^2J_{\text{C-F}}=31.61\text{Hz}$), 131.3, 126.8 (q, $^3J_{\text{C-F}}=4.02\text{Hz}$), 123.2

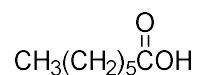
Compound 3J:



^1H -NMR (ppm): 2.35 (t, $^3J=7.61\text{Hz}$, 2H), 1.64 (m, 2H), 1.32 (m, 4H), 0.90 (m, 3H)

^{13}C -NMR (ppm): 179.9, 34.0, 31.2, 24.3, 22.3, 13.9

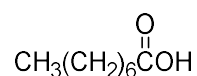
Compound 3K:



^1H -NMR (ppm): 2.35 (t, $^3J=7.61\text{Hz}$, 2H), 1.63 (m, 2H), 1.30 (m, 6H), 0.89 (m, 3H)

^{13}C -NMR (ppm): 178.3, 33.7, 31.4, 28.7, 24.6, 22.5, 14.0

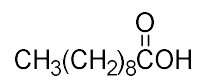
Compound 3L:



^1H -NMR (ppm): 2.35 (t, $^3J=7.61\text{Hz}$, 2H), 1.63 (m, 2H), 1.29 (m, 8H), 0.88 (m, 3H)

^{13}C -NMR (ppm): 180.8, 34.6, 32.2, 29.6, 29.5, 25.2, 23.2, 14.6

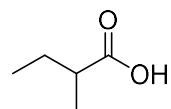
Compound 3M:



^1H -NMR (ppm): 2.35 (t, $^3J=7.61\text{Hz}$, 2H), 1.63 (m, 2H), 1.26 (m, 12H), 0.88 (m, 3H)

^{13}C -NMR (ppm): 179.0, 33.8, 31.8, 29.4, 29.2, 29.0, 24.7, 22.6, 14.1

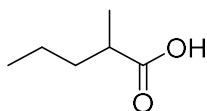
Compound 3N:



$^1\text{H-NMR}$ (ppm): 2.40 (m, $^3J=6.73\text{Hz}$, 2H), 1.69 1.50 (dm, 2H), 1.18 (d, $^3J=7.02\text{Hz}$, 3H), 0.95 (t, $^3J=7.32\text{Hz}$, 3H)

$^{13}\text{C-NMR}$ (ppm): 183.1, 40.8, 26.5, 16.3, 11.5

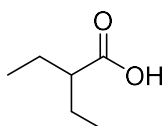
Compound 3O:



$^1\text{H-NMR}$ (ppm): 2.47 (m, $^3J=7.02\text{Hz}$, 1H), 1.66 1.43(dm, 2H), 1.37 (m, 2H), 1.18 (d, $^3J=6.73\text{Hz}$, 3H), 0.92 (m, 3H)

$^{13}\text{C-NMR}$ (ppm): 183.1, 39.1, 35.7, 20.3, 16.8, 13.9

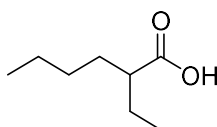
Compound 3P:



$^1\text{H-NMR}$ (ppm): 2.23 (m, 1H), 1.57 (m, 4H), 0.94 (t, $^3J=7.32\text{Hz}$, 6H)

$^{13}\text{C-NMR}$ (ppm): 183.2, 49.2, 25.3, 12.3

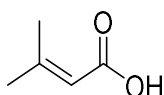
Compound 3Q:



$^1\text{H-NMR}$ (ppm): 2.29 (m, 1H), 1.57 (dm, 4H), 1.30 (m, 4H), 0.93 (m, 6H)

$^{13}\text{C-NMR}$ (ppm): 182.4, 47.0, 31.4, 29.5, 25.2, 22.6, 13.9, 11.7

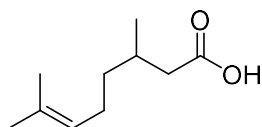
Compound 3R:



$^1\text{H-NMR}$ (ppm): 5.71 (m, 1H), 2.18 (d, $^4J=1.17\text{Hz}$, 3H), 1.93 (d, $^4J=1.17\text{Hz}$, 3H)

^{13}C -NMR (ppm): 170.6, 159.7, 115.3, 27.7, 20.5

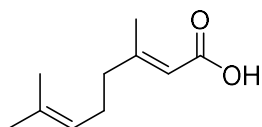
Compound 3S:



^1H -NMR (ppm): 5.09 (m, 1H), 2.37 2.15 (dm, $^2J=14.92\text{Hz}$, $^3J=5.85\text{Hz}$, 2H), 1.99 (m, 2H), 1.68 (s, 3H), 1.60 (s, 3H), 1.31 (dm, 2H), 0.98 (d, $^3J=6.44\text{Hz}$, 3H)

^{13}C -NMR (ppm): 178.7, 131.7, 124.1, 41.3, 36.7, 29.8, 25.7, 25.4, 19.6, 17.6

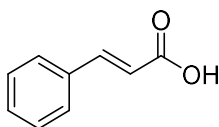
Compound 3T:



^1H -NMR (ppm): 5.70 (m, 1H), 5.07 (m, 1H), 2.18 (m, 7H), 1.69 (s, 3H), 1.61 (s, 3H)

^{13}C -NMR (ppm): 170.5, 163.0, 132.7, 122.8, 114.7, 41.2, 26.0, 25.7, 17.7(2 signals)

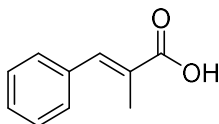
Compound 3U:



^1H -NMR (ppm): 12.26 (br, 1H), 7.66 (m, 2H), 7.58 (d, $^3J_{\text{trans}}=16.09\text{Hz}$, 1H), 7.39 (m, 3H), 6.51 (d, $^3J_{\text{trans}}=16.09\text{Hz}$, 1H)

^{13}C -NMR (ppm): 168.0, 144.4, 134.7, 130.7, 129.3, 128.6, 119.7

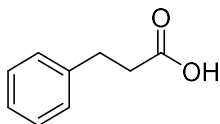
Compound 3V:



^1H -NMR (ppm): 12.54 (br, 1H), 7.58 (d, $^4J=1.46\text{Hz}$, 1H), 7.44 (m, 5H), 2.00 (d, $^4J=1.46\text{Hz}$, 3H)

^{13}C -NMR (ppm): 169.8, 138.1, 136.0, 130.0, 128.9, 128.8, 14.4

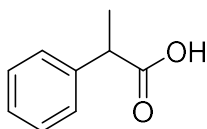
Compound 3W:



^1H -NMR (ppm): 7.31 (m, 2H), 7.23 (m, 3H), 2.97 (t, $^3J=8.19\text{Hz}$, 2H), 2.70 (t, $^3J=8.19\text{Hz}$, 2H)

^{13}C -NMR (ppm): 179.1, 140.1, 128.6, 128.3, 126.4, 35.6, 30.6

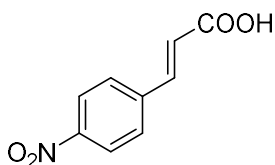
Compound 3X:



^1H -NMR (ppm): 11.96 (br, 1H), 7.36 (m, 5H), 3.78 (q, $^3J=7.32\text{Hz}$, 1H), 1.56 (d, $^3J=7.32\text{Hz}$, 3H)

^{13}C -NMR (ppm): 181.2, 139.8, 128.7, 127.6, 127.4, 45.4, 18.1

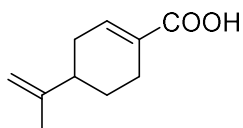
Compound 3Y:



^1H -NMR (ppm): 12.77 (br, 1H), 8.22 (d, $^3J=8.78\text{Hz}$, 2H), 7.96 (d, $^3J=8.78\text{Hz}$, 2H), 7.68 (d, $^3J_{\text{trans}}=16.09\text{Hz}$, 1H), 6.72 (d, $^3J_{\text{trans}}=16.09\text{Hz}$, 1H)

^{13}C -NMR (ppm): 167.5, 148.4, 141.8, 141.2, 131.1, 129.7, 124.4

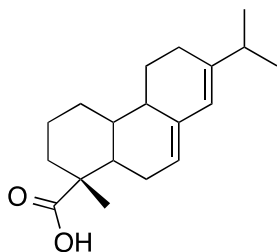
Compound 3Z:



^1H -NMR (ppm): 12.11 (br, 1H), 6.86 (m, 1H), 4.71 (m, 2H), 2.28 2.08 (dm, 2H), 2.07 (m, 1H), 1.78 1.38 (dm, 2H), 1.70 (s, 3H)

^{13}C -NMR (ppm): 168.4, 149.0, 138.7, 130.5, 109.7, 30.8, 27.1, 24.7, 21.0 (one signal was blocked by DMSO- d_6 solvent signal)

Compound 53:



^1H -NMR (ppm): 5.80 (s, 1H), 5.40 (m, 1H), 2.25 (m, 1H), 2.10 (m, 3H), 1.97 (m, 1H), 1.90 (m, 1H), 1.83 (m, 2H), 1.70 (m, 1H), 1.60 (m, 1H), 1.28 (s, 3H), 1.26 (m, 3H), 1.03 (m, 6H), 0.91 (m, 1H), 0.86 (s, 3H)

^{13}C -NMR (ppm): 185.4, 145.2, 135.6, 122.4, 120.5, 51.0, 46.4, 44.9, 38.3, 37.2, 34.9, 34.5, 27.5, 25.6, 21.4, 20.9, 16.7, 14.0

4.6 References

- [1] a) Yao, X.; Li, C.-J. *Org. Lett.* 2005, **7**, 4395; b) Yu, M.; Skouta, R.; Zhou, L.; Jiang, H.-F.; Yao, X.; Li, C.-J. *J. Org. Chem.* 2009, **74**, 3378; c) Deng, G.-J.; Li, C.-J. *Synlett* 2008, 1571; d) Jia, Z. Li, X.; Chan, A. S. C.; Li, C.-J. *Synlett* 2012, **23**, 2758; e) Fu, X.-P.; Liu, L.; Wang, D.; Chen, Y.-J.; Li, C.-J. *Green Chem.* 2011, **13**, 549.
- [2] Perez-Miller, S. J.; Hurley, T. D. *Biochemistry*. 2003, **42**, 7100–7108.
- [3] Benet, W. E.; Lewis, G. S.; Yang, L. Z.; Hugn, D. E. P. *J. Chem. Res.* 2011, 675-677.
- [4] *Advanced organic chemistry*, page 314, Jerry March (4th Ed), Wiley-Interscience.
- [5] Jia, Z.; Zhou, F.; Liu, M.; Li, X.; Chan, A. S. C.; Li, C.-J. *Angew. Chem. Int. Ed.* 2013, **52**, 11871-11874.
- [6] Kascatan-Neibiolglu, A.; Panzner, M. J.; Tessier, C. A.; Cannon, C. L.; Youngs, W. J. *Coord. Chem. Rev.* 2007, **251**, 884-895
- [7] Whittaker, A. M.; Dong, V. M. *Angew. Chem. Int. Ed.* 2015, **54**, 1312-1315.
- [8] Gonzalez, M.A.; Correa-Royero, J.; Agudelo, L.; Mesa, A.; Betancur-Galvis, L.; *Eur. J. Med. Chem.* 2009, **44**, 2468-2472.

Chapter 5 – Catalytic Fehling, a copper-catalyzed aerobic oxidation of aldehyde in water

5.1 Background and hypothesis

In chapter 4, we have developed an efficient silver(I)-catalyzed aerobic oxidation of aldehyde towards the carboxylic acid. However, certain problems remain, as silver is still a relatively expensive element, which will be endangered in the next 100 years [1]. To develop efficient oxidation of aldehyde towards carboxylic acid, we noticed that historically, the Fehling oxidation and the Tollens oxidation were both of great application. They require water as the sole solvent. The oxidation is carried on at very mild condition (only require a warm water bath). Vast variety of different aldehydes can all be transformed into the corresponding carboxylic acid very quickly, making those reactions even applicable for titration analysis. The Achilles' heel, however, is the requirement of stoichiometric amount of copper(II) and silver(I) salt, which generates vast amount of silver(0) and copper(I) waste. It would be highly desirable to eliminate the need of stoichiometric metal for these reactions. We then started to question the feasibility of using similar strategy in developing our catalytic Tollens' reaction (Figure 5.1), towards the development of a new generation of aldehyde aerobic oxidation catalyst that use more abundant copper as catalyst – a catalytic Fehling's oxidation.

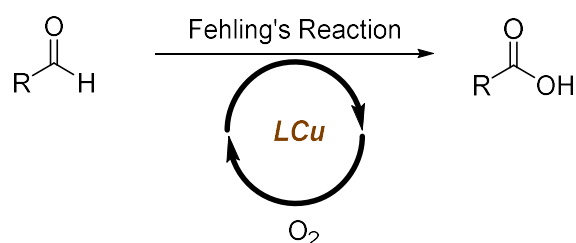


Figure 5.1 Our proposed catalytic Fehling's reaction

5.2 Feasibility investigation

Historically, copper has been widely used as aerobic oxidation catalyst, which can afford a variety of oxidation mechanisms [2]. One of the common examples is the Cu(I)/Cu(II)/ O_2 'electron relay'. Since aerobic oxidation of Cu(I) into Cu(II) is generally fast [3], in such step, electron in Cu(I) is efficiently extracted by oxygen to generate Cu(II). The active Cu(II) species can then extract electrons from a variety of substrates and oxidize them into the desired product (Figure 5.2). The most well-known application for the above-mentioned relay is the classic Wacker's process [4]. After β -hydride elimination, the electron was extracted from Pd(II)-H to generate H^+ and Cu(I),

which transfer the electron to oxygen as the terminal electron acceptor. A similar process was used by Adimurthy and co-workers in their Cu-catalyzed aerobic oxidation of amine to imine [5], where Cu(II) extracted electrons from amine and ultimately transfer those electrons to oxygen. Other than those examples in which 2 electrons were relayed, single electron transfer (SET) of such ‘electron relay’ with copper is also well-studied, such as the Cu-catalyzed oxidative cyclization of hydrazonoketone and ammonium into 1,2,3-triazole [6], and copper-catalyzed aerobic oxidation of amine into formamide [7].

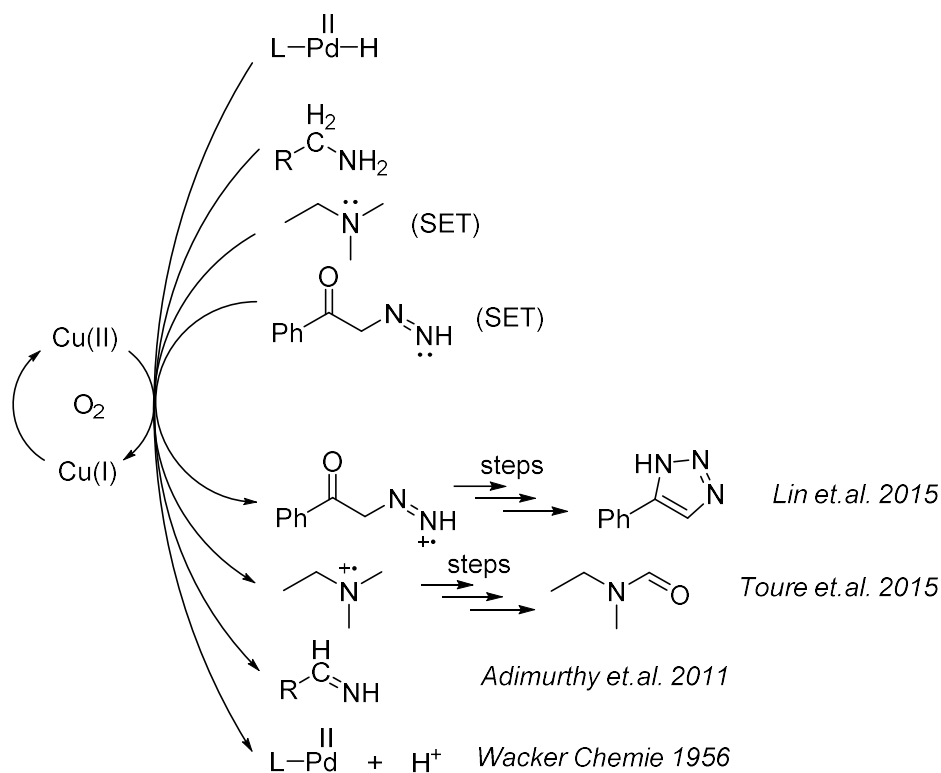


Figure 5.2 Applications of Cu(I)/Cu(II)/O₂ relay

Among all the example of Cu-catalyzed aerobic oxidation, alcohol oxidation is probably one of the most intensively-studied. Although the fixation of oxygen was still done by Cu(I) to generate Cu(II), however, an additional hydrogen-extractor is often required to achieve homolysis of the α -C-H bond (Figure 5.3). For example, TEMPO [8] and other hydroxylamine-based radical reagent. [9] In 2004, Marko and co-workers reported the use of di-tert-butyl azodicarboxylate as hydrogen-extractor to achieve alcohol oxidation [10]. Although innovative, the requirement of hydrogen-extractor was still irreplaceable. In 2015, Lumb and Arndtsen reported a bio-mimic copper-

catalyzed aerobic oxidation of alcohol without hydrogen-extractor [11]. However, this method suffers from the requirement of strict anhydrous condition and hazardous solvent (CH_2Cl_2). Recently, Kumar and co-workers demonstrated the feasibility of O_2 fixation by Cu(II) [12], which is different from the classic O_2 fixation by Cu(I) and achieved β -hydrogen extraction without the need of additional extractor. However, the Cu(III) intermediate involved in this report is still relatively rare and unstable.

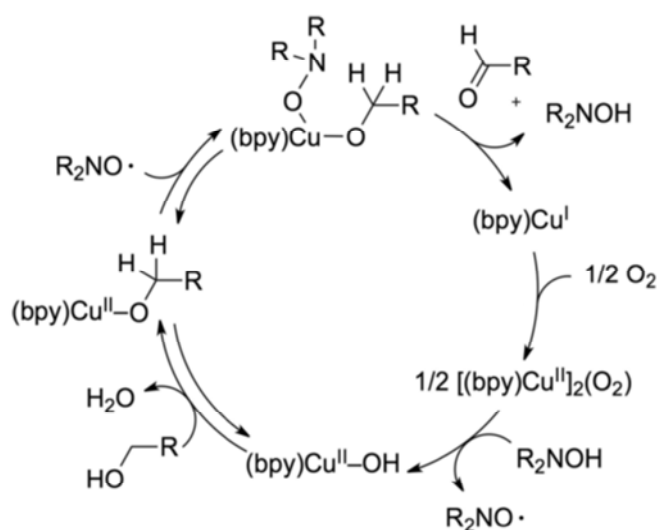


Figure 5.3 A typical Cu-catalyzed alcohol oxidation with hydrogen extractor (R_2NO in this case)

Based on our preliminary investigation, we concluded that the re-oxidation of Cu(I) generated in Fehling's oxidation back into Cu(II) is potentially feasible. As stoichiometric Cu(II) alone can readily achieve aldehyde oxidation, no hydrogen-extractor shall be necessary in our chemistry. The introduction of ligand can facilitate the re-oxidation by pushing the equilibrium forward and stabilize the Cu catalyst.

5.3 Result and discussion

5.3.1 Condition optimization

To begin our investigation, we used a common copper(II) salt, CuCl_2 , which was premixed with 2,2'-bipyridyl ligand as catalyst, along with stoichiometric amount of NaOH to consume the product and push the equilibrium forward. In 100 °C water and atmospheric oxygen sealed in the reaction vessel (Table 5.1), our standard substrate benzaldehyde (1a) gave 5 % oxidation product

of the corresponding benzoic acid (2a, entry 1). When Cu(I)Cl was used, the yield decreased to 1 % (entry 2). The same reaction using CuCl₂ gave 13 % yield when the reaction temperature was lowered to 50 °C (entry 3). Keeping the other condition unchanged, switching CuCl₂ to CuBr₂ gave a reduced 3 % yield (entry 4), and the use of CuO eliminates the formation of product (entry 5). To our delight, the use of Cu(OAc)₂ increased the yield to 68 % (entry 6), and Cu(acac)₂ gave almost quantitative oxidation (entry 7). The yield dropped to 50 % in the absence of bipy ligand (entry 8). When examine the current condition with piperonal (1b), a more functionalized aldehyde,

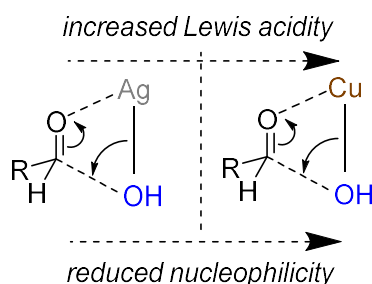


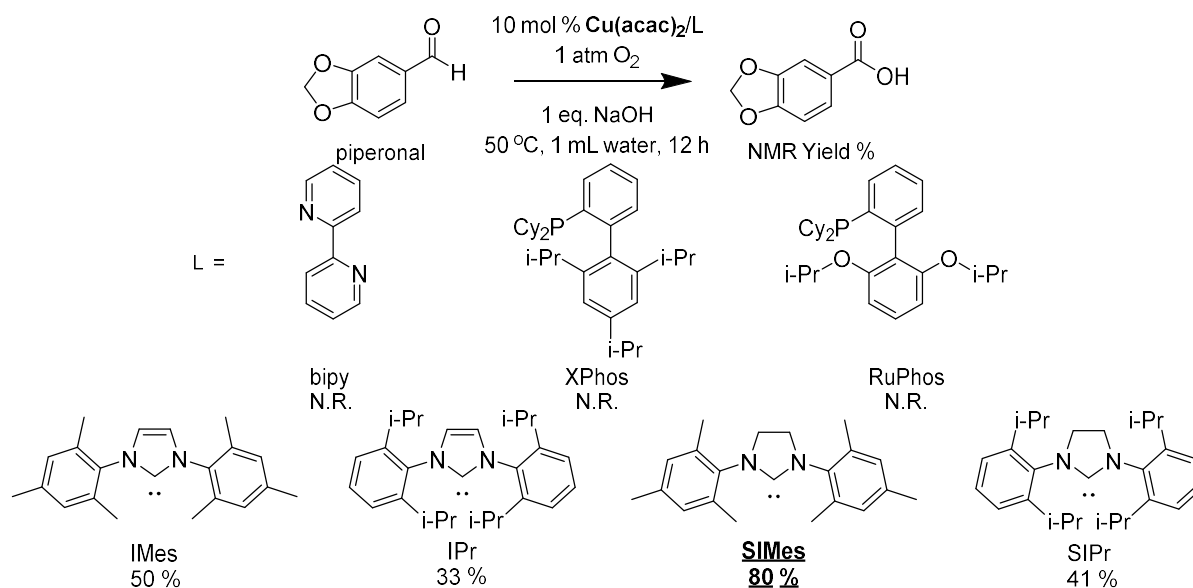
Figure 5.4 Comparison of silver and copper in our catalysis

no product of the corresponding piperonylic acid (2b) was obtained (entry 9). Considering the great functional tolerance of our previous silver(I) catalyst (Figure 5.4), we designed a solution to overcome this problem by using very electron-rich ligand to make copper cation into a softer acid, that is, more ‘silver like’. The use of electron-rich Buckwald-type ligand also did not overcome this limitation (entry 10, 11). When more electron-rich N-heterocyclic carbene (NHC) ligand IMes was used, 50 % 2b was obtained (entry 12). Other NHC ligands such as IPr, SIMes, SIPr gave 33 %, 80 %, 41 % yield of 2b, respectively (entry 13-15). Keeping Cu(acac)₂ and SIMes as the optimized catalyst, lowering the catalyst load to 5 mol% only gave a slightly yield drop into 78 % (entry 16). The free carbene cannot give the desired oxidation by itself (entry 17). And no product was obtained without pre-mixing Cu salt and the carbene ligand (entry 18).

5.3.2 Scope investigation

A series of selected aldehyde candidate was examined towards our aerobic oxidation condition, in order to investigate its functional tolerance (Table 5.2). Benzaldehyde gave quantitative yield of benzoic acid (**3a**). Other aromatic aldehydes such as 5-indancarboxaldehyde and 2-naphthalenecarboxaldehyde also gave quantitative oxidation of their corresponding carboxylic acid (**3c**, **3d**). Piperonal gave 77 % yield of the corresponding piperonylic acid (**3e**). Other electron-

Table 5.1. Optimization of reaction condition



Entry	[Cu]/L ^a	NMR Yield	Entry	[Cu]/L ^a	NMR Yield ^b
1	CuCl ₂ /bipy ^c	5 %	10	Cu(acac) ₂ /XPhos ^d	N.R.
2	CuCl/bipy ^c	1 %	11	Cu(acac) ₂ /RuPhos ^d	N.R.
3	CuCl ₂ /bipy	13 %	12	Cu(acac) ₂ /IMes ^d	50 %
4	CuBr ₂ /bipy	3 %	13	Cu(acac) ₂ /IPr ^d	33 %
5	CuO/bipy	N.R.	14	Cu(acac) ₂ /SIMes ^d	80 %
6	Cu(OAc) ₂ /bipy	68 %	15	Cu(acac) ₂ /SIPr ^d	41 %
7	Cu(acac) ₂ /bipy	99 %	16	Cu(acac) ₂ /SIMes ^{de}	78 % (77 %) ^f
8	Cu(acac) ₂ /no ligand	50 %	17	no copper/IMes ^d	N.R.
9	Cu(acac) ₂ /bipy ^d	N.R.	18	Cu(acac) ₂ /SIMes ^{dg}	N.R.

^a: The copper catalyst was generated prior to the oxidation by mixing copper salt with the ligand under argon in acetonitrile. Cu(acac)₂/NHC type catalyst can be generated either by mixing Cu(acac)₂ salt with the corresponding imidazolium salt in acetonitrile under argon for 24 h, or treating the imidazolium salt with n-BuLi under argon in THF then adding Cu(acac)₂ salt. The result was unaffected;

^b: NMR yields were determined by 1,3,5-mesitylene as the internal standard;

^c: This reaction was performed with 100 °C temperature;

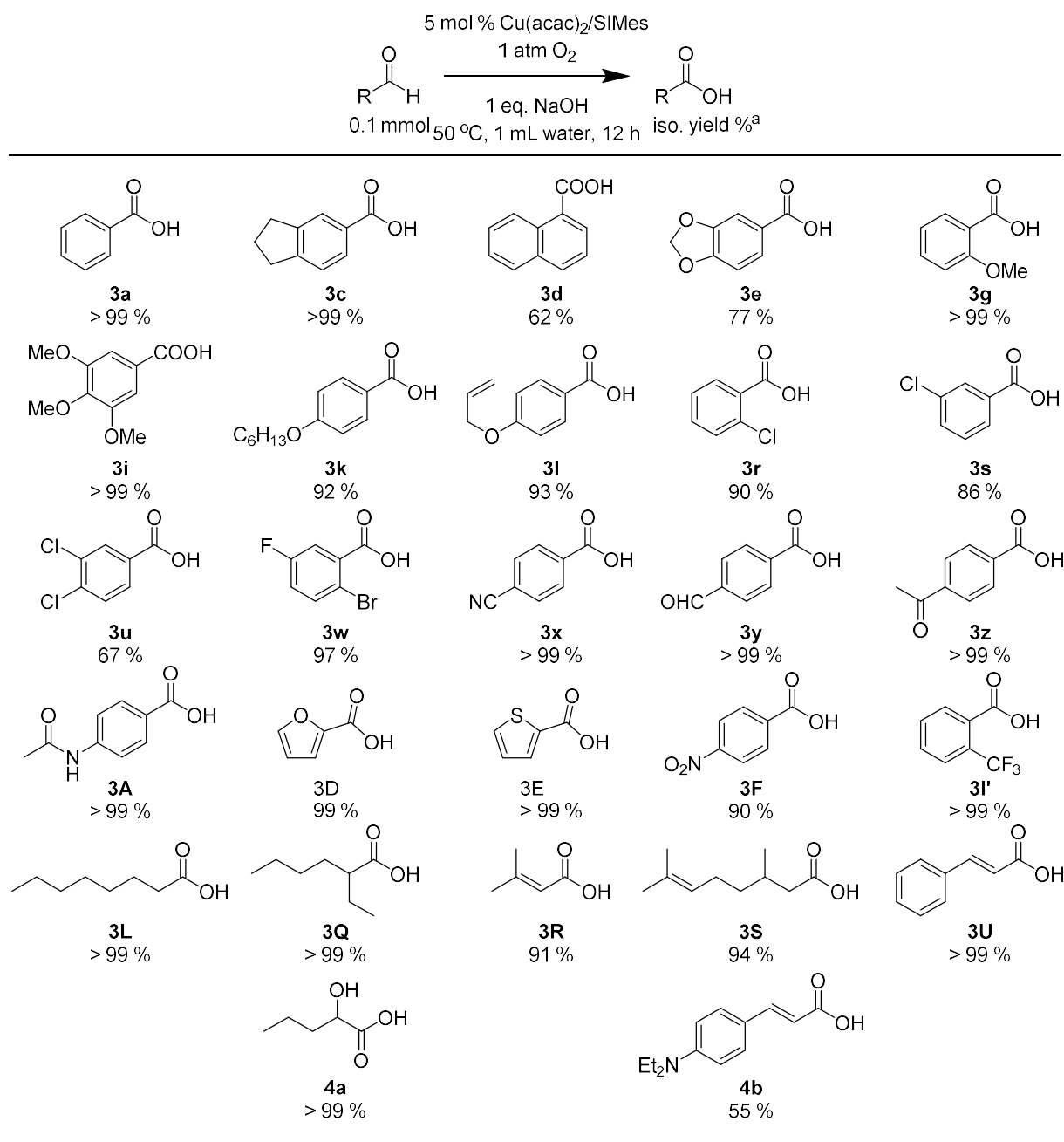
^d: This reaction was performed using piperonal as starting material;

^e: This reaction was performed with 5 mol % catalyst loading;

^f: Isolated yield;

^g: Cu(acac)₂ and SIMes were directly introduced to the reaction without premix.

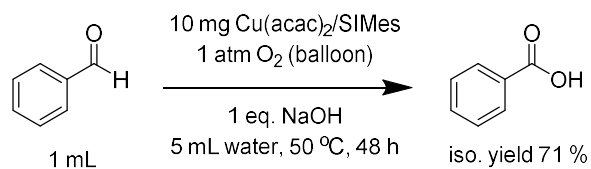
Table 5.2. Scope investigation



^a All reaction were conducted with the standard oxidation procedure (details available in electronic supporting information). Aldehyde (0.1 mmol), Cu catalyst (0.005 mmol, 5 mol %), NaOH (0.1 mmol, 1 equiv.) was mixed in 1 mL water and non-pressurized oxygen with stirring at 50 °C for 12 h

rich aromatic aldehydes such as 2-anisaldehyde, 3,4,5-trimethoxybenzaldehyde, 4-hexoxybenzaldehyde and 4-allyloxybenzaldehyde all gave satisfying oxidation, giving

quantitative, quantitative, 92 % and 93 % yield of the corresponding carboxylic acid respectively (**3g**, **3i**, **3k**, **3l**). No C=C bond oxidation or rearranging was observed for **3l**. Halogen substituted aromatic aldehyde, such as 2-chlorobenzaldehyde, 3-chlorobenzaldehyde, 3,4-dichlorobenzaldehyde, and 2-bromo-5-fluorobenzaldehyde gave 90 %, 86 %, 67 %, and 97 % isolated yield of their corresponding carboxylic acid (**3r**, **3s**, **3u**, **3w**). Electron-deficient aromatic aldehyde such as 4-cyanobenzaldehyde, terephthalaldehyde, and 4-acetylbenzaldehyde all gave quantitative oxidation into their corresponding carboxylic acid (**3x**, **3y**, **3z**). Further oxidation of **3y** into the dicarboxylic acid was not observed, possibly due to strong water-solubility of **3y** in basic aqueous solution separate it from hydrophobic catalyst. 4-acetaminobenzaldehyde also gave 90 % isolated yield of 4-acetaminobenzoic acid (**3A**). Other substrate examples include furfural and 2-thiophenecarboxaldehyde, which all gave almost quantitative yield of 2-furoic acid and 2-thiophenecarboxylic acid (**3D**, **3E**). 4-nitrobenzaldehyde gave 62 % isolated yield of 4-nitrobenzoic acid (**3F**), possibly due to side reactions on the phenyl ring or nitro group. α , α , α -trifluoro-2-tolualdehyde gave the corresponding acid quantitatively (**3I'**). Simple long-chain aliphatic aldehyde such as octanal and 2-ethylhexanal gave quantitative yield of their corresponding carboxylic acid too (**3L**, **3Q**). Unsaturated aliphatic aldehyde, such as 3,3-dimethylacrolein, citronellal and cinnamaldehyde gave 91 %, 94 %, and quantitative yield of their corresponding carboxylic acid (**3R**, **3S**, **3U**). 2-hydroxypentanal gave quantitative oxidation of the corresponding 2-hydroxypentanoic acid (**4a**). p-diethylaminocinnamaldehyde gave a reduced 55 % yield of p-diethylaminocinnamic acid (**4b**), possibly due to this unnatural amino acid is in constant ionic form, therefore increased its water-solubility. Gram-scale oxidation of benzaldehyde was also achieved with 10 mg of [Cu(acac)₂]/SIMes catalyst oxidizing 1 mL benzaldehyde in a prolonged time. 71 % isolated yield of benzoic acid was obtained (Scheme 5.1).



Scheme 5.1. Gram-scale experimental result

5.3.3 Mechanism investigation

At this stage, we were very curious about the mechanism behind this oxidation. We started by investigating the composition of our catalyst, as to the best of our knowledge no previous report concerns the reaction between $\text{Cu}(\text{acac})_2$ and in situ generated NHC. According to Nechaev's work [13], most $\text{Cu}(\text{II})$ -NHC complexes are unstable, unless chelated by covalent oxygen donor from either NHC or acetate. The green-colored catalyst of our oxidation was then recrystallized in hexane/chloroform by slow diffusion. Two types of crystal were isolated. The X-ray diffraction experiment suggest one of the crystal being a 2-coordinated $\text{Cu}(\text{I})$ complex, NHC-Cu-Cl and the other being $\text{Cu}(\text{acac})_2$. No $\text{NHC-Cu}(\text{II})$ complex was detected. Under our standard oxidation conditions, the NHC-Cu-Cl alone was able to catalyze the aerobic oxidation of piperonal and gave 55 % yield, whereas no oxidation was observed when $\text{Cu}(\text{acac})_2$ alone was used. However, keeping the overall $[\text{Cu}]$ load unchanged, when the 2 crystals were mixed, 73 % yield of piperonylic acid was granted, which is similar to the 77 % yield obtained under our optimized condition (Figure 5.5A). We suggested that the NHC-Cu-Cl is the actual catalyst of our reaction, while $\text{Cu}(\text{acac})_2$ serves as an efficient additive which function is so far unknown. One possibility is that the $\text{Cu}(\text{II})$ is oxidizing the $\text{Cu}(\text{I})$ in NHC-Cu-Cl into $\text{Cu}(\text{II})$, then regenerated by oxygen oxidation, similar to the Wacker's process [4] whereas $\text{Cu}(\text{II})$ was used to oxidize $\text{Pd}(0)$ to $\text{Pd}(\text{II})$ and the generated $\text{Cu}(\text{I})$ was re-oxidized by oxygen. Oxidizing $\text{Cu}(\text{I})$ to $\text{Cu}(\text{II})$ is also much easier than oxidizing $\text{Pd}(0)$ to $\text{Pd}(\text{II})$ judging by standard redox electrode potential [14]. To examine this possibility, our oxidation of piperonal was performed in argon with freeze-pump-thaw-degassed water and air-tight equipment. We first found that stoichiometric amount of NHC-Cu-OH , which was generated by anion exchange from previous NHC-Cu-Cl , was able to oxidize piperonal into piperonylic acid in 91 % yield, whereas no product was obtained with stoichiometric amount of NHC-Cu-Cl . This not only indicating the possibility of NHC-Cu-Cl can transform into NHC-Cu-OH in the presence of NaOH in our system and become the active catalyst species, but also suggest that at least the first step of our oxidation does not necessarily need oxygen and oxidation of $\text{Cu}(\text{I})$ into $\text{Cu}(\text{II})$. Then we lower the NHC-Cu-OH load into 5 mol%, and the yield of piperonylic acid also dropped to approximately 5 %. Keeping other reaction conditions unchanged, 1 equiv of $\text{Cu}(\text{acac})_2$ was added to the system. Surprisingly, the yield of piperonylic acid was still approximately 5 % (Figure 5.5B). Although we still cannot completely rule out the possibility for a Wacker-like mechanism,

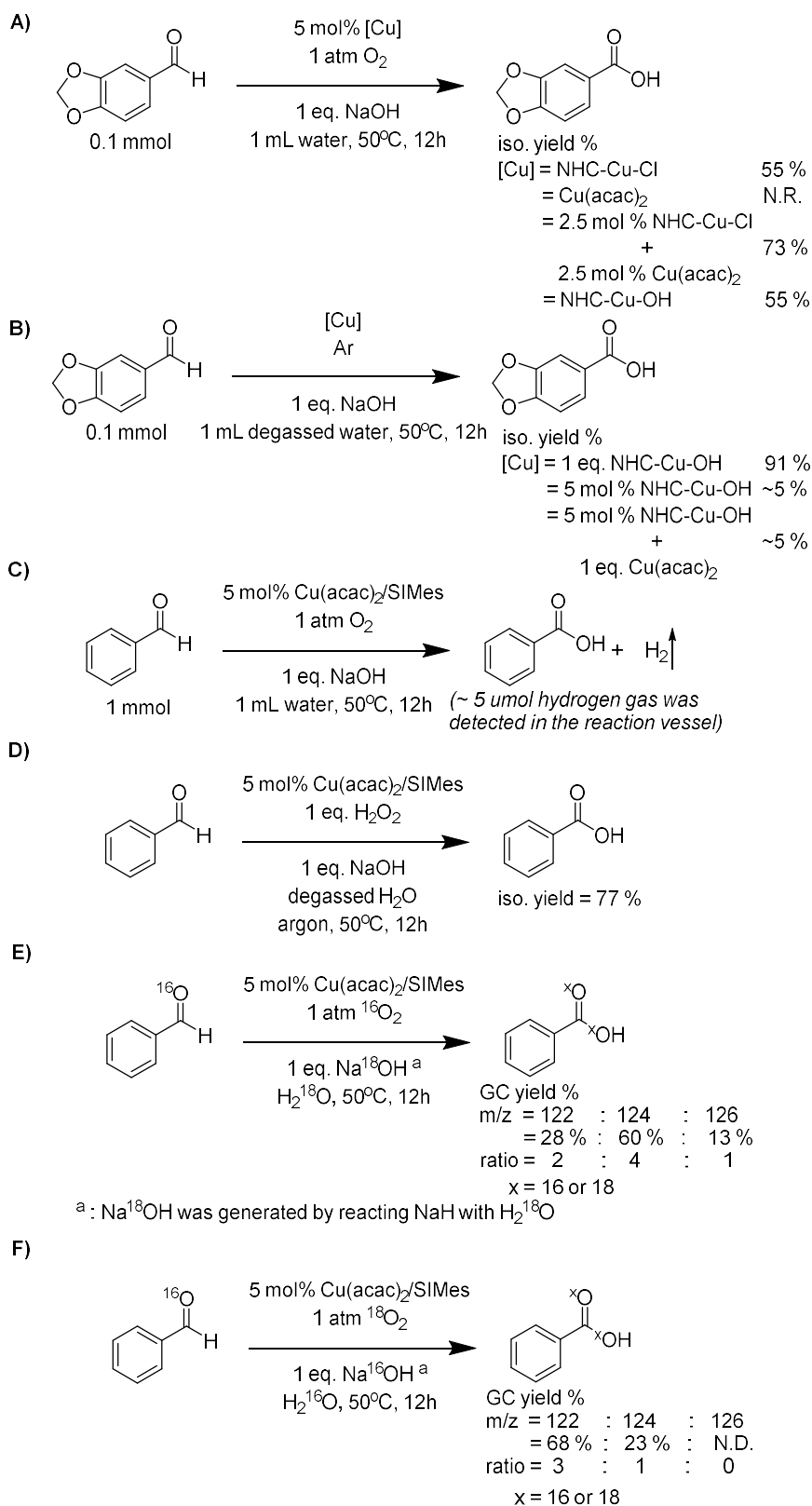


Figure 5.5. Mechanism investigation

as the true function of Cu(II) in our system is still unknown, those experimental data we obtained strongly oppose such suggestion. Then, the atmosphere in the sealed reaction vessel of our standard aerobic oxidation was examined. A low but notable concentration of hydrogen was detected (Figure 5.5C), suggesting a possible metal-hydride intermediate which can undergo minor hydrolysis. This similar phenomenon was also observed in the previous catalytic Tollens reaction in chapter 4. Considering this similarity and both Cu(I) and Ag(I) being coinage metal, we proposed that the first stage of these 2 transformations are similar via -OH nucleophilic attack/ β -H elimination to give the desired metal-hydride species. The hydride is then reducing molecular oxygen. If the reducing product is -OH, the active catalyst species will be directly regenerated and the next catalytic cycle shall begin with no external hydroxide necessary. This is inconsistent with our observations as 50 % yield of benzaldehyde was obtained when NaOH load dropped to 0.5 equiv. Another possibility is that the metal-hydride is reducing oxygen into a hydroperoxyl-species. The nucleophilic attack of this hydroperoxyl to aldehyde carbonyl should be easier than previous -OH attack due to α -effect, then the hydroperoxyl oxidize the aldehyde hydride and give the carboxylate product, which is substituted by external hydroxide anion to release the product and regenerate the active catalyst species. We conducted the experiment using H₂O₂ instead of oxygen as the oxidant, the result was consistent with our hypothesis (Figure 5.5D). To further examine this hypothesis, an isotope-labelling experiment was conducted for the standard aerobic oxidation of benzaldehyde. When isotope-labelled H₂¹⁸O and Na¹⁸OH was introduced with normal ¹⁶O₂, an m:m+2:m+4 product ratio of 2:4:1 was observed (Figure 5.5E). Although the presence of m+4 product indicates not all the oxygen atom of the product came from oxygen, we realized that oxygen in benzaldehyde can spontaneously exchange with oxygen in water without the oxidation [15]. Therefore another isotope-labelling experiment using isotope-labelled ¹⁸O₂ and normal H₂¹⁶O/Na¹⁶OH was conducted, showing m:m+2:m+4 ratio of 3:1:0 (Figure 5.5F). This is consistent with our hypothesis and previous experiment, indicating the oxygen in carboxylic acid product does not fully come from oxygen, supporting our second mechanism hypothesis involves hydroperoxyl intermediate, whereas the first mechanism hypothesis, which suggests metal hydride reduce oxygen into -OH, was negated, as all the oxygen in carboxylic acid product should come from oxygen in that case.

We concluded our mechanism assumptions and experimental observations, and came up with a proposed reaction mechanism (Figure 5.6). The first phase of reaction mechanism is similar to our

previous catalytic-Tollens reaction: the nucleophilic attack of -OH on copper to the aldehyde carbonyl, followed by $\beta\text{-H}$ elimination to release the product and generate the copper-hydride intermediate. The minor hydrolysis of this intermediate is responsible for the detection of hydrogen gas. The hydride then fixes one molecule of oxygen, generating a copper-hydroperoxide intermediate. This hydroperoxyl group attacks another molecule of aldehyde, then oxidizing the aldehyde hydride and generates the carboxylate product, which is released by hydroxide anion substitution to regenerate the active catalyst species at the same time.

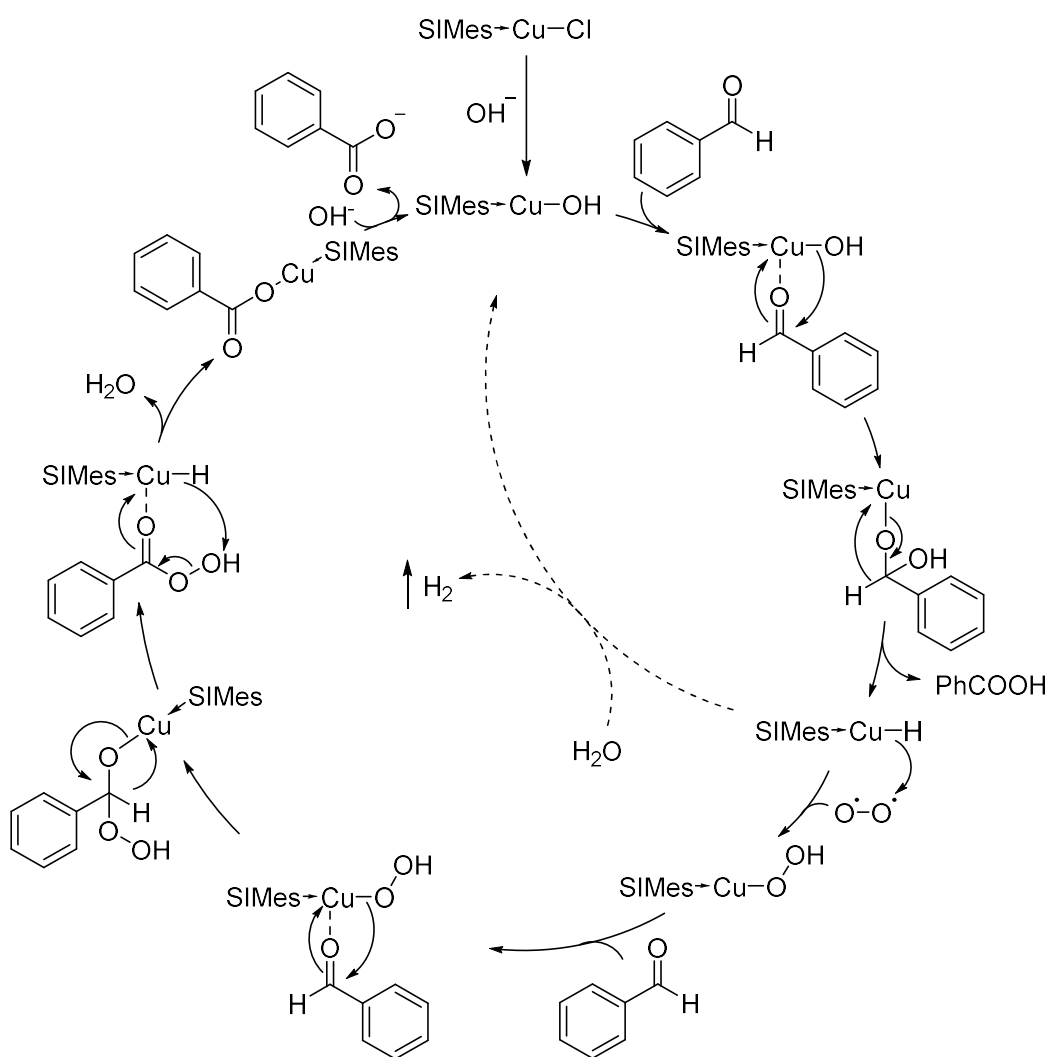


Figure 5.6. Proposed mechanism of our catalytic Fehling's reaction

5.4 Conclusion and perspective

In this chapter, we have developed a highly efficient and cost-effective aldehyde oxidation method, using oxygen as the sole oxidant and water as the sole solvent. The development of this method was inspired by both the classical Fehling's reaction and the function of copper as a classic aerobic oxidation catalyst. Using a copper-NHC complex as the optimized catalyst, proceeding via an unprecedented copper-catalyzed aerobic oxidation mechanism, extremely high efficiency and wide functional tolerance were both obtained. With our newly developed method added to the arsenal of copper-catalyzed aerobic oxidations, the development of copper catalyst towards the oxidation of more complex substrates can be enabled. For example, the aerobic oxidative cleavage of biomass, which can serve as an effort towards the development of sustainable alternative carbon source than fossil. Such work has already underway in our lab.

5.5 Contributions of authors

The designing of research directions and experiments in this project was the result of discussions between Prof. Chao-Jun Li and me. I was in charge of carrying out all the experiments (including but not limited to condition optimization, substrate scope investigation, and all mechanism study experiments except for the X-ray Crystallography, which was carried out by Dr. Thierry Maris in Université de Montréal.) and identifications using NMR spectrometer.

5.6 Experimental

5.6.1 General information

Unless otherwise noted, all oxidations were carried out in Biotage Microwave Reaction Vials size 10-15 mL equipped with a magnetic stir-bar unless otherwise noticed. All reactions were in sealed closed system: no open-vial reaction was involved and no balloon containing extra volume of gas was attached to the vessel unless otherwise noted. No microwave was involved during the entire investigation. All manipulation and purification procedures were carried out with reagent-grade solvents. Aldehydes which are in liquid form under normal conditions were redistilled under reduced pressure. The corresponding aldehyde of **4a** was generated via oxidation of 1,2-pentadiol according to reported method [16]. SIMes-Cu-Cl was also synthesized via reported method [17]. Drying of solvent was performed with IOCB AS CR Pure-Solv solvent purification system. Analytical thin-layer chromatography (TLC) was performed using E. Merck silica gel 60 F₂₅₄ pre-coated plates (0.25 mm). Flash chromatography was generally not necessary, but could be

performed using Biotage Isolera One Flash Purification System equipped with Biotage SNAP Ultra 25g prepared column for further purification requirements. Nuclear magnetic resonance (NMR) spectra were recorded on a Varian MERCURY plus-300 spectrometer (^1H 300 MHz, ^{13}C 75 MHz) or a Bruker Ascend 500 spectrometer (^1H 500 MHz, ^{13}C 125 MHz). Chemical shifts for ^1H NMR spectra are reported in parts per million (ppm) from tetramethylsilane with the solvent resonance as the internal standard (CDCl_3 : δ 7.26 ppm, DMSO: δ 2.46 ppm). Chemical shifts for ^{13}C NMR spectra are reported in parts per million (ppm) from tetramethylsilane with the solvent as the internal standard (CDCl_3 : δ 77.0 ppm, DMSO: δ 40.0 ppm). Data are reported as following: chemical shift, multiplicity (s = singlet, d = doublet, dd = doublet of doublets, t = triplet, q = quartet, m = multiplet, br = broad signal), and integration.

5.6.2 General procedures

General procedures for the catalyst generation: Method A: An oven-dried reaction vessel, charged with copper(II) acetylacetonate (26.2 mg, 0.1 mmol, 1 equiv) and 1,3-bis(2,4,6-trimethylphenyl)-4,5-dihydroimidazolium chloride ($\text{SIMes}\cdot\text{HCl}$, 34.2 mg, 0.1 mmol, 1 equiv), was flushed with argon 3 times. Dry acetonitrile (2.5 mL) was added into the vessel. The vessel was then sealed and stirred at room temperature for 24 h. **Method B:** An oven-dried reaction vessel was charged with 1,3-bis(2,4,6-trimethylphenyl)-4,5-dihydroimidazolium chloride ($\text{SIMes}\cdot\text{HCl}$, 34.3 mg, 0.1 mmol, 1 equiv) and flushed with argon 3 times. of dry tetrahydrofuran (2.5 mL) was added into the vessel. n-butyllithium hexane solution (40 μL , 0.1 mmol, 2.5 M concentration) was added into the reaction mixture and allowed to stir for 5 min. A clear, pale-white solution was obtained followed by the addition of copper(II) acetylacetonate (26.2 mg, 0.1 mmol, 1 equiv) and further stirred for 5 min. The resulting mixture in both cases were then stripped of solvent with rotary evaporator and the resulting solid were kept in a desiccator for later use.

General procedure for the oxidation of aldehydes: A reaction vessel, charged with $\text{Cu}(\text{acac})_2/\text{SIMes}$ catalyst (4.7 mg, 0.005 mmol, 5 mol %) and sodium hydroxide (4 mg, 0.1 mmol, 1 equiv) was gently flushed with oxygen of ordinary purity using a balloon or gas valve. After this, distilled water (1 mL) was added to the vessel. The reaction mixture was then warmed up to 50 $^\circ\text{C}$ before the aldehyde (0.1 mmol, 1 equiv) was added. The reaction vessel was then sealed and kept at 50 $^\circ\text{C}$ for 12 h. After this, the reaction mixture was washed with methylene chloride (DCM) three times with a total DCM volume of 10 mL and the pH of the aqueous phase was then adjusted

to 2 with 0.1 M HCl. The aqueous phase was then extracted with ethyl ether 3 times with a total ether volume of 10 mL and the combined ether phase was dried over anhydrous sodium sulfate and evaporated *in vacuo* to obtain the carboxylic acid product.

Procedure for oxidation with SIMes-Cu-OH: A reaction vessel, charged with SIMes-Cu-Cl (2.0 mg, 0.005 mmol, 5 mol%) and KOH (0.6 mg, 0.0107 mmol, 10.7 mol %), was flushed with argon and anhydrous THF (0.1 mL) was added. The vessel was then sealed and stirred at 50 °C for 12 h before it was cooled to room temperature and filtered through a syringe filterer plug. Additional THF (0.5 mL) was used to rinse the reaction vessel and the filterer. The combined organic phase was evaporated in a standard 10 mL reaction vessel before piperonal (15 mg, 0.1 mmol) and NaOH (4 mg, 0.1 mmol, 1 equiv) was added. Oxygen was then gently flushed into the reaction vessel followed by the addition of 1 mL distilled water. The reaction vessel was then sealed and stirred at 50 °C for 12 h. The reaction mixture was then washed with dichloromethane (DCM) 3 time with a combined volume of 10 mL, acidified to pH = 2 with 0.1 M HCl, and extracted with diethyl ether 3 times with a combined volume of 10 mL. The combined ether phase was then evaporated using rotary evaporator to give the piperonylic acid product (55 % yield).

Procedure for stoichiometric [Cu] experiment: A reaction vessel, charged with SIMes-Cu-OH (38 mg, 0.1 mmol, 1 equiv) and NaOH (4 mg, 0.1 mmol, 1 equiv), was flushed with argon 3 times before 1 mL Freeze-Pump-Thaw degassed distilled water was added. The resulting mixture was stirred for 5 min at room temperature followed by the addition of piperonal (15 mg, 0.1 mmol, 1 equiv). The reaction vessel was then sealed and stirred at 50 °C for 12 h before allowed to cool to room temperature. The organic phase was washed with DCM 3 times, then acidified and extracted with ether 3 times. The combined ether phase was dried and evaporated to give piperonylic acid product (91 % yield).

Procedure for the hydrogen detection: Following a standard oxidation procedure, with a reaction with 10 times the scale compared to the above general procedure (1 mmol of the aldehyde and NaOH, 0.05 mmol catalyst, 10 mL water, in a 50 mL reaction vial) was conducted. Upon completion, a 5 mL syringe equipped with a 15 gauge needle was inserted into the sealed plug for the reaction vessel and 5 mL gas sample inside the reaction vessel was taken. The needle was plugged using a normal septum before it was inserted into a heat-conductivity-GC and injected all its component at once. About 0.5 μ mol H₂ was detected for the 5 mL gas sample.

Procedure for the oxidation with hydrogen peroxide: A reaction vessel, charged with Cu(acac)₂/SIMes (4.7 mg, 0.005 mmol, 5 mol %) and NaOH (0.4 mg, 0.1 mmol, 1 equiv), was flushed with argon 3 times before water (1 mL, degassed carefully with freeze-pump-thaw for 5 cycles) was added along with benzaldehyde (10 µL, 0.1 mmol) and 30 % commercially available hydrogen peroxide (10.2 µL, 0.1 mmol, 1 equiv). The reaction vessel was sealed and stirred at 50 °C for 12 h before cooled to room temperature. The aqueous reaction mixture was washed with DCM 3 times, acidified, and extracted with ether. The combined ether phase was evaporated to give benzoic acid product in 77 % yield.

Procedure for the H₂¹⁸O isotope labelled experiment*: A reaction vessel, charged with Cu(acac)₂/SIMes (4.7 mg, 0.005 mmol, 5 mol %) and NaH (0.3 mg, 0.12 mmol, 1.2 equiv), was added benzaldehyde (10 µL, 0.1 mmol) and H₂¹⁸O (0.1 mL). The reaction vessel was then sealed and stirred for 12 h at 50 °C before cooled to room temperature. The aqueous reaction mixture was washed with DCM 3 times, acidified, extracted with ether 3 times and evaporated to give the product, which was used for GC-MS analysis.

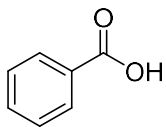
Procedure for the ¹⁸O₂ isotope labeling experiment: A reaction vessel, charged with Cu(acac)₂/SIMes (4.7 mg, 0.005 mmol, 5 mol %) and NaOH (0.4 mg, 0.1 mmol, 1 equiv), was vacuumed with oil pump before a balloon of ¹⁸O₂ was plugged on, followed by the addition of benzaldehyde (10 µL, 0.1 mmol) and Freeze-Pump-Thaw degassed H₂O (0.1 mL). The reaction vessel was then sealed and stirred for 12 h at 50 °C before cooled to room temperature. The aqueous reaction mixture was washed with DCM 3 times, acidified, extracted with ether 3 times and evaporated to give the product, which was used for GC-MS analysis.

*: Note that the m+4 product of this experiment was possibly generated by oxidation of benzaldehyde-¹⁸O, which resulted from the fast hydration-dehydration process in basic aqueous conditions. ^[18]

5.6.3 Identification of products.

All compounds are previously known and the data reported herein are consistent with the literature reports. ^[19]

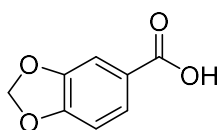
Compound 3a:



$^1\text{H-NMR}$ (CDCl_3 , 500 MHz, ppm): 11-13 (br, 1H), 8.16 (m, 2H), 7.65 (tt, $^3\text{J}=7.32\text{Hz}$, $^4\text{J}=2.05\text{Hz}$, 1H), 7.50 (t, $^3\text{J}=7.32\text{Hz}$, 2H),

$^{13}\text{C-NMR}$ (CDCl_3 , 125 MHz, ppm): 172.3, 133.8, 130.2, 129.3, 128.5

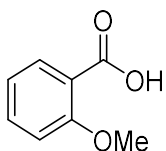
Compound 3e:



$^1\text{H-NMR}$ (DMSO-D_6 , 500 MHz, ppm): 12.5-13.0 (br, 1H), 7.55 (dd, $^3\text{J}=8.24\text{Hz}$, $^4\text{J}=1.83\text{Hz}$, 1H), 7.36 (d, $^4\text{J}=1.83\text{Hz}$, 1H), 7.00 (d, $^3\text{J}=8.24\text{Hz}$, 1H), 6.12 (s, 2H)

$^{13}\text{C-NMR}$ (DMSO-D_6 , 125 MHz, ppm): 167.1, 151.6, 147.9, 125.4, 125.1, 109.2, 108.5, 102.4

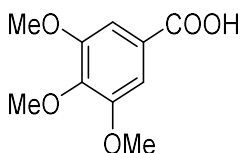
Compound 3g:



$^1\text{H-NMR}$ (DMSO-D_6 , 500 MHz, ppm): 12.57 (br, 1H) 7.61 (dd, $^3\text{J}=7.90\text{Hz}$, $^4\text{J}=2.05\text{Hz}$, 1H), 7.48 (m, 1H), 7.10 (d, $^3\text{J}=8.49\text{Hz}$, 1H), 6.97 (dt, $^3\text{J}=7.32\text{Hz}$, $^4\text{J}=0.88\text{Hz}$, 1H), 3.79 (s, 3H)

$^{13}\text{C-NMR}$ (DMSO-D_6 , 125 MHz, ppm): 167.8, 158.5, 133.5, 131.0, 121.7, 120.4, 112.8, 56.1

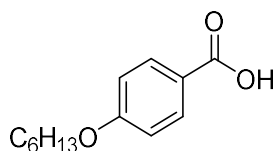
Compound 3i:



$^1\text{H-NMR}$ (DMSO-D_6 , 300 MHz, ppm): 12.7-13.0 (br, 1H), 7.21 (s, 2H), 3.80 (s, 6H), 3.70 (s, 3H)

^{13}C -NMR (DMSO- D_6 , 75 MHz, ppm): 167.4, 153.1, 141.8, 126.4, 107.0, 60.6, 56.4

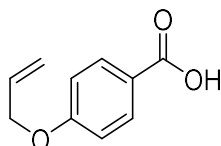
Compound 3k:



^1H -NMR (DMSO- D_6 , 500 MHz, ppm): 12.58 (br, 1H), 7.88 (d, $^3J=8.78\text{Hz}$, 2H), 7.00 (d, $^3J=8.78\text{Hz}$, 2H), 4.04 (t, $^3J=6.73\text{Hz}$, 2H), 1.73 (m, 1.42 (m, 2H), 1.32 (m, 4H), 0.88 (m, 3H)

^{13}C -NMR (CDCl_3 , 125 MHz, ppm): 171.1, 163.7, 132.3, 121.7, 114.2, 68.3, 31.5, 29.0, 25.6, 22.6, 14.01

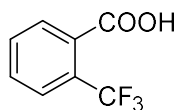
Compound 3l:



^1H -NMR (DMSO- D_6 , 300 MHz, ppm): 12.59 (br, 1H), 7.86 (dt, $^3J=9.07\text{Hz}$, $^4J=2.05\text{Hz}$, 2H), 7.00 (dt, $^3J=9.07\text{Hz}$, $^4J=2.05\text{Hz}$, 2H), 6.02 (m, 1H), 5.32 (m, $J=17.26\text{Hz}$, $J=10.53$, 2H), 4.62 (dt, $^3J=5.27\text{Hz}$, $^4J=1.46\text{Hz}$, 2H)

^{13}C -NMR (DMSO- D_6 , 75 MHz, ppm): 167.4, 162.2, 133.6, 131.8, 123.5, 118.3, 114.9, 68.8

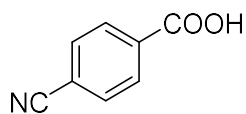
Compound 3l':



^1H -NMR (DMSO- D_6 , 500 MHz, ppm): 13.57 (br, 1H), 7.70-7.85 (m, 4H)

^{13}C -NMR (DMSO- D_6 , 125 MHz, ppm): 168.3, 133.1, 132.8 (m), 131.6, 130.1, 127.0 (q, $J=5.49\text{Hz}$), 125.1, 122.9

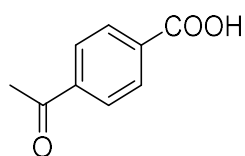
Compound 3x:



$^1\text{H-NMR}$ (DMSO- D_6 , 500 MHz, ppm): 13.55 (br, 1H), 8.09 (d, $^3J=8.49\text{Hz}$, 2H), 7.98 (d, $^3J=8.49\text{Hz}$, 2H)

$^{13}\text{C-NMR}$ (DMSO- D_6 , 125 MHz, ppm): 166.5, 135.3, 133.1, 130.4, 118.6, 115.5

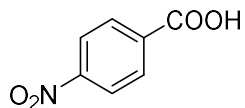
Compound 3z:



$^1\text{H-NMR}$ (DMSO- D_6 , 300 MHz, ppm): 13.18 (br, 1H), 8.03 (m, 4H), 2.61 (s, 3H)

$^{13}\text{C-NMR}$ (DMSO- D_6 , 75 MHz, ppm): 198.1, 167.1, 140.3, 134.9, 130.0, 128.7, 27.4

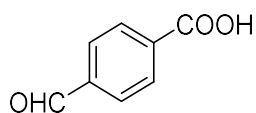
Compound 3F:



$^1\text{H-NMR}$ (DMSO- D_6 , 300 MHz, ppm): 13.61 (br, 1H), 8.30 (d, $^3J=9.07\text{Hz}$, 2H), 8.15 (d, $^3J=9.07\text{Hz}$, 2H),

$^{13}\text{C-NMR}$ (DMSO- D_6 , 75 MHz, ppm): 166.2, 150.5, 136.9, 131.1, 124.2

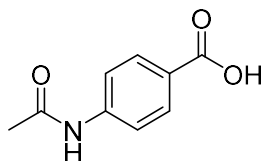
Compound 3y:



$^1\text{H-NMR}$ (DMSO- D_6 , 500 MHz, ppm): 13.37 (br, 1H), 10.11 (s, 1H), 8.15 (d, $^3J=8.49\text{Hz}$, 2H), 8.05 (d, $^3J=8.49\text{Hz}$, 2H)

$^{13}\text{C-NMR}$ (DMSO- D_6 , 125 MHz, ppm): 193.5, 167.0, 139.4, 136.1, 130.4, 130.0

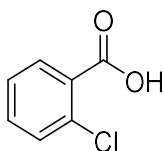
Compound 3A:



$^1\text{H-NMR}$ (DMSO- D_6 , 300 MHz, ppm): 12.64 (br, 1H), 10.22 (s, 1H), 7.86 (d, $^3\text{J}=8.78\text{Hz}$, 2H), 7.66 (d, $^3\text{J}=8.78\text{Hz}$, 2H), 2.06 (s, 3H)

$^{13}\text{C-NMR}$ (DMSO- D_6 , 75 MHz, ppm): 169.3, 167.4, 143.8, 130.8, 125.3, 118.6, 24.6

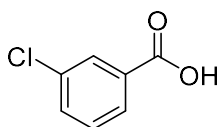
Compound 3r:



$^1\text{H-NMR}$ (DMSO- D_6 , 500 MHz, ppm): 13.36 (br, 1H), 7.79 (m, 1H), 7.55 (m, 2H), 7.43 (m, 1H)

$^{13}\text{C-NMR}$ (DMSO- D_6 , 125 MHz, ppm): 167.2, 133.0, 132.0, 131.9, 131.3, 131.1, 127.7

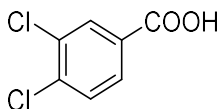
Compound 3s:



$^1\text{H-NMR}$ (DMSO- D_6 , 500 MHz, ppm): 13.31 (br, 1H), 7.91 (m, 2H), 7.70 (m, 1H), 7.55 (t, $^3\text{J}=7.90\text{Hz}$, 1H)

$^{13}\text{C-NMR}$ (DMSO- D_6 , 125 MHz, ppm): 166.5, 133.8, 133.3, 133.2, 131.1, 129.3, 128.4

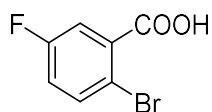
Compound 3u:



$^1\text{H-NMR}$ (DMSO- D_6 , 300 MHz, ppm): 13.47 (br, 1H), 8.04 (d, $^4\text{J}=2.05\text{Hz}$, 1H), 7.86 (dd, $^3\text{J}=8.19\text{Hz}$, $^4\text{J}=2.05\text{Hz}$, 1H), 7.76 (d, $^3\text{J}=8.19\text{Hz}$, 1H)

$^{13}\text{C-NMR}$ (DMSO- D_6 , 75 MHz, ppm): 165.9, 136.2, 132.0, 131.9, 131.5, 131.4, 129.8

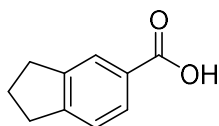
Compound 3w:



$^1\text{H-NMR}$ (DMSO- D_6 , 300 MHz, ppm): 13.66 (br, 1H), 7.74 (dd, $^3J=8.78\text{Hz}$, $^4J_{\text{H-F}}=4.97$, 1H), 7.57 (dd, $^3J_{\text{H-F}}=8.78\text{Hz}$, $^4J=3.22\text{Hz}$, 1H), 7.32 (dt, $^3J=^3J_{\text{H-F}}=8.78\text{Hz}$, $^4J=3.22\text{Hz}$, 1H)

$^{13}\text{C-NMR}$ (DMSO- D_6 , 75 MHz, ppm): 166.7, 163.0, 159.7 ($^1J_{\text{C-F}}=246.56\text{Hz}$), 136.1, 136.0 ($^3J_{\text{C-F}}=8.05\text{Hz}$, 2C), 120.3, 120.0 ($^2J_{\text{C-F}}=22.91\text{Hz}$), 118.0, 117.7 ($^2J_{\text{C-F}}=22.91\text{Hz}$), 115.0 115.0 ($^4J_{\text{C-F}}=2.87\text{Hz}$)

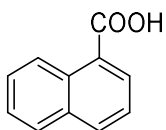
Compound 3c:



$^1\text{H-NMR}$ (DMSO- D_6 , 500 MHz, ppm): 12.70 (br, 1H), 7.79 (s, 1H), 7.72 (d, $^3J=7.90\text{Hz}$, 1H), 7.33 (d, $^3J=7.90$, 1H), 2.91 (t, $^3J=7.61\text{Hz}$, 4H), 2.04 (m, $^3J=7.61\text{Hz}$, 2H)

$^{13}\text{C-NMR}$ (DMSO- D_6 , 125 MHz, ppm): 172.5, 151.0, 144.7, 128.6, 127.3, 126.1, 124.3, 33.1, 32.5, 25.4

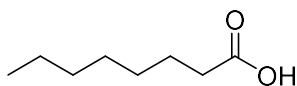
Compound 3d:



$^1\text{H-NMR}$ (DMSO- D_6 , 300 MHz, ppm): 13.12 (br, 1H), 8.84 (m, 1H), 8.14 (m, 2H), 7.99 (m, 1H), 7.57 (m, 3H)

$^{13}\text{C-NMR}$ (DMSO- D_6 , 75 MHz, ppm): 169.1, 133.9, 133.4, 130.5, 130.3, 129.1, 128.7, 126.6, 126.5, 125.9, 125.3

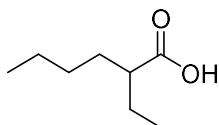
Compound 3L:



$^1\text{H-NMR}$ (CDCl_3 , 500 MHz, ppm): 11.2-12.0 (br, 1H), 2.35 (t, $^3J=7.61\text{Hz}$, 2H), 1.63 (m, 2H), 1.29 (m, 8H), 0.88 (m, 3H)

$^{13}\text{C-NMR}$ (CDCl_3 , 125 MHz, ppm): 180.8, 34.6, 32.2, 29.6, 29.5, 25.2, 23.2, 14.6

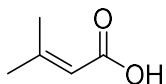
Compound 3Q:



$^1\text{H-NMR}$ (DMSO-D_6 , 300 MHz, ppm): 12.00 (br, 1H), 2.10 (m, 1H), 1.43 (dm, 4H), 1.22 (m, 4H), 0.82 (m, 6H)

$^{13}\text{C-NMR}$ (DMSO-D_6 , 75 MHz, ppm): 177.3, 46.9, 31.6, 29.6, 25.3, 22.6, 14.3, 12.1

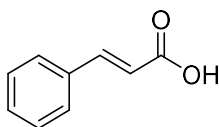
Compound 3R:



$^1\text{H-NMR}$ (DMSO-D_6 , 500 MHz, ppm): 12.21 (br, 1H), 6.74 (m, 1H), 1.75 (m, 6H)

$^{13}\text{C-NMR}$ (DMSO-D_6 , 125 MHz, ppm): 170.6, 159.7, 115.3, 27.7, 20.5

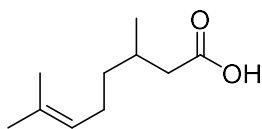
Compound 3U:



$^1\text{H-NMR}$ (DMSO-D_6 , 500 MHz, ppm): 12.30 (br, 1H), 7.69 (m, 2H), 7.60 (d, $^3J_{\text{trans}}=16.09\text{Hz}$, 1H), 7.42 (m, 3H), 6.53 (d, $^3J_{\text{trans}}=16.09\text{Hz}$, 1H)

$^{13}\text{C-NMR}$ (DMSO-D_6 , 125 MHz, ppm): 168.0, 144.4, 134.7, 130.7, 129.4, 128.7, 119.7

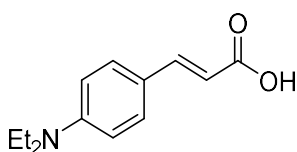
Compound 3S:



$^1\text{H-NMR}$ (DMSO- D_6 , 500 MHz, ppm): 11.99 (br, 1H), 5.08 (m, 1H), 1.70-2.22 (m, 5H), 1.65 (d, 3H), 1.57 (d, 3H), 0.99-1.36 (m, 2H), 0.88 (d, 3H)

$^{13}\text{C-NMR}$ (CDCl_3 , 125 MHz, ppm): 178.5, 131.7, 124.1, 41.3, 36.7, 29.8, 25.7, 25.4, 19.6, 17.6

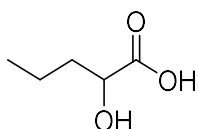
Compound 4b:



$^1\text{H-NMR}$ (DMSO- D_6 , 500 MHz, ppm): 11.9 (br, 1H), 7.46 (m, 3H), 6.66 (d, 2H), 6.16 (d, $^3J_{\text{trans}}=15.80\text{Hz}$, 1H), 3.39 (m, 4H), 1.11 (t, $^3J=7.02\text{Hz}$, 6H)

$^{13}\text{C-NMR}$ (DMSO- D_6 , 75 MHz, ppm): 168.7, 149.4, 145.1, 130.5, 121.1, 112.7, 111.5, 44.2, 12.9

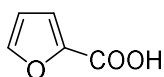
Compound 4a:



$^1\text{H-NMR}$ (DMSO- D_6 , 500 MHz, ppm): 12.32 (br, 1H), 3.92 (t, 1H), 1.45-1.65 (m, 2H) 1.36 (m, 2H), 0.88 (t, $^3J=7.32\text{Hz}$, 3H)

$^{13}\text{C-NMR}$ (DMSO- D_6 , 125 MHz, ppm): 176.4, 69.8, 36.5, 18.5, 14.2

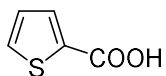
Compound 3D:



$^1\text{H-NMR}$ (DMSO- D_6 , 300 MHz, ppm): 12.92 (br, 1H), 7.90 (m, 1H), 7.20 (dd, $^3J=3.51\text{Hz}$, $^4J=0.88\text{Hz}$, 1H), 6.63 (dd, $^3J=3.51\text{Hz}$, $^4J=1.76\text{Hz}$, 1H)

$^{13}\text{C-NMR}$ (DMSO- D_6 , 75 MHz, ppm): 159.7, 147.5, 145.3, 118.1, 112.5

Compound 3E:

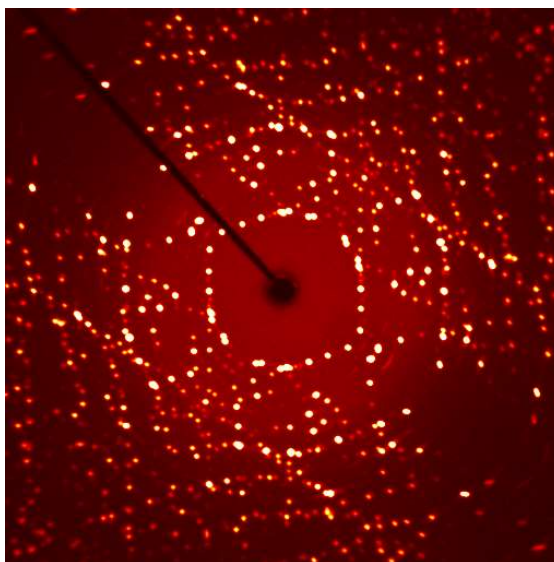


$^1\text{H-NMR}$ (DMSO- D_6 , 300 MHz, ppm): 13.31 (br, 1H), 7.87 (dd, $^3J=3.80\text{Hz}$, $^4J=1.17\text{Hz}$, 1H), 7.71 (dd, $^3J=4.97\text{Hz}$, $^4J=1.15\text{Hz}$, 1H), 7.17 (dd, $^3J=3.80\text{Hz}$, $^3J=4.97$, 1H)

$^{13}\text{C-NMR}$ (DMSO- D_6 , 75 MHz, ppm): 163.3, 135.1, 133.6, 128.7

5.6.4 X-ray single crystallography result

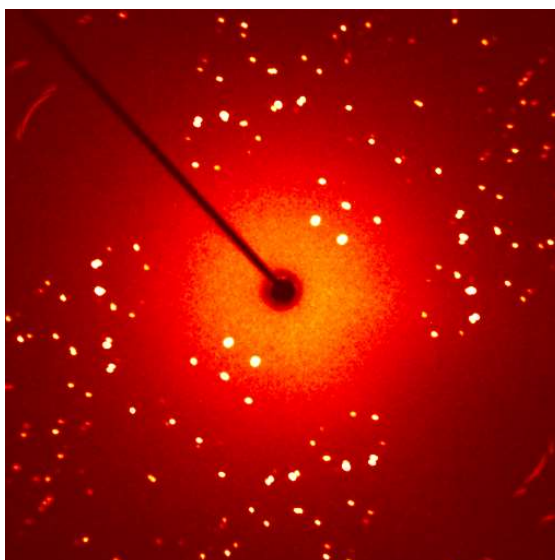
CHAOJ1(1) - Colorless Crystal 0.17 * 0.20 * 0.22 mm³, T = 100 K



Unit Cell:

a /Å	8.7675(7)
b /Å	15.3649(1)
c /Å	30.137(2)
α /°	90
β /°	90
γ /°	90
V /Å ³	4059.8(6)
Space Group	<i>Pbca</i>

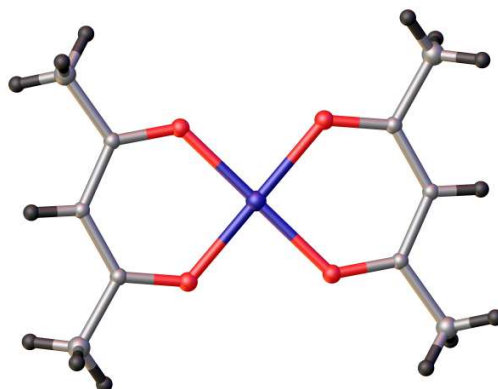
Identified as (SIMes)CuCl, CSD REFCODE PAPDOA (J. Org. Chem 70 (2005) p4784).



Unit Cell:

a /Å	10.2721(19)
b /Å	4.6297(9)
c /Å	11.288(2)
α /°	90
β /°	92.360(3)
γ /°	90
V /Å ³	536.34(18)
Space Group	<i>P</i> 2 ₁ / <i>n</i>

Identified as Cu(acac)₂, CSD REFCODE ACACCU02.



5.7 References

- [1] D. A. Atwood in *The Rare Earth Elements: Fundamentals and Applications*, Wiley, Chichester, 2012, pp. 21–25.
- [2] Elwell, C. E.; Gagnon, N. L.; Neisen, B. D.; Dhar, D.; Spaeth, A. D.; Yee, G. M.; Tolman, W. B. *Chem. Rev.* 2017, **117**, 2059-2107.
- [3] McCann, S. D.; Stahl, S. S. *J. Am. Chem. Soc.* 2016, **138**, 199-206.
- [4] Jira, R. *Angew. Chem. Int. Ed.* 2009, **48**, 9034-9037
- [5] Patil, R. D.; Adimurthy, S. *Adv. Synth. Catal.* 2011, **353**, 1695-1700.
- [6] Wu, L.; Guo, S.; Wang, X.; Guo, Z.; Yao, G.; Lin, Q.; Wu, M. *Tetrahedron Lett.* 2015, **56**, 2145-2148.
- [7] Genovino, J.; Sames, D.; Toure, B. B. *Tetrahedron Lett.* 2015, **56**, 3066-3069.
- [8] Zhang, G.; Han, X.; Luan, Y.; Wang, Y.; Wen, X.; Ding, C. *Chem. Commun.* 2013, **49**, 7908-7910.
- [9] Lopez, M. C.; Chavant, P. Y.; Molton, F.; Royal, G.; Blandin, V. *ChemistrySelect* 2017, **2**, 443-450.
- [10] Marko, I. E.; Gautier, A.; Dumeunier, R.; Doda, K.; Philippart, F.; Brown, S. M.; Urch, C. J. *Angew. Chem. Int. Ed.* 2004, **43**, 1588-1591.
- [11] Xu, B.; Lumb, J.-P.; Arndtsen, B. A. *Angew. Chem. Int. Ed.* 2015, **54**, 4208-4211.
- [12] Kumar, Y.; Jaiswal, Y.; Kumar, A. *J. Org. Chem.* 2016, **81**, 12247-12257.
- [13] Kolychev, E. L.; Shuntikov, V. V.; Khrustalev, V. N.; Bush, A. A.; Nechaev, M. S. *Dalton Trans.* 2011, **40**, 3074-3076
- [14] Lide, David R., ed. (2006). *CRC Handbook of Chemistry and Physics* (87th ed.). Boca Raton, FL: CRC Press.
- [15] McClelland, R.A.; Coe, M. *J. Am. Chem. Soc.* 1983, **105**, 2718-2725
- [16] Siedlecka, R.; Skarzewski, J.; Miochowski, J. *Tetrahedron Lett.* 1990, **31**, 2177-2180
- [17] a) Kaur, H.; Zinn, F. K.; Stevens, E. D.; Nolan, S. P. *Organometallics* 2004, **23**, 1157-1160; b) Di'ez-Gonza'lez, S.; Kaur, H.; Zinn, F. K.; Stevens, E. D.; Nolan, S. P. *J. Org. Chem.* 2005, **70**, 4784-4796.
- [18] McClelland, R. A.; Coe, M. *J. Am. Chem. Soc.* 1983, **105**, 2718-2725.

[19] For selected literature reports on those compounds, see: a) Tian, Q.; Shi, D.; Sha, Y.; *Molecules* 2008, **13**, 948-957; b) Yoshida, M.; Katagiri, Y.; Zhu, W.-B.; Shishido, K.; *Org. Biomol. Chem.* 2009, **7**, 4062-4066; c) Chiang, P.-C.; Bode, J. W. *Org. Lett.* 2011, **13**, 2422-2425; d) Mita, T.; Suga, K.; Sato, K.; Sato, Y. *Org. Lett.* 2015, **17**, 5276-5279; e) Sun, J.; Wang, Y.; Han, L.; Xu, D.; Chen, Y.; Peng, X. Guo, H. *Org. Chem. Front.*, 2014, **1**, 1201–1204; f) Brauer, G. M.; Stansbury, J. W.; Antonucci, J. M. *J. Dent. Res.* 1981, **60**, 1343-1348; h) Maruyama, Y.; Sezaki, T.; Tekawa, M.; Sakamoto, T.; Shimizu, I.; Yamamoto, A. *J. Organomet. Chem.* 1994, **473**, 257-264.

Chapter 6 – Contribution to fundamental knowledge

In this thesis, we have established a series of silver/copper catalyzed aldehyde reduction and aerobic oxidation methods. We have discussed the first homogeneous silver-catalyzed transfer hydrogenation of aldehyde in water using formate as reductant, which implying the first decarboxylation of silver(I)-formate (AgO_2CH) to afford silver(I)-hydride. The discovery of such process potentially enables cost-effective and environmental-friendly reduction of other substrates, such as ketone, etc.

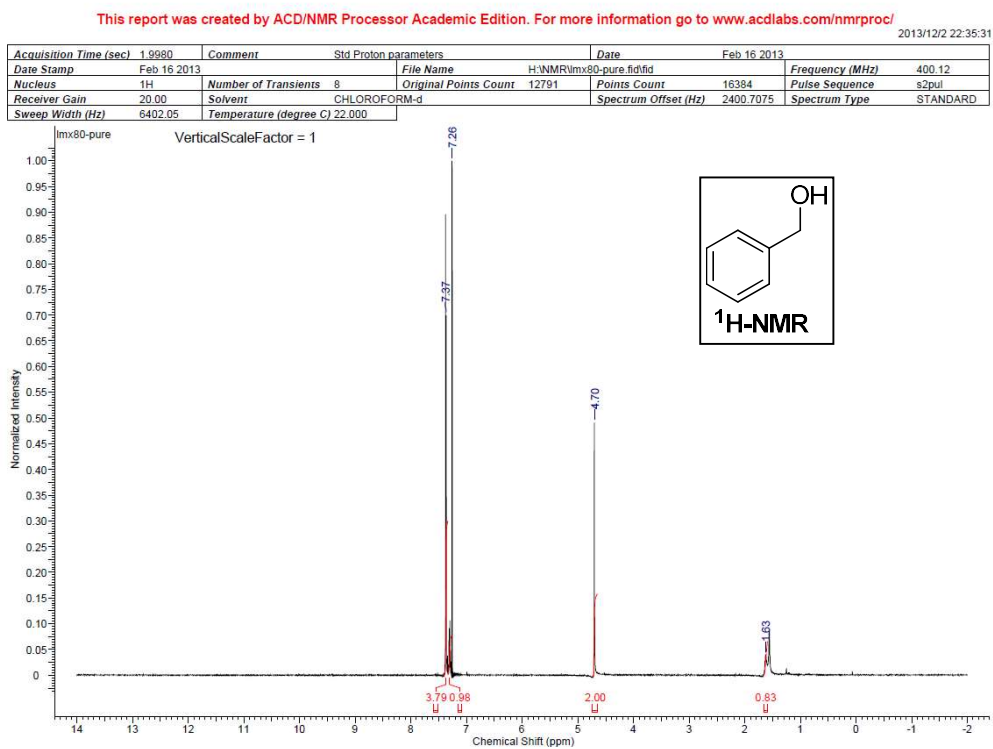
Inspired by Silver-Mirror reaction, as one of the most powerful aldehyde oxidations in the history, we have developed an innovative silver-catalyzed aerobic oxidation of aldehyde. The developed reaction, like the historic Silver-Mirror reaction, shows powerful functional tolerance and adaptability for a wide section of aldehyde, including natural products, in mild condition. This is the first report concerning β -H elimination of a silver(I)-(gem-diol-anion) complex $[\text{AgOCH}(\text{OH})\text{R}]$. Generally, β -H elimination of silver(I) complex was rarely reported. It is also the first time that hydrogen gas was detected in aerobic oxidation of aldehyde, implying the effectiveness of a silver(I)-hydride in activating molecular oxygen, which is unprecedented in aldehyde oxidation chemistry.

The catalytic version of another historically important aldehyde reaction, the Fehling's reaction, was also developed. While achieving most of the advantages for the previous catalytic-silver-mirror, including wide adaptability, high catalyst efficiency, mild condition, and easy purification, the catalytic-Fehling is particularly advantageous since global silver conservation is suffering from fast depletion. Among all the previous Cu-catalyzed aerobic oxidation chemistry, no report demonstrated that the activation of oxygen was done by Cu-H, which was suggested by our study.

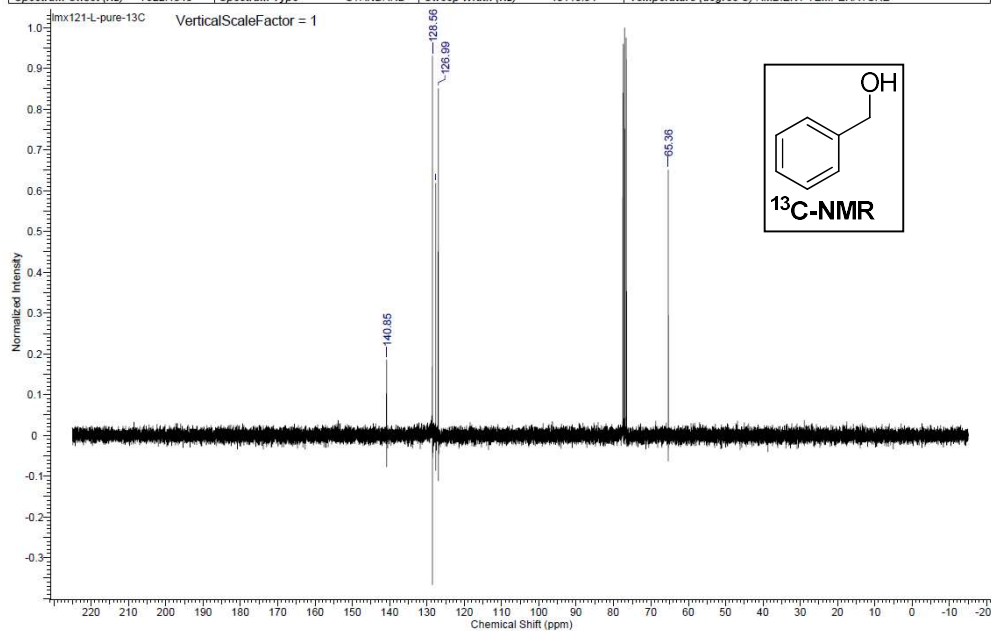
Also, notably, it was suggested that all the described reactions, both reduction and oxidation, proceed via a unified nucleophilic attack mechanism. All reactions involve a key metal-hydride intermediate, which attacks the carbonyl to give alkoxide in reduction and activates oxygen into hydroperoxide in oxidation. Such unified mechanism implies that the complex relationship between reduction and oxidation in chemistry may also be unified in mechanistic level. This hypothesis has already inspired us to pursue further examinations and developments of new applications from those ideas.

Appendix

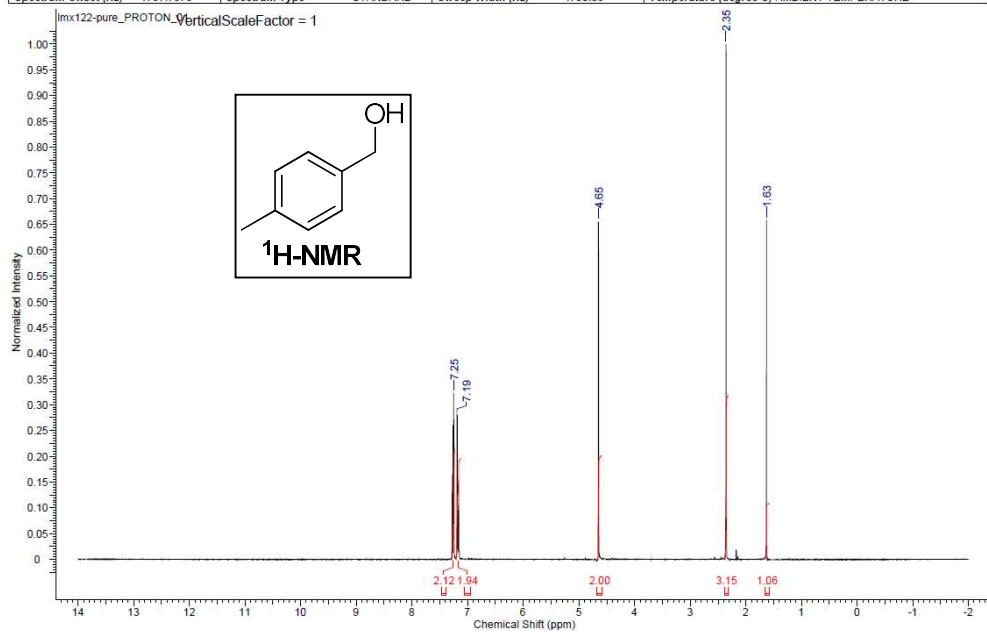
NMR spectra of products described in chapter 3



Acquisition Time (sec)	1.3005	Comment	Std Carbon experiment	Date	Mar 5 2013
Date Stamp	Mar 5 2013	File Name	H:\NMR\lmx121-L-pure-13C.fid.tif	Frequency (MHz)	75.46
Nucleus	13C	Number of Transients	500	Original Points Count	23560
Pulse Sequence	s2pul	Receiver Gain	20.00	Points Count	32768
Spectrum Offset (Hz)	7922.1348	Spectrum Type	STANDARD	Solvent	CHLOROFORM-d
				Sweep Width (Hz)	18115.94
				Temperature (degree C)	AMBIENT TEMPERATURE



Acquisition Time (sec)	2.0480	Date	Dec 2 2013	Date Stamp	Dec 2 2013		
File Name	C:\Users\IML\W\Desktop\NMR\mx122-pure_PROTON_01.fid.fid				Frequency (MHz)	299.63	
Nucleus	¹ H	Number of Transients	8	Original Points Count	9818	Points Count	16384
Pulse Sequence	s2pul	Receiver Gain	30.00	Solvent	CHLOROFORM-d		
Spectrum Offset (Hz)	1797.7676	Spectrum Type	STANDARD	Sweep Width (Hz)	4793.86	Temperature (degree C)	AMBIENT TEMPERATURE

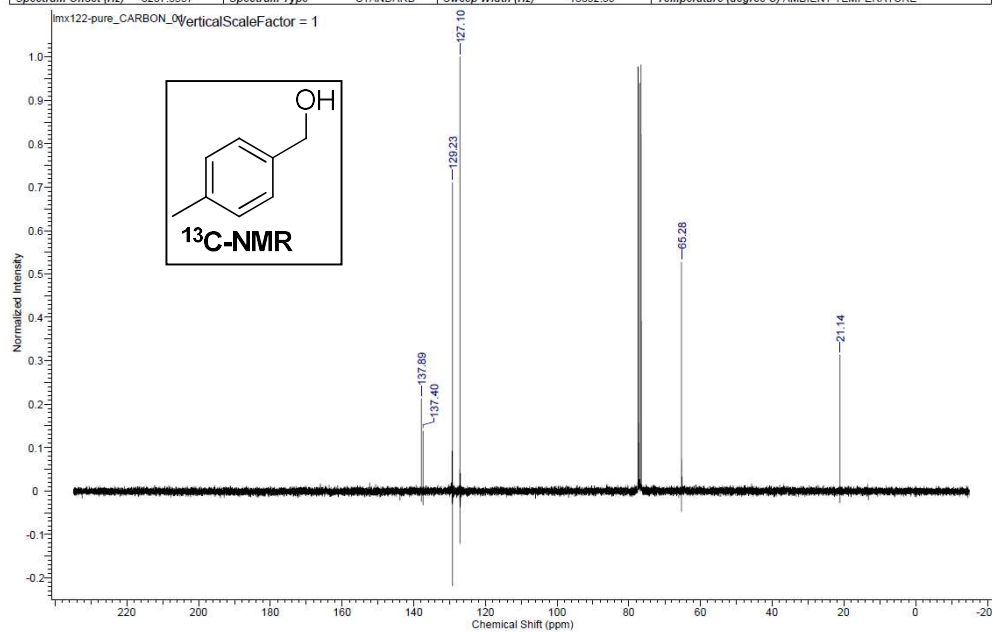


This report was created by ACD/NMR Processor Academic Edition. For more information go to www.acdlabs.com/nmrproc/

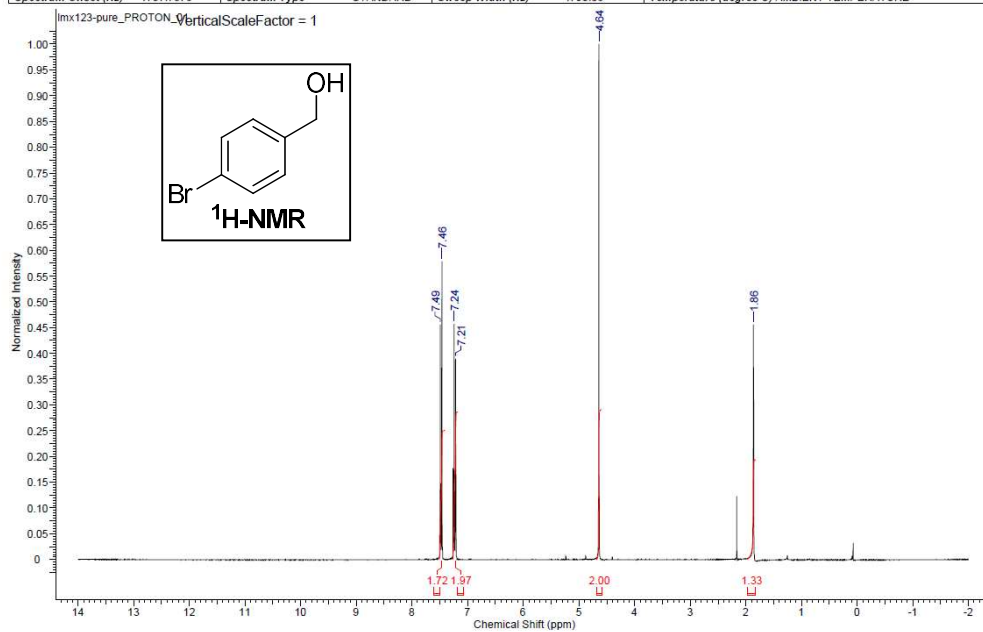
2013/12/2 22:40:46

2013/12/22 22:40:4

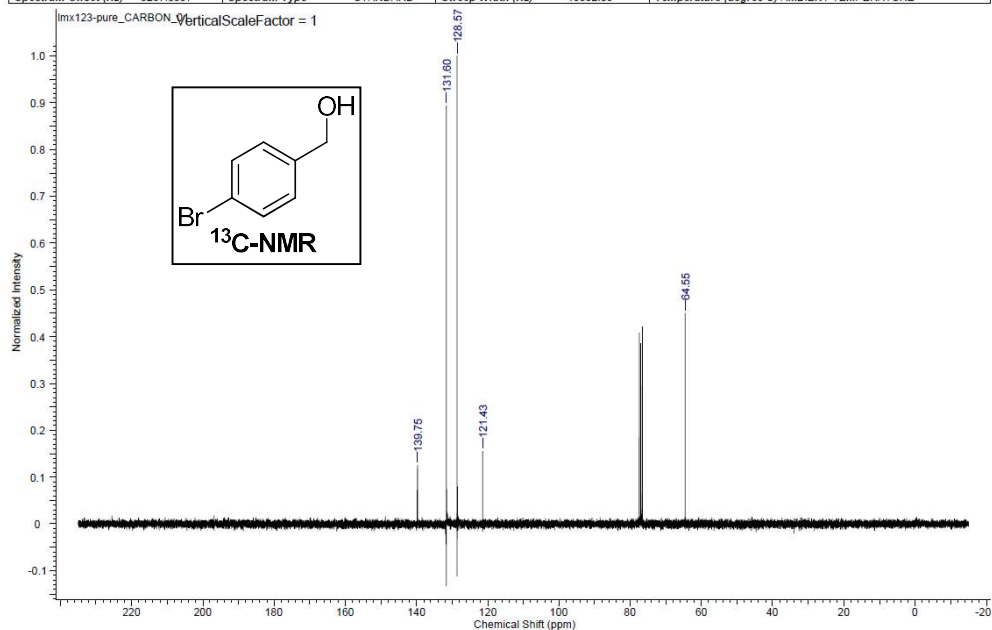
Acquisition Time (sec)	1.0420	Date	Dec. 2 2013	Date Stamp	Dec. 2 2013		
File Name	C:\Users\MMLWW\Desktop\NMR\lmx122-pure_CARBON_01.fid.tif					Frequency (MHz)	75.35
Nucleus	¹³ C	Number of Transients	3300	Original Points Count	19624	Points Count	32768
Pulse Sequence	s2pul	Receiver Gain	30.00	Solvent	CHLOROFORM-d		
Spectrum Offset (Hz)	8287.5557	Spectrum Type	STANDARD	Sweep Width (Hz)	18832.39	Temperature (degree C)	AMBIENT TEMPERATURE



Acquisition Time (sec)	2.0480	Date	Dec 2 2013	Date Stamp	Dec 2 2013
File Name	C:\Users\IML\W\Desktop\NMR\mx123-pure_PROTON_01.fid.fid	Frequency (MHz)	299.63	Points Count	16384
Nucleus	¹ H	Number of Transients	8	Original Points Count	9818
Pulse Sequence	s2pul	Receiver Gain	30.00	Solvent	CHLOROFORM-d
Spectrum Offset (Hz)	1797.7676	Spectrum Type	STANDARD	Sweep Width (Hz)	4793.86
				Temperature (degree C)	AMBIENT TEMPERATURE



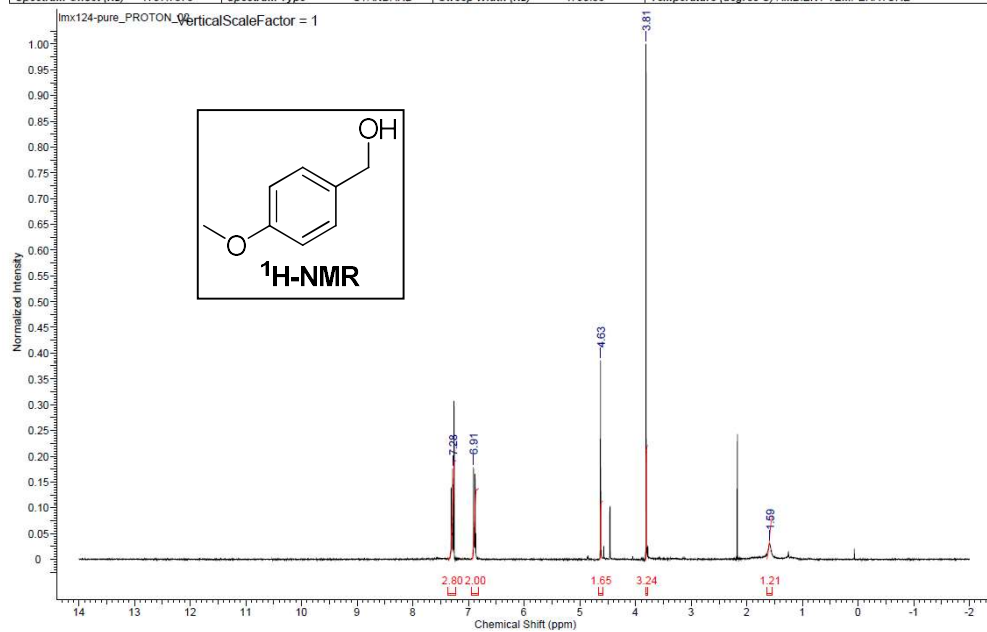
Acquisition Time (sec)	1.0420	Date	Dec 2 2013	Date Stamp	Dec 2 2013
File Name	C:\Users\IMLW\Desktop\NMR\mx123-pure_CARBON_01.fid.tif	Frequency (MHz)	75.35		
Nucleus	¹³ C	Number of Transients	832	Original Points Count	19624
				Points Count	32768
Pulse Sequence	s2pul	Receiver Gain	30.00	Solvent	CHLOROFORM-d
Spectrum Offset (Hz)	8287.5557	Spectrum Type	STANDARD	Sweep Width (Hz)	18832.39
				Temperature (degree C)	AMBIENT TEMPERATURE



This report was created by ACD/NMR Processor Academic Edition. For more information go to www.acdlabs.com/nmrproc/

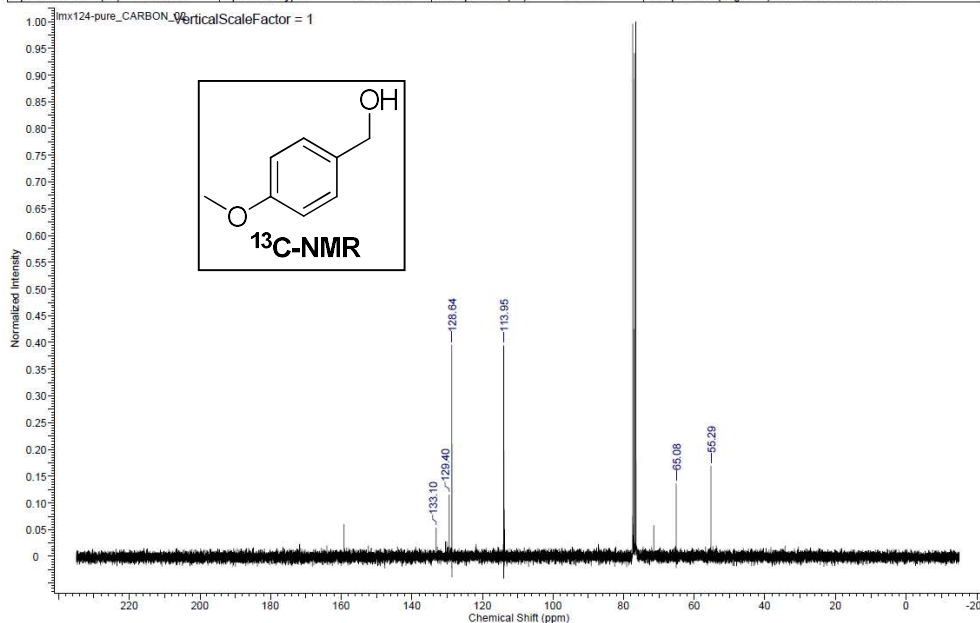
2013/12/2 22:42:36

Acquisition Time (sec)	2.0480	Date	Dec 2 2013	Date Stamp	Dec 2 2013		
File Name	C:\Users\IML\W\Desktop\NMR\lmx124-pure_PROTON_02.fid				Frequency (MHz)	299.63	
Nucleus	¹ H	Number of Transients	8	Original Points Count	9818	Points Count	16384
Pulse Sequence	s2pul	Receiver Gain	39.00	Solvent	CHLOROFORM-d		
Spectrum Offset (Hz)	1797.7676	Spectrum Type	STANDARD	Sweep Width (Hz)	4793.86	Temperature (degree C)	AMBIENT TEMPERATURE



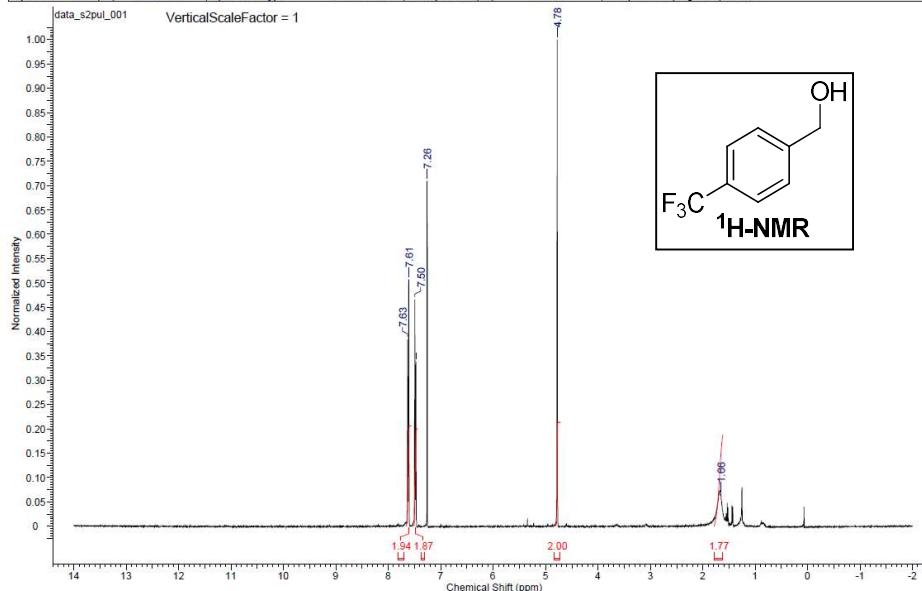
2013/12/2 22:43:10

Acquisition Time (sec)	1.0420	Date	Dec. 2 2013	Date Stamp	Dec. 2 2013
File Name	C:\Users\MMLWW\Desktop\NMR\lrx124-pure_CARBON_02.fidfid	Frequency (MHz)	75.35	Points Count	32768
Nucleus	¹³ C	Number of Transients	3300	Original Points Count	19624
Pulse Sequence	s2pul	Receiver Gain	30.00	Solvent	CHLOROFORM-d
Spectrum Offset (Hz)	6287.5557	Spectrum Type	STANDARD	Sweep Width (Hz)	18832.39
Temperature (degree C) AMBIENT TEMPERATURE					

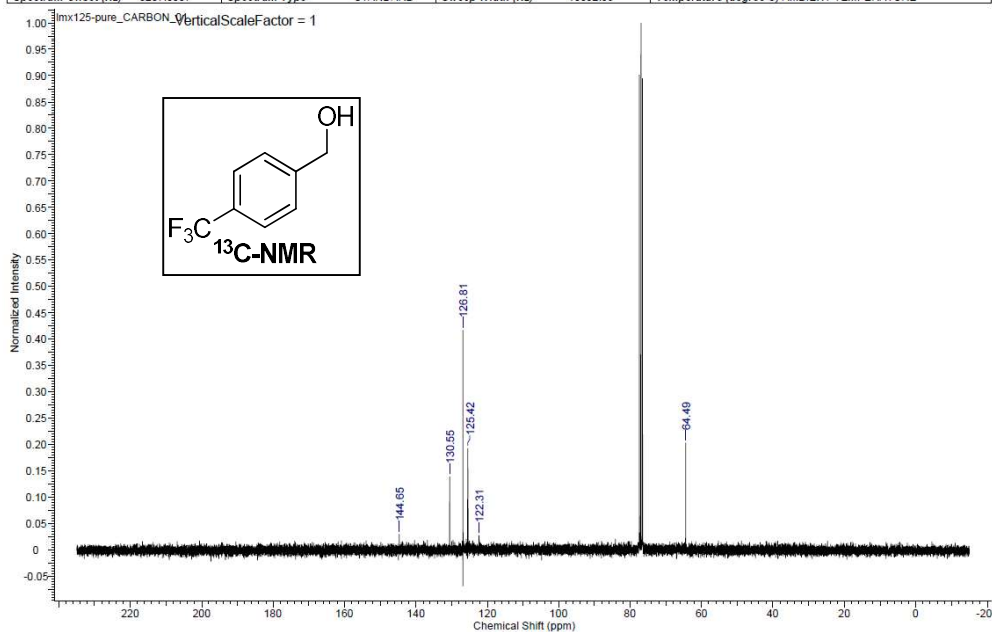


2013/12/3 11:45:33

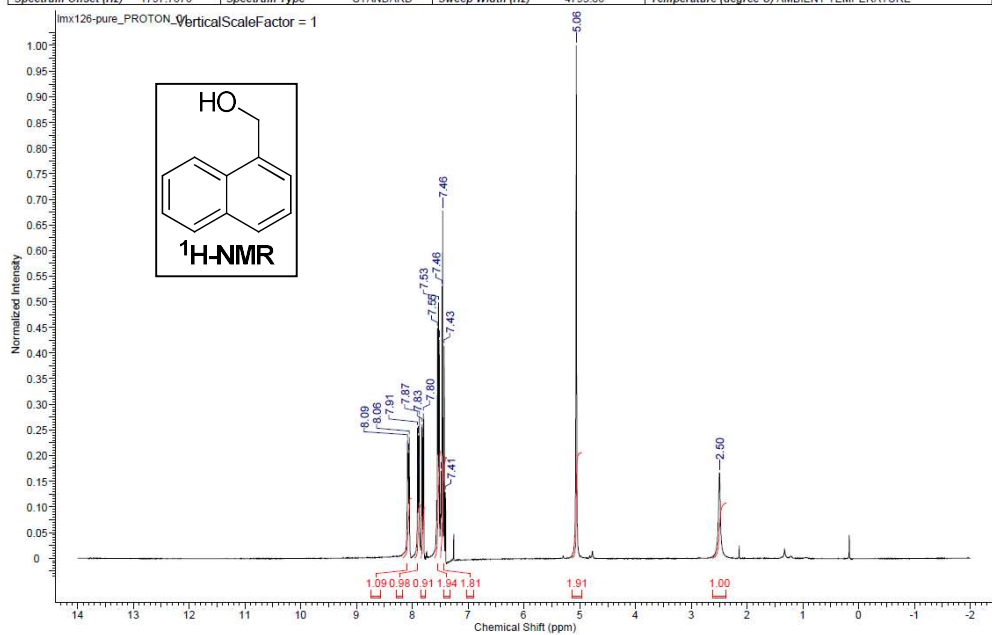
Acquisition Time (sec)	2.5592	Comment	lrx125-new	Date	Dec. 3 2013	Date Stamp	Dec. 3 2013
File Name	C:\Users\MMLWW\Desktop\NMR\lrx125-new_20131203_01\data_s2pul_001.fidfid				Frequency (MHz)	400.12	
Nucleus	1H	Number of Transients	8	Original Points Count	16384	Points Count	16384
Pulse Sequence	s2pul	Receiver Gain	24.00	Solvent	CHLOROFORM-d		
Spectrum Offset (Hz)	2400.7075	Spectrum Type	STANDARD	Sweep Width (Hz)	6402.05	Temperature (degree C)	23.000



Acquisition Time (sec)	1.0420	Date	Dec 3 2013	Date Stamp	Dec 3 2013
File Name	C:\Users\IMML\W\Desktop\NMR\mx125-pure_CARBON_01.fid	Frequency (MHz)	75.35	Points Count	32768
Nucleus	¹³ C	Number of Transients	3300	Original Points Count	19624
Pulse Sequence	s2pul	Receiver Gain	30.00	Solvent	CHLOROFORM-d
Spectrum Offset (Hz)	8287.5557	Spectrum Type	STANDARD	Sweep Width (Hz)	18832.39
		Temperature (degree C)	AMBIENT TEMPERATURE		

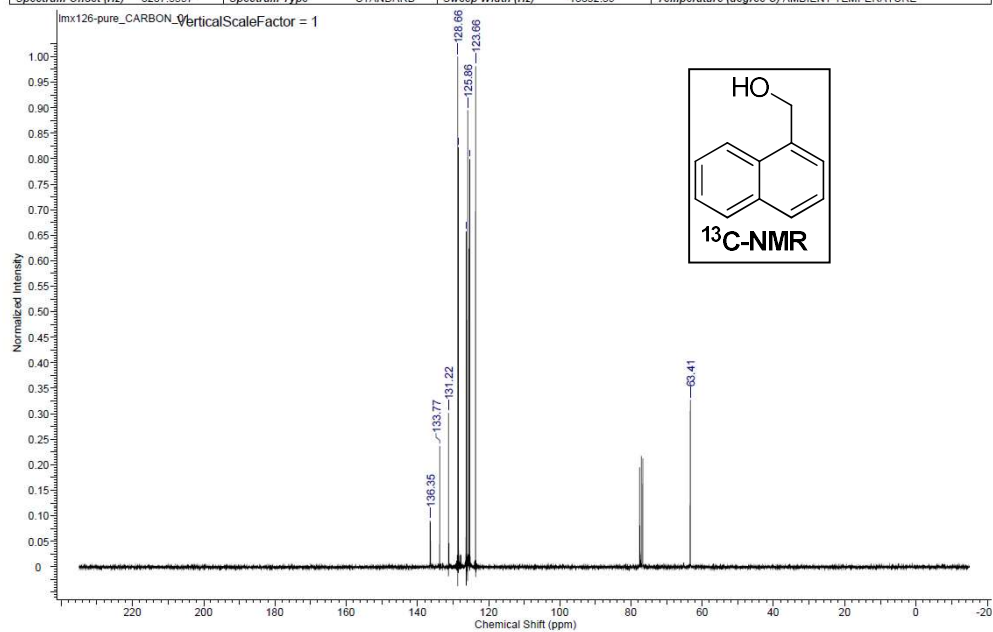


Acquisition Time (sec)	2.0480	Date	Dec 2 2013	Date Stamp	Dec 2 2013
File Name	C:\Users\IMML\W\Desktop\NMR\mx126-pure_PROTON_01.fid	Frequency (MHz)	299.63	Points Count	16384
Nucleus	¹ H	Number of Transients	8	Original Points Count	9818
Pulse Sequence	s2pul	Receiver Gain	16.00	Solvent	CHLOROFORM-d
Spectrum Offset (Hz)	1797.7876	Spectrum Type	STANDARD	Sweep Width (Hz)	4793.86
		Temperature (degree C)	AMBIENT TEMPERATURE		

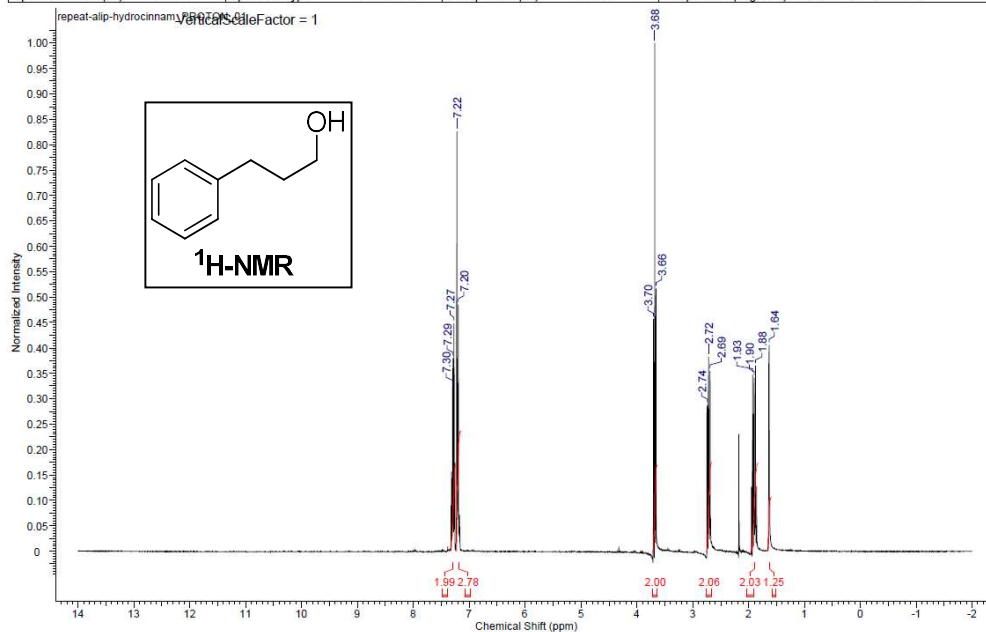


2013/12/22, 44

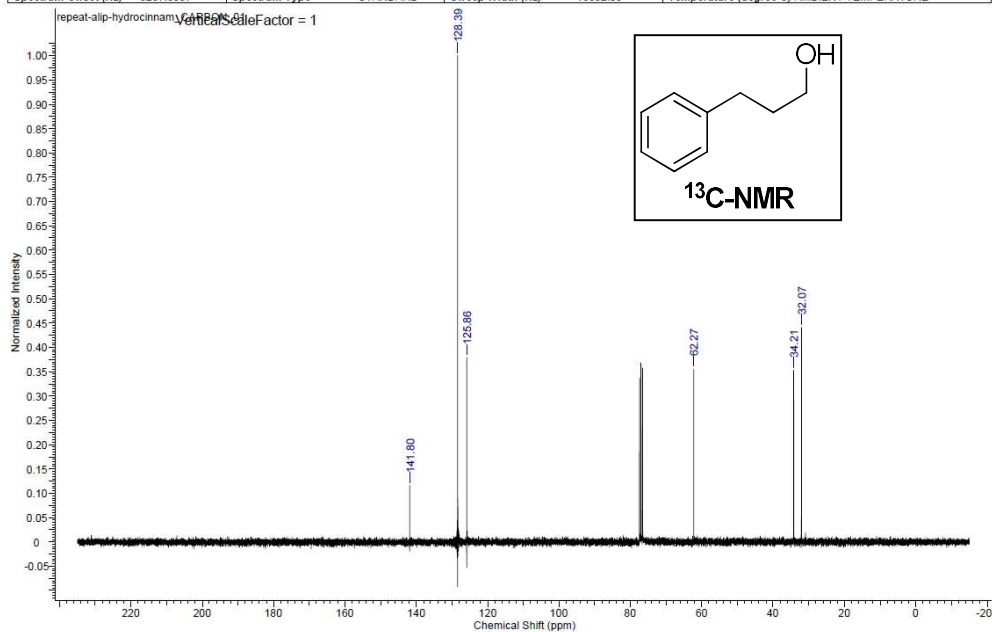
Acquisition Time (sec)	1.0420	Date	Dec. 2 2013	Date Stamp	Dec. 2 2013		
File Name	C:\Users\MMLWW\Desktop\NMR\mx126-pure_CARBON_01.fid.tif					Frequency (MHz)	75.35
Nucleus	¹³ C	Number of Transients	2112	Original Points Count	19624	Points Count	32768
Pulse Sequence	s2pul	Receiver Gain	30.00	Solvent	CHLOROFORM-d		
Spectrum Offset (Hz)	8287.5557	Spectrum Type	STANDARD	Sweep Width (Hz)	18832.39	Temperature (degree C)	AMBIENT TEMPERATURE



Acquisition Time (sec)	2.0480	Date	Dec 2 2013	Date Stamp	Dec 2 2013
File Name	C:\Users\IMLW\Desktop\NMR\repeat-alip-hydrocinnam	PROTON_01.fid.tif	Frequency (MHz)	299.63	
Nucleus	¹ H	Number of Transients	8	Original Points Count	9818
Pulse Sequence	s2pul	Receiver Gain	26.00	Solvent	CHLOROFORM-d
Spectrum Offset (Hz)	1797.7676	Spectrum Type	STANDARD	Sweep Width (Hz)	4793.86
				Temperature (degree C)	AMBIENT TEMPERATURE



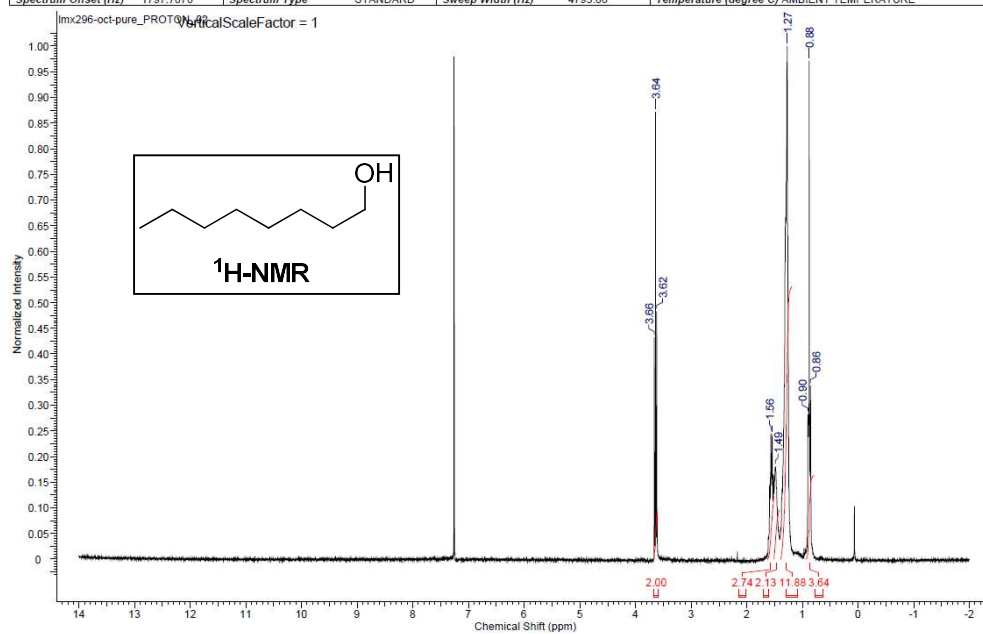
Acquisition Time (sec)	1.0420	Date	Dec. 2 2013	Date Stamp	Dec. 2 2013
File Name	C:\Users\MMLWW\Desktop\NMR\repeat-alip-hydrocinnam_CARBON_01.fid	Frequency (MHz)	75.35	Points Count	32768
Nucleus	¹³ C	Number of Transients	1024	Original Points Count	19624
Pulse Sequence	s2pul	Receiver Gain	30.00	Solvent	CHLOROFORM-d
Spectrum Offset (Hz)	8287.5557	Spectrum Type	STANDARD	Sweep Width (Hz)	18832.39
				Temperature (degree C)	AMBIENT TEMPERATURE



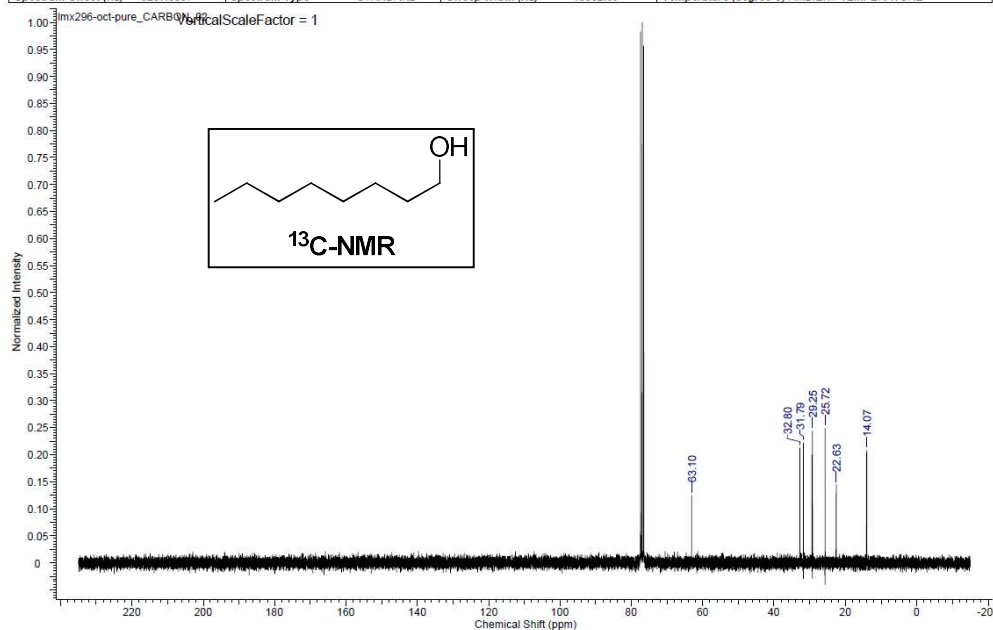
This report was created by ACD/NMR Processor Academic Edition. For more information go to www.acdlabs.com/nmrproc/

2013/12/2 22:47:41

Acquisition Time (sec)	2.0480	Date	Aug 19 2013	Date Stamp	Aug 19 2013		
File Name	C:\Users\IMLW\Desktop\NMR\mx296-oct-pure_PROTON_02.fid				Frequency (MHz)	299.63	
Nucleus	¹ H	Number of Transients	8	Original Points Count	9818	Points Count	16384
Pulse Sequence	s2pul	Receiver Gain	36.00	Solvent	CHLOROFORM-d		
Spectrum Offset (Hz)	1797.7676	Spectrum Type	STANDARD	Sweep Width (Hz)	4793.86	Temperature (degree C)	AMBIENT TEMPERATURE



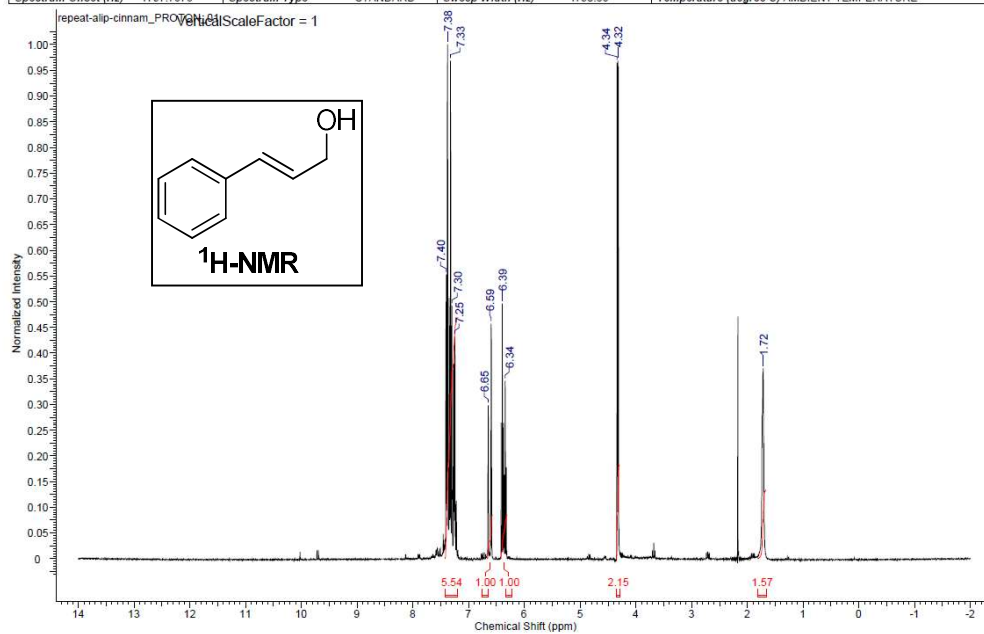
Acquisition Time (sec)	1.0420	Date	Aug 19 2013	Date Stamp	Aug 19 2013
File Name	C:\Users\IMLW\My Desktop\NMR\m296-oct-pure_CARBON_02.fid	Frequency (MHz)	75.35	Points Count	32768
Nucleus	¹³ C	Number of Transients	3300	Original Points Count	19624
Pulse Sequence	s2pul	Receiver Gain	30.00	Solvent	CHLOROFORM-d
Spectrum Offset (Hz)	8287.5557	Spectrum Type	STANDARD	Sweep Width (Hz)	18832.39
				Temperature (degree C)	AMBIENT TEMPERATURE



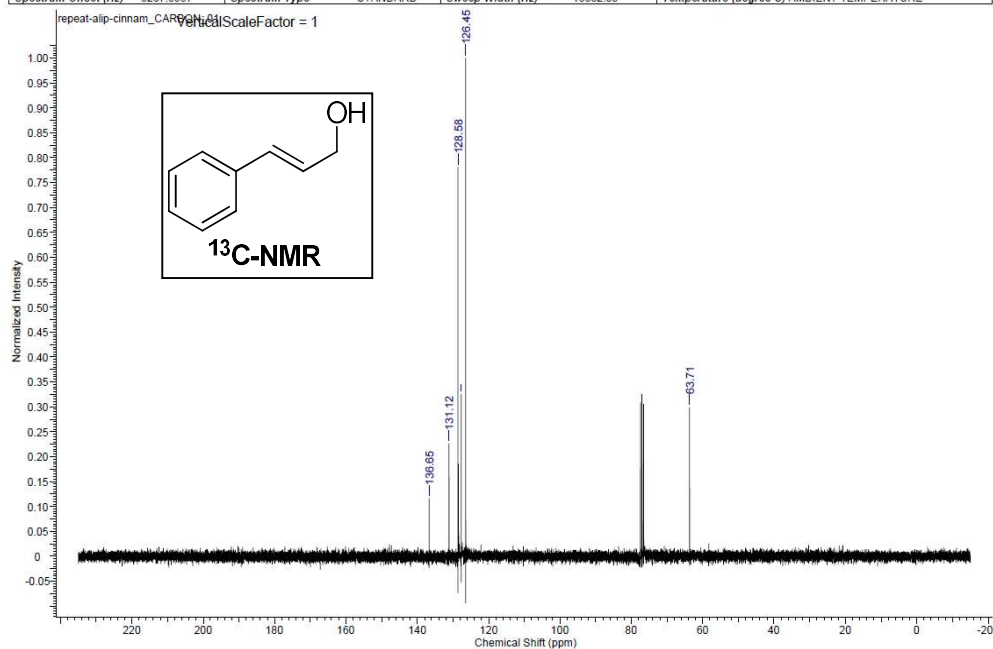
This report was created by ACD/NMR Processor Academic Edition. For more information go to www.acdlabs.com/nmrproc/

2013/12/2 22:49:56

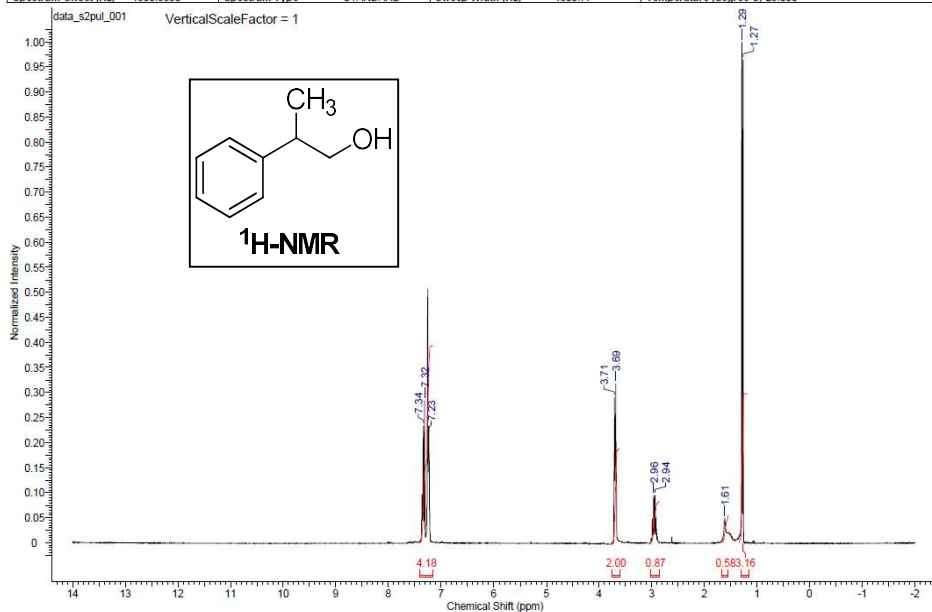
Acquisition Time (sec)	2.0480	Date	Dec 2 2013	Date Stamp	Dec 2 2013	
File Name	C:\Users\MMLW\Desktop\NMR\repeat-alip-cinnam_PROTON_01.fid				Frequency (MHz)	299.63
Nucleus	¹ H	Number of Transients	8	Original Points Count	9818	Points Count 16384
Pulse Sequence	s2pul	Receiver Gain	30.00	Solvent	CHLOROFORM-d	
Spectrum Offset (Hz)	1797.7676	Spectrum Type	STANDARD	Sweep Width (Hz)	4793.86	Temperature (degree C) AMBIENT TEMPERATURE



Acquisition Time (sec)	1.0420	Date	Dec 2 2013	Date Stamp	Dec 2 2013
File Name	C:\Users\MML\W\Desktop\NMR\repeat-alip-cinnam_CARBON_01.fid	Frequency (MHz)	75.35	Points Count	32768
Nucleus	¹³ C	Number of Transients	320	Original Points Count	19624
Pulse Sequence	s2pul	Receiver Gain	30.00	Solvent	CHLOROFORM-d
Spectrum Offset (Hz)	8287.5557	Spectrum Type	STANDARD	Sweep Width (Hz)	18832.39
				Temperature (degree C)	AMBIENT TEMPERATURE



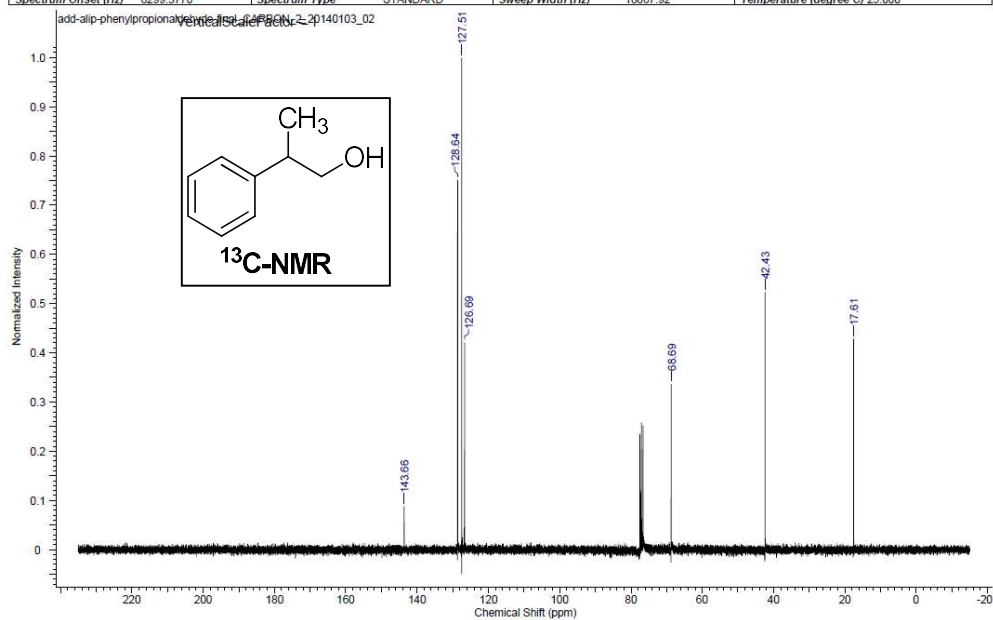
Acquisition Time (sec)	2.0480	Comment	add-alip-phenylpropionaldehyde-final	Date	Jan 3 2014
Date Stamp	Jan 3 2014	File Name	C:\Users\MML\W\Desktop\add-alip-phenylpropionaldehyde-final	20140103_01\data_s2pul_001.fid	
Frequency (MHz)	300.06	Nucleus	¹ H	Number of Transients	8
Points Count	16384	Pulse Sequence	s2pul	Receiver Gain	24.00
Spectrum Offset (Hz)	1800.3330	Spectrum Type	STANDARD	Sweep Width (Hz)	4800.77
				Temperature (degree C)	25.000



This report was created by ACD/NMR Processor Academic Edition. For more information go to www.acdlabs.com/nmrproc/

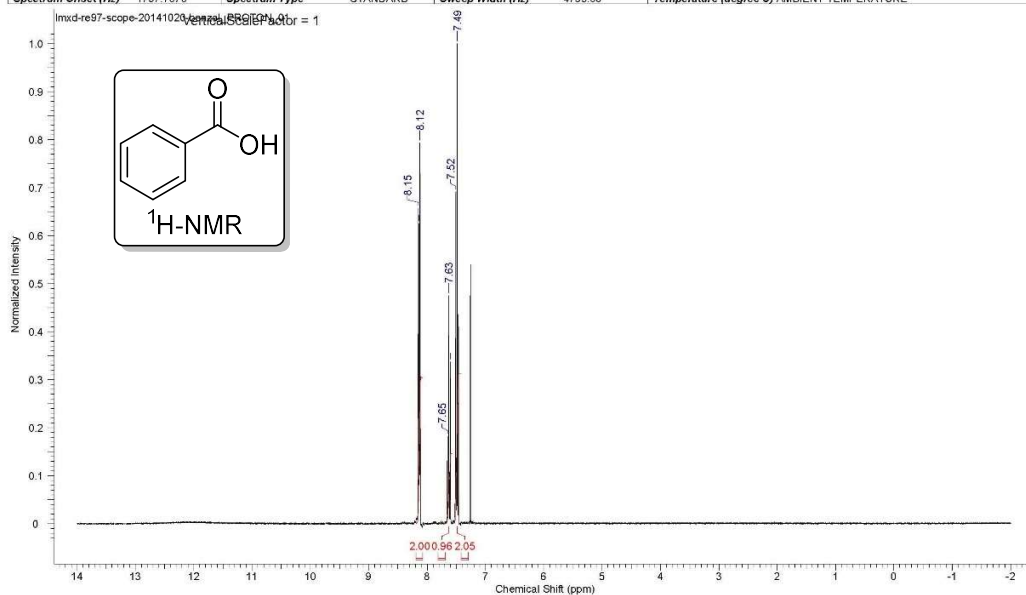
2014/1/6 18:27:17

Acquisition Time (sec)	1.0420	Comment	add-alip-phenylpropionaldehyde-final	Date	Jan. 3 2014
Date Stamp	Jan. 3 2014				
File Name	C:\Users\IMMLWW\Desktop\add-alip-phenylpropionaldehyde-final_20140103_02\add-alip-phenylpropionaldehyde-final			CARBON_2_20140103_02.fid.tif	
Frequency (MHz)	75.46	Nucleus	¹³ C	Number of Transients	1651
Points Count	32768	Pulse Sequence	zgpg30	Original Points Count	19661
Spectrum Offset (Hz)	8299.3770	Spectrum Type	STANDARD	Receiver Gain	30.00
				Solvent	CHLOROFORM-d
				Sweep Width (Hz)	18867.92
				Temperature (degree C)	25.000

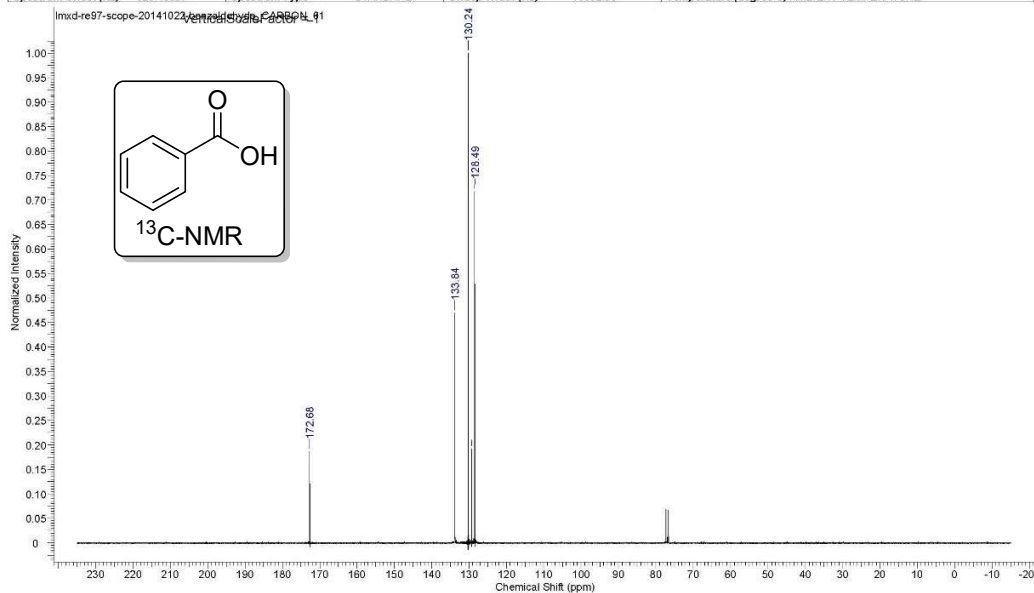


NMR spectra of products described in chapter 4

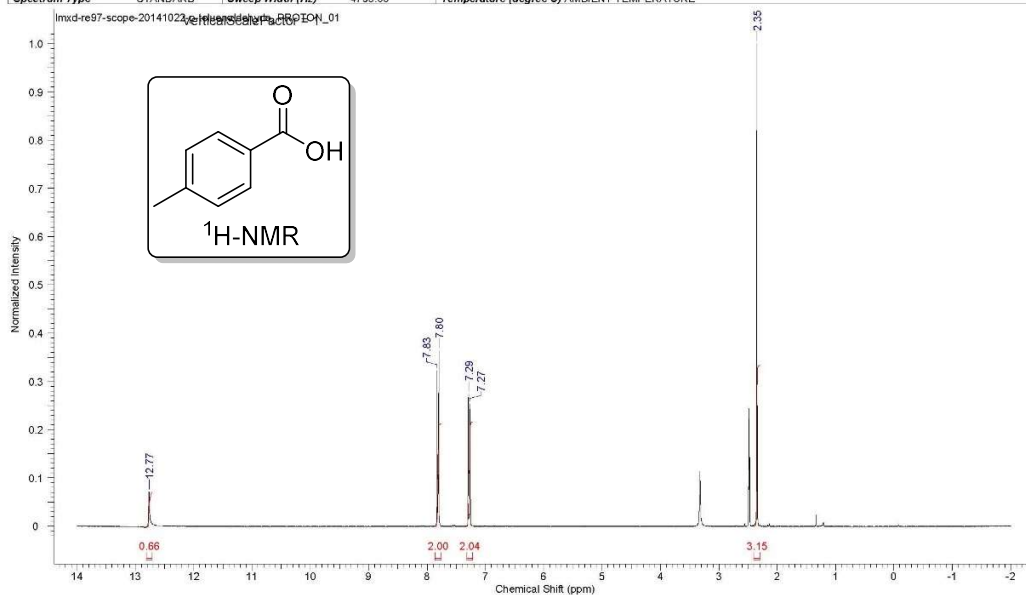
Acquisition Time (sec)	2.0480	Date	Oct 20 2014	Date Stamp	Oct 20 2014
File Name	G:\20140818-scope\additional\lmsd-re97-scope-20141020-benzal_PROTON_01.fid	Number of Transients	8	Original Points Count	9818
Nucleus	¹ H	Receiver Gain	39.00	Solvent	CHLOROFORM-d
Pulse Sequence	s2pul	Spectrum Type	STANDARD	Sweep Width (Hz)	4793.86
Spectrum Offset (Hz)	1797.7676			Temperature (degree C)	AMBIENT TEMPERATURE



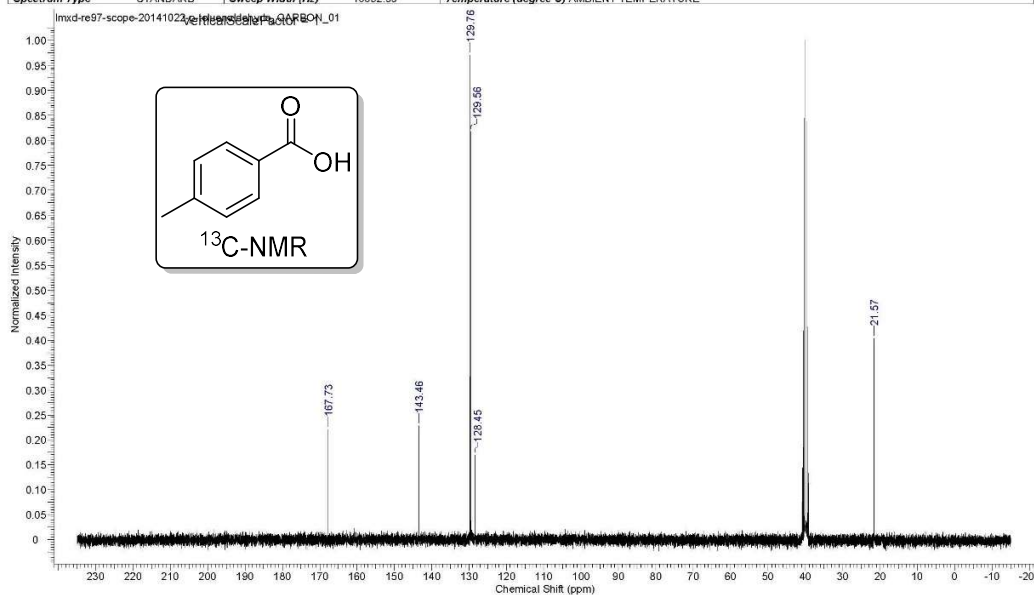
Acquisition Time (sec)	1.0420	Date	Oct 23 2014	Date Stamp	Oct 23 2014
File Name	G:\20140818-scope\additional\lmsd-re97-scope-20141022-benzaldehyde_CARBON_01.fid	Number of Transients	1750	Original Points Count	19624
Nucleus	¹³ C	Receiver Gain	30.00	Solvent	CHLOROFORM-d
Pulse Sequence	s2pul	Spectrum Type	STANDARD	Sweep Width (Hz)	18832.39
Spectrum Offset (Hz)	6287.5557			Temperature (degree C)	AMBIENT TEMPERATURE



Acquisition Time (sec)	2.0480	Date	Oct 22 2014	Date Stamp	Oct 22 2014
File Name	G:\20140818-scope\additional\lmsd-re97-scope-20141022-p-toluenaldehyde_PROTON_01.fid	Frequency (MHz)	299.63		
Nucleus	¹ H	Number of Transients	8	Original Points Count	9818
Pulse Sequence	s2pul	Receiver Gain	36.00	Solvent	DMSO-d6
Spectrum Type	STANDARD	Sweep Width (Hz)	4793.86	Temperature (degree C)	AMBIENT TEMPERATURE
				Spectrum Offset (Hz)	1797.7788

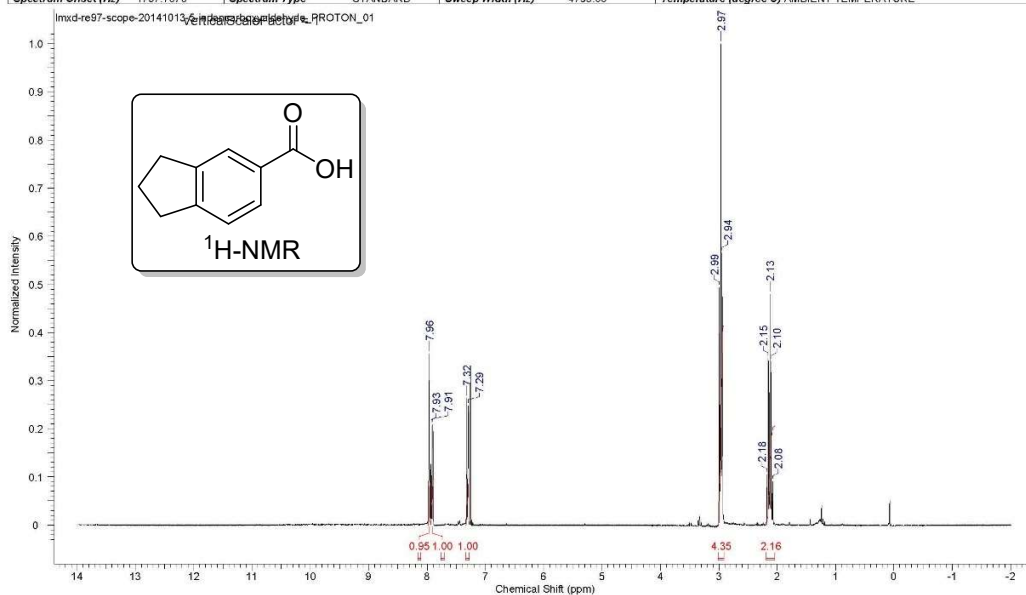


Acquisition Time (sec)	1.0420	Date	Oct 22 2014	Date Stamp	Oct 22 2014
File Name	G:\20140818-scope\additional\lmsd-re97-scope-20141022-p-toluenaldehyde_CARBON_01.fid	Frequency (MHz)	75.35		
Nucleus	¹³ C	Number of Transients	1700	Original Points Count	19624
Pulse Sequence	s2pul	Receiver Gain	30.00	Solvent	DMSO-d6
Spectrum Type	STANDARD	Sweep Width (Hz)	18832.39	Temperature (degree C)	AMBIENT TEMPERATURE
				Spectrum Offset (Hz)	8287.6016



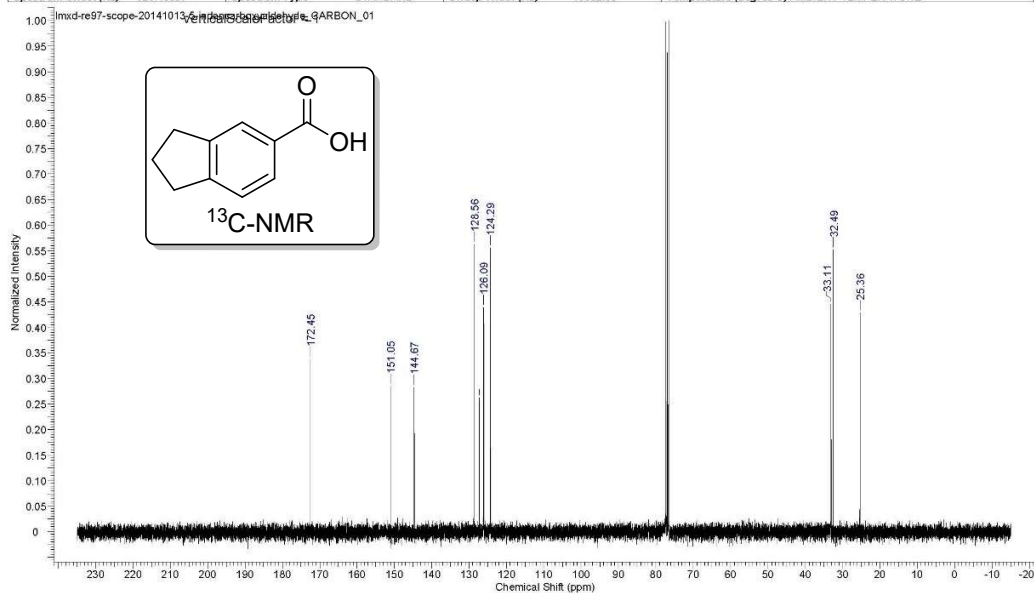
20/10/2014 9:47:29 PM

Acquisition Time (sec)	2.0480	Date	Oct 14 2014	Date Stamp	Oct 14 2014
File Name	G:\20140818-scope\lmsd-re97-scope-20141013-5-indancarboxaldehyde_PROTON_01.fid	Frequency (MHz)	299.63		
Nucleus	¹ H	Number of Transients	8	Original Points Count	9818
Pulse Sequence	s2pul	Receiver Gain	36.00	Solvent	CHLOROFORM-d
Spectrum Offset (Hz)	1797.7676	Spectrum Type	STANDARD	Sweep Width (Hz)	4793.86
				Temperature (degree C)	AMBIENT TEMPERATURE



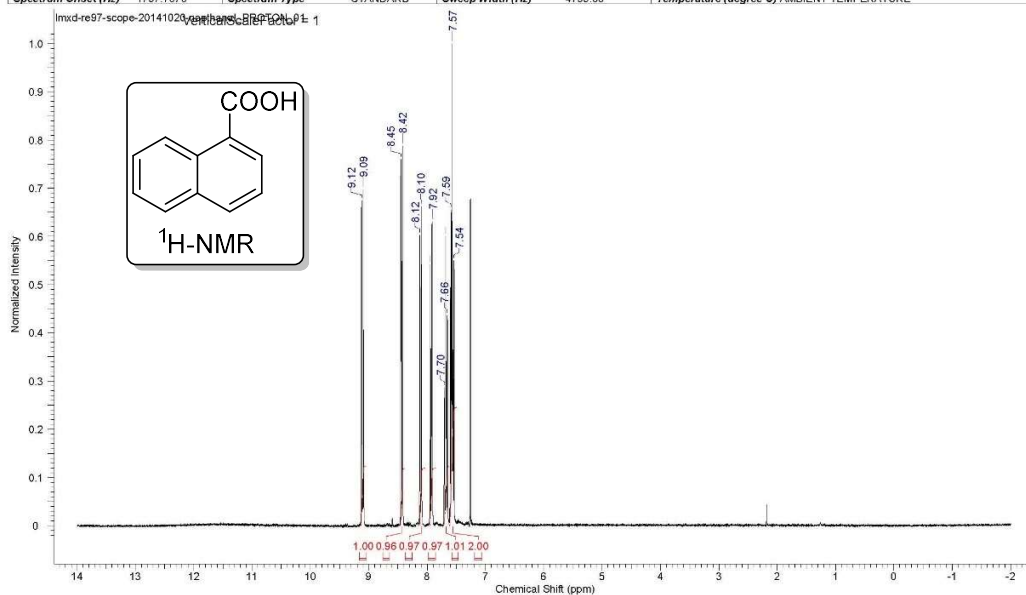
20/10/2014 9:48:09 PM

Acquisition Time (sec)	1.0420	Date	Oct 14 2014	Date Stamp	Oct 14 2014
File Name	G:\20140818-scope\lmsd-re97-scope-20141013-5-indancarboxaldehyde_CARBON_01.fid	Frequency (MHz)	75.35		
Nucleus	¹³ C	Number of Transients	1700	Original Points Count	19624
Pulse Sequence	s2pul	Receiver Gain	30.00	Solvent	CHLOROFORM-d
Spectrum Offset (Hz)	6287.5557	Spectrum Type	STANDARD	Sweep Width (Hz)	18832.39
				Temperature (degree C)	AMBIENT TEMPERATURE



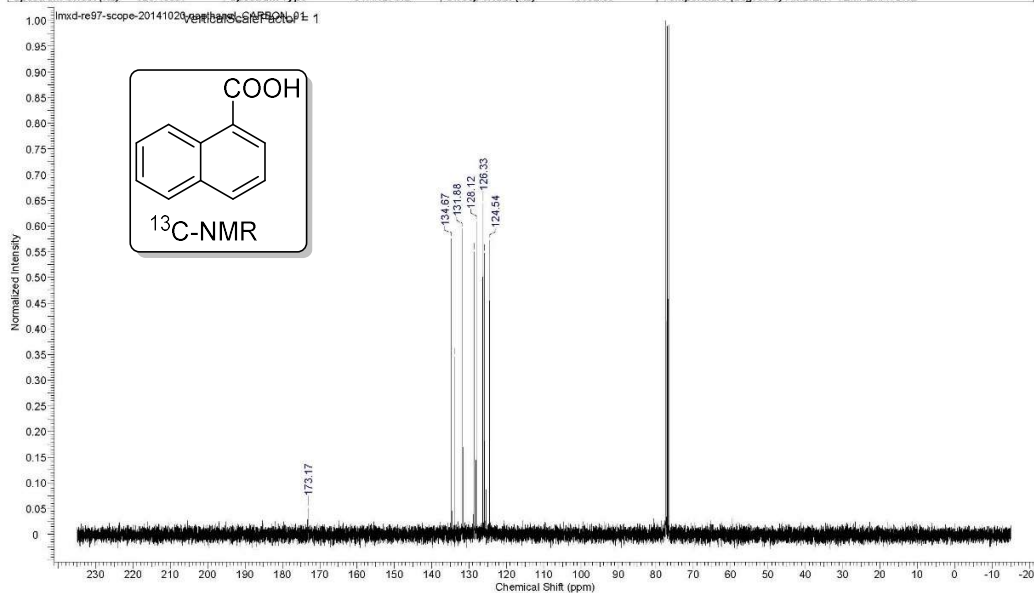
21/10/2014 8:20:22 AM

Acquisition Time (sec)	2.0480	Date	Oct 20 2014	Date Stamp	Oct 20 2014
File Name	G:\20140818-scope\additional\imxd-re97-scope-20141020-naphthal_PROTON_01.fid			Frequency (MHz)	299.63
Nucleus	¹ H	Number of Transients	8	Original Points Count	9818
Pulse Sequence	s2pul	Receiver Gain	36.00	Solvent	CHLOROFORM-d
Spectrum Offset (Hz)	1797.7676	Spectrum Type	STANDARD	Sweep Width (Hz)	4793.86
				Temperature (degree C)	AMBIENT TEMPERATURE



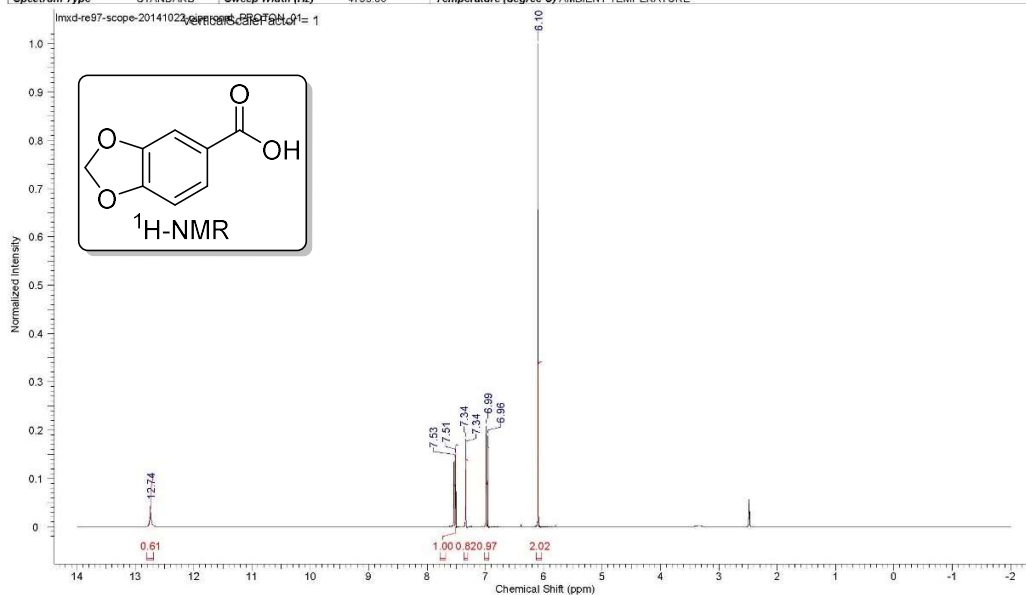
21/10/2014 8:21:23 AM

Acquisition Time (sec)	1.0420	Date	Oct 20 2014	Date Stamp	Oct 20 2014
File Name	G:\20140818-scope\additional\imxd-re97-scope-20141020-naphthal_CARBON_01.fid			Frequency (MHz)	75.35
Nucleus	¹³ C	Number of Transients	1700	Original Points Count	19624
Pulse Sequence	s2pul	Receiver Gain	30.00	Solvent	CHLOROFORM-d
Spectrum Offset (Hz)	6287.5557	Spectrum Type	STANDARD	Sweep Width (Hz)	18832.39
				Temperature (degree C)	AMBIENT TEMPERATURE



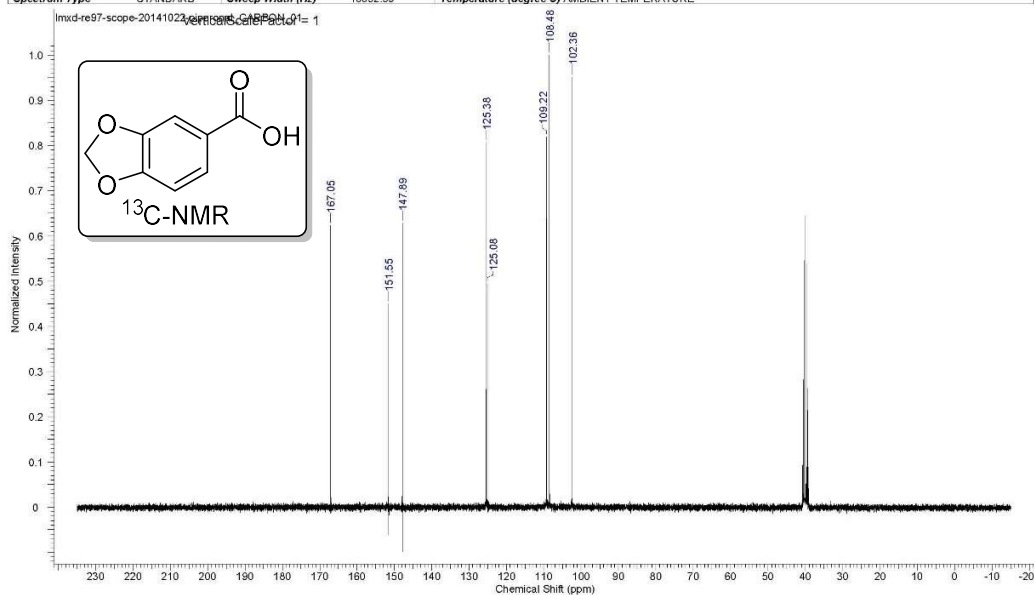
22/10/2014 11:05:35 PM

Acquisition Time (sec)	2.0480	Date	Oct 22 2014	Date Stamp	Oct 22 2014
File Name	G:\20140818-scope\additional\lmsd-re97-scope-20141022-piperonal_PROTON_01.fid	Frequency (MHz)	299.63		
Nucleus	¹ H	Number of Transients	8	Original Points Count	9818
Pulse Sequence	s2pul	Receiver Gain	30.00	Solvent	DMSO-d6
Spectrum Type	STANDARD	Sweep Width (Hz)	4793.86	Temperature (degree C)	AMBIENT TEMPERATURE
				Spectrum Offset (Hz)	1797.7788



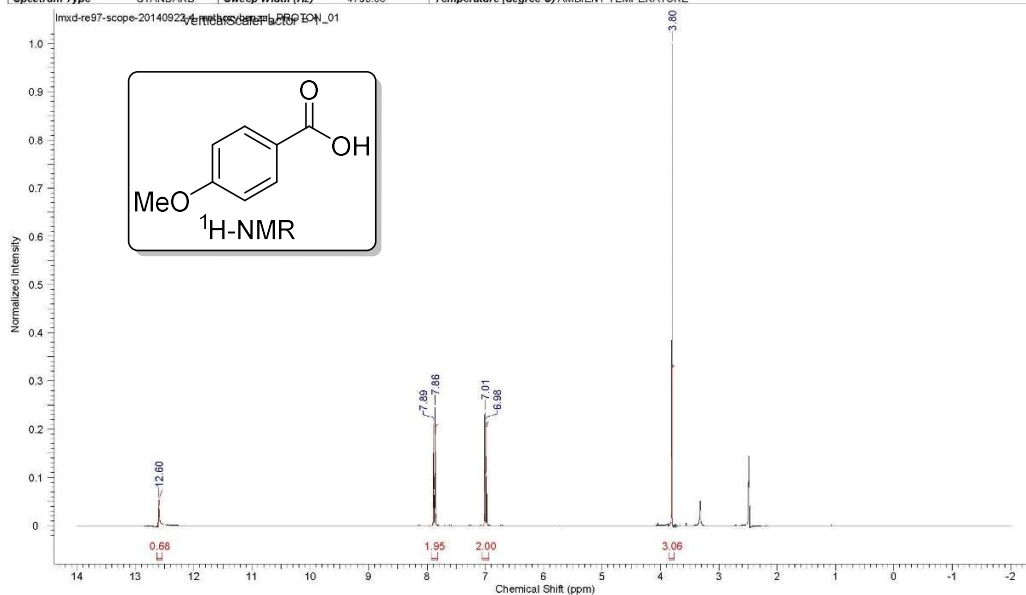
23/10/2014 7:27:03 PM

Acquisition Time (sec)	1.0420	Date	Oct 22 2014	Date Stamp	Oct 22 2014
File Name	G:\20140818-scope\additional\lmsd-re97-scope-20141022-piperonal_CARBOON_01.fid	Frequency (MHz)	75.35		
Nucleus	¹³ C	Number of Transients	1750	Original Points Count	19624
Pulse Sequence	s2pul	Receiver Gain	30.00	Solvent	DMSO-d6
Spectrum Type	STANDARD	Sweep Width (Hz)	18832.39	Temperature (degree C)	AMBIENT TEMPERATURE
				Spectrum Offset (Hz)	8287.6016



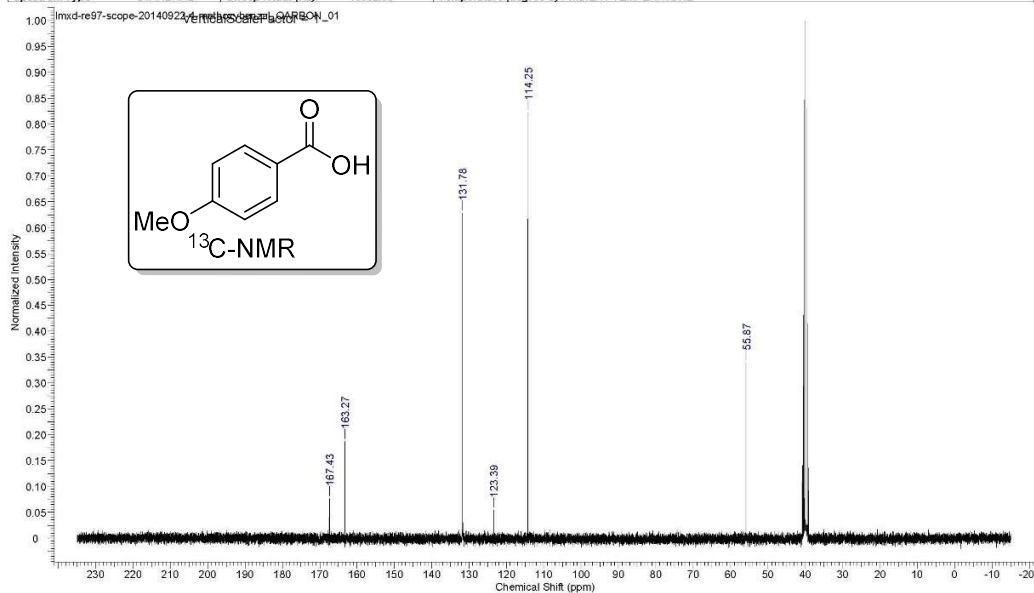
20/10/2014 9:48:34 PM

Acquisition Time (sec)	2.0480	Date	Sep 22 2014	Date Stamp	Sep 22 2014
File Name	G:\20140818-scope\lmsd-re97-scope-20140922-4-methoxybenzal_PROTON_01.fid	Number of Transients	8	Original Points Count	9818
Nucleus	¹ H	Receiver Gain	30.00	Solvent	DMSO-d6
Pulse Sequence	s2pul	Sweep Width (Hz)	4793.86	Temperature (degree C)	AMBIENT TEMPERATURE
Spectrum Type	STANDARD			Frequency (MHz)	299.63
				Points Count	16364
				Spectrum Offset (Hz)	1797.7788



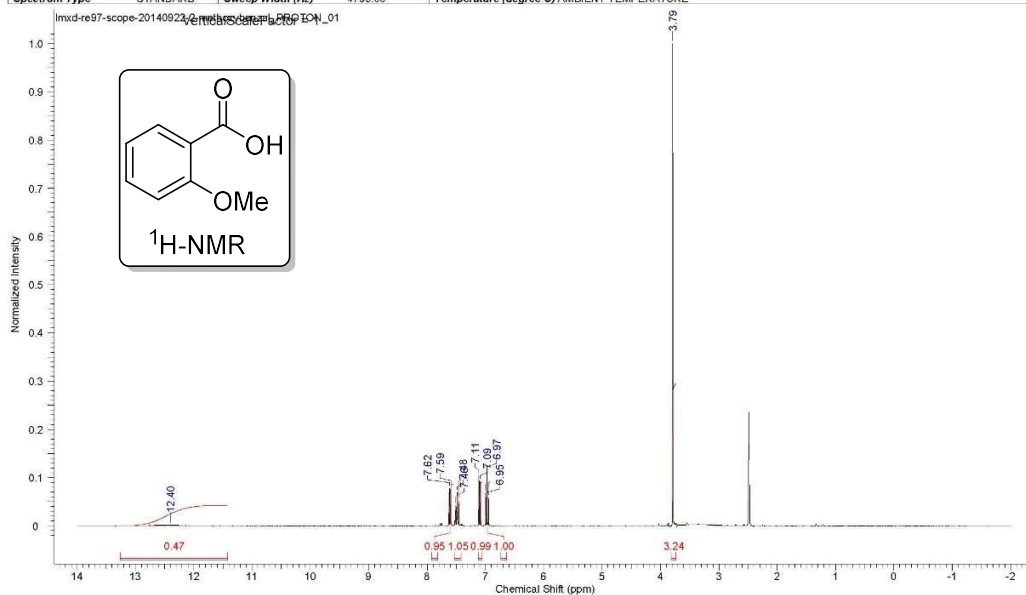
20/10/2014 9:48:17 PM

Acquisition Time (sec)	1.0420	Date	Sep 23 2014	Date Stamp	Sep 23 2014
File Name	G:\20140818-scope\lmsd-re97-scope-20140922-4-methoxybenzal_CARBON_01.fid	Number of Transients	1696	Original Points Count	19624
Nucleus	¹³ C	Receiver Gain	30.00	Solvent	DMSO-d6
Pulse Sequence	s2pul	Sweep Width (Hz)	18832.39	Temperature (degree C)	AMBIENT TEMPERATURE
Spectrum Type	STANDARD			Frequency (MHz)	75.35
				Points Count	32768
				Spectrum Offset (Hz)	8287.6016



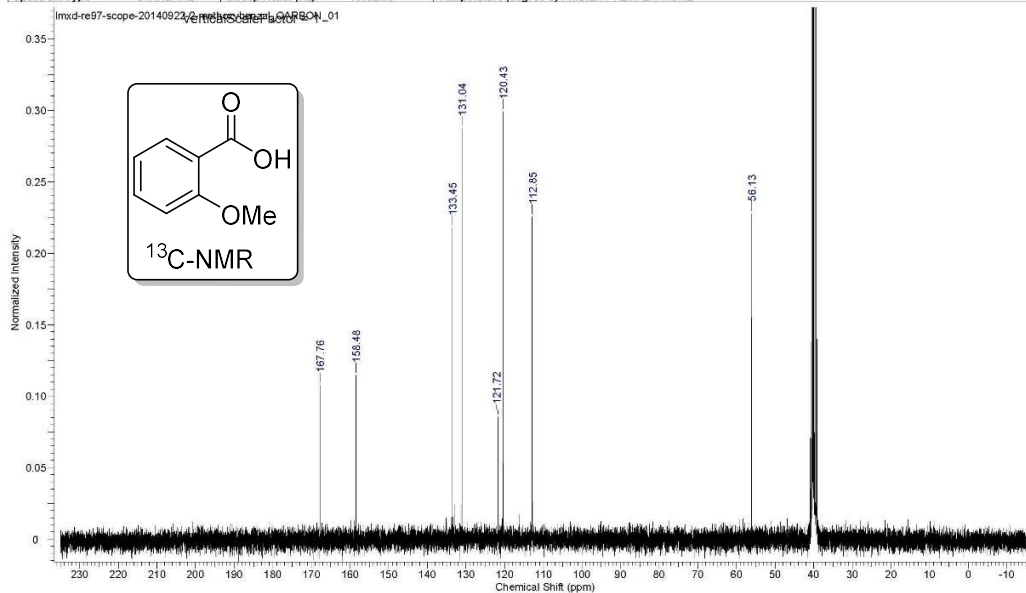
20/10/2014 10:46:49 PM

Acquisition Time (sec)	2.0480	Date	Sep 22 2014	Date Stamp	Sep 22 2014
File Name	G:\20140818-scope\lmsd-re97-scope-20140922-2-methoxybenzal_PROTON_01.fid	Number of Transients	8	Original Points Count	9818
Nucleus	¹ H	Receiver Gain	39.00	Solvent	DMSO-d6
Pulse Sequence	s2pul	Sweep Width (Hz)	4793.86	Temperature (degree C)	AMBIENT TEMPERATURE
Spectrum Type	STANDARD			Frequency (MHz)	299.63
				Points Count	16364
				Spectrum Offset (Hz)	1797.7788



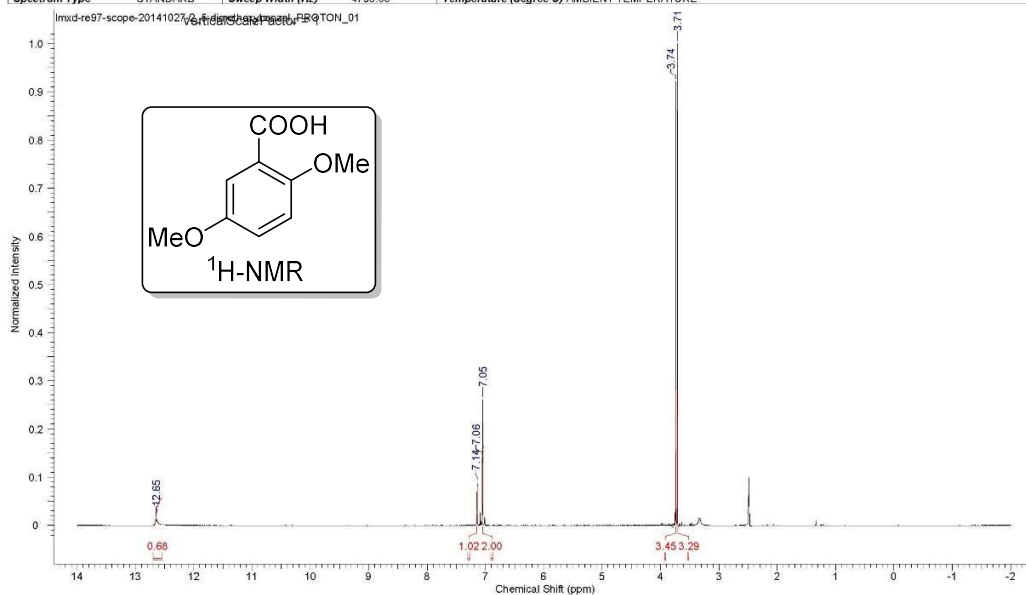
20/10/2014 10:47:57 PM

Acquisition Time (sec)	1.0420	Date	Sep 23 2014	Date Stamp	Sep 23 2014
File Name	G:\20140818-scope\lmsd-re97-scope-20140922-2-methoxybenzal_CARBON_01.fid	Number of Transients	3300	Original Points Count	19624
Nucleus	¹³ C	Receiver Gain	30.00	Solvent	DMSO-d6
Pulse Sequence	s2pul	Sweep Width (Hz)	18832.39	Temperature (degree C)	AMBIENT TEMPERATURE
Spectrum Type	STANDARD			Frequency (MHz)	75.35
				Points Count	32768
				Spectrum Offset (Hz)	8287.6016



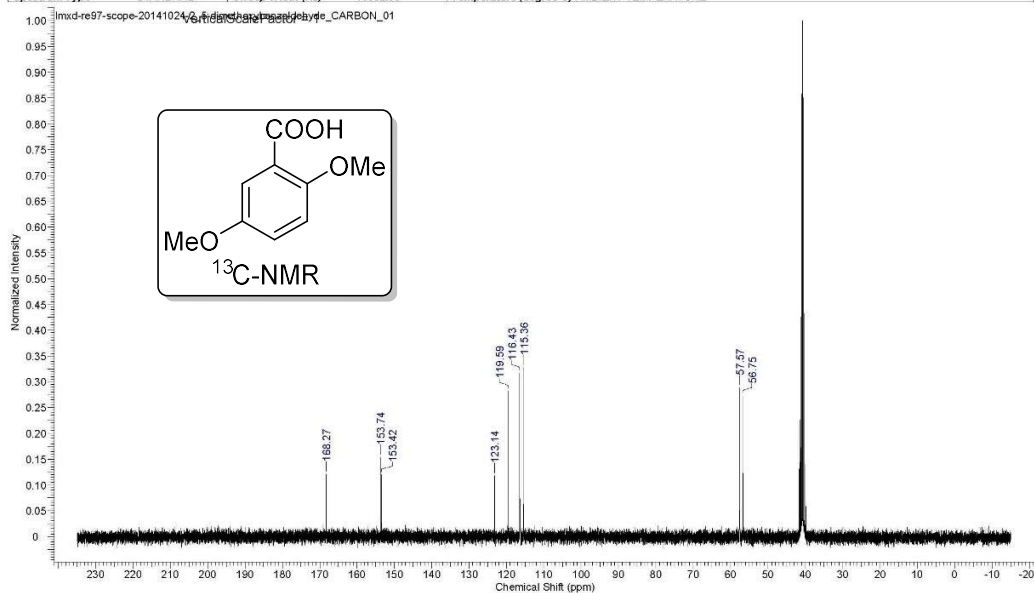
07/11/2014 11:04:32 PM

Acquisition Time (sec)	2.0480	Date	Oct 27 2014	Date Stamp	Oct 27 2014
File Name	C:\Users\MMLWW\Desktop\lmsd-re97-scope-20141027-2_5-dimethoxybenzaldehyde_PROTON_01.fid				Frequency (MHz)
Nucleus	¹ H	Number of Transients	8	Original Points Count	8818
Pulse Sequence	s2pul	Receiver Gain	30.00	Solvent	DMSO-d6
Spectrum Type	STANDARD	Sweep Width (Hz)	4793.86	Temperature (degree C)	AMBIENT TEMPERATURE
					Points Count
					Spectrum Offset (Hz)



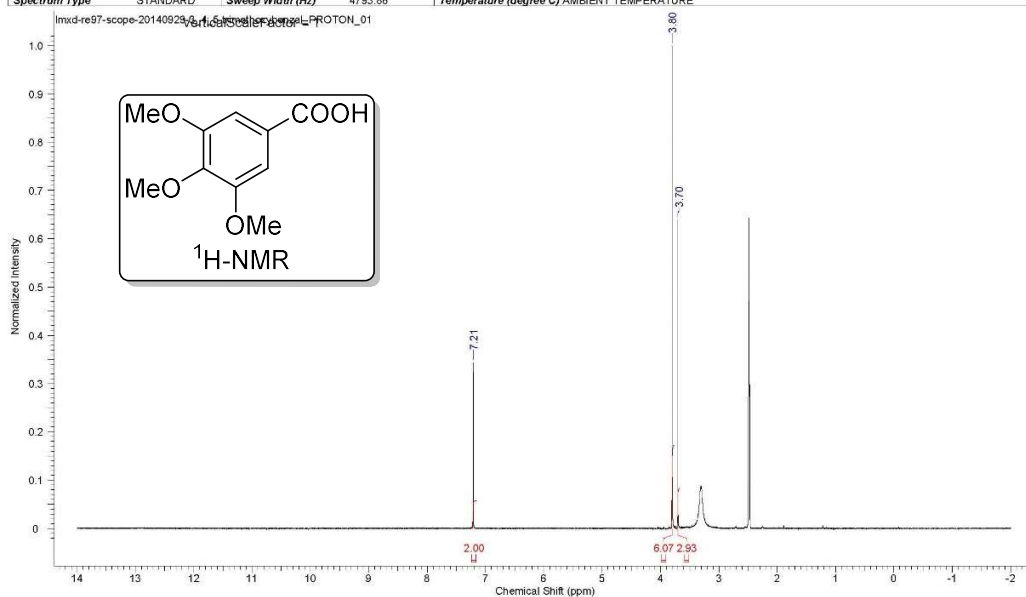
07/11/2014 11:05:58 PM

Acquisition Time (sec)	1.0420	Date	Oct 24 2014	Date Stamp	Oct 24 2014
File Name	C:\Users\MMLWW\Desktop\lmsd-re97-scope-20141024-2_5-dimethoxybenzaldehyde_CARBOON_01.fid				Frequency (MHz)
Nucleus	¹³ C	Number of Transients	1700	Original Points Count	19624
Pulse Sequence	s2pul	Receiver Gain	30.00	Solvent	DMSO-d6
Spectrum Type	STANDARD	Sweep Width (Hz)	18832.39	Temperature (degree C)	AMBIENT TEMPERATURE
					Points Count
					Spectrum Offset (Hz)



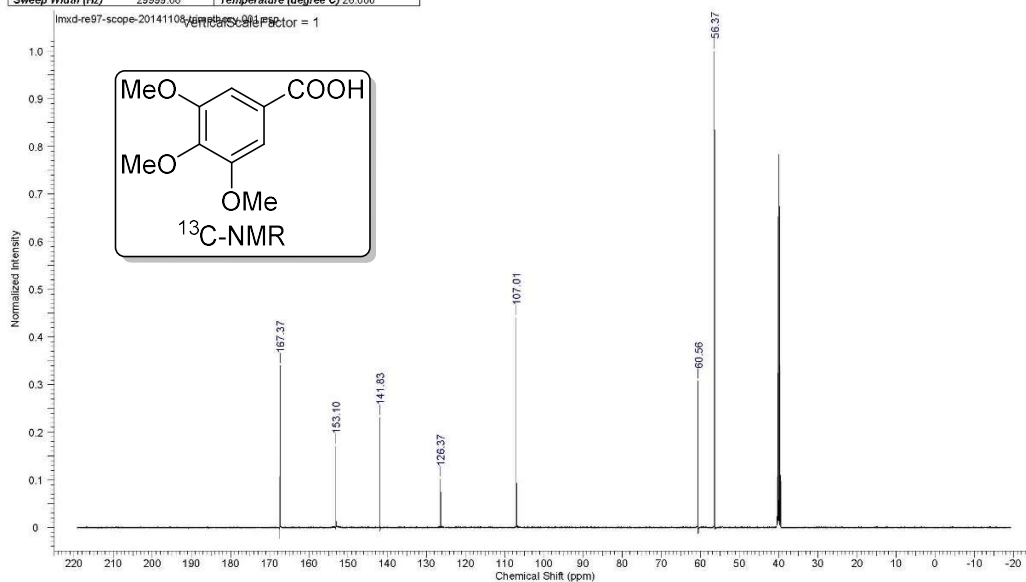
07/11/2014 10:38:29 PM

Acquisition Time (sec)	2.0480	Date	Sep 29 2014	Date Stamp	Sep 29 2014
File Name	G:\20140818-scope\mx-d-re97-scope-20140929-3_4_5-trimethoxybenzal_PROTON_01.fid	Frequency (MHz)	299.63	Points Count	16364
Nucleus	¹ H	Number of Transients	8	Original Points Count	9818
Pulse Sequence	s2pul	Receiver Gain	39.00	Solvent	DMSO-d6
Spectrum Type	STANDARD	Sweep Width (Hz)	4793.86	Temperature (degree C)	AMBIENT TEMPERATURE
				Spectrum Offset (Hz)	1797.7768

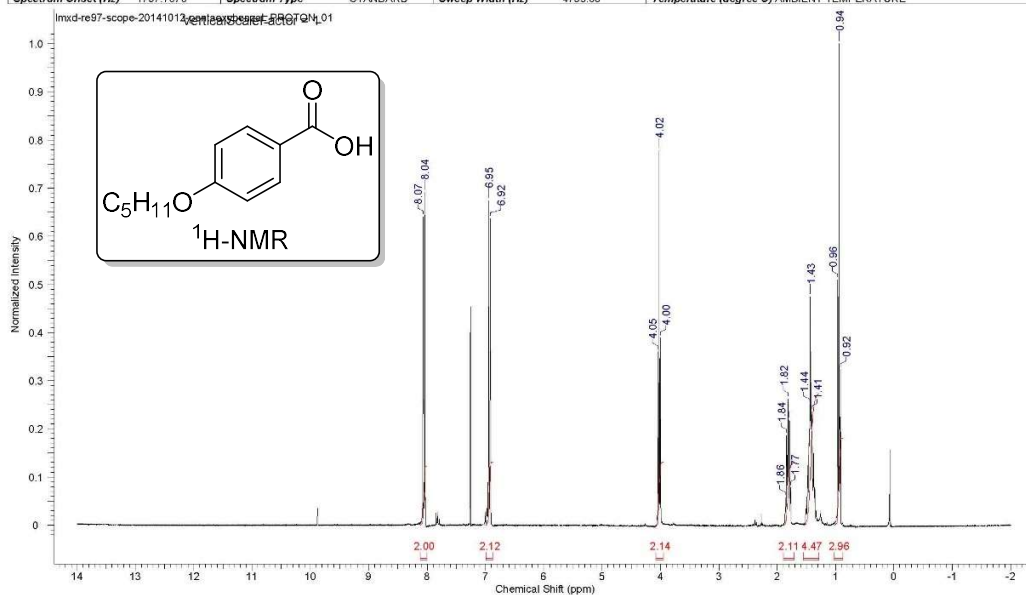


08/11/2014 8:50:08 PM

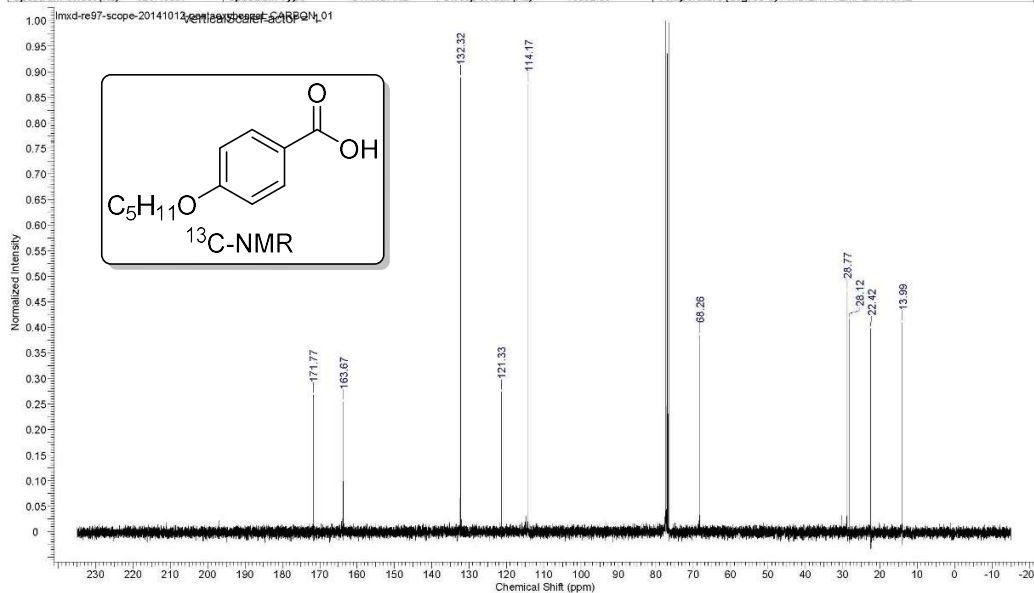
Acquisition Time (sec)	1.0923	Date	08 Nov 2014 14:33:20	Date Stamp	08 Nov 2014 14:33:20
File Name	C:\Users\MML\My Desktop\mx-d-re97-scope-20141108-trimethoxy11.fid	Frequency (MHz)	125.81	Points Count	32768
Nucleus	¹³ C	Number of Transients	3400	Original Points Count	32768
Owner	mcgillnmr	Points Count	32768	Pulse Sequence	zgpg30
SW (cyclic) (Hz)	30000.00	Solvent	DMSO-d6	Spectrum Offset (Hz)	12578.9238
Sweep Width (Hz)	29999.08	Temperature (degree C)	26.000	Receiver Gain	192.72
				Spectrum Type	STANDARD



Acquisition Time (sec)	2.0480	Date	Oct 12 2014	Date Stamp	Oct 12 2014
File Name	G:\20140818-scope\lmsd-re97-scope-20141012-pentaoxybenzal	PROTON_01.fid.fid	Frequency (MHz)	299.63	
Nucleus	¹ H	Number of Transients	8	Original Points Count	9818
Pulse Sequence	s2pul	Receiver Gain	36.00	Solvent	CHLOROFORM-d
Spectrum Offset (Hz)	1797.7676	Spectrum Type	STANDARD	Sweep Width (Hz)	4793.86
				Temperature (degree C)	AMBIENT TEMPERATURE

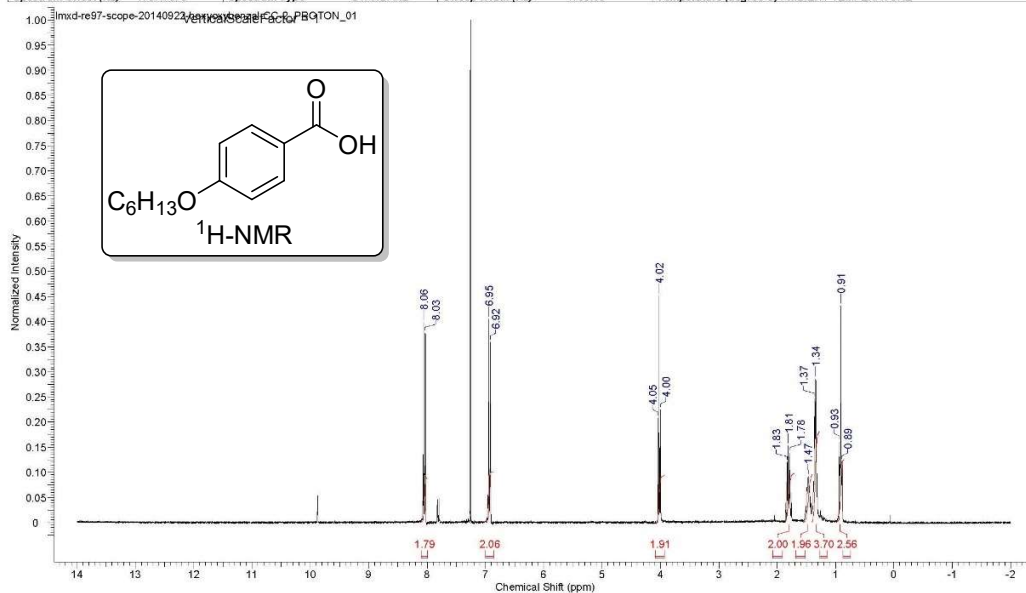


Acquisition Time (sec)	1.0420	Date	Oct 12 2014	Date Stamp	Oct 12 2014
File Name	G:\20140818-scope\lmsd-re97-scope-20141012-pentaoxybenzal	CARBON_01.fid.fid	Frequency (MHz)	75.35	
Nucleus	¹³ C	Number of Transients	3300	Original Points Count	19624
Pulse Sequence	s2pul	Receiver Gain	30.00	Solvent	CHLOROFORM-d
Spectrum Offset (Hz)	6287.5557	Spectrum Type	STANDARD	Sweep Width (Hz)	18832.39
				Temperature (degree C)	AMBIENT TEMPERATURE



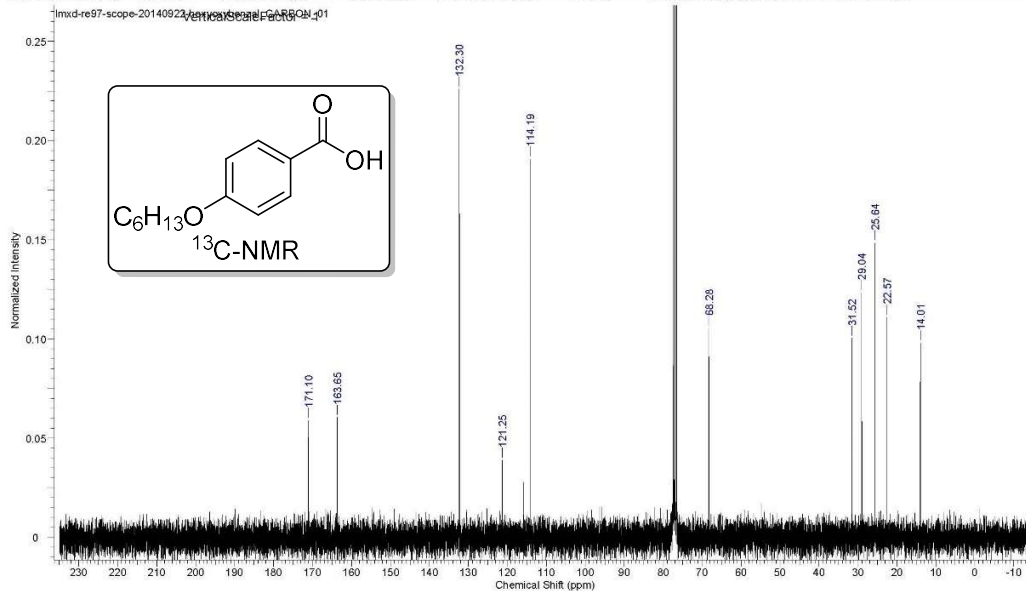
20/10/2014 10:59:38 PM

Acquisition Time (sec)	2.0480	Date	Sep 22 2014	Date Stamp	Sep 22 2014
File Name	G:\20140818-scope\imxd-re97-scope-20140922-hexyloxybenzoic acid	Number of Transients	8	Original Points Count	9818
Nucleus	¹ H	Receiver Gain	39.00	Solvent	CHLOROFORM-d
Pulse Sequence	s2pul	Spectrum Type	STANDARD	Sweep Width (Hz)	4793.86
Spectrum Offset (Hz)	1797.7676			Temperature (degree C)	AMBIENT TEMPERATURE



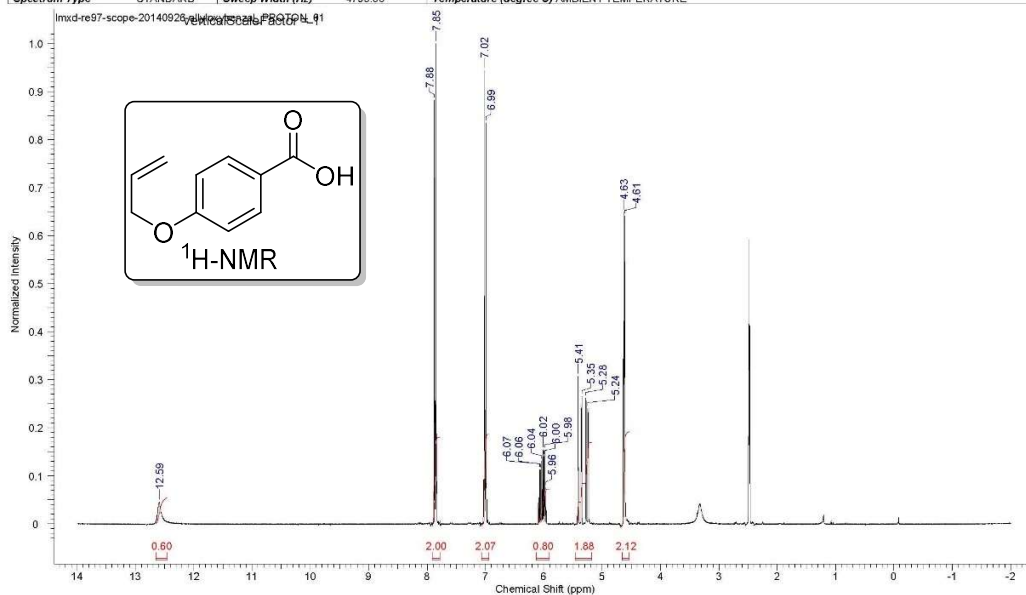
20/10/2014 11:01:09 PM

Acquisition Time (sec)	1.0420	Date	Sep 23 2014	Date Stamp	Sep 23 2014
File Name	G:\20140818-scope\imxd-re97-scope-20140922-hexyloxybenzoic acid	Number of Transients	3300	Original Points Count	19624
Nucleus	¹³ C	Receiver Gain	30.00	Solvent	CHLOROFORM-d
Pulse Sequence	s2pul	Spectrum Type	STANDARD	Sweep Width (Hz)	18832.39
Spectrum Offset (Hz)	8287.5557			Temperature (degree C)	AMBIENT TEMPERATURE



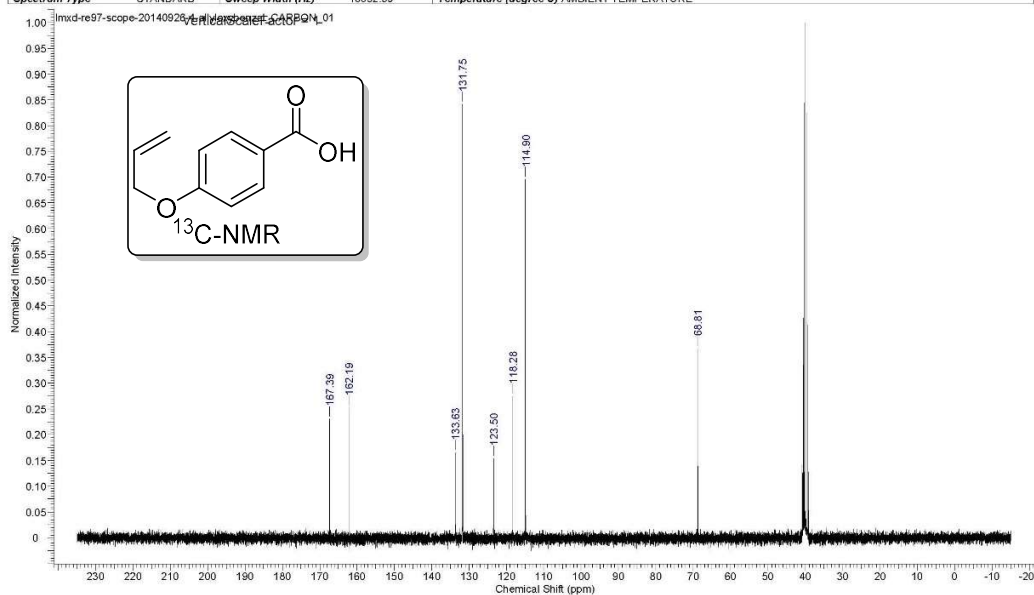
21/10/2014 12:52:32 AM

Acquisition Time (sec)	2.0480	Date	Sep 26 2014	Date Stamp	Sep 26 2014
File Name	G:\20140818-scope\lmsd-re97-scope-20140926-allyloxybenzaldehyde-PROTON_01.fid	Frequency (MHz)	299.63	Points Count	16384
Nucleus	¹ H	Number of Transients	8	Original Points Count	9818
Pulse Sequence	s2pul	Receiver Gain	36.00	Solvent	DMSO-d6
Spectrum Type	STANDARD	Sweep Width (Hz)	4793.86	Temperature (degree C)	AMBIENT TEMPERATURE
				Spectrum Offset (Hz)	1797.7788

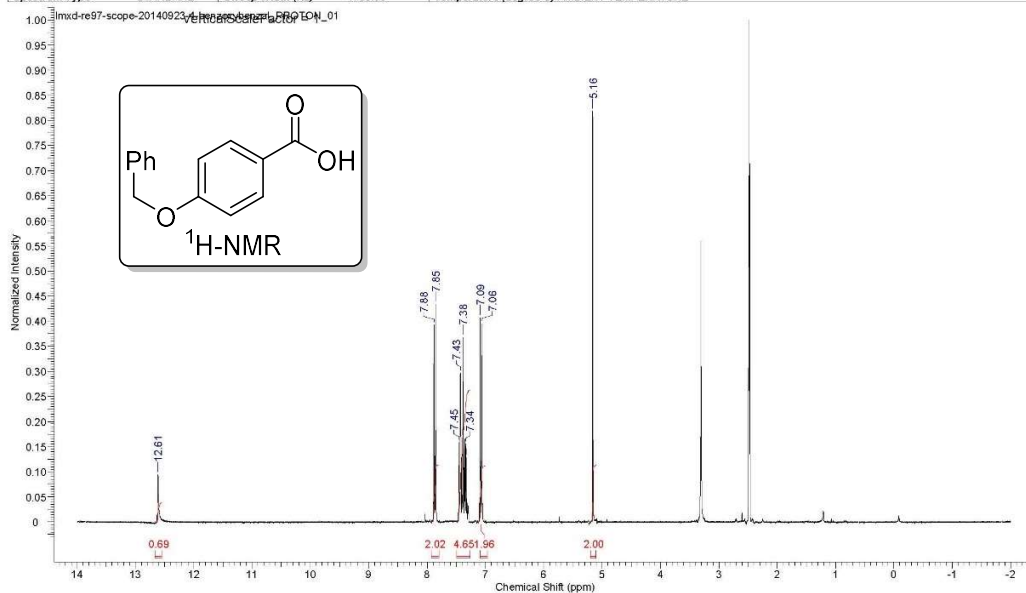


21/10/2014 12:44:40 AM

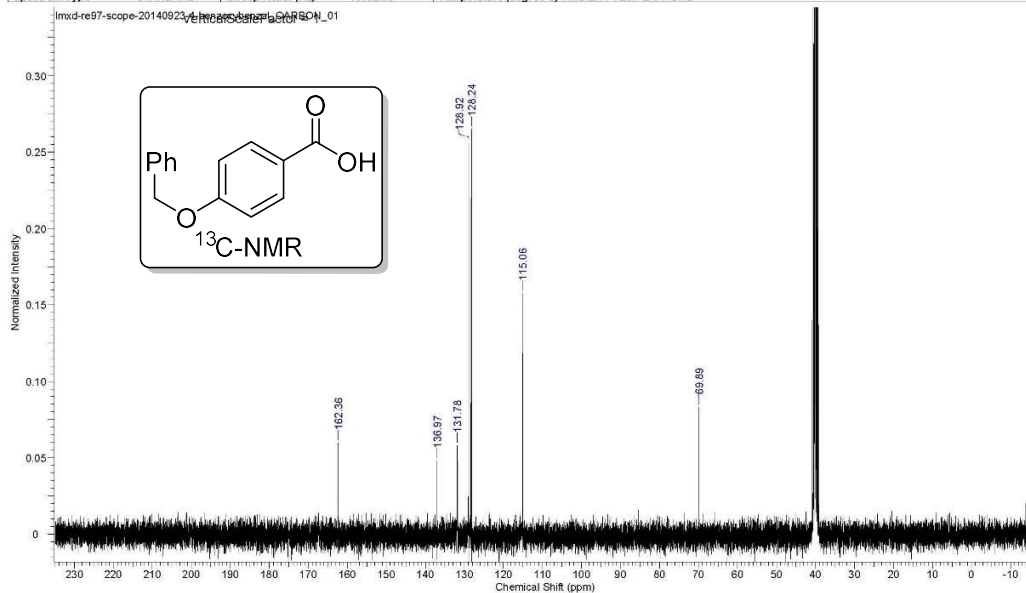
Acquisition Time (sec)	1.0420	Date	Sep 26 2014	Date Stamp	Sep 26 2014
File Name	G:\20140818-scope\lmsd-re97-scope-20140926-allyloxybenzaldehyde-CARBON_01.fid	Frequency (MHz)	75.35	Points Count	32768
Nucleus	¹³ C	Number of Transients	1700	Original Points Count	19624
Pulse Sequence	s2pul	Receiver Gain	30.00	Solvent	DMSO-d6
Spectrum Type	STANDARD	Sweep Width (Hz)	18832.39	Temperature (degree C)	AMBIENT TEMPERATURE
				Spectrum Offset (Hz)	8287.6016



Acquisition Time (sec)	2.0480	Date	Sep 24 2014	Date Stamp	Sep 24 2014
File Name	G:\20140818-scope\lmsd-re97-scope-20140923-4-benzoylbenzal_PROTON_01.fid	Frequency (MHz)	299.63		
Nucleus	¹ H	Number of Transients	8	Original Points Count	9818
Pulse Sequence	s2pul	Receiver Gain	39.00	Solvent	DMSO-d6
Spectrum Type	STANDARD	Sweep Width (Hz)	4793.66	Temperature (degree C)	AMBIENT TEMPERATURE
				Points Count	16384
				Spectrum Offset (Hz)	1797.7768

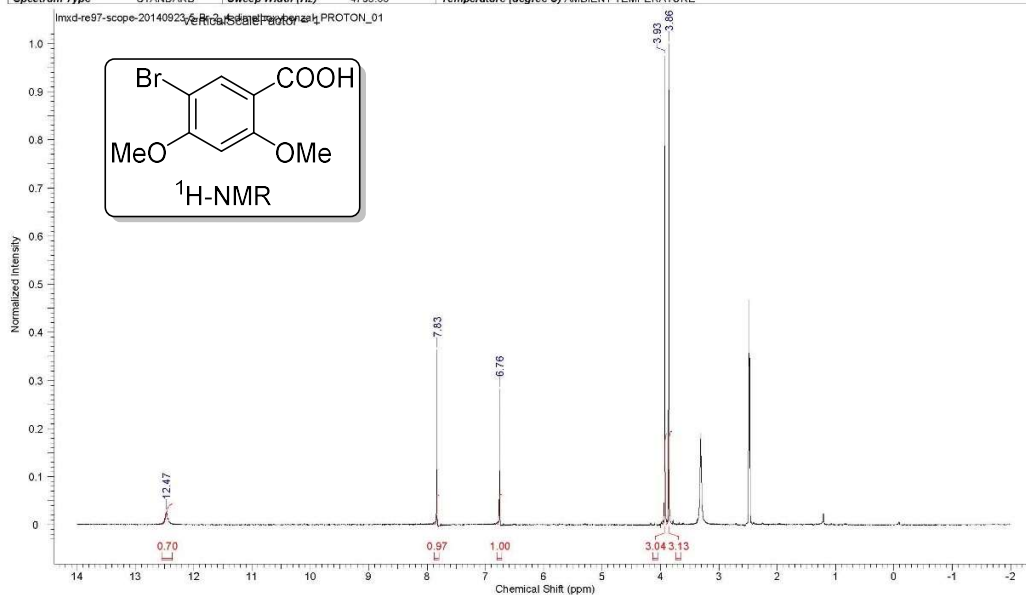


Acquisition Time (sec)	1.0420	Date	Sep 25 2014	Date Stamp	Sep 25 2014
File Name	G:\20140818-scope\lmsd-re97-scope-20140923-4-benzoylbenzal_CARBON_01.fid	Frequency (MHz)	75.35		
Nucleus	¹³ C	Number of Transients	1700	Original Points Count	19624
Pulse Sequence	s2pul	Receiver Gain	30.00	Solvent	DMSO-d6
Spectrum Type	STANDARD	Sweep Width (Hz)	18832.39	Temperature (degree C)	AMBIENT TEMPERATURE
				Points Count	32768
				Spectrum Offset (Hz)	8287.6016



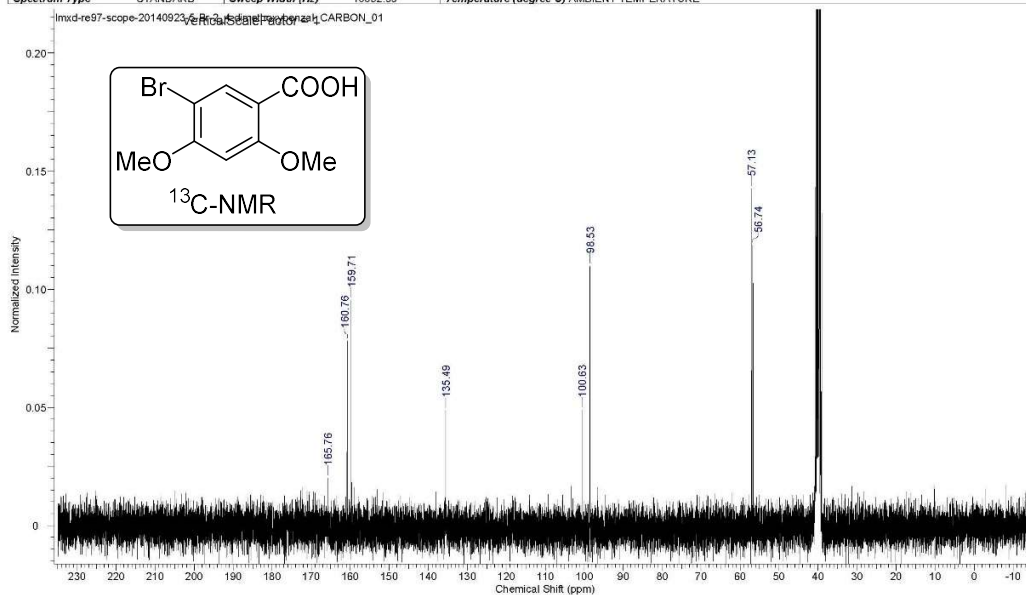
21/10/2014 12:33:06 AM

Acquisition Time (sec)	2.0480	Date	Sep 24 2014	Date Stamp	Sep 24 2014
File Name	G:\20140818-scope\lmsd-re97-scope-20140923-5-Br-2_4-dimethoxybenzal_PROTON_01.fid	Number of Transients	8	Original Points Count	9818
Nucleus	¹ H	Receiver Gain	39.00	Solvent	DMSO-d6
Pulse Sequence	s2pul	Sweep Width (Hz)	4793.86	Temperature (degree C)	AMBIENT TEMPERATURE
Spectrum Type	STANDARD				

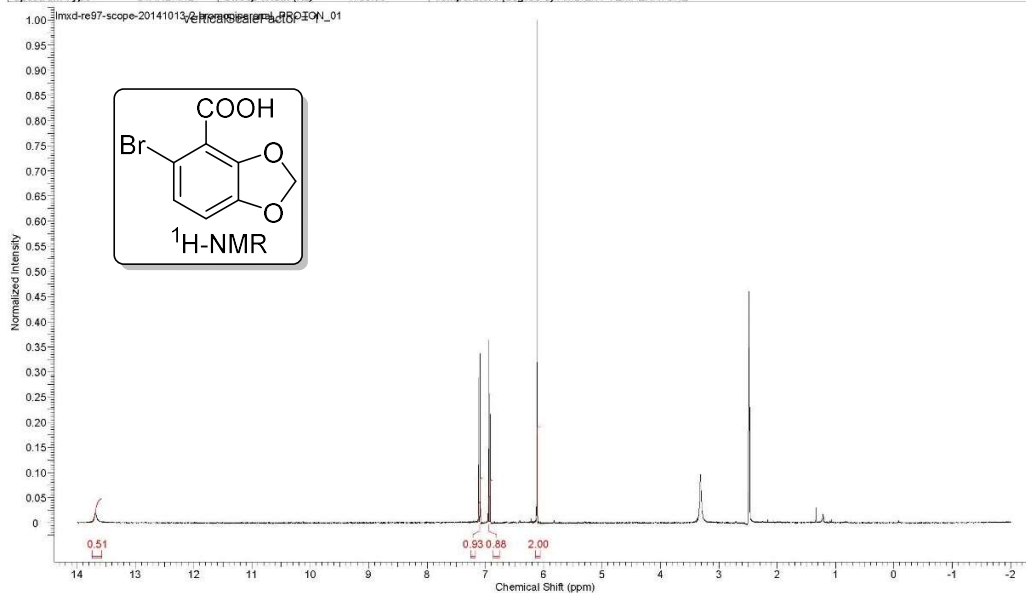


21/10/2014 12:35:54 AM

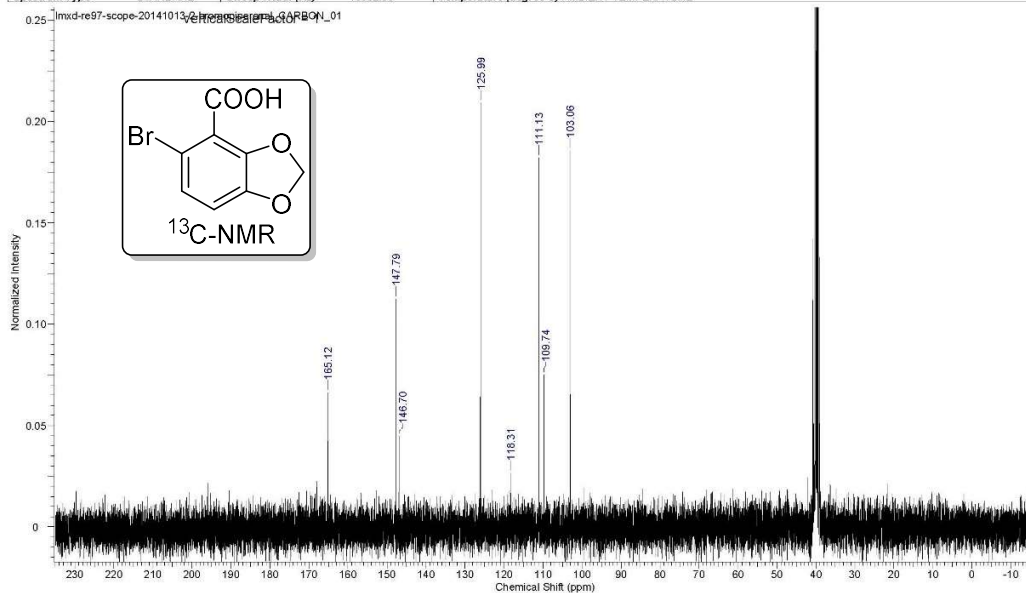
Acquisition Time (sec)	1.0420	Date	Sep 24 2014	Date Stamp	Sep 24 2014
File Name	G:\20140818-scope\lmsd-re97-scope-20140923-5-Br-2_4-dimethoxybenzal_CARBON_01.fid	Number of Transients	1700	Original Points Count	19624
Nucleus	¹³ C	Receiver Gain	30.00	Solvent	DMSO-d6
Pulse Sequence	s2pul	Sweep Width (Hz)	18832.39	Temperature (degree C)	AMBIENT TEMPERATURE
Spectrum Type	STANDARD				



Acquisition Time (sec)	2.0480	Date	Oct 14 2014	Date Stamp	Oct 14 2014
File Name	G:\20140818-scope\mxid-re97-scope-20141013-2-bromopiperonal_PROTON_01.fid	Frequency (MHz)	299.63		
Nucleus	¹ H	Number of Transients	8	Original Points Count	9818
Pulse Sequence	s2pul	Receiver Gain	39.00	Solvent	DMSO-d6
Spectrum Type	STANDARD	Sweep Width (Hz)	4793.86	Temperature (degree C)	AMBIENT TEMPERATURE
				Points Count	16364
				Spectrum Offset (Hz)	1797.7788

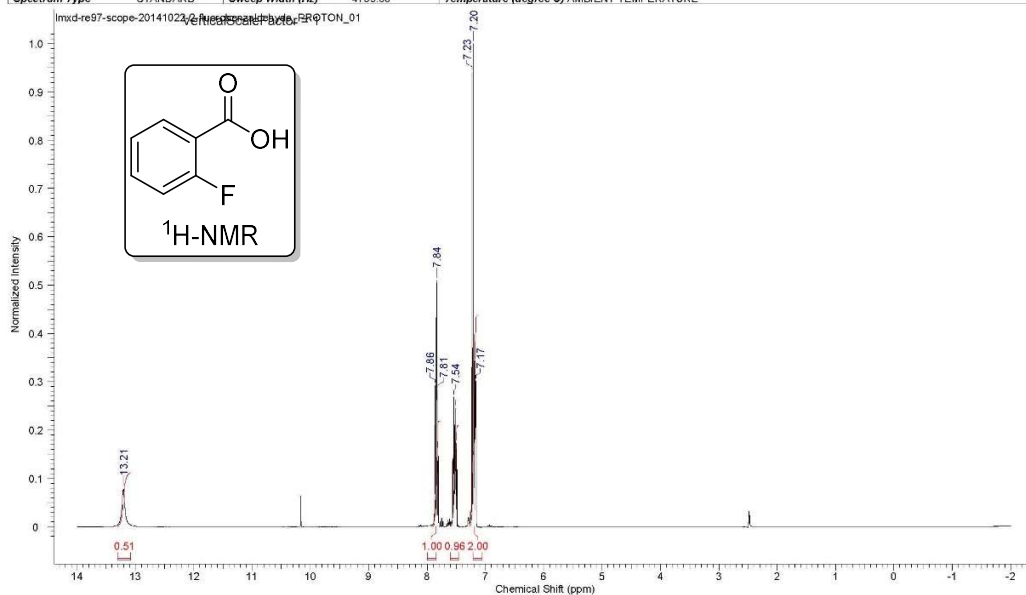


Acquisition Time (sec)	1.0420	Date	Oct 14 2014	Date Stamp	Oct 14 2014
File Name	G:\20140818-scope\mxid-re97-scope-20141013-2-bromopiperonal_CARBON_01.fid	Frequency (MHz)	75.35		
Nucleus	¹³ C	Number of Transients	1700	Original Points Count	19624
Pulse Sequence	s2pul	Receiver Gain	30.00	Solvent	DMSO-d6
Spectrum Type	STANDARD	Sweep Width (Hz)	18832.39	Temperature (degree C)	AMBIENT TEMPERATURE
				Points Count	32768
				Spectrum Offset (Hz)	8287.6016



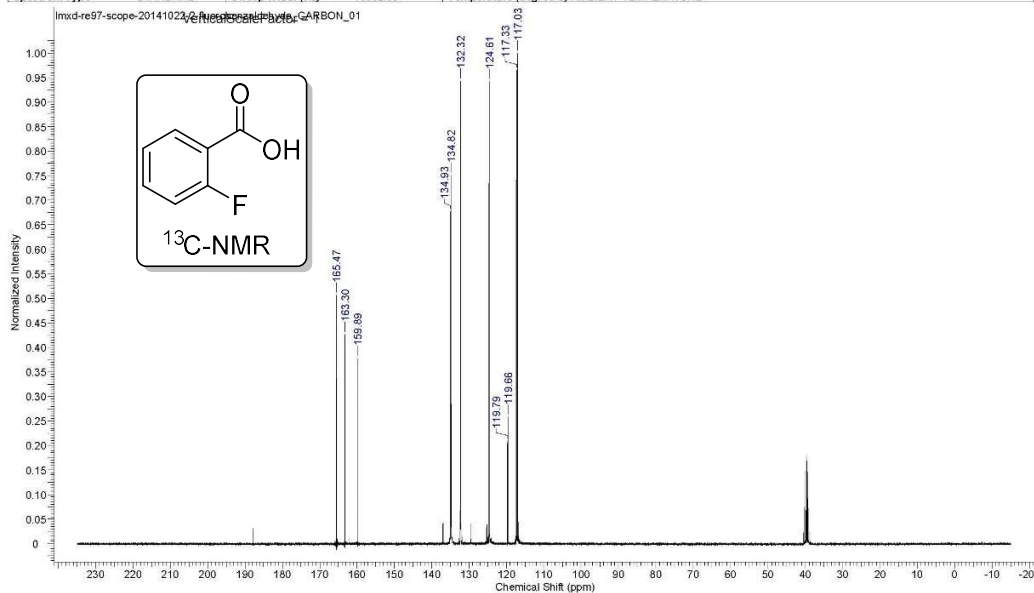
22/10/2014 10:18:27 PM

Acquisition Time (sec)	2.0480	Date	Oct 22 2014	Date Stamp	Oct 22 2014
File Name	G:\20140818-scope\additional\lmsd-re97-scope-20141022-2-fluorobenzaldehyde_PROTON_01.fid	Number of Transients	8	Original Points Count	9818
Nucleus	¹ H	Receiver Gain	16.00	Solvent	DMSO-d6
Pulse Sequence	s2pul	Sweep Width (Hz)	4793.86	Temperature (degree C)	AMBIENT TEMPERATURE
Spectrum Type	STANDARD				



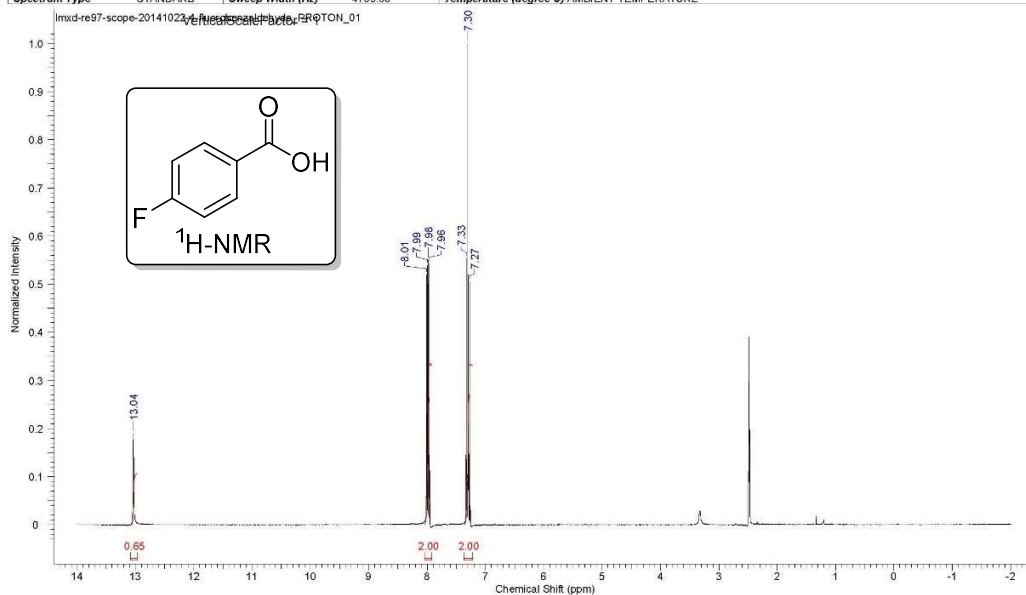
22/10/2014 10:35:49 PM

Acquisition Time (sec)	1.0420	Date	Oct 22 2014	Date Stamp	Oct 22 2014
File Name	G:\20140818-scope\additional\lmsd-re97-scope-20141022-2-fluorobenzaldehyde_CARBON_01.fid	Number of Transients	1750	Original Points Count	19624
Nucleus	¹³ C	Receiver Gain	30.00	Solvent	DMSO-d6
Pulse Sequence	s2pul	Sweep Width (Hz)	18832.39	Temperature (degree C)	AMBIENT TEMPERATURE
Spectrum Type	STANDARD				



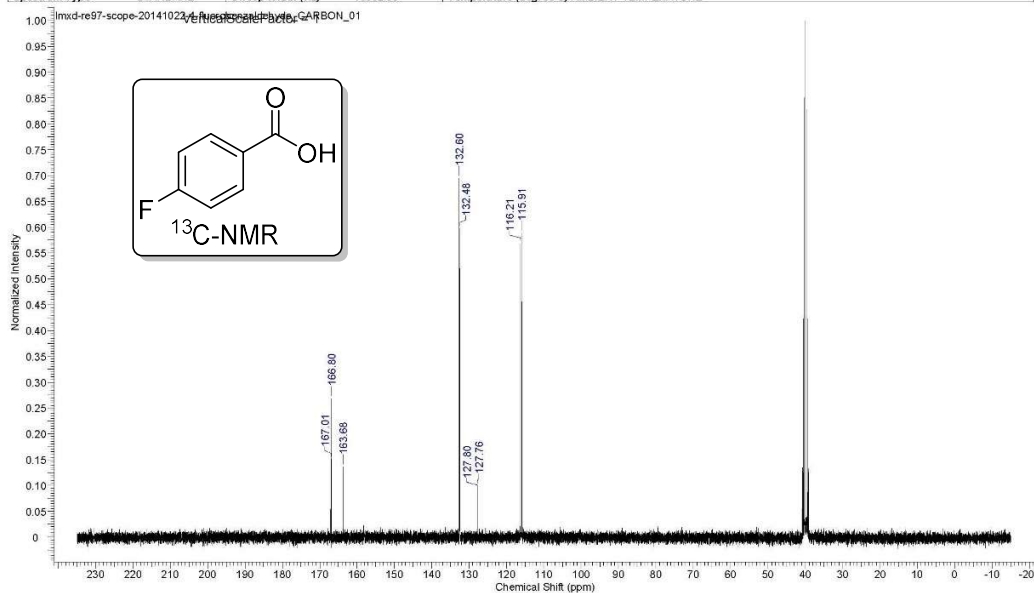
22/10/2014 10:39:57 PM

Acquisition Time (sec)	2.0480	Date	Oct 22 2014	Date Stamp	Oct 22 2014
File Name	G:\20140818-scope\additional\imxd-re97-scope-20141022-4-fluorobenzaldehyde_PROTON_01.fid\fid				Frequency (MHz)
Nucleus	¹ H	Number of Transients	8	Original Points Count	9816
Pulse Sequence	s2pul	Receiver Gain	36.00	Solvent	DMSO-d6
Spectrum Type	STANDARD	Sweep Width (Hz)	4793.86	Temperature (degree C)	AMBIENT TEMPERATURE
					Points Count
					Spectrum Offset (Hz)



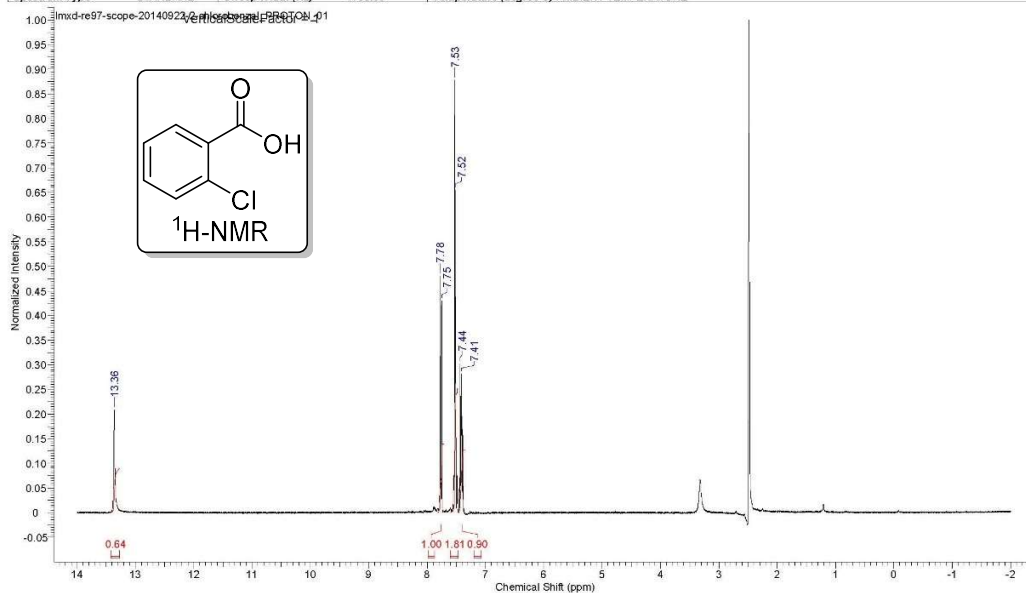
22/10/2014 10:43:54 PM

Acquisition Time (sec)	1.0420	Date	Oct 22 2014	Date Stamp	Oct 22 2014
File Name	G:\20140818-scope\additional\imxd-re97-scope-20141022-4-fluorobenzaldehyde_CARBON_01.fid\fid				Frequency (MHz)
Nucleus	¹³ C	Number of Transients	1750	Original Points Count	19624
Pulse Sequence	s2pul	Receiver Gain	30.00	Solvent	DMSO-d6
Spectrum Type	STANDARD	Sweep Width (Hz)	18832.39	Temperature (degree C)	AMBIENT TEMPERATURE
					Points Count
					Spectrum Offset (Hz)



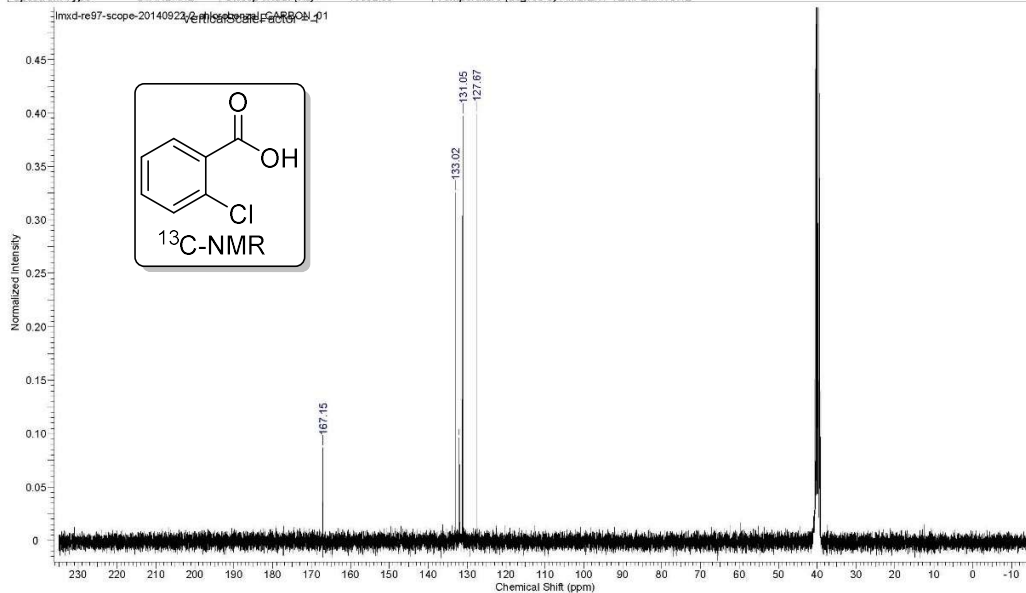
20/10/2014 10:43:35 PM

Acquisition Time (sec)	2.0480	Date	Sep 22 2014	Date Stamp	Sep 22 2014
File Name	G:\20140818-scope\lmsd-re97-scope-20140922-2-chlorobenzal_PROTON_01.fid.fid	Frequency (MHz)	299.63		
Nucleus	¹ H	Number of Transients	8	Original Points Count	9818
Pulse Sequence	s2pul	Receiver Gain	39.00	Solvent	DMSO-d6
Spectrum Type	STANDARD	Sweep Width (Hz)	4793.86	Temperature (degree C)	AMBIENT TEMPERATURE
				Spectrum Offset (Hz)	1797.7788



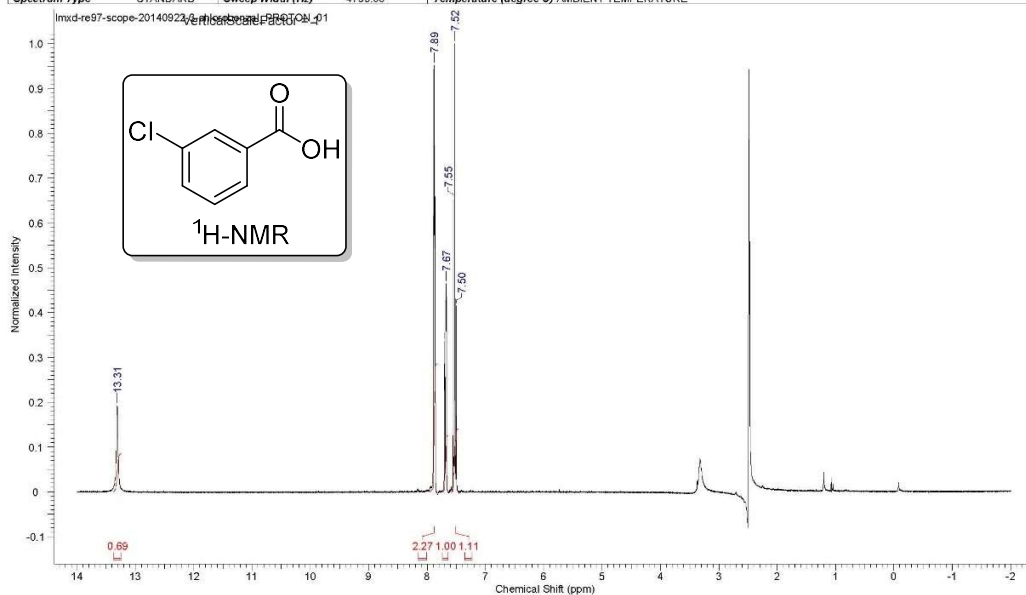
20/10/2014 10:44:18 PM

Acquisition Time (sec)	1.0420	Date	Sep 22 2014	Date Stamp	Sep 22 2014
File Name	G:\20140818-scope\lmsd-re97-scope-20140922-2-chlorobenzal_CARBON_01.fid.fid	Frequency (MHz)	75.35		
Nucleus	¹³ C	Number of Transients	2368	Original Points Count	19624
Pulse Sequence	s2pul	Receiver Gain	30.00	Solvent	DMSO-d6
Spectrum Type	STANDARD	Sweep Width (Hz)	18832.39	Temperature (degree C)	AMBIENT TEMPERATURE
				Spectrum Offset (Hz)	6287.6016



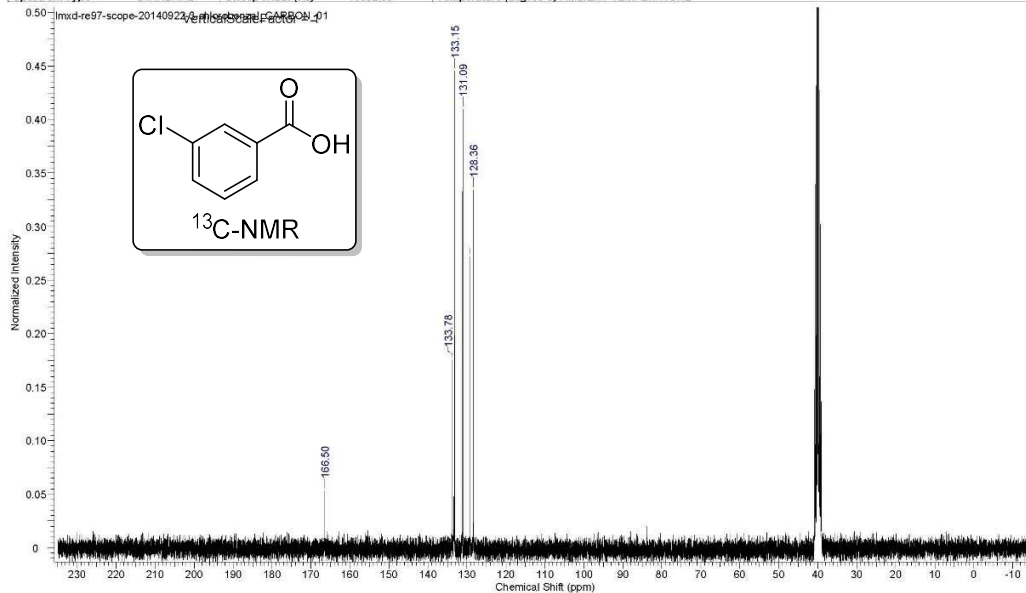
20/10/2014 10:49:40 PM

Acquisition Time (sec)	2.0480	Date	Sep 22 2014	Date Stamp	Sep 22 2014
File Name	G:\20140818-scope\lmsd-re97-scope-20140922-3-chlorobenzal_PROTON_01.fid	Frequency (MHz)	299.63	Points Count	16384
Nucleus	¹ H	Number of Transients	8	Original Points Count	9818
Pulse Sequence	s2pul	Receiver Gain	36.00	Solvent	DMSO-d6
Spectrum Type	STANDARD	Sweep Width (Hz)	4793.86	Temperature (degree C)	AMBIENT TEMPERATURE
				Spectrum Offset (Hz)	1797.7788

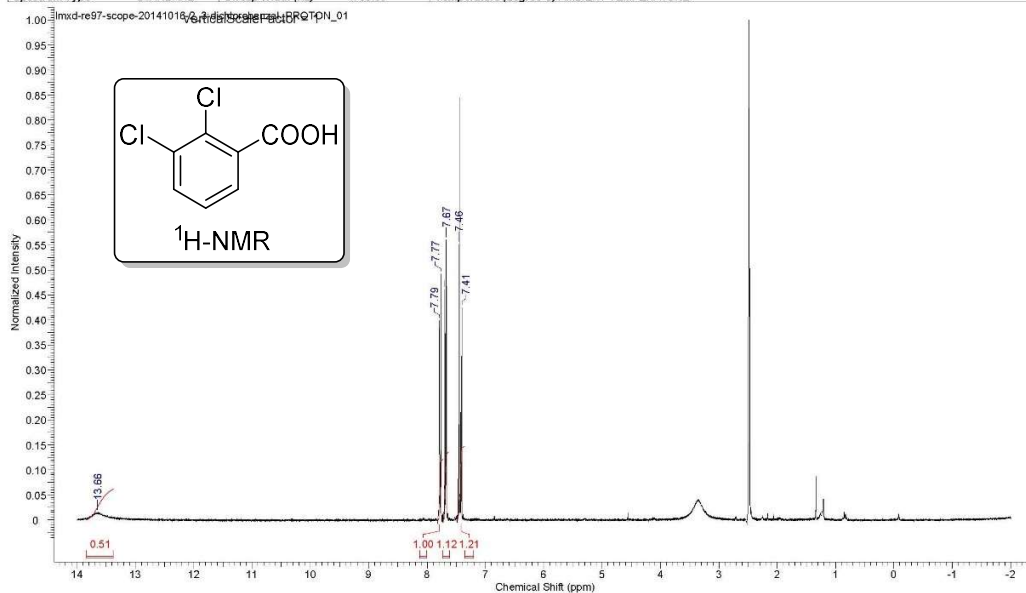


20/10/2014 10:50:29 PM

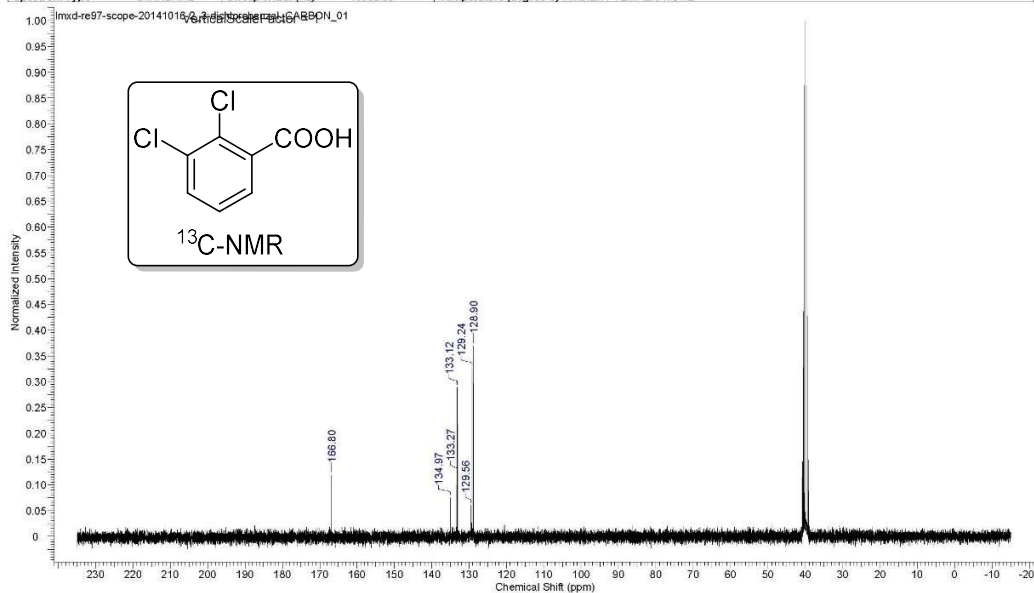
Acquisition Time (sec)	1.0420	Date	Sep 23 2014	Date Stamp	Sep 23 2014
File Name	G:\20140818-scope\lmsd-re97-scope-20140922-3-chlorobenzal_CARBON_01.fid	Frequency (MHz)	75.35	Points Count	32768
Nucleus	¹³ C	Number of Transients	1696	Original Points Count	19624
Pulse Sequence	s2pul	Receiver Gain	30.00	Solvent	DMSO-d6
Spectrum Type	STANDARD	Sweep Width (Hz)	18832.39	Temperature (degree C)	AMBIENT TEMPERATURE
				Spectrum Offset (Hz)	6287.6016



Acquisition Time (sec)	2.0480	Date	Oct 16 2014	Date Stamp	Oct 16 2014
File Name	G:\20140818-scope\mxid-re97-scope-20141016-2_3-dichlorobenzal_PROTON_01.fid	Frequency (MHz)	299.63		
Nucleus	¹ H	Number of Transients	8	Original Points Count	9818
Pulse Sequence	s2pul	Receiver Gain	39.00	Solvent	DMSO-d6
Spectrum Type	STANDARD	Sweep Width (Hz)	4793.86	Temperature (degree C)	AMBIENT TEMPERATURE
				Spectrum Offset (Hz)	1797.7788

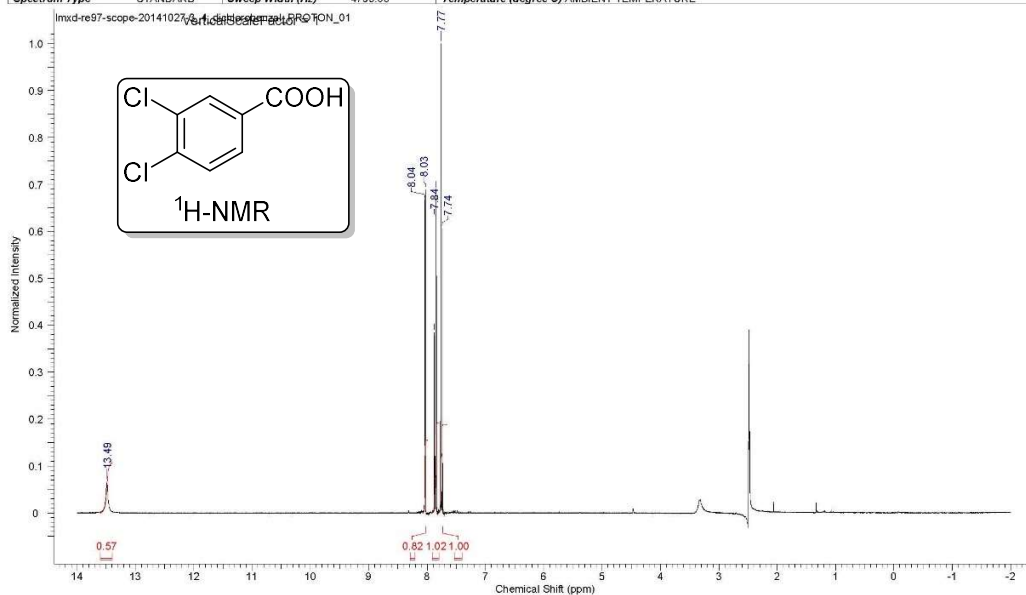


Acquisition Time (sec)	1.0420	Date	Oct 16 2014	Date Stamp	Oct 16 2014
File Name	G:\20140818-scope\mxid-re97-scope-20141016-2_3-dichlorobenzal_CARBON_01.fid	Frequency (MHz)	75.35		
Nucleus	¹³ C	Number of Transients	1700	Original Points Count	19624
Pulse Sequence	s2pul	Receiver Gain	30.00	Solvent	DMSO-d6
Spectrum Type	STANDARD	Sweep Width (Hz)	18832.39	Temperature (degree C)	AMBIENT TEMPERATURE
				Spectrum Offset (Hz)	8287.6016



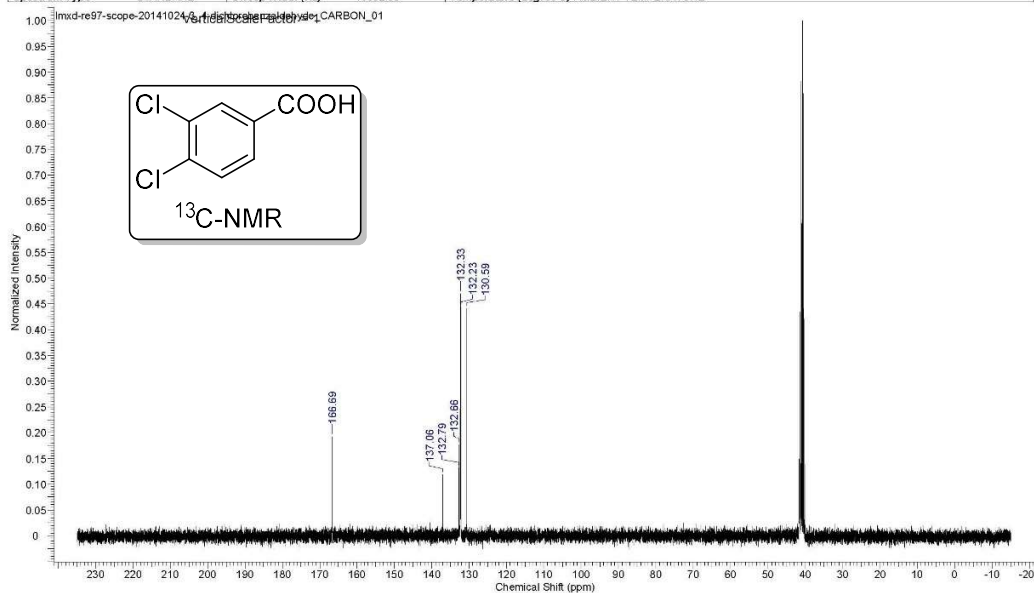
07/11/2014 11:06:47 PM

Acquisition Time (sec)	2.0480	Date	Oct 27 2014	Date Stamp	Oct 27 2014		
File Name	C:\Users\MML\My Desktop\lmsd-re97-scope-20141027-3_4_dichlorobenzaldehyde_PROTON_01.fid				Frequency (MHz)	299.63	
Nucleus	¹ H	Number of Transients	8	Original Points Count	9518	Points Count	16384
Pulse Sequence	s2pul	Receiver Gain	36.00	Solvent	DMSO-d6	Spectrum Offset (Hz)	1797.7788
Spectrum Type	STANDARD	Sweep Width (Hz)	4793.86	Temperature (degree C)	AMBIENT TEMPERATURE		



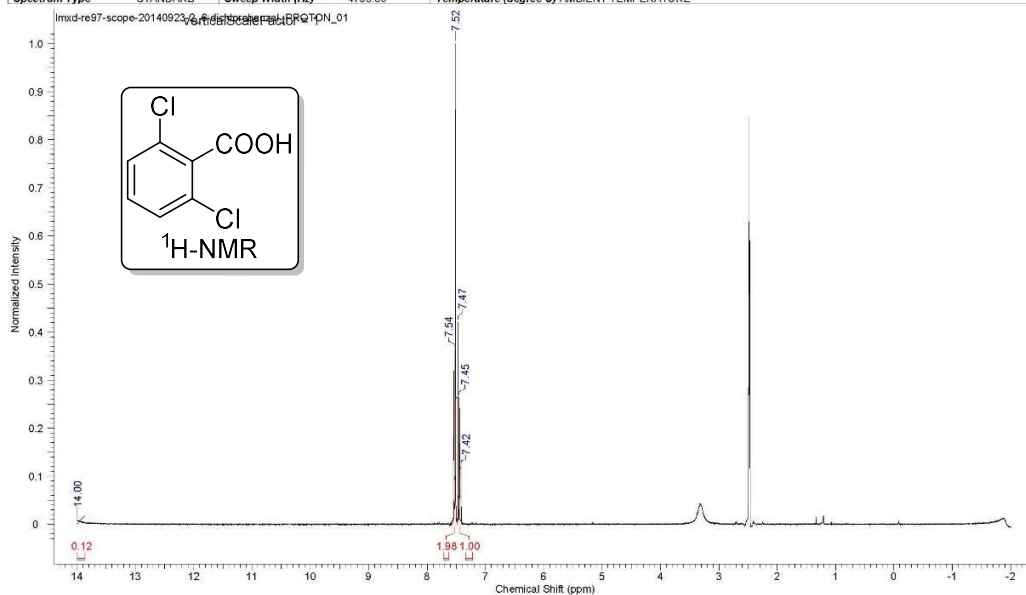
07/11/2014 11:07:16 PM

Acquisition Time (sec)	1.0420	Date	Oct 24 2014	Date Stamp	Oct 24 2014		
File Name	C:\Users\MML\My Desktop\lmsd-re97-scope-20141024-3_4-dichlorobenzaldehyde_CARBON_01.fid					Frequency (MHz)	75.35
Nucleus	¹³ C	Number of Transients	1700	Original Points Count	19624	Points Count	32768
Pulse Sequence	s2pul	Receiver Gain	30.00	Solvent	DMSO-d6	Spectrum Offset (Hz)	8287.6016
Spectrum Type	STANDARD	Sweep Width (Hz)	18832.39	Temperature (degree C)	AMBIENT TEMPERATURE		



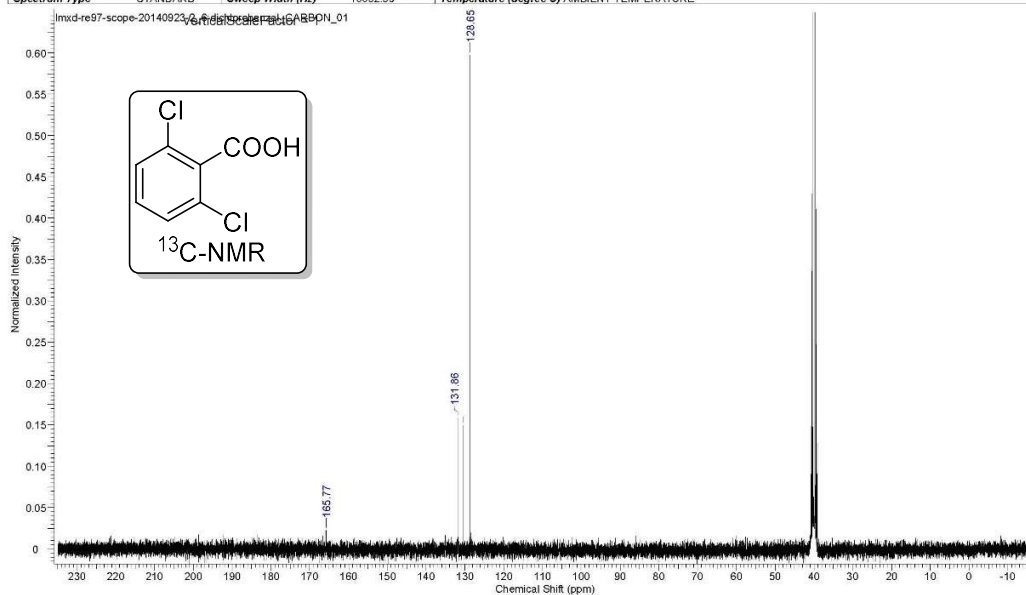
20/10/2014 11:02:30 PM

Acquisition Time (sec)	2.0480	Date	Sep 24 2014	Date Stamp	Sep 24 2014	
File Name	G:\20140818-scope\lmsd-re97-scope-20140923-2_6-dichlorobenzal_PROTON_01.fid					
Nucleus	¹ H	Number of Transients	8	Original Points Count	9818	
Pulse Sequence	s2pul	Receiver Gain	39.00	Solvent	DMSO-d6	
Spectrum Type	STANDARD	Sweep Width (Hz)	4793.86	Temperature (degree C)	AMBIENT TEMPERATURE	
					Spectrum Offset (Hz)	1797.7788

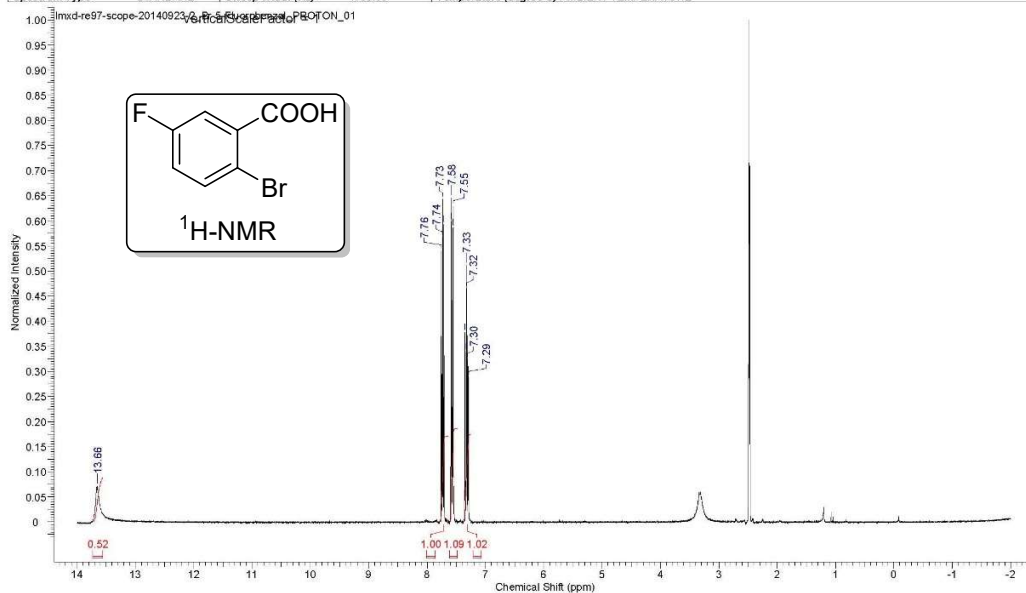


20/10/2014 11:04:39 PM

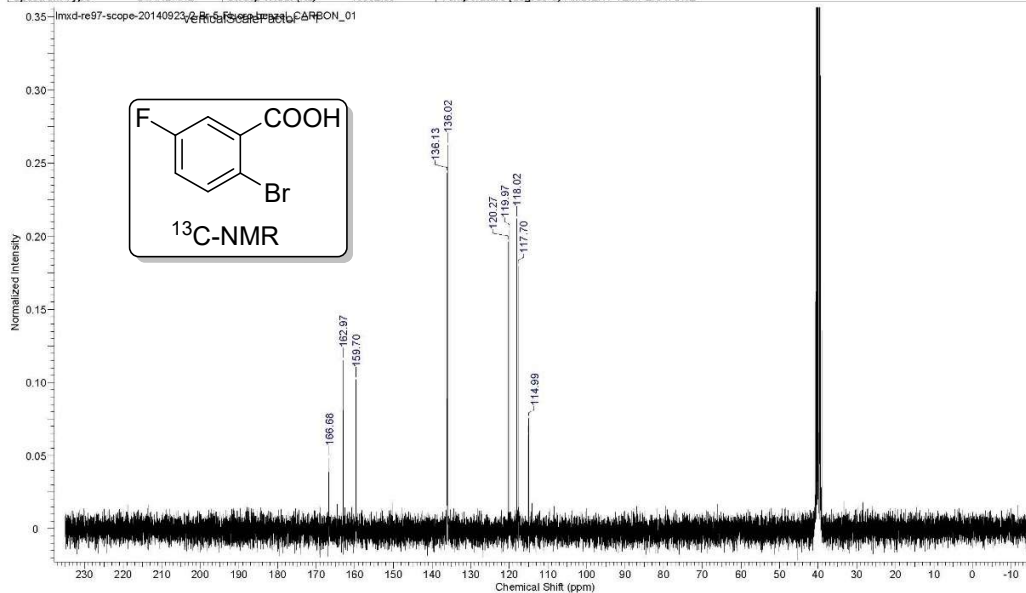
Acquisition Time (sec)	1.0420	Date	Sep 24 2014	Date Stamp	Sep 24 2014		
File Name	G:\20140818-scope\lmsd-re97-scope-20140923-2_6-dichlorobenzal_CARBON_01.fid					Frequency (MHz)	75.35
Nucleus	¹³ C	Number of Transients	1700	Original Points Count	19624	Points Count	32768
Pulse Sequence	s2pul	Receiver Gain	30.00	Solvent	DMSO-d6	Spectrum Offset (Hz)	8287.6016
Spectrum Type	STANDARD	Sweep Width (Hz)	18832.39	Temperature (degree C)	AMBIENT TEMPERATURE		



Acquisition Time (sec)	2.0480	Date	Sep 24 2014	Date Stamp	Sep 24 2014
File Name	G:\20140818-scope\mxid-re97-scope-20140923-2-Br-5-Fluorobenzal_FROTON_01.fid.tif			Frequency (MHz)	299.63
Nucleus	¹ H	Number of Transients	8	Original Points Count	9818
Pulse Sequence	s2pul	Receiver Gain	39.00	Solvent	DMSO-d6
Spectrum Type	STANDARD	Sweep Width (Hz)	4793.86	Temperature (degree C)	AMBIENT TEMPERATURE
				Points Count	16384
				Spectrum Offset (Hz)	1797.7788

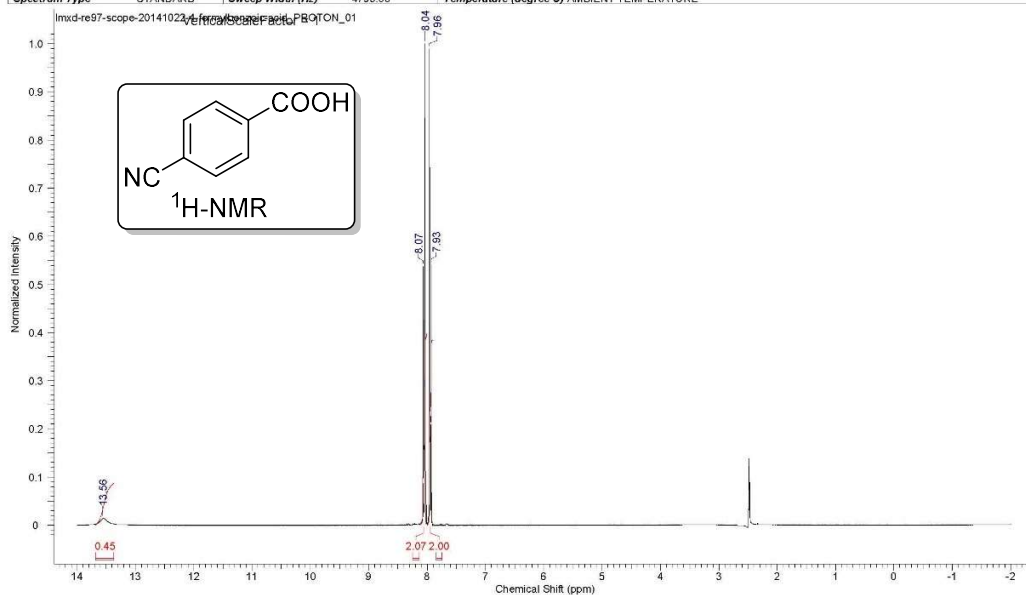


Acquisition Time (sec)	1.0420	Date	Sep 24 2014	Date Stamp	Sep 24 2014
File Name	G:\20140818-scope\mxid-re97-scope-20140923-2-Br-5-Fluorobenzal_CARBON_01.fid.tif			Frequency (MHz)	75.35
Nucleus	¹³ C	Number of Transients	1700	Original Points Count	19624
Pulse Sequence	s2pul	Receiver Gain	30.00	Solvent	DMSO-d6
Spectrum Type	STANDARD	Sweep Width (Hz)	18832.39	Temperature (degree C)	AMBIENT TEMPERATURE
				Points Count	32768
				Spectrum Offset (Hz)	6287.6016



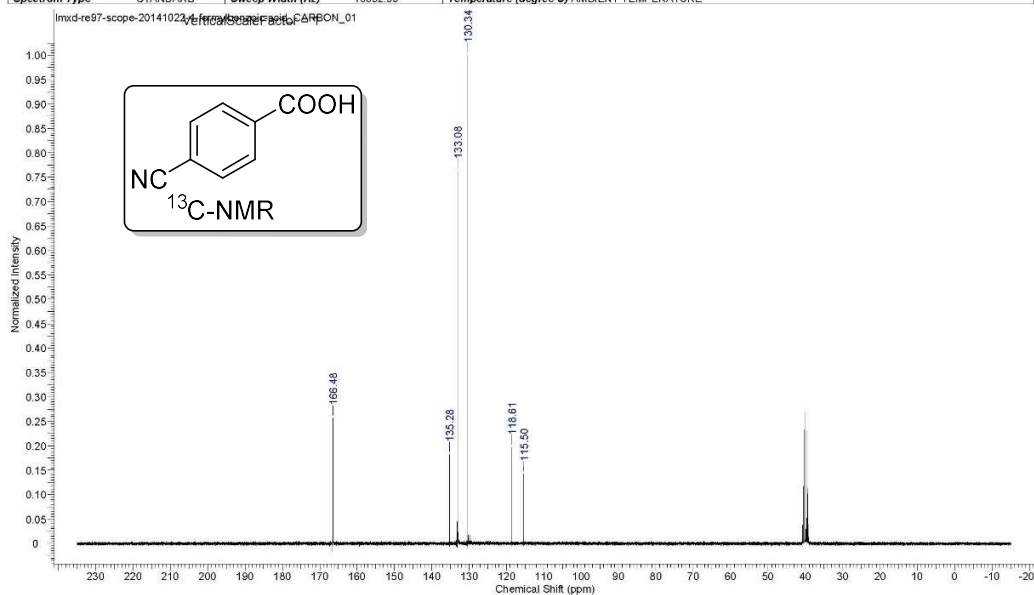
23/10/2014 7:44:05 PM

Acquisition Time (sec)	2.0480	Date	Oct 23 2014	Date Stamp	Oct 23 2014
File Name	G:\20140818-scope\additional\lmsd-re97-scope-20141022-4-formylbenzoic-acid_PROTON_01.fid				Frequency (MHz)
Nucleus	¹ H	Number of Transients	8	Original Points Count	9818
Pulse Sequence	s2pul	Receiver Gain	30.00	Solvent	DMSO-d6
Spectrum Type	STANDARD	Sweep Width (Hz)	4793.86	Temperature (degree C)	AMBIENT TEMPERATURE
					Points Count
					Spectrum Offset (Hz)



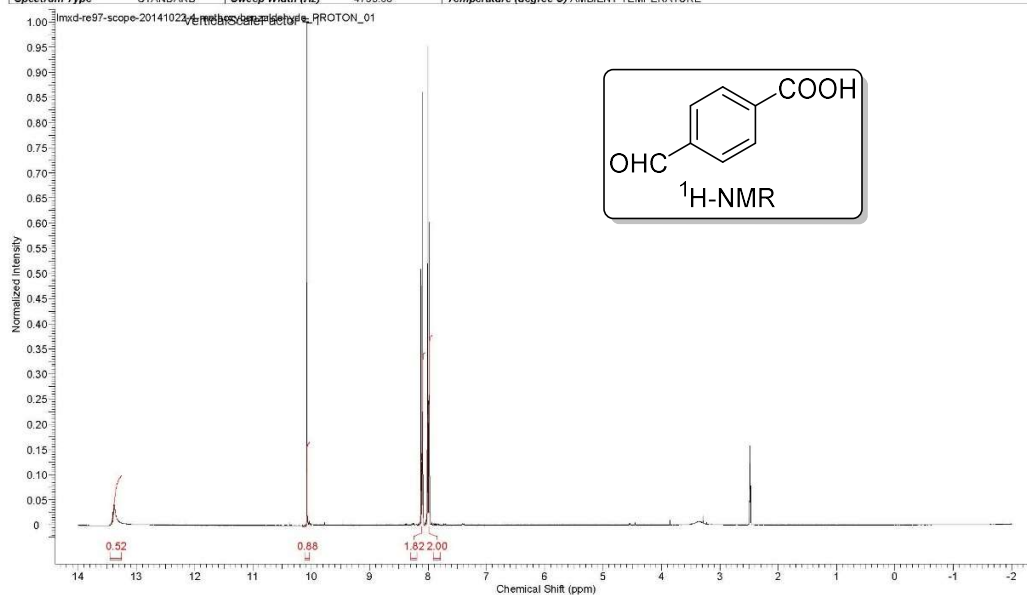
23/10/2014 7:44:22 PM

Acquisition Time (sec)	1.0420	Date	Oct 23 2014	Date Stamp	Oct 23 2014
File Name	G:\20140818-scope\additional\lmsd-re97-scope-20141022-4-formylbenzoic-acid_CARBON_01.fid				Frequency (MHz)
Nucleus	¹³ C	Number of Transients	1750	Original Points Count	19624
Pulse Sequence	s2pul	Receiver Gain	30.00	Solvent	DMSO-d6
Spectrum Type	STANDARD	Sweep Width (Hz)	18832.39	Temperature (degree C)	AMBIENT TEMPERATURE
					Points Count
					Spectrum Offset (Hz)



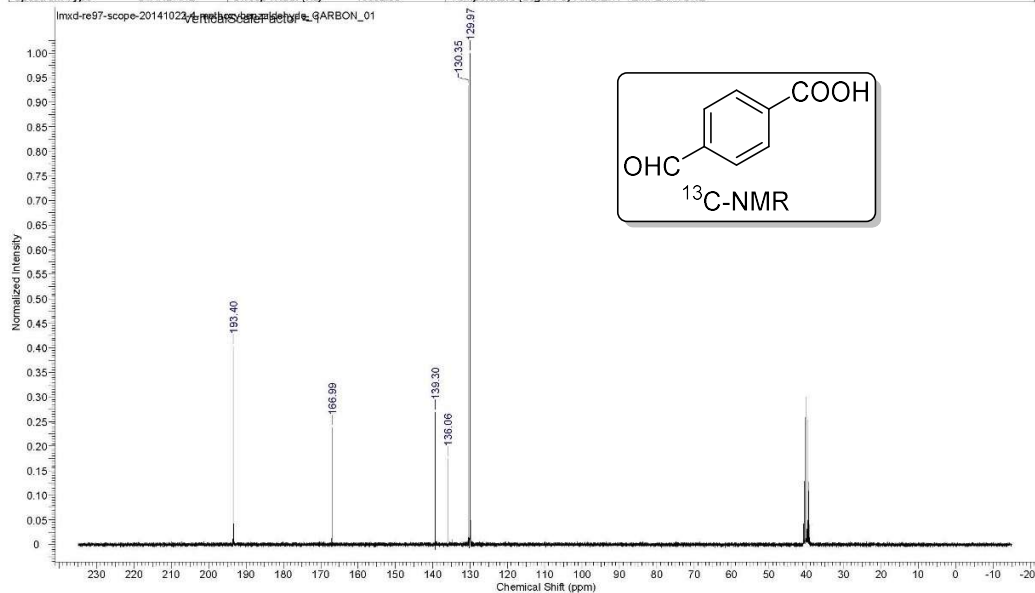
23/10/2014 7:32:23 PM

Acquisition Time (sec)	2.0480	Date	Oct 22 2014	Date Stamp	Oct 22 2014
File Name	G:\20140818-scope\additional\mxd-re97-scope-20141022-4-methoxybenzaldehyde_PROTON_01.fid	Frequency (MHz)	299.63		
Nucleus	¹ H	Number of Transients	8	Original Points Count	9818
Pulse Sequence	s2pul	Receiver Gain	30.00	Solvent	DMSO-d6
Spectrum Type	STANDARD	Sweep Width (Hz)	4793.86	Temperature (degree C)	AMBIENT TEMPERATURE
				Spectrum Offset (Hz)	1797.7788

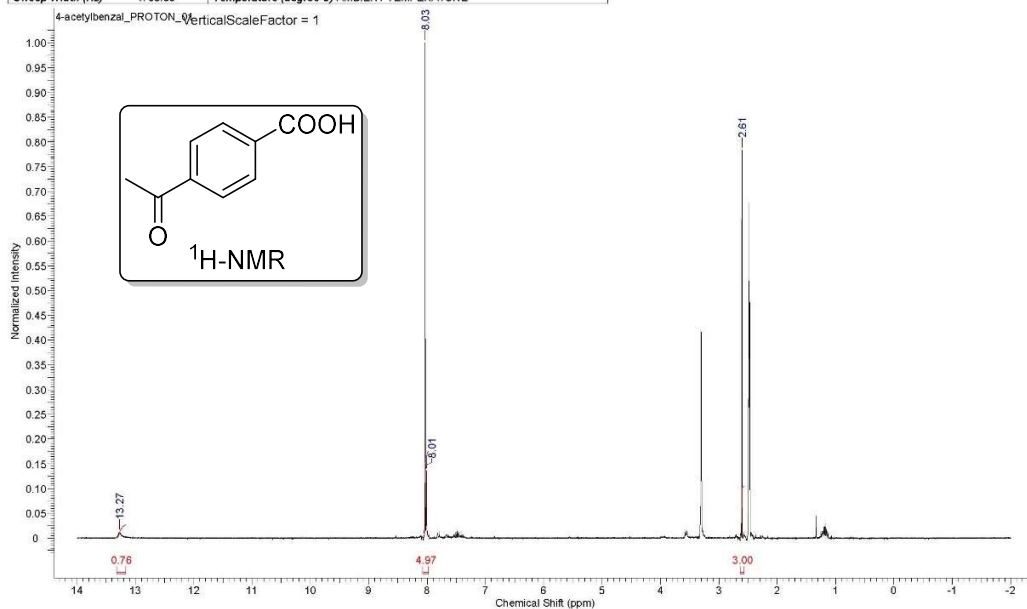


23/10/2014 7:33:10 PM

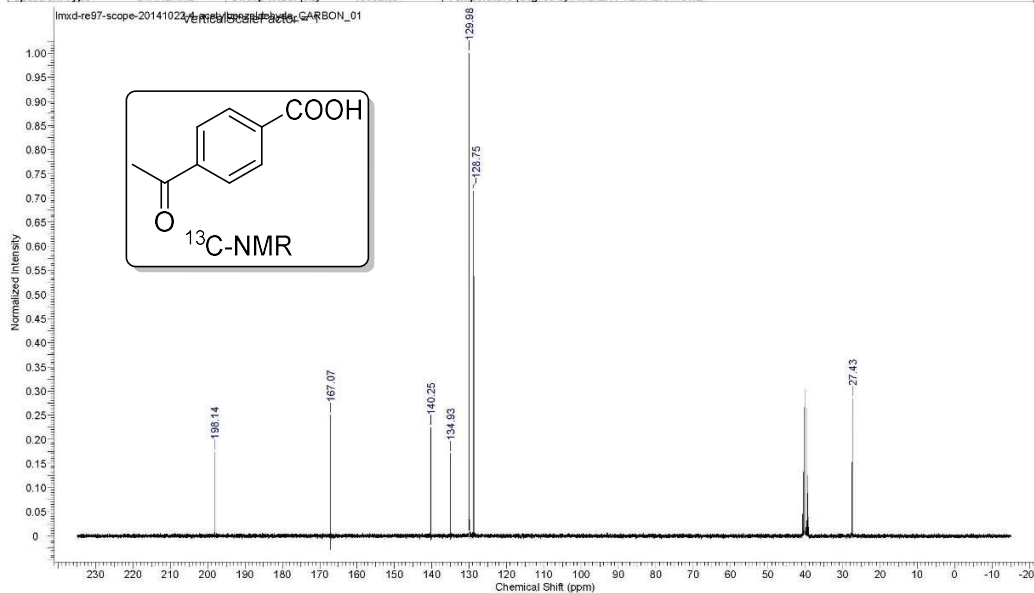
Acquisition Time (sec)	1.0420	Date	Oct 22 2014	Date Stamp	Oct 22 2014
File Name	G:\20140818-scope\additional\mxd-re97-scope-20141022-4-methoxybenzaldehyde_CARBON_01.fid	Frequency (MHz)	75.35		
Nucleus	¹³ C	Number of Transients	1750	Original Points Count	19624
Pulse Sequence	s2pul	Receiver Gain	30.00	Solvent	DMSO-d6
Spectrum Type	STANDARD	Sweep Width (Hz)	18832.39	Temperature (degree C)	AMBIENT TEMPERATURE
				Spectrum Offset (Hz)	8287.6016



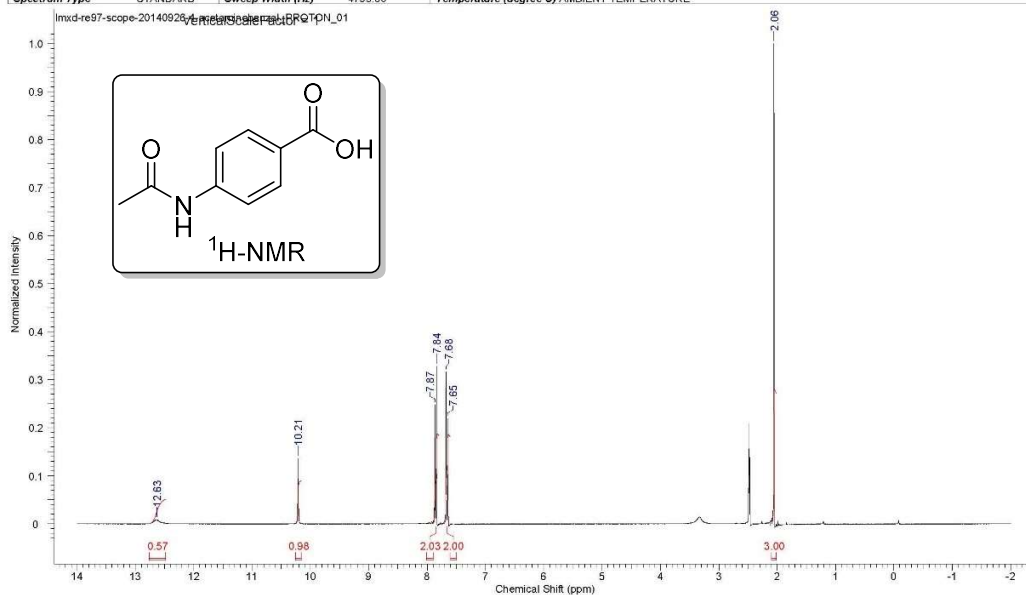
Acquisition Time (sec)	2.0480	Date	Sep 24 2014	Date Stamp	Sep 24 2014	File Name	G:\20140818-scope\4-acetylbenzaldehyde_PROTON_01.fid
Frequency (MHz)	299.63	Nucleus	¹ H	Number of Transients	8	Original Points Count	9618
Pulse Sequence	s2pul	Receiver Gain	39.00	Solvent	DMSO-d6	Points Count	16384
Sweep Width (Hz)	4793.66	Temperature (degree C)	AMBIENT TEMPERATURE			Spectrum Offset (Hz)	1797.7788
						Spectrum Type	STANDARD



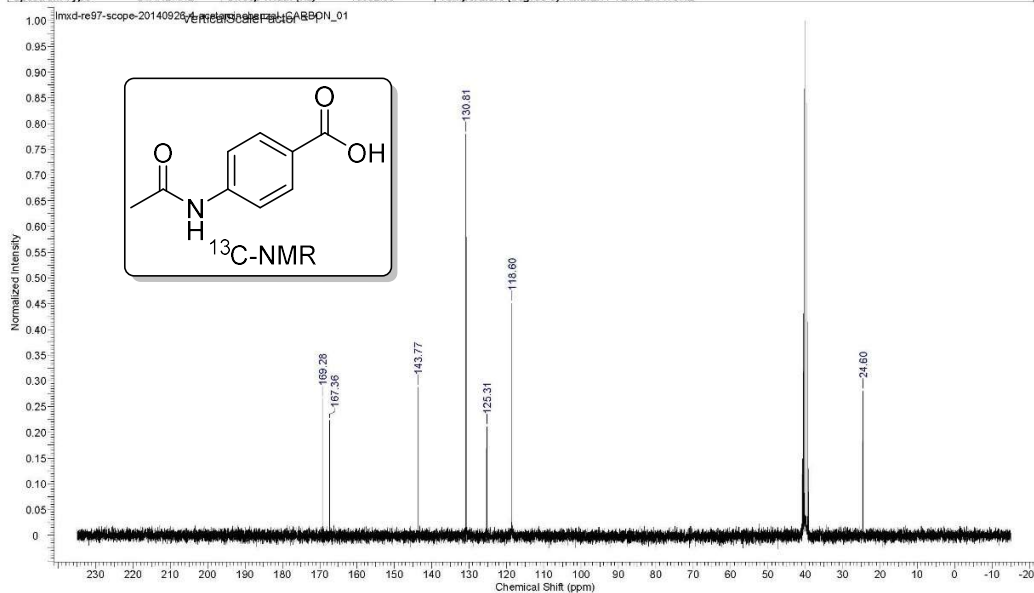
Acquisition Time (sec)	1.0420	Date	Oct 23 2014	Date Stamp	Oct 23 2014	File Name	G:\20140818-scope\additional\1022-4-acetylbenzaldehyde_CARBO_01.fid
Frequency (MHz)	75.35	Nucleus	¹³ C	Number of Transients	1750	Original Points Count	19624
Pulse Sequence	s2pul	Receiver Gain	30.00	Solvent	DMSO-d6	Points Count	32768
Spectrum Type	STANDARD	Sweep Width (Hz)	18832.39	Temperature (degree C)	AMBIENT TEMPERATURE	Spectrum Offset (Hz)	8287.6016



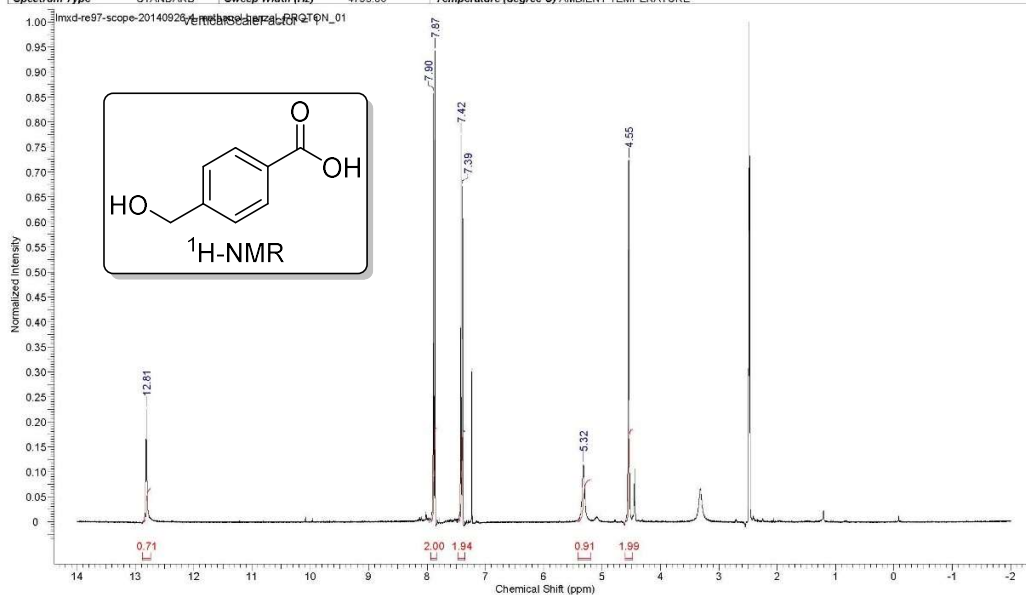
Acquisition Time (sec)	2.0480	Date	Sep 26 2014	Date Stamp	Sep 26 2014
File Name	G:\20140818-scope\lmsd-re97-scope-20140926-4-acetaminobenzal_PROTON_01.fid	Frequency (MHz)	299.63		
Nucleus	¹ H	Number of Transients	8	Original Points Count	9818
Pulse Sequence	s2pul	Receiver Gain	30.00	Solvent	DMSO-d6
Spectrum Type	STANDARD	Sweep Width (Hz)	4793.86	Temperature (degree C)	AMBIENT TEMPERATURE
				Points Count	16384
				Spectrum Offset (Hz)	1797.7788



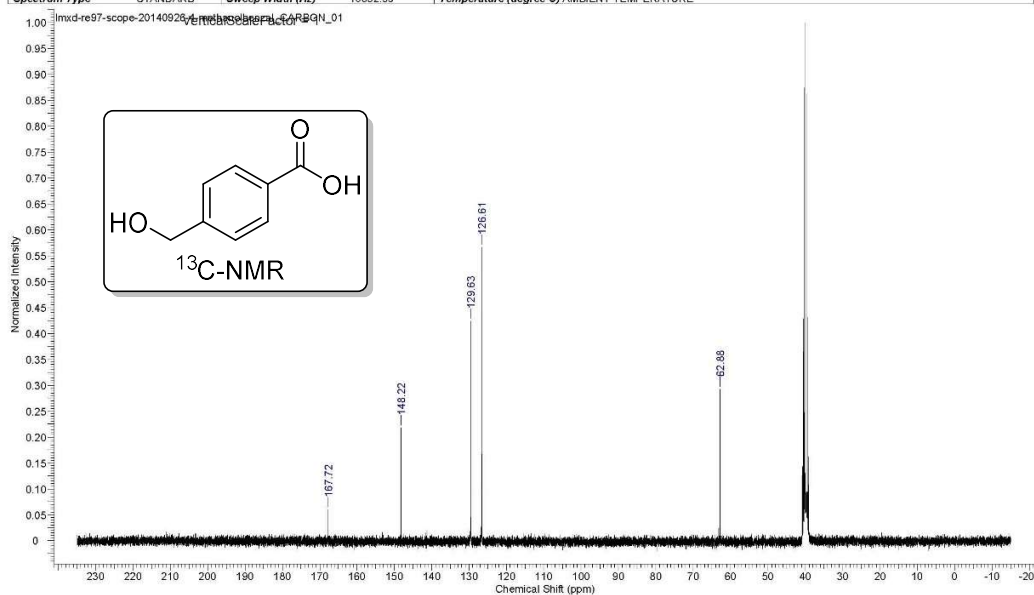
Acquisition Time (sec)	1.0420	Date	Sep 26 2014	Date Stamp	Sep 26 2014
File Name	G:\20140818-scope\lmsd-re97-scope-20140926-4-acetaminobenzal_CARBON_01.fid	Frequency (MHz)	75.35		
Nucleus	¹³ C	Number of Transients	1700	Original Points Count	19624
Pulse Sequence	s2pul	Receiver Gain	30.00	Solvent	DMSO-d6
Spectrum Type	STANDARD	Sweep Width (Hz)	18832.39	Temperature (degree C)	AMBIENT TEMPERATURE
				Points Count	32788
				Spectrum Offset (Hz)	8287.6016



Acquisition Time (sec)	2.0480	Date	Sep 26 2014	Date Stamp	Sep 26 2014
File Name	G:\20140818-scope\mxid-re97-scope-20140926-4-methanol-benzal_PROTON_01.fid	Frequency (MHz)	299.63		
Nucleus	¹ H	Number of Transients	8	Original Points Count	9818
Pulse Sequence	s2pul	Receiver Gain	36.00	Solvent	DMSO-d6
Spectrum Type	STANDARD	Sweep Width (Hz)	4793.86	Temperature (degree C)	AMBIENT TEMPERATURE
				Points Count	16384
				Spectrum Offset (Hz)	1797.7788

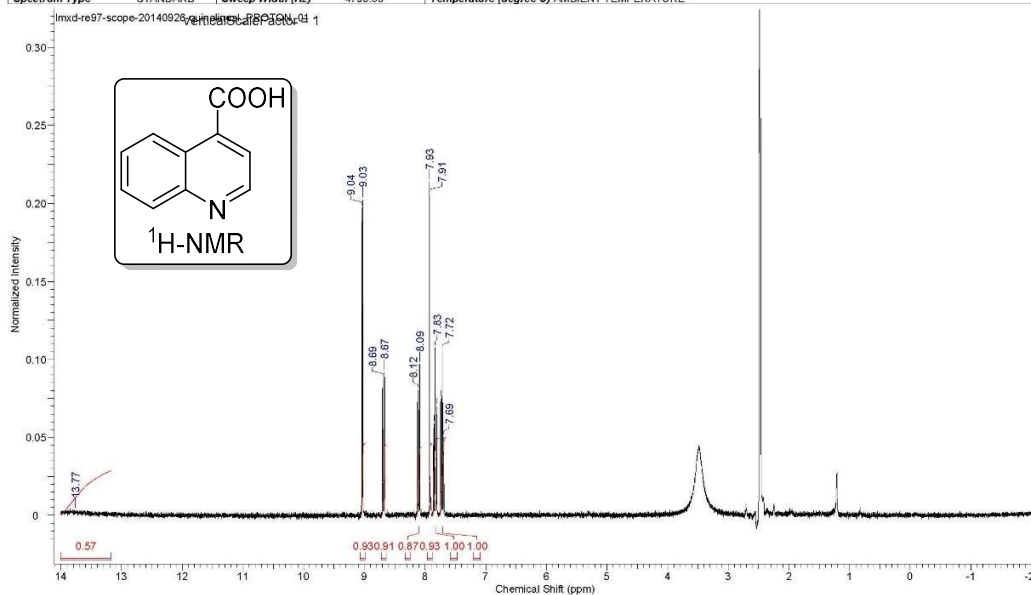


Acquisition Time (sec)	1.0420	Date	Sep 26 2014	Date Stamp	Sep 26 2014
File Name	G:\20140818-scope\mxid-re97-scope-20140926-4-methanol-benzal_CARBON_01.fid	Frequency (MHz)	75.35		
Nucleus	¹³ C	Number of Transients	1700	Original Points Count	19624
Pulse Sequence	s2pul	Receiver Gain	30.00	Solvent	DMSO-d6
Spectrum Type	STANDARD	Sweep Width (Hz)	18832.39	Temperature (degree C)	AMBIENT TEMPERATURE
				Points Count	32768
				Spectrum Offset (Hz)	8287.6016



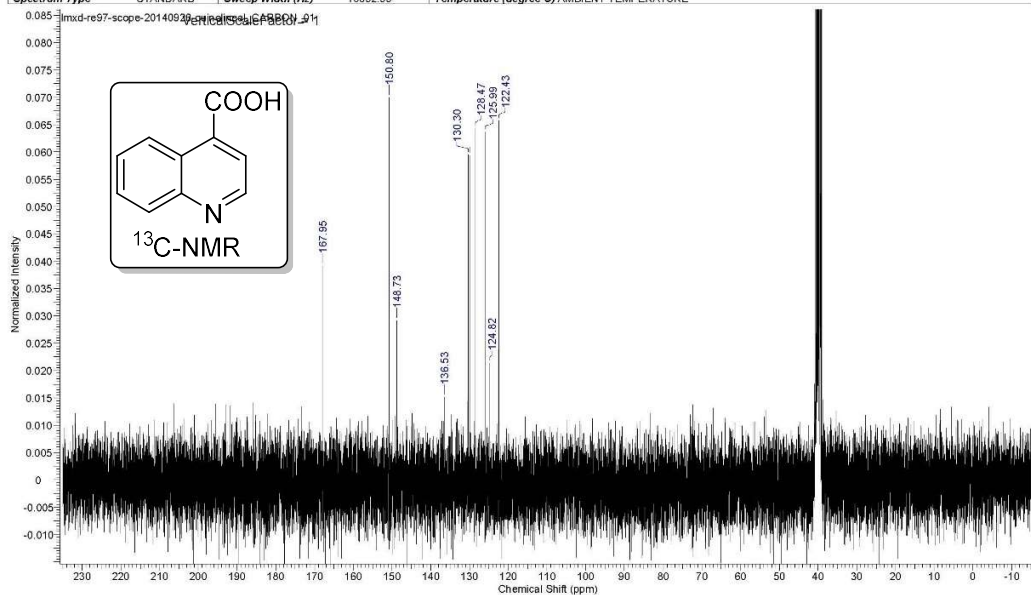
21/10/2014 12:55:02 AM

Acquisition Time (sec)	2.0480	Date	Sep 26 2014	Date Stamp	Sep 26 2014
File Name	G:\20140818-scope\lmsd-re97-scope-20140926-quinolineal	PROTON_01.fid	Frequency (MHz)	299.63	
Nucleus	¹ H	Number of Transients	8	Points Count	16384
Pulse Sequence	s2pul	Receiver Gain	39.00	Solvent	DMSO-d6
Spectrum Type	STANDARD	Sweep Width (Hz)	4793.86	Temperature (degree C)	AMBIENT TEMPERATURE
				Spectrum Offset (Hz)	1797.7786



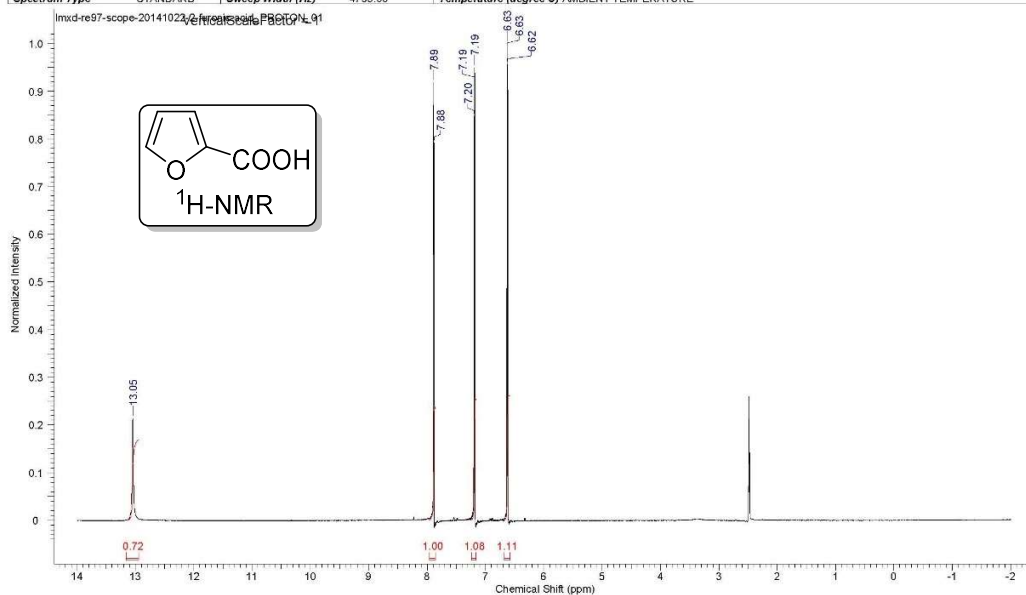
21/10/2014 12:57:28 AM

Acquisition Time (sec)	1.0420	Date	Sep 26 2014	Date Stamp	Sep 26 2014
File Name	G:\20140818-scope\lmsd-re97-scope-20140926-quinolineal	CARBON_01.fid	Frequency (MHz)	75.35	
Nucleus	¹³ C	Number of Transients	3300	Points Count	32768
Pulse Sequence	s2pul	Receiver Gain	30.00	Solvent	DMSO-d6
Spectrum Type	STANDARD	Sweep Width (Hz)	18832.39	Temperature (degree C)	AMBIENT TEMPERATURE
				Spectrum Offset (Hz)	8287.6016



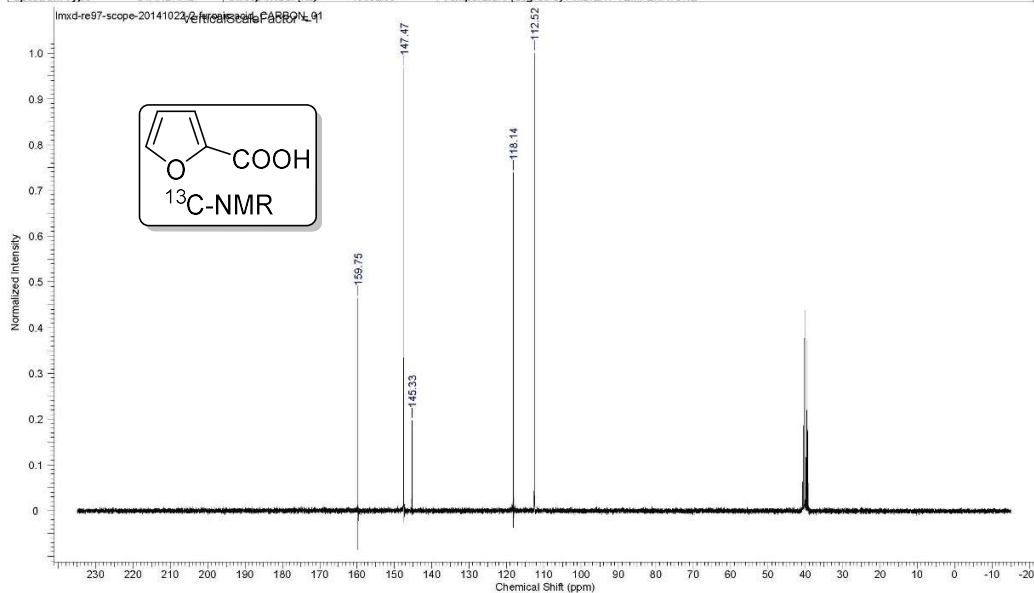
23/10/2014 7:46:53 PM

Acquisition Time (sec)	2.0480	Date	Oct 23 2014	Date Stamp	Oct 23 2014
File Name	G:\20140818-scope\additional\lmsd-re97-scope-20141022-2-furonic-acid_PROTON_01.fid	Frequency (MHz)	299.63		
Nucleus	¹ H	Number of Transients	8	Original Points Count	9618
Pulse Sequence	s2pul	Receiver Gain	30.00	Solvent	DMSO-d6
Spectrum Type	STANDARD	Sweep Width (Hz)	4793.86	Temperature (degree C)	AMBIENT TEMPERATURE
				Spectrum Offset (Hz)	1797.7768



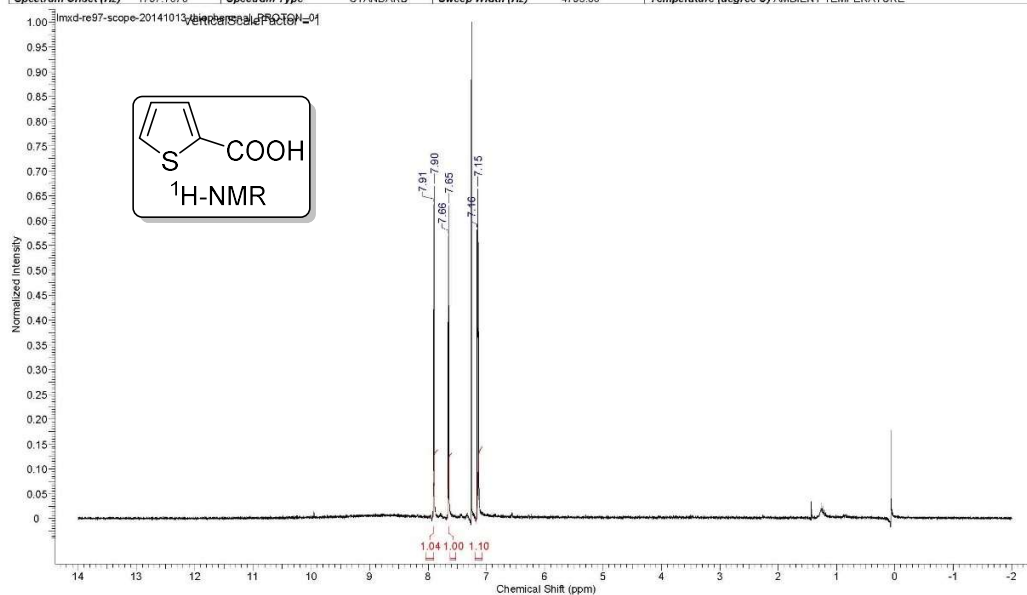
23/10/2014 7:47:30 PM

Acquisition Time (sec)	1.0420	Date	Oct 23 2014	Date Stamp	Oct 23 2014
File Name	G:\20140818-scope\additional\lmsd-re97-scope-20141022-2-furonic-acid_CARBON_01.fid	Frequency (MHz)	75.35		
Nucleus	¹³ C	Number of Transients	1750	Original Points Count	19624
Pulse Sequence	s2pul	Receiver Gain	30.00	Solvent	DMSO-d6
Spectrum Type	STANDARD	Sweep Width (Hz)	18832.39	Temperature (degree C)	AMBIENT TEMPERATURE
				Spectrum Offset (Hz)	8287.6016



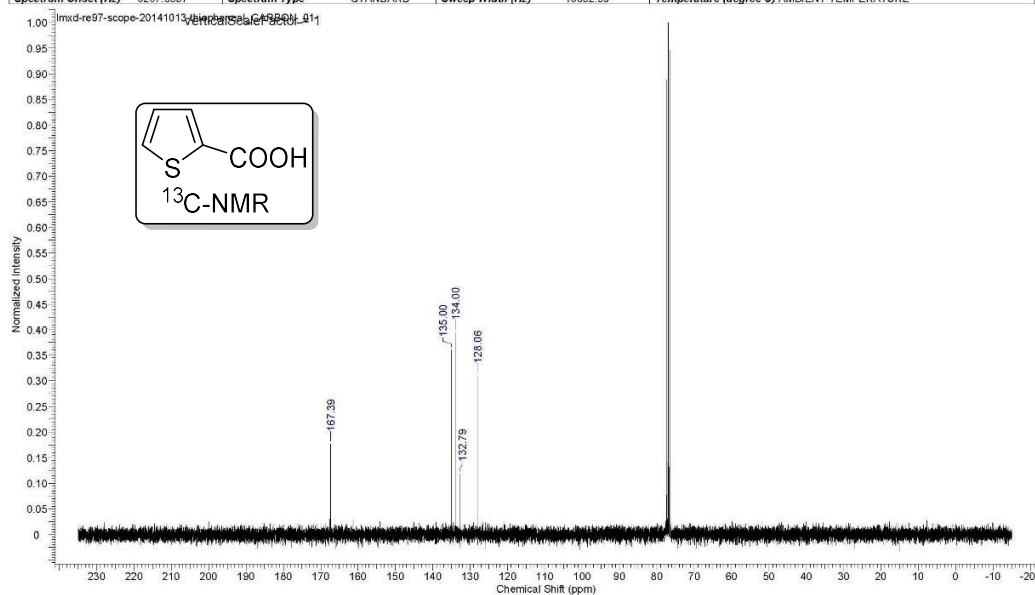
21/10/2014 1:23:45 AM

Acquisition Time (sec)	2.0480	Date	Oct 14 2014	Date Stamp	Oct 14 2014
File Name	G:\20140818-scope\lmsd-re97-scope-20141013-thiopheneal	PROTON_01.fid	Frequency (MHz)	299.63	
Nucleus	¹ H	Number of Transients	8	Original Points Count	9818
Pulse Sequence	s2pul	Receiver Gain	39.00	Solvent	CHLOROFORM-d
Spectrum Offset (Hz)	1797.7676	Spectrum Type	STANDARD	Sweep Width (Hz)	4793.86
				Temperature (degree C)	AMBIENT TEMPERATURE



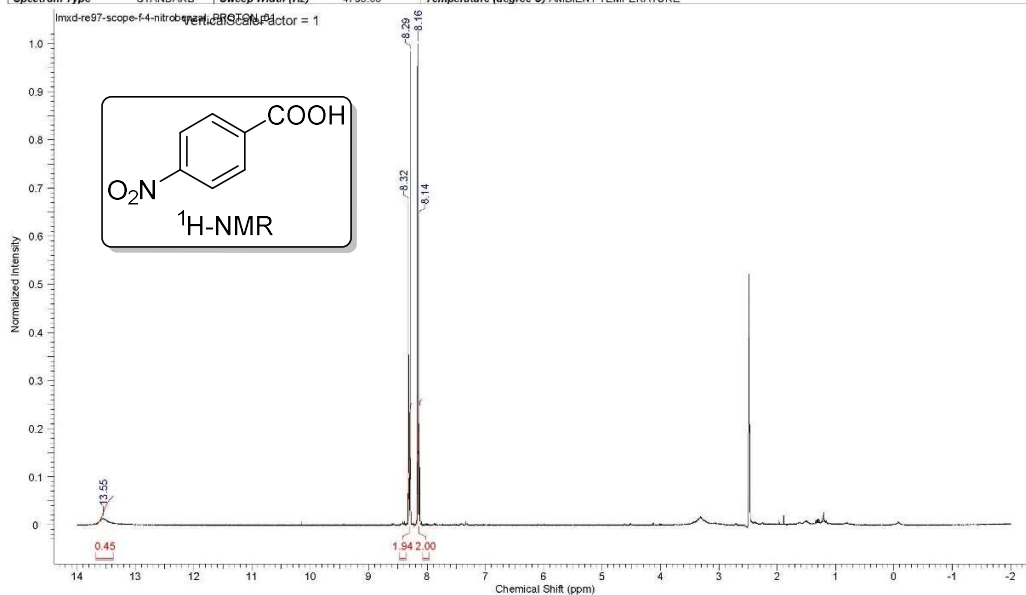
21/10/2014 1:24:30 AM

Acquisition Time (sec)	1.0420	Date	Oct 15 2014	Date Stamp	Oct 15 2014
File Name	G:\20140818-scope\lmsd-re97-scope-20141013-thiopheneal	CARBON_01.fid	Frequency (MHz)	75.35	
Nucleus	¹³ C	Number of Transients	1700	Original Points Count	19624
Pulse Sequence	s2pul	Receiver Gain	30.00	Solvent	CHLOROFORM-d
Spectrum Offset (Hz)	6287.5557	Spectrum Type	STANDARD	Sweep Width (Hz)	18832.39
				Temperature (degree C)	AMBIENT TEMPERATURE



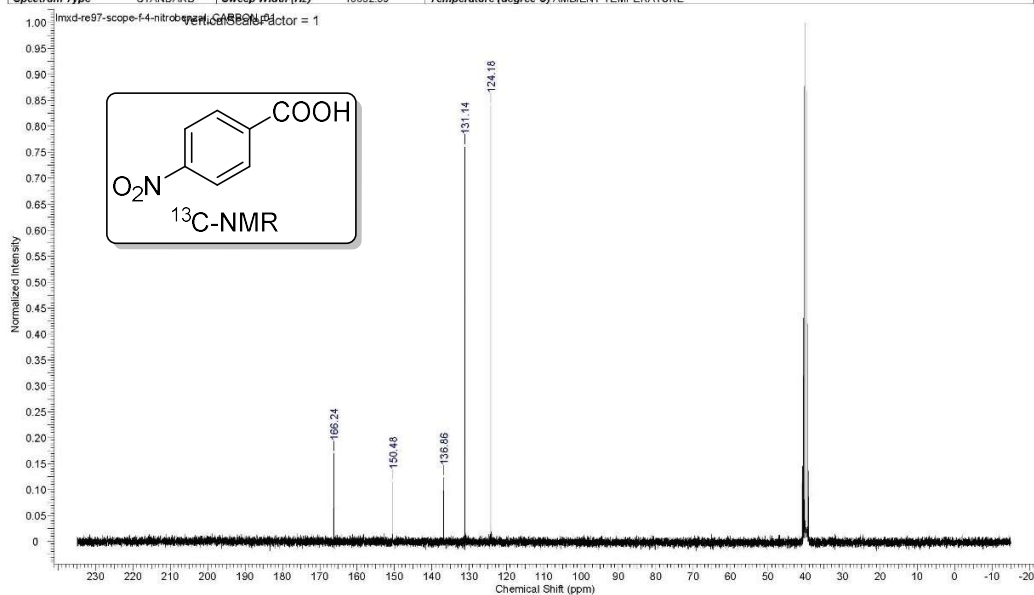
21/10/2014 1:38:08 AM

Acquisition Time (sec)	2.0480	Date	Aug 31 2014	Date Stamp	Aug 31 2014
File Name	G:\20140818-scope\lmsd-re97-scope-f-4-nitrobenzal_PROTON_01.fid	Frequency (MHz)	299.63		
Nucleus	¹ H	Number of Transients	8	Original Points Count	9818
Pulse Sequence	s2pul	Receiver Gain	39.00	Solvent	DMSO-d6
Spectrum Type	STANDARD	Sweep Width (Hz)	4793.86	Temperature (degree C)	AMBIENT TEMPERATURE
Spectrum Offset (Hz)					
1797.7788					



21/10/2014 1:38:41 AM

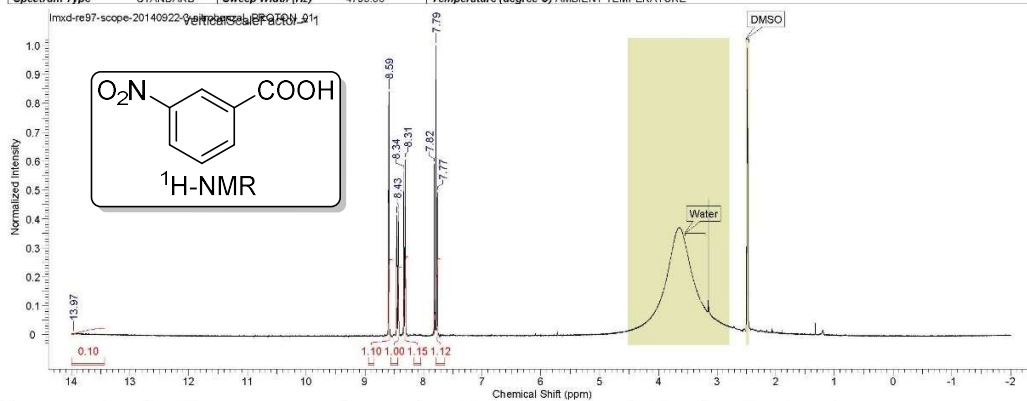
Acquisition Time (sec)	1.0420	Date	Aug 31 2014	Date Stamp	Aug 31 2014
File Name	G:\20140818-scope\lmsd-re97-scope-f-4-nitrobenzal_CARBON_01.fid	Frequency (MHz)	75.35		
Nucleus	¹³ C	Number of Transients	3300	Original Points Count	19624
Pulse Sequence	s2pul	Receiver Gain	30.00	Solvent	DMSO-d6
Spectrum Type	STANDARD	Sweep Width (Hz)	18832.39	Temperature (degree C)	AMBIENT TEMPERATURE
Spectrum Offset (Hz)					
8287.6016					



This report was created by ACD/NMR Processor Academic Edition. For more information go to www.acdlabs.com/nmrproc/

20/10/2014 10:54:20 PM

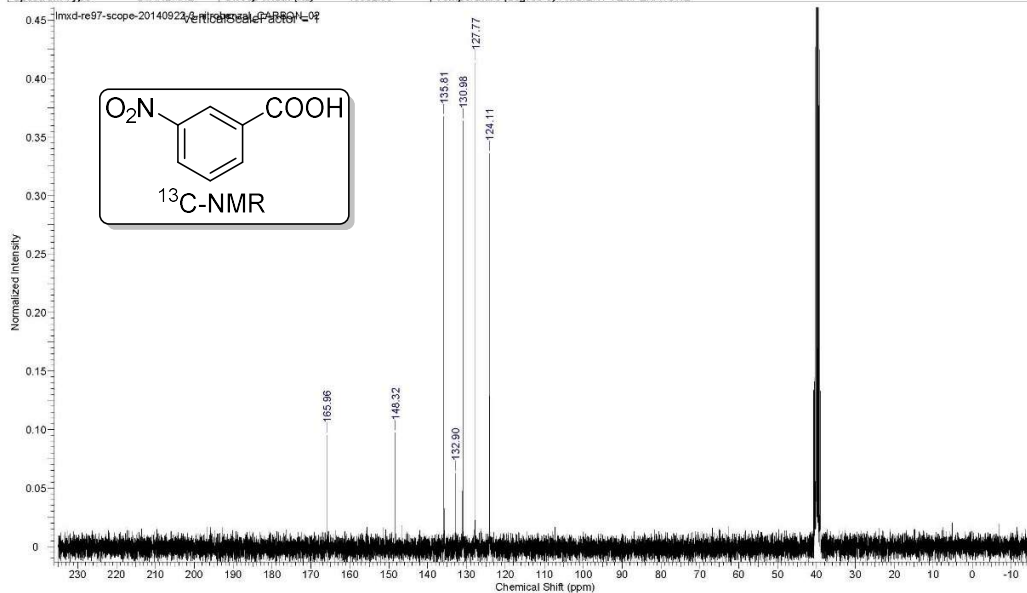
Acquisition Time (sec)	2.0480	Date	Sep 22 2014	Date Stamp	Sep 22 2014
File Name	G:\20140818-scope\imxd-re97-scope-20140922-3-nitrobenzal	PROTON_01.fid	Frequency (MHz)	299.83	
Nucleus	¹ H	Number of Transients	6	Original Points Count	9818
Pulse Sequence	s2pul	Receiver Gain	24.00	Solvent	DMSO-d6
Spectrum Type	STANDARD	Sweep Width (Hz)	4793.86	Temperature (degree C)	AMBIENT TEMPERATURE
				Spectrum Offset (Hz)	1797.7788



This report was created by ACD/NMR Processor Academic Edition. For more information go to www.acdlabs.com/nmrproc/

20/10/2014 10:54:58 PM

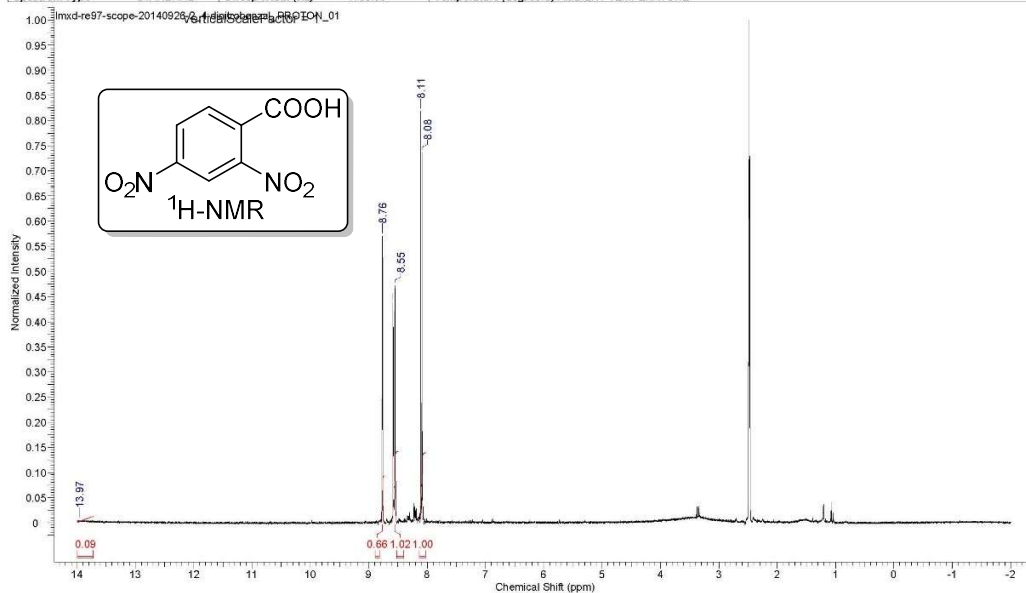
Acquisition Time (sec)	1.0420	Date	Sep 23 2014	Date Stamp	Sep 23 2014
File Name	G:\20140818-scope\imxd-re97-scope-20140922-3-nitrobenzal	CARBON_02.fid	Frequency (MHz)	75.35	
Nucleus	¹³ C	Number of Transients	1696	Original Points Count	19624
Pulse Sequence	s2pul	Receiver Gain	30.00	Solvent	DMSO-d6
Spectrum Type	STANDARD	Sweep Width (Hz)	18832.39	Temperature (degree C)	AMBIENT TEMPERATURE
				Spectrum Offset (Hz)	8287.6016



This report was created by ACD/NMR Processor Academic Edition. For more information go to www.acdlabs.com/nmrproc/

21/10/2014 12:40:34 AM

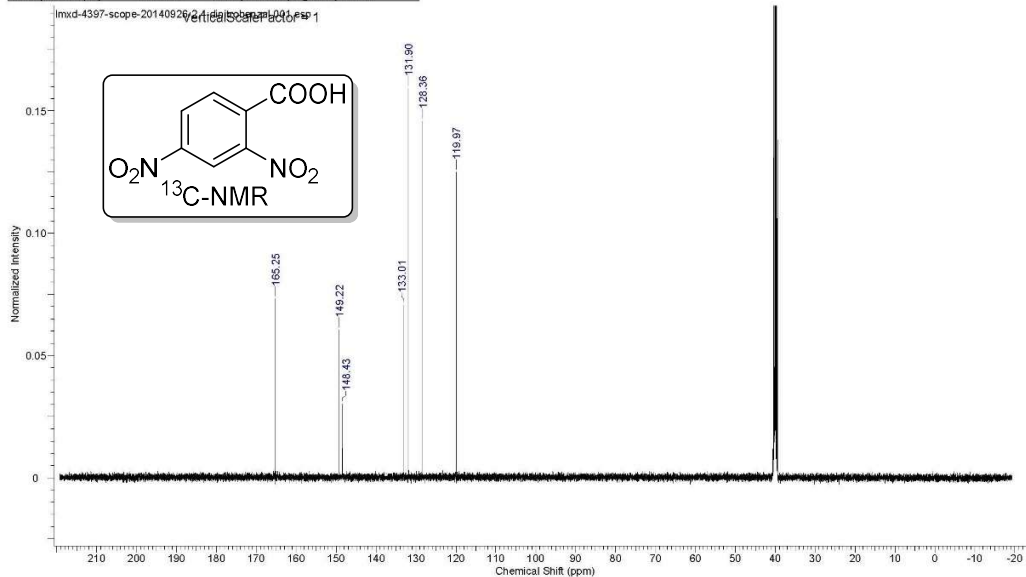
Acquisition Time (sec)	2.0480	Date	Sep 26 2014	Date Stamp	Sep 26 2014
File Name	G:\20140818-scope\lmsd-re97-scope-20140926-2,4-dinitrobenzal_PROTON_01.fid	Frequency (MHz)	299.63		
Nucleus	¹ H	Number of Transients	8	Original Points Count	9818
Pulse Sequence	s2pul	Receiver Gain	39.00	Solvent	DMSO-d6
Spectrum Type	STANDARD	Sweep Width (Hz)	4793.86	Temperature (degree C)	AMBIENT TEMPERATURE
				Spectrum Offset (Hz)	1797.7788



This report was created by ACD/NMR Processor Academic Edition. For more information go to www.acdlabs.com/nmrproc/

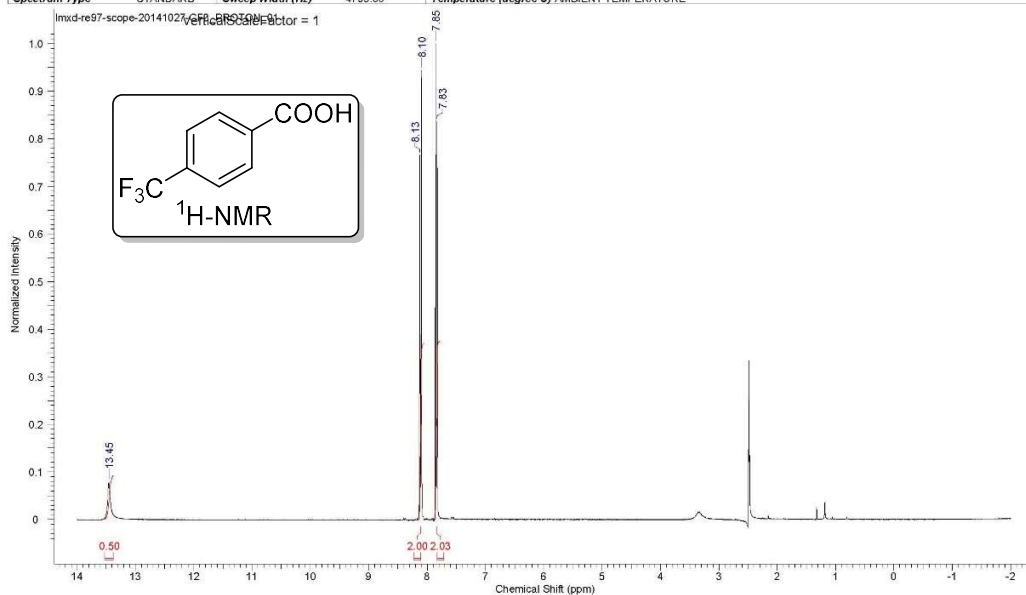
20/10/2014 9:58:19 PM

Acquisition Time (sec)	1.0923	Date	27 Sep 2014 22:50:40	Date Stamp	27 Sep 2014 22:50:40
File Name	G:\20140818-scope\lmsd-4397-scope-20140926-2,4-dinitrobenzal_13C.fid	Frequency (MHz)	125.80		
Nucleus	¹³ C	Number of Transients	3300	Original Points Count	32768
Owner	mcgillnmr	Points Count	32768	Pulse Sequence	zgpg30
SW (Hz)	30000.00	Solvent	DMSO-d6	Spectrum Offset (Hz)	12578.9248
Sweep Width (Hz)	29999.08	Temperature (degree C)	24.999	Receiver Gain	192.72
				Spectrum Type	STANDARD



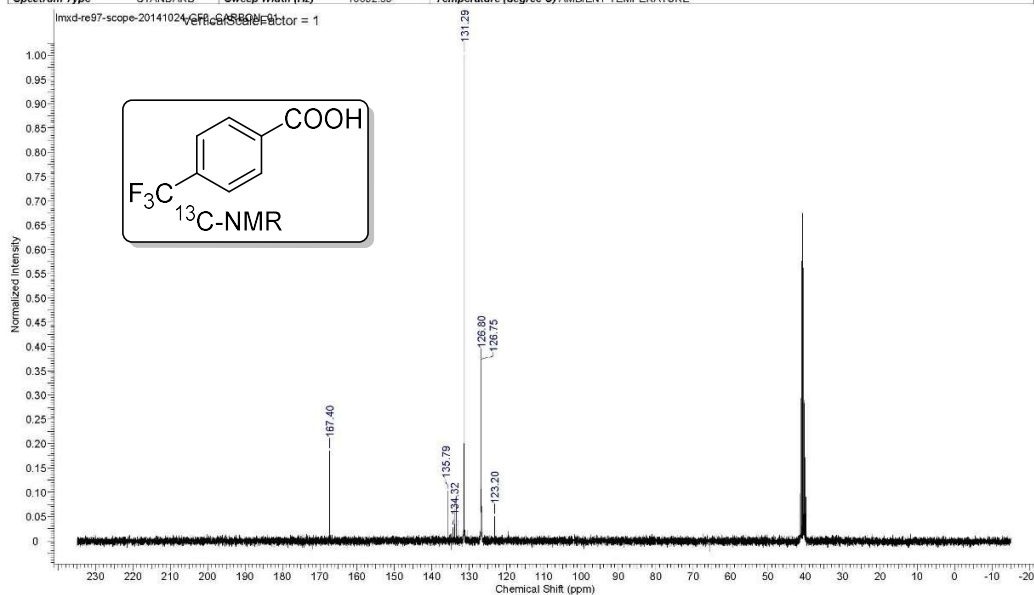
07/11/2014 10:41:38 PM

Acquisition Time (sec)	2.0480	Date	Oct 27 2014	Date Stamp	Oct 27 2014
File Name	C:\Users\MML\My Documents\mxid-re97-scope-20141027-CF3_PROTON_01.fid	Frequency (MHz)	299.63	Points Count	16384
Nucleus	¹ H	Number of Transients	8	Original Points Count	9818
Pulse Sequence	s2pul	Receiver Gain	30.00	Solvent	DMSO-d6
Spectrum Type	STANDARD	Sweep Width (Hz)	4793.86	Temperature (degree C)	AMBIENT TEMPERATURE
				Spectrum Offset (Hz)	1797.7788



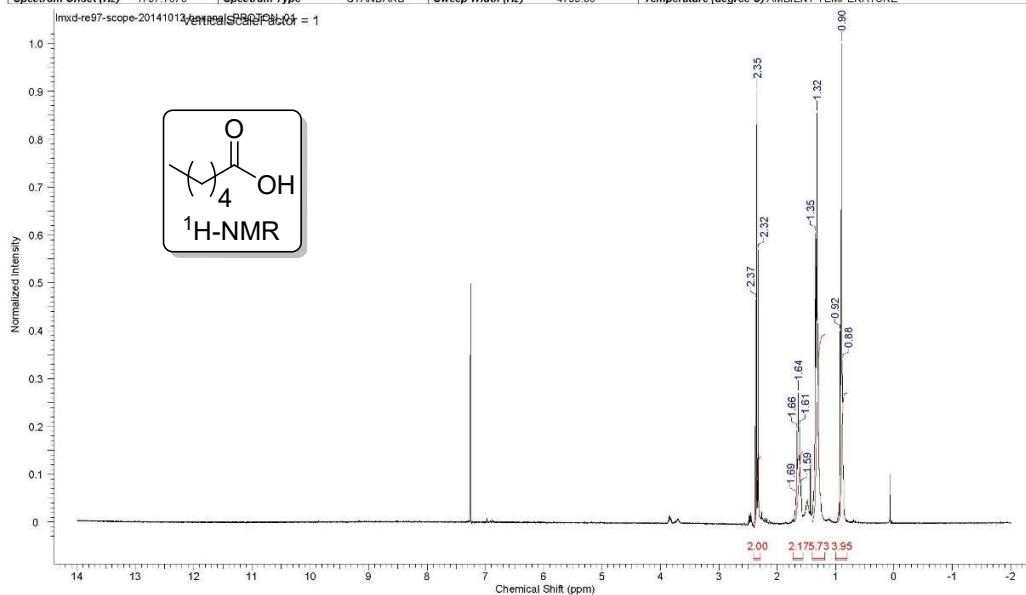
07/11/2014 10:50:04 PM

Acquisition Time (sec)	1.0420	Date	Oct 25 2014	Date Stamp	Oct 25 2014
File Name	C:\Users\MML\My Documents\mxid-re97-scope-20141024-CF3_CARBON_01.fid	Frequency (MHz)	75.35	Points Count	32768
Nucleus	¹³ C	Number of Transients	1700	Original Points Count	19624
Pulse Sequence	s2pul	Receiver Gain	30.00	Solvent	DMSO-d6
Spectrum Type	STANDARD	Sweep Width (Hz)	18832.39	Temperature (degree C)	AMBIENT TEMPERATURE
				Spectrum Offset (Hz)	8287.6016



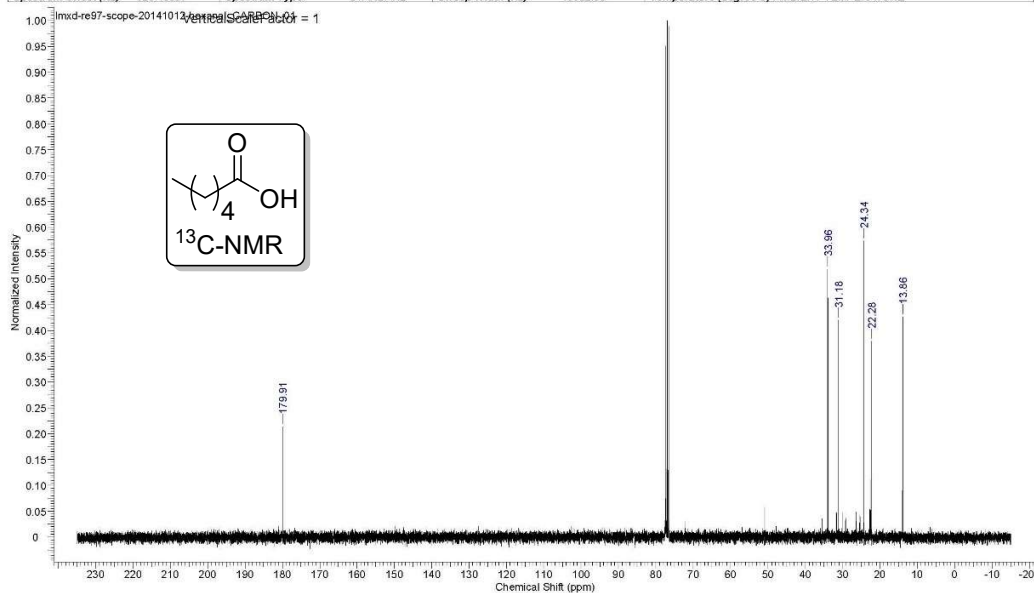
21/10/2014 1:11:50 AM

Acquisition Time (sec)	2.0480	Date	Oct 12 2014	Date Stamp	Oct 12 2014
File Name	G:\20140818-scope\lmsd-re97-scope-20141012-hexanal_PROTON_01.fid	Frequency (MHz)	299.63		
Nucleus	¹ H	Number of Transients	8	Original Points Count	9818
Pulse Sequence	s2pul	Receiver Gain	30.00	Solvent	CHLOROFORM-d
Spectrum Offset (Hz)	1797.7676	Spectrum Type	STANDARD	Sweep Width (Hz)	4793.86
		Temperature (degree C) AMBIENT TEMPERATURE			



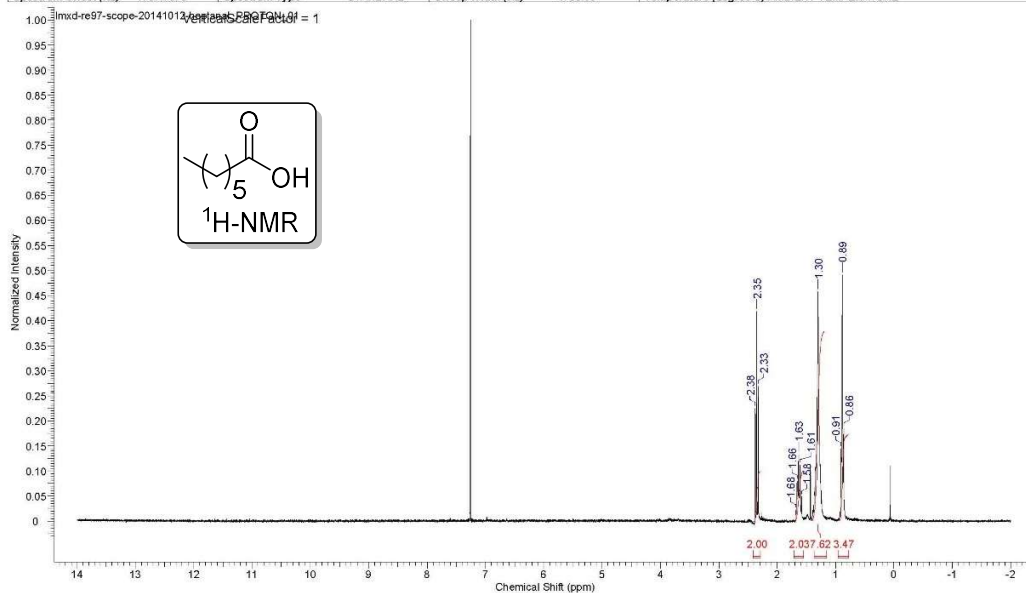
21/10/2014 1:12:28 AM

Acquisition Time (sec)	1.0420	Date	Oct 12 2014	Date Stamp	Oct 12 2014
File Name	G:\20140818-scope\lmsd-re97-scope-20141012-hexanal_CARBO_01.fid	Frequency (MHz)	75.35		
Nucleus	¹³ C	Number of Transients	3300	Original Points Count	19624
Pulse Sequence	s2pul	Receiver Gain	30.00	Solvent	CHLOROFORM-d
Spectrum Offset (Hz)	8287.5557	Spectrum Type	STANDARD	Sweep Width (Hz)	18832.39
		Temperature (degree C) AMBIENT TEMPERATURE			



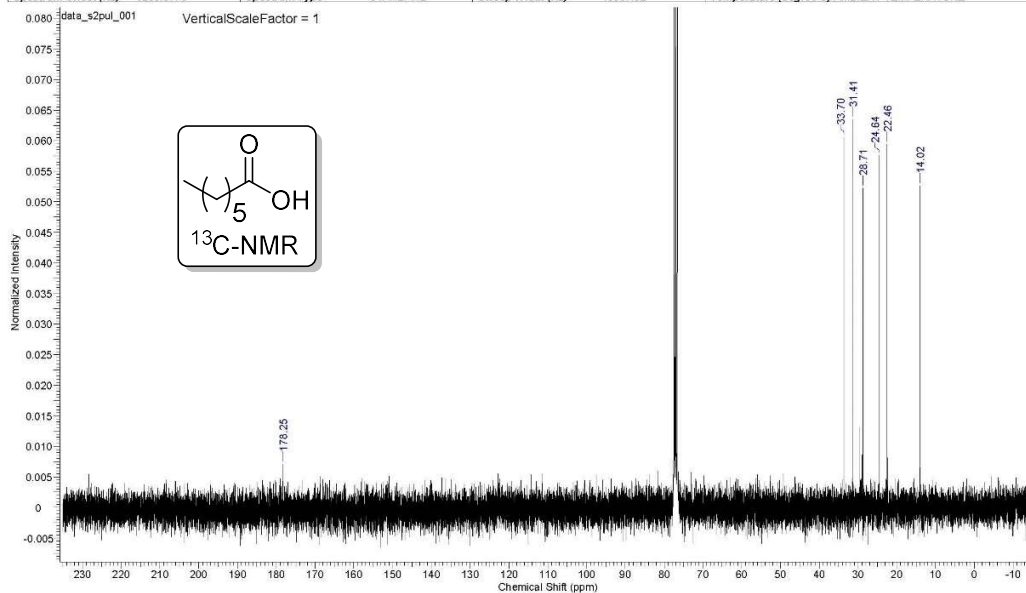
21/10/2014 1:09:51 AM

Acquisition Time (sec)	2.0480	Date	Oct 12 2014	Date Stamp	Oct 12 2014		
File Name	G:\20140818-scope\lmsd-re97-scope-20141012-heptanal_PROTON_01.fid				Frequency (MHz)	299.63	
Nucleus	¹ H	Number of Transients	8	Original Points Count	9818	Points Count	16384
Pulse Sequence	s2pul	Receiver Gain	39.00	Solvent	CHLOROFORM-d		
Spectrum Offset (Hz)	1797.7676	Spectrum Type	STANDARD	Sweep Width (Hz)	4793.86	Temperature (degree C)	AMBIENT TEMPERATURE



23/10/2014 7:54:53 PM

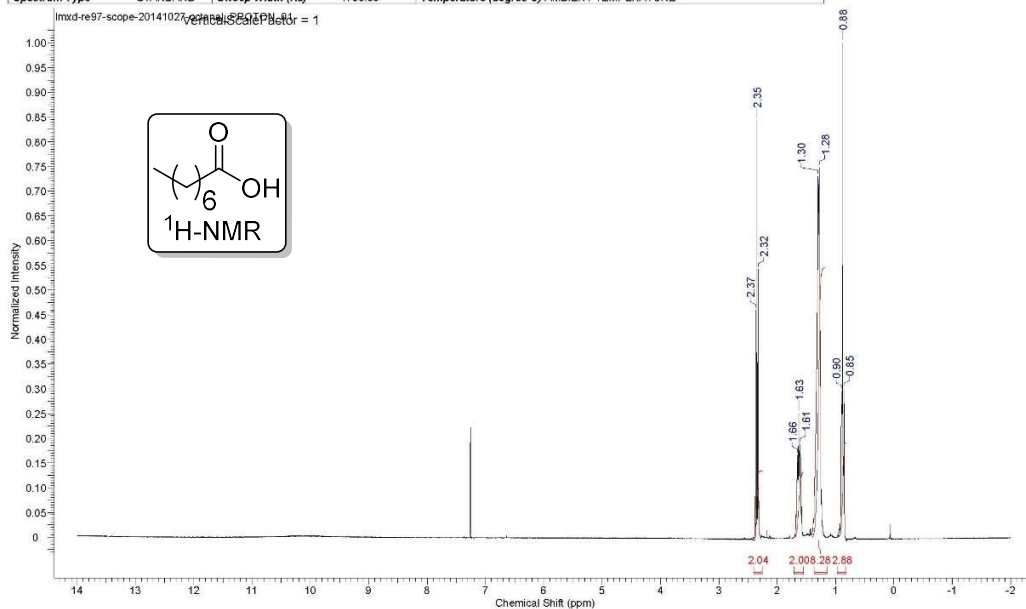
Acquisition Time (sec)	1.0420	Comment	lmsd-re97-scope_20141022-heptanal-13C		Date	Oct 22 2014	
Date Stamp	Oct 22 2014	File Name	G:\20140818-scope\additional\lmsd-re97-scope_20141022-heptanal-13C_20141022_01\data_s2pul_001.fid				
Frequency (MHz)	75.46	Nucleus	¹³ C	Number of Transients	23800	Original Points Count	19661
Points Count	32768	Pulse Sequence	s2pul	Receiver Gain	30.00	Solvent	CHLOROFORM-d
Spectrum Offset (Hz)	8299.3770	Spectrum Type	STANDARD	Sweep Width (Hz)	18867.92	Temperature (degree C)	AMBIENT TEMPERATURE



This report was created by ACD/NMR Processor Academic Edition. For more information go to www.acdlabs.com/nmrproc/

07/11/2014 10:07:59 PM

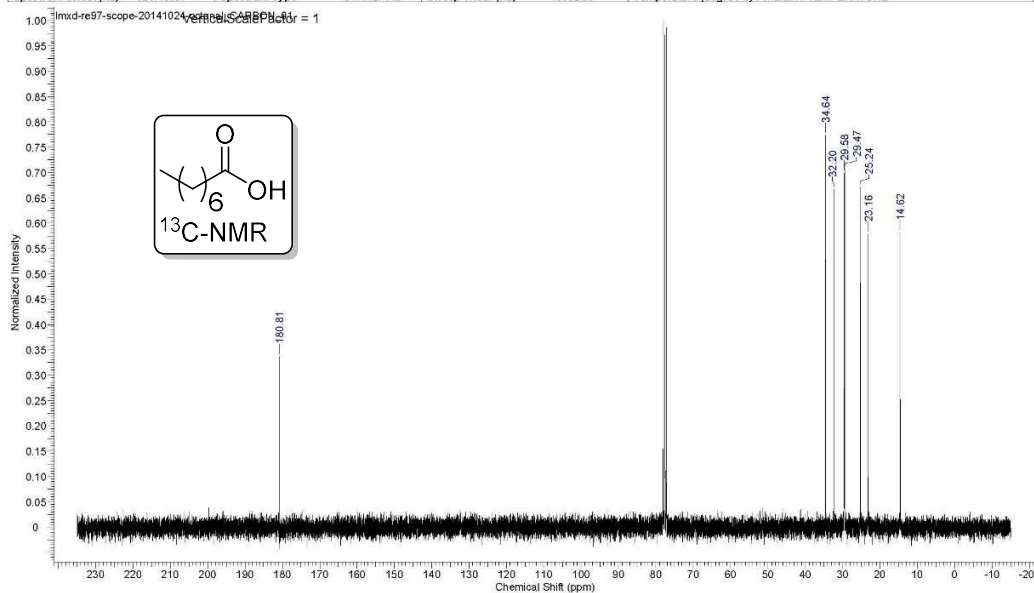
Acquisition Time (sec)	2.0480	Date	Oct 27 2014	Date Stamp	Oct 27 2014	File Name	G:\mxid-re97-scope-20141027-octanal_PROTON_01.fid\fid
Frequency (MHz)	299.63	Nucleus	¹ H	Number of Transients	8	Original Points Count	9818
Pulse Sequence	s2pul	Receiver Gain	24.00	Solvent	CHLOROFORM-d	Points Count	16384
Spectrum Type	STANDARD	Sweep Width (Hz)	4793.86	Temperature (degree C)	AMBIENT TEMPERATURE	Spectrum Offset (Hz)	1797.7676



This report was created by ACD/NMR Processor Academic Edition. For more information go to www.acdlabs.com/nmrproc/

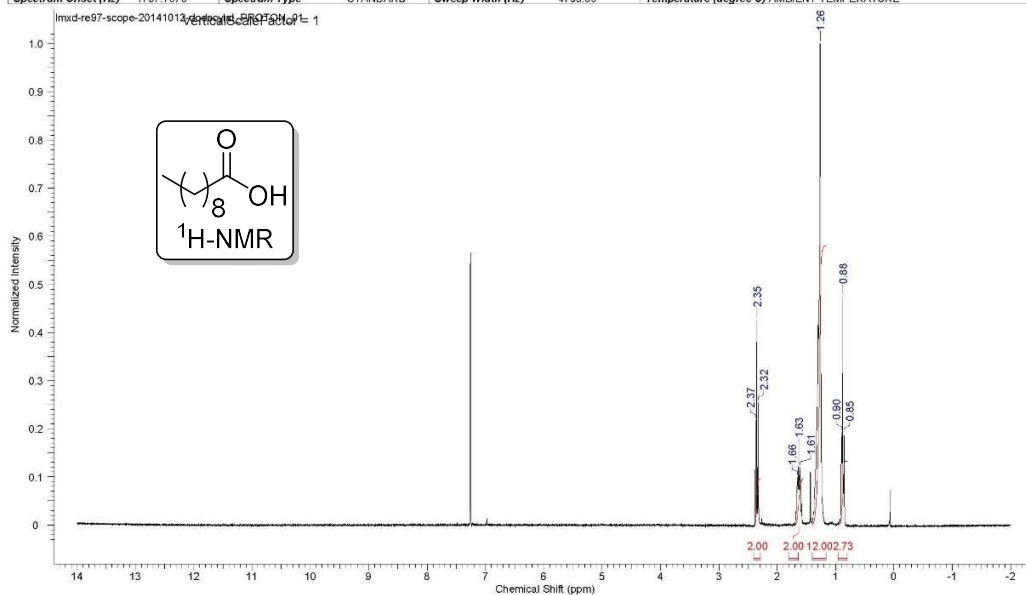
07/11/2014 10:09:10 PM

Acquisition Time (sec)	1.0420	Date	Oct 25 2014	Date Stamp	Oct 25 2014	File Name	G:\mxid-re97-scope-20141024-octanal_CARBO_01.fid 2.fid
Frequency (MHz)	75.35	Nucleus	¹³ C	Number of Transients	1700	Original Points Count	19624
Pulse Sequence	s2pul	Receiver Gain	30.00	Solvent	CHLOROFORM-d	Points Count	32768
Spectrum Offset (Hz)	6287.5557	Spectrum Type	STANDARD	Sweep Width (Hz)	18832.39	Temperature (degree C)	AMBIENT TEMPERATURE



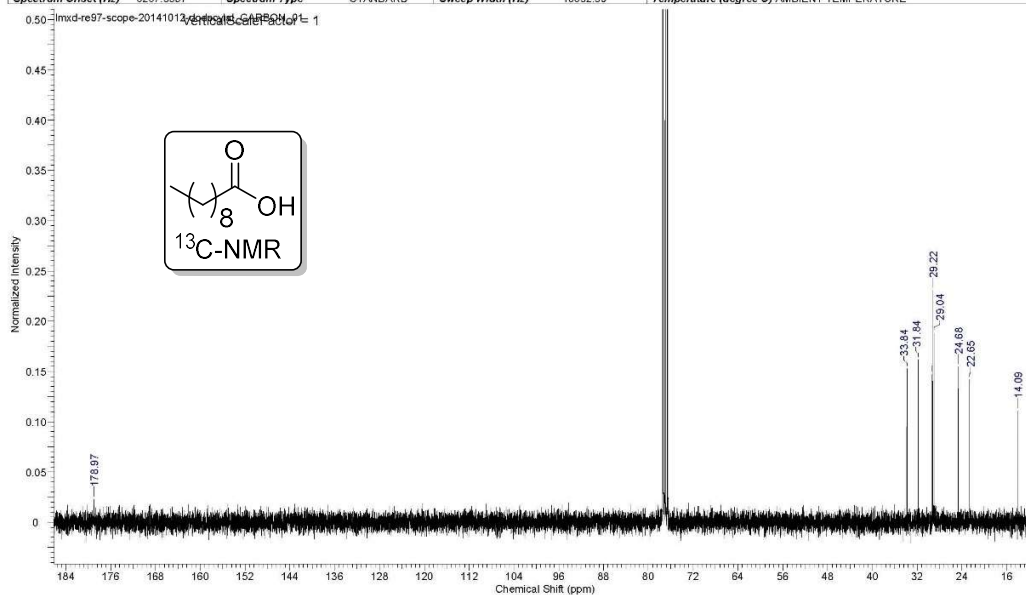
21/10/2014 1:06:31 AM

Acquisition Time (sec)	2.0480	Date	Oct 12 2014	Date Stamp	Oct 12 2014
File Name	G:\20140818-scope\lmsd-re97-scope-20141012-dodecylal_PROTON_01.fid				Frequency (MHz)
Nucleus	¹ H	Number of Transients	8	Original Points Count	9818
Pulse Sequence	s2pul	Receiver Gain	39.00	Solvent	CHLOROFORM-d
Spectrum Offset (Hz)	1797.7676	Spectrum Type	STANDARD	Sweep Width (Hz)	4793.86
					Temperature (degree C)

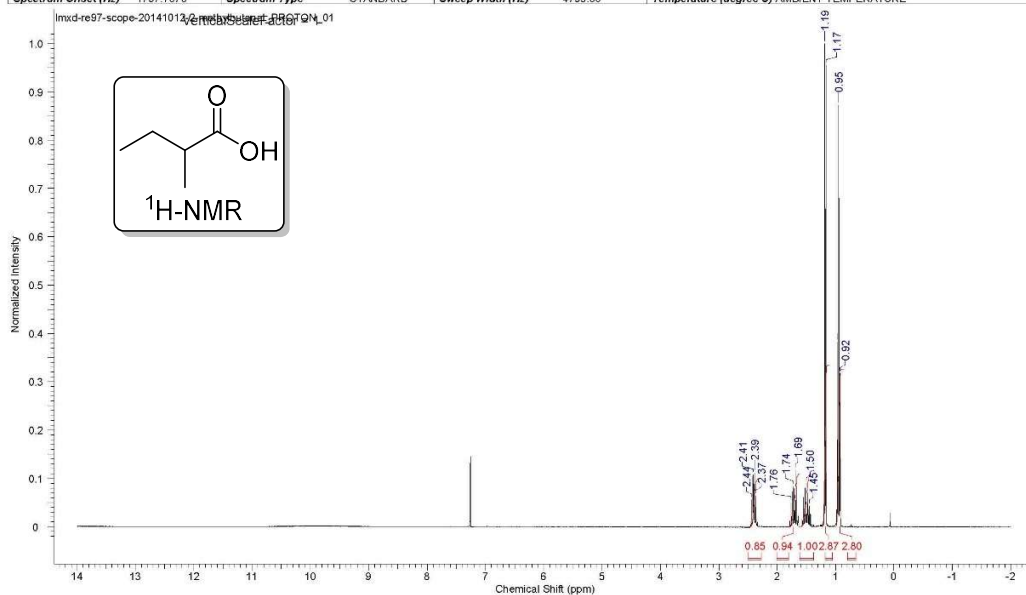


21/10/2014 1:08:36 AM

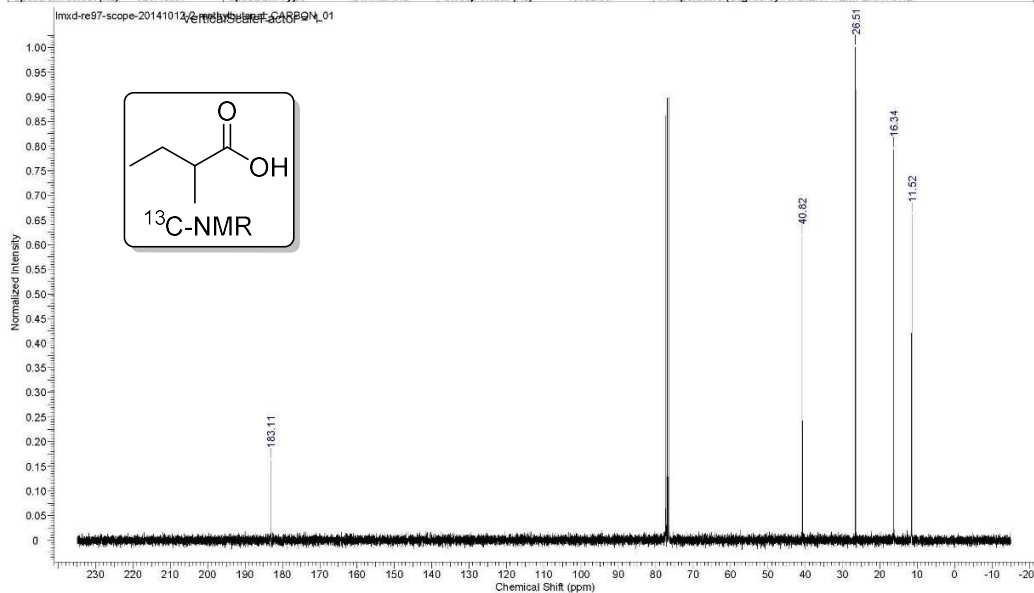
Acquisition Time (sec)	1.0420	Date	Oct 12 2014	Date Stamp	Oct 12 2014
File Name	G:\20140818-scope\lmsd-re97-scope-20141012-dodecylal_CARBON_01.fid				Frequency (MHz)
Nucleus	¹³ C	Number of Transients	3300	Original Points Count	19624
Pulse Sequence	s2pul	Receiver Gain	30.00	Solvent	CHLOROFORM-d
Spectrum Offset (Hz)	8287.5557	Spectrum Type	STANDARD	Sweep Width (Hz)	18832.39
					Temperature (degree C)



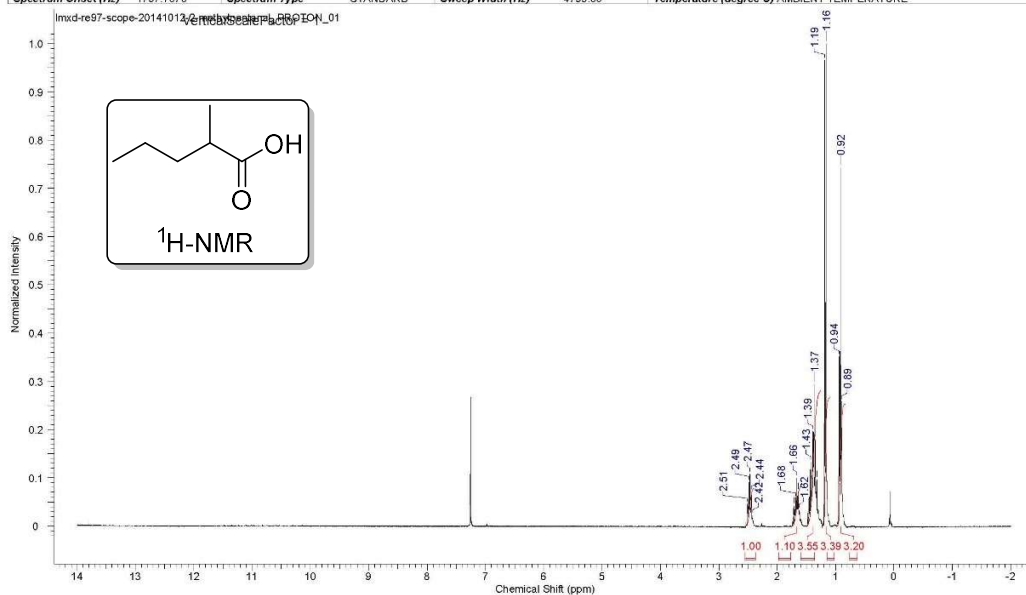
Acquisition Time (sec)	2.0480	Date	Oct 12 2014	Date Stamp	Oct 12 2014
File Name	G:\20140818-scope\mxid-re97-scope-20141012-2-methylbutanal_PROTON_01.fid	Frequency (MHz)	299.63		
Nucleus	¹ H	Number of Transients	8	Original Points Count	9818
Pulse Sequence	s2pul	Receiver Gain	30.00	Solvent	CHLOROFORM-d
Spectrum Offset (Hz)	1797.7676	Spectrum Type	STANDARD	Sweep Width (Hz)	4793.86
		Temperature (degree C) AMBIENT TEMPERATURE			



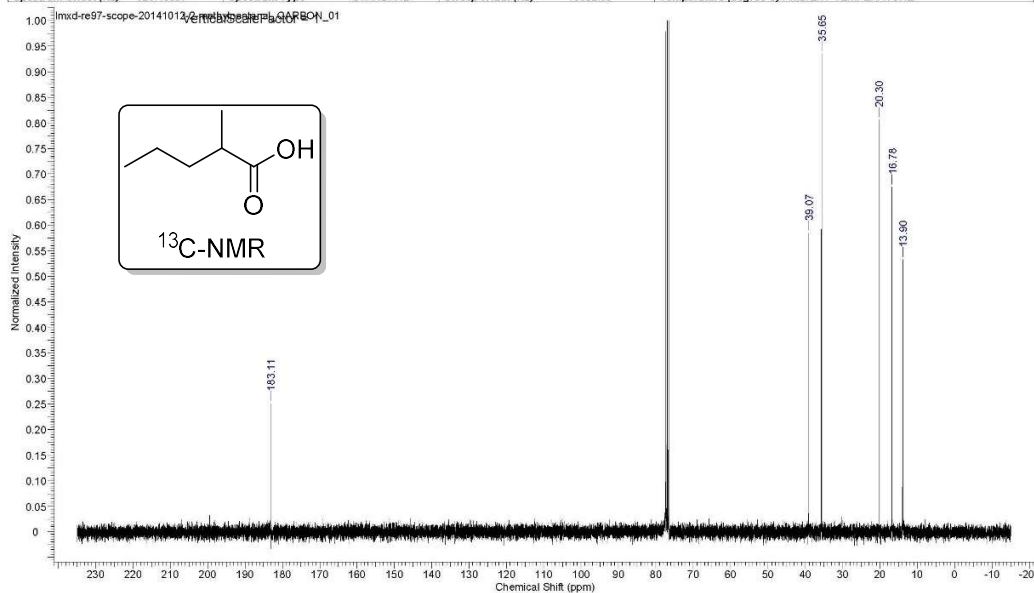
Acquisition Time (sec)	1.0420	Date	Oct 12 2014	Date Stamp	Oct 12 2014
File Name	G:\20140818-scope\mxid-re97-scope-20141012-2-methylbutanal_CARBON_01.fid	Frequency (MHz)	75.35		
Nucleus	¹³ C	Number of Transients	3300	Original Points Count	19624
Pulse Sequence	s2pul	Receiver Gain	30.00	Solvent	CHLOROFORM-d
Spectrum Offset (Hz)	6287.5557	Spectrum Type	STANDARD	Sweep Width (Hz)	18832.39
		Temperature (degree C) AMBIENT TEMPERATURE			



Acquisition Time (sec)	2.0480	Date	Oct 12 2014	Date Stamp	Oct 12 2014
File Name	G:\20140818-scope\mxid-re97-scope-20141012-2-methylpentanal_PROTON_01.fid	Frequency (MHz)	299.63		
Nucleus	¹ H	Number of Transients	8	Original Points Count	9818
Pulse Sequence	s2pul	Receiver Gain	30.00	Solvent	CHLOROFORM-d
Spectrum Offset (Hz)	1797.7676	Spectrum Type	STANDARD	Sweep Width (Hz)	4793.86
					Temperature (degree C) AMBIENT TEMPERATURE

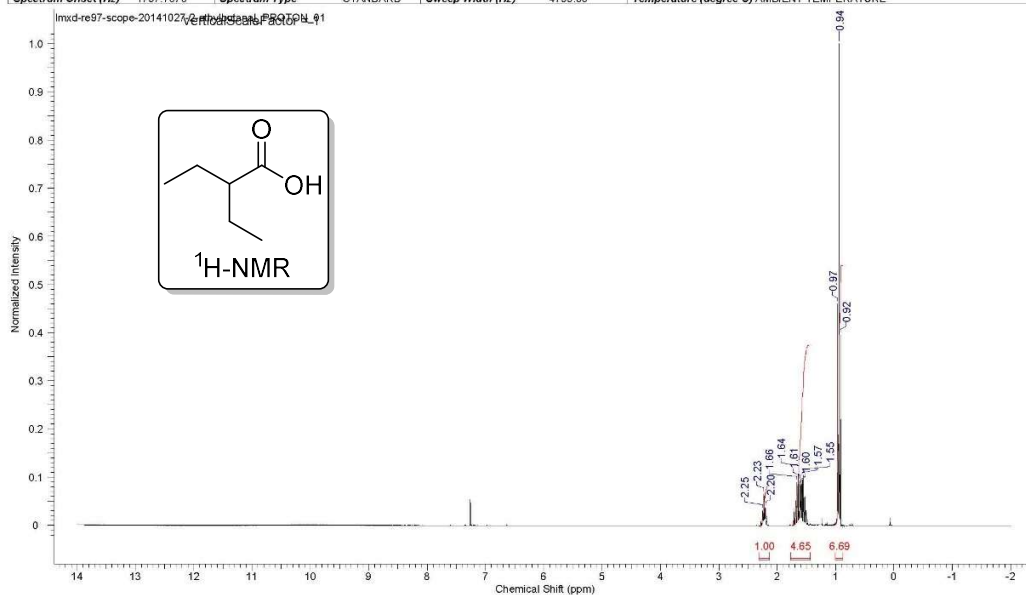


Acquisition Time (sec)	1.0420	Date	Oct 12 2014	Date Stamp	Oct 12 2014
File Name	G:\20140818-scope\mxid-re97-scope-20141012-2-methylpentanal_CARBON_01.fid	Frequency (MHz)	75.35		
Nucleus	¹³ C	Number of Transients	3300	Original Points Count	19624
Pulse Sequence	s2pul	Receiver Gain	30.00	Solvent	CHLOROFORM-d
Spectrum Offset (Hz)	6287.5557	Spectrum Type	STANDARD	Sweep Width (Hz)	18832.39
					Temperature (degree C) AMBIENT TEMPERATURE



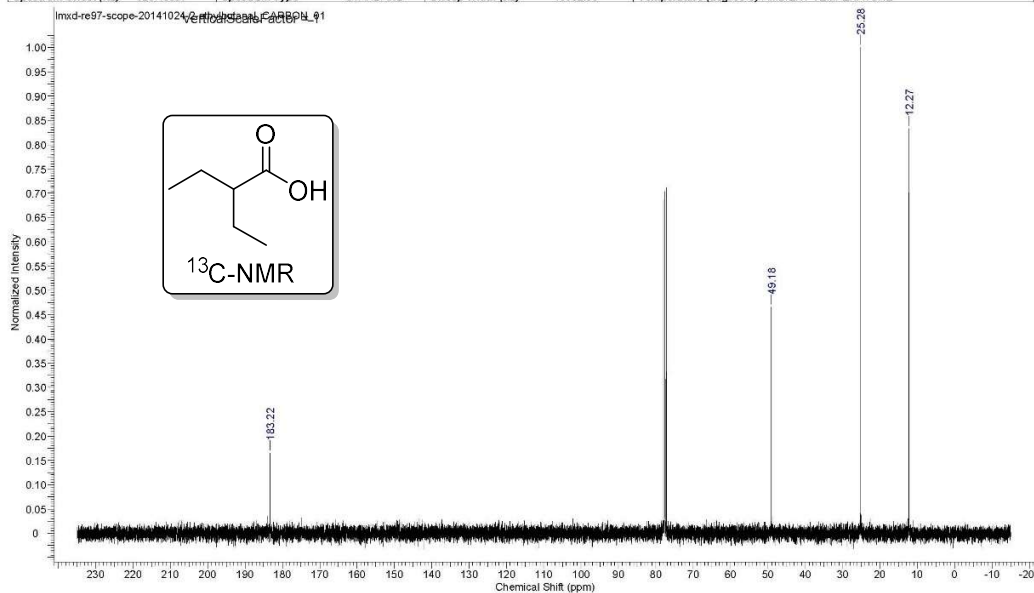
07/11/2014 10:10:01 PM

Acquisition Time (sec)	2.0480	Date	Oct 27 2014	Date Stamp	Oct 27 2014
File Name	G:\mxid-re97-scope-20141027-2-ethylbutanal_PROTON_01.fid	Frequency (MHz)	299.63		
Nucleus	¹ H	Number of Transients	8	Original Points Count	9818
Pulse Sequence	s2pul	Receiver Gain	30.00	Solvent	CHLOROFORM-d
Spectrum Offset (Hz)	1797.7676	Spectrum Type	STANDARD	Sweep Width (Hz)	4793.86
		Temperature (degree C) AMBIENT TEMPERATURE			

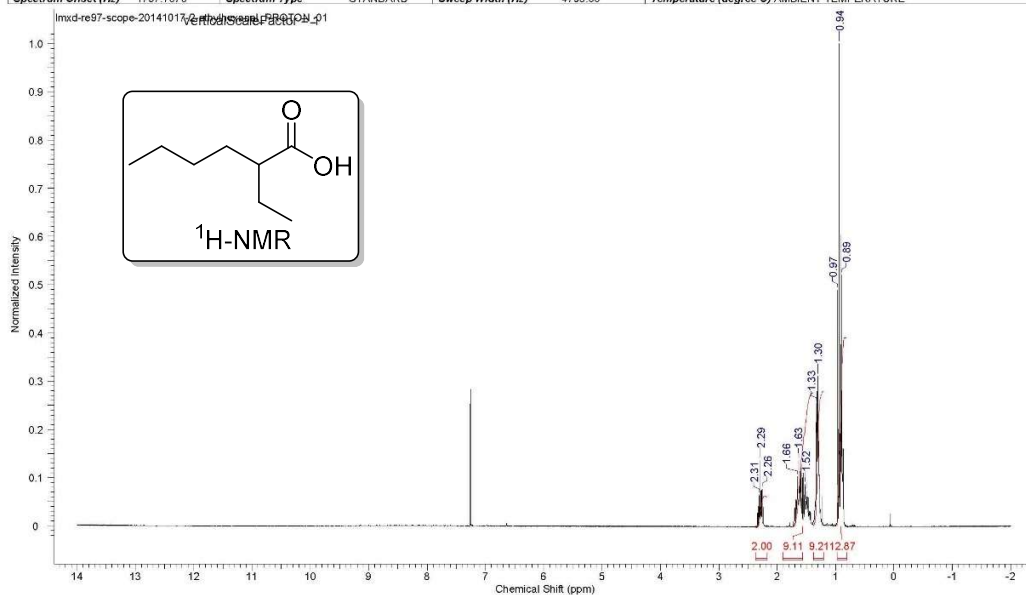


07/11/2014 10:10:26 PM

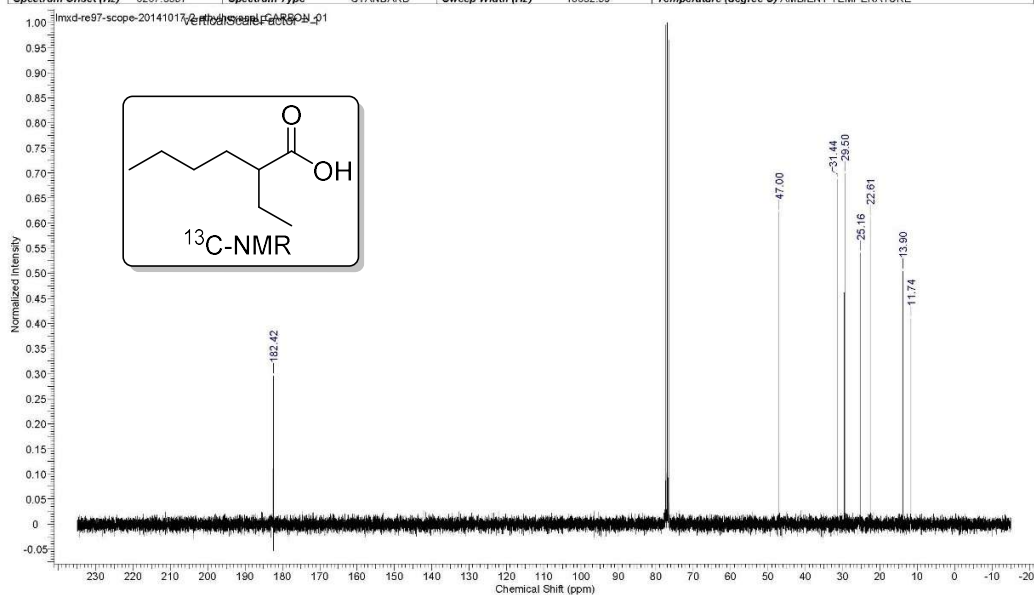
Acquisition Time (sec)	1.0420	Date	Oct 24 2014	Date Stamp	Oct 24 2014
File Name	G:\mxid-re97-scope-20141024-2-ethylbutanal_CARBON_01.fid	Frequency (MHz)	75.35		
Nucleus	¹³ C	Number of Transients	1700	Original Points Count	19624
Pulse Sequence	s2pul	Receiver Gain	30.00	Solvent	CHLOROFORM-d
Spectrum Offset (Hz)	6287.5557	Spectrum Type	STANDARD	Sweep Width (Hz)	18832.39
		Temperature (degree C) AMBIENT TEMPERATURE			



Acquisition Time (sec)	2.0480	Date	Oct 17 2014	Date Stamp	Oct 17 2014
File Name	G:\20140818-scope\lmsd-re97-scope-20141017-2-ethylhexanal	PROTON_01.fid.tif	Frequency (MHz)	299.63	
Nucleus	¹ H	Number of Transients	8	Original Points Count	9818
Pulse Sequence	s2pul	Receiver Gain	30.00	Solvent	CHLOROFORM-d
Spectrum Offset (Hz)	1797.7676	Spectrum Type	STANDARD	Sweep Width (Hz)	4793.86
				Temperature (degree C)	AMBIENT TEMPERATURE

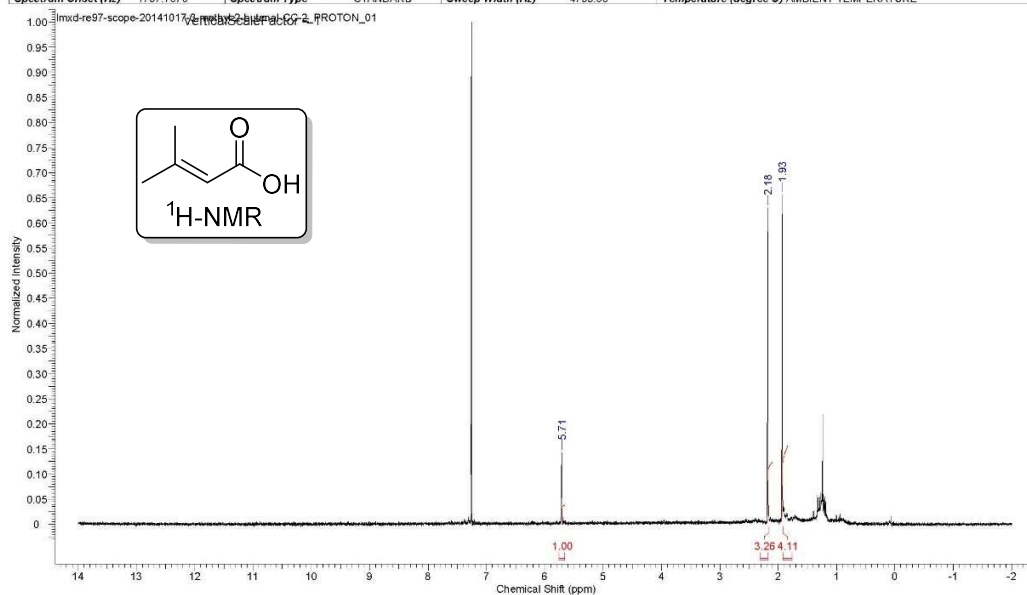


Acquisition Time (sec)	1.0420	Date	Oct 17 2014	Date Stamp	Oct 17 2014
File Name	G:\20140818-scope\lmsd-re97-scope-20141017-2-ethylhexanal	CARBON_01.fid.tif	Frequency (MHz)	75.35	
Nucleus	¹³ C	Number of Transients	1700	Original Points Count	19624
Pulse Sequence	s2pul	Receiver Gain	30.00	Solvent	CHLOROFORM-d
Spectrum Offset (Hz)	6287.5557	Spectrum Type	STANDARD	Sweep Width (Hz)	18832.39
				Temperature (degree C)	AMBIENT TEMPERATURE



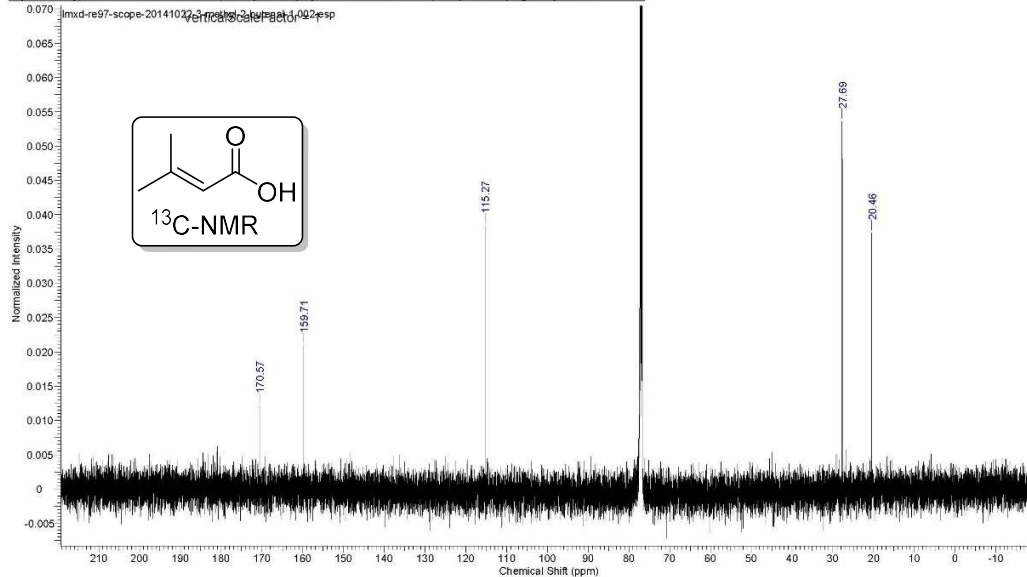
21/10/2014 1:49:08 AM

Acquisition Time (sec)	2.0480	Date	Oct 17 2014	Date Stamp	Oct 17 2014
File Name	G:\20140818-scope\lmsd-re97-scope-20141017-3-methyl-2-butenal-CC-2_PROTON_01.fid	Frequency (MHz)	299.63		
Nucleus	¹ H	Number of Transients	8	Original Points Count	9818
Pulse Sequence	zgpg30	Receiver Gain	39.00	Solvent	CHLOROFORM-d
Spectrum Offset (Hz)	1797.7676	Spectrum Type	STANDARD	Sweep Width (Hz)	4793.86
				Temperature (degree C)	AMBIENT TEMPERATURE



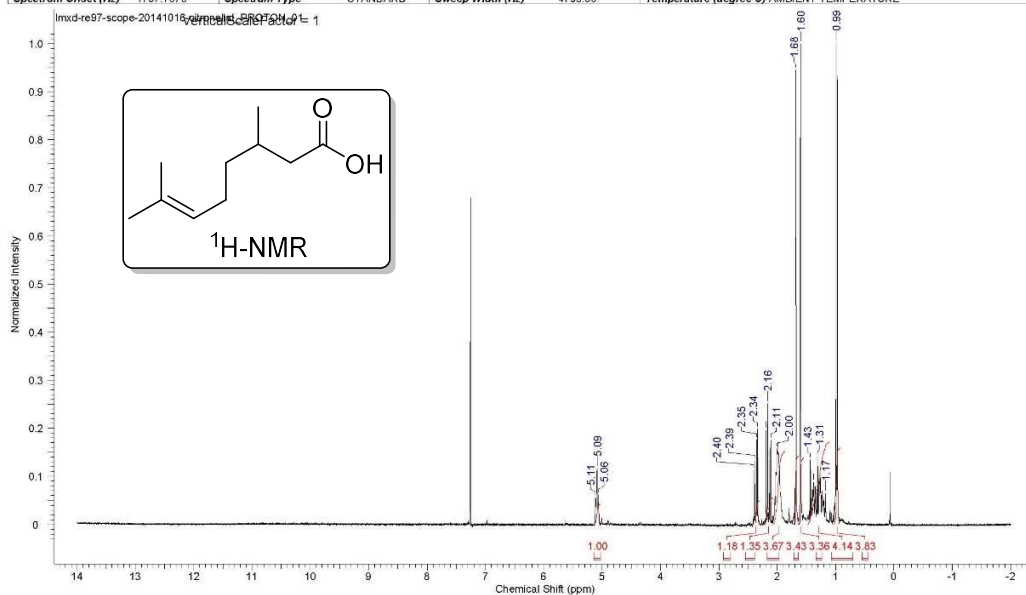
22/10/2014 10:06:07 PM

Acquisition Time (sec)	1.0923	Date	22 Oct 2014 21:08:16	Date Stamp	22 Oct 2014 21:08:16
File Name	G:\20140818-scope\additional\lmsd-re97-scope-20141022-3-methyl-2-butenal-13.fid	Frequency (MHz)	125.81		
Nucleus	¹³ C	Number of Transients	3400	Origin	AVII1500HD
Owner	mcgillnmr	Points Count	32768	Pulse Sequence	zgpg30
SW (Hz)	30000.00	Solvent	CHLOROFORM-d	Receiver Gain	192.72
Spectrum Type	STANDARD	Sweep Width (Hz)	29999.08	Temperature (degree C)	24.998
				Spectrum Offset (Hz)	12578.9238



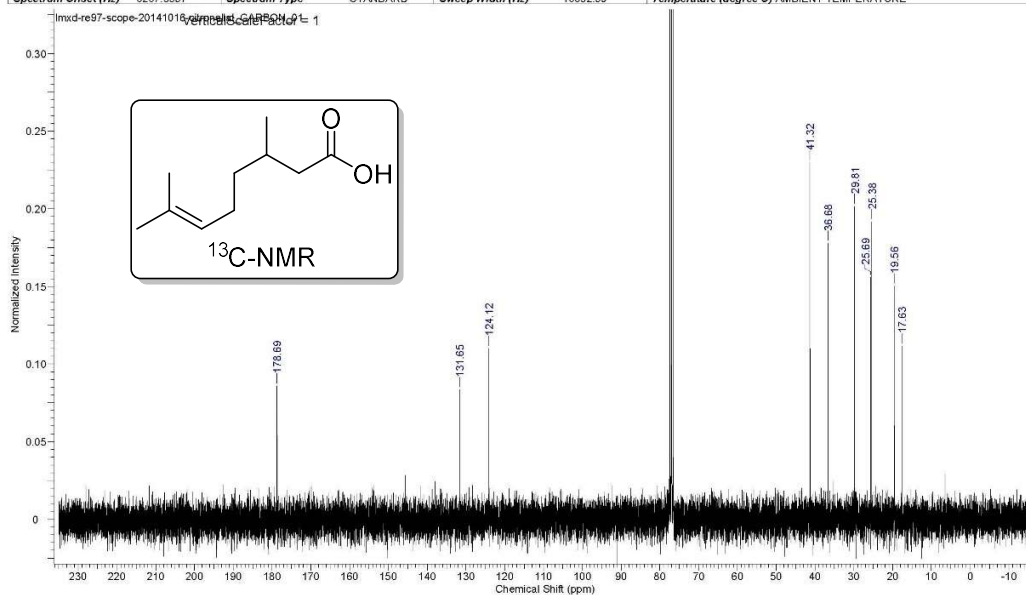
21/10/2014 1:44:56 AM

Acquisition Time (sec)	2.0480	Date	Oct 16 2014	Date Stamp	Oct 16 2014
File Name	G:\20140818-scope\lmsd-re97-scope-20141016-citronella_PROTON_01.fid	Frequency (MHz)	299.63		
Nucleus	¹ H	Number of Transients	8	Original Points Count	9818
Pulse Sequence	s2pul	Receiver Gain	39.00	Solvent	CHLOROFORM-d
Spectrum Offset (Hz)	1797.7676	Spectrum Type	STANDARD	Sweep Width (Hz)	4793.86
		Temperature (degree C) AMBIENT TEMPERATURE			



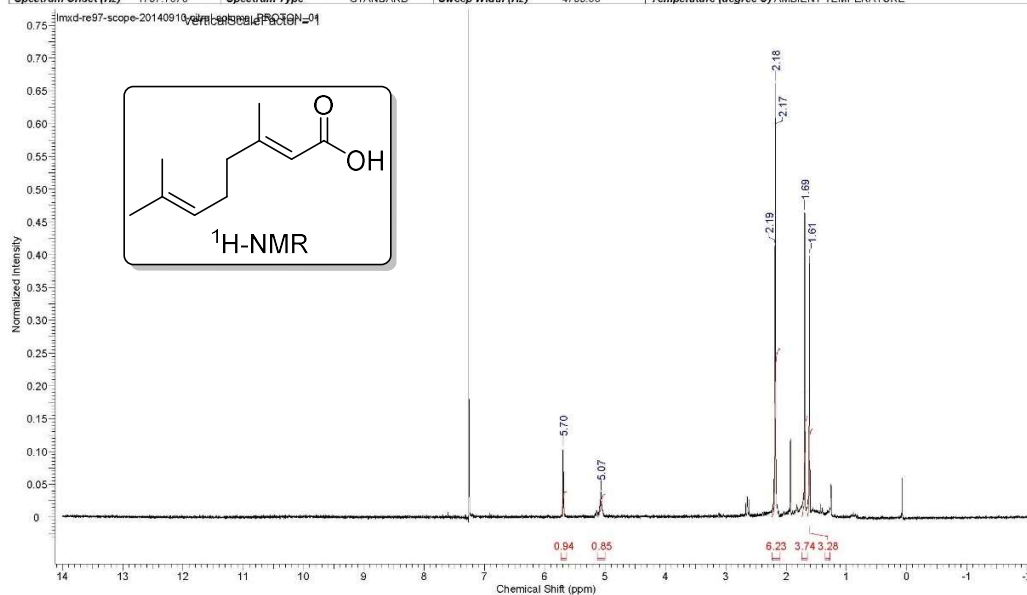
21/10/2014 1:45:47 AM

Acquisition Time (sec)	1.0420	Date	Oct 16 2014	Date Stamp	Oct 16 2014
File Name	G:\20140818-scope\lmsd-re97-scope-20141016-citronella_CARBON_01.fid	Frequency (MHz)	75.35		
Nucleus	¹³ C	Number of Transients	1700	Original Points Count	19624
Pulse Sequence	s2pul	Receiver Gain	30.00	Solvent	CHLOROFORM-d
Spectrum Offset (Hz)	8287.5557	Spectrum Type	STANDARD	Sweep Width (Hz)	18832.39
		Temperature (degree C) AMBIENT TEMPERATURE			



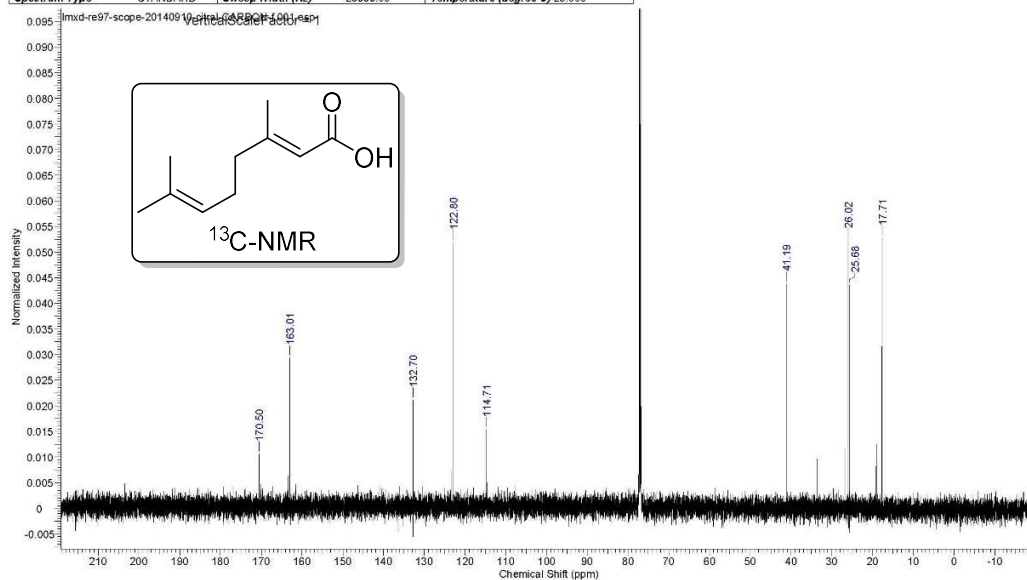
20/10/2014 10:16:22 PM

Acquisition Time (sec)	2.0480	Date	Sep 10 2014	Date Stamp	Sep 10 2014
File Name	G:\20140818-scope\lmsd-re97-scope-20140910-citral-column	PROTON_01.fid		Frequency (MHz)	299.63
Nucleus	¹ H	Number of Transients	8	Original Points Count	9818
Pulse Sequence	zgpg30	Receiver Gain	39.00	Solvent	CHLOROFORM-d
Spectrum Offset (Hz)	1797.7676	Spectrum Type	STANDARD	Sweep Width (Hz)	4793.86
				Temperature (degree C)	AMBIENT TEMPERATURE



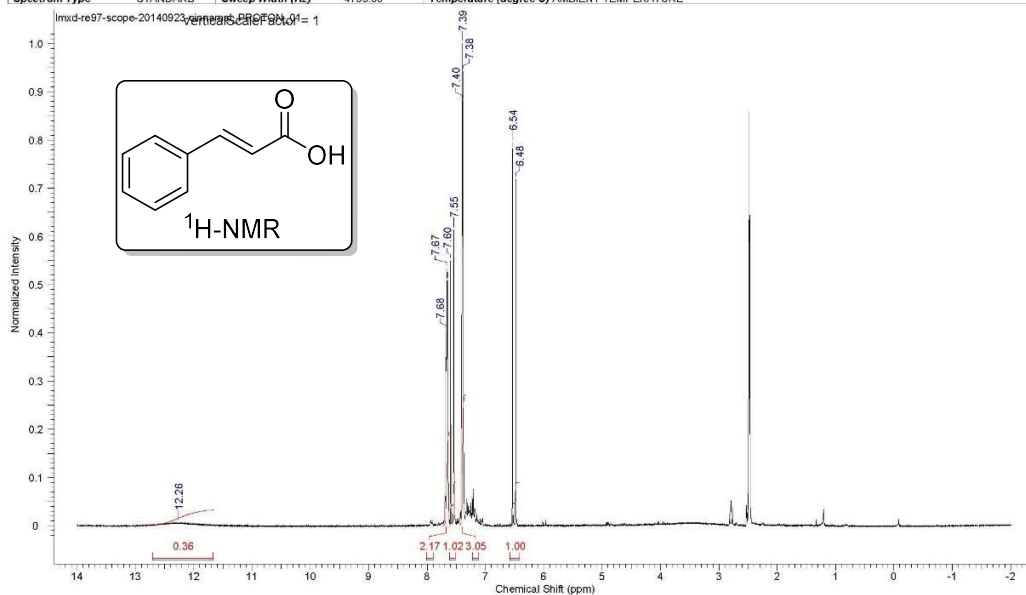
20/10/2014 10:18:47 PM

Acquisition Time (sec)	1.0923	Date	11 Sep 2014 01:09:20	Date Stamp	11 Sep 2014 01:09:20
File Name	G:\20140818-scope\lmsd-re97-scope-20140910-citral-CARBON-f1.fid			Frequency (MHz)	125.81
Nucleus	¹³ C	Number of Transients	3300	Origin	AVIII500HD
Owner	mcgillnmr	Points Count	32768	Pulse Sequence	zgpg30
SW (Hz)	30000.00	Solvent	CHLOROFORM-d	Receiver Gain	192.72
Spectrum Type	STANDARD	Sweep Width (Hz)	29999.08	Temperature (degree C)	25.000
				Spectrum Offset (Hz)	12578.9238



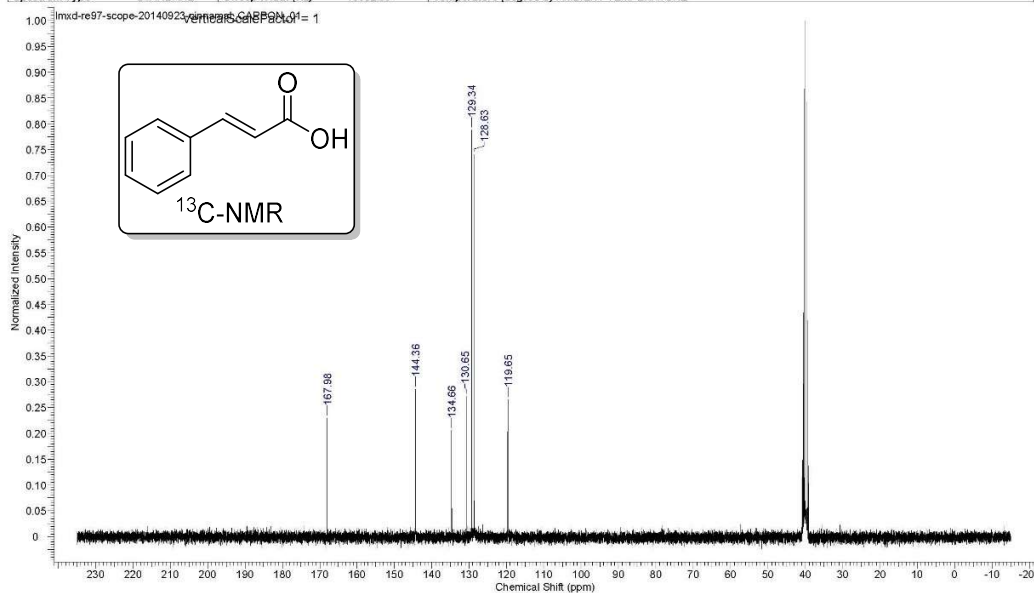
21/10/2014 12:37:40 AM

Acquisition Time (sec)	2.0480	Date	Sep 24 2014	Date Stamp	Sep 24 2014
File Name	G:\20140818-scope\lmsd-re97-scope-20140923-cinnamal_PROTON_01.fid	Frequency (MHz)	299.63	Points Count	16384
Nucleus	¹ H	Number of Transients	8	Original Points Count	9818
Pulse Sequence	s2pul	Receiver Gain	36.00	Solvent	DMSO-d6
Spectrum Type	STANDARD	Sweep Width (Hz)	4793.86	Temperature (degree C)	AMBIENT TEMPERATURE
				Spectrum Offset (Hz)	1797.7768



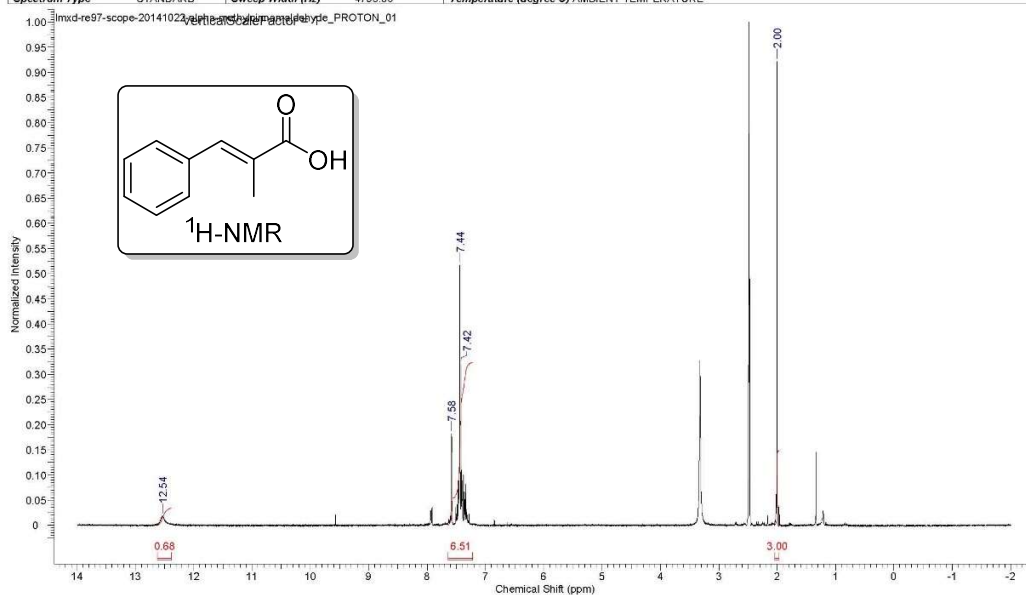
21/10/2014 12:38:27 AM

Acquisition Time (sec)	1.0420	Date	Sep 25 2014	Date Stamp	Sep 25 2014
File Name	G:\20140818-scope\lmsd-re97-scope-20140923-cinnamal_CARBON_01.fid	Frequency (MHz)	75.35	Points Count	32768
Nucleus	¹³ C	Number of Transients	1700	Original Points Count	19624
Pulse Sequence	s2pul	Receiver Gain	30.00	Solvent	DMSO-d6
Spectrum Type	STANDARD	Sweep Width (Hz)	18632.39	Temperature (degree C)	AMBIENT TEMPERATURE
				Spectrum Offset (Hz)	8287.6016



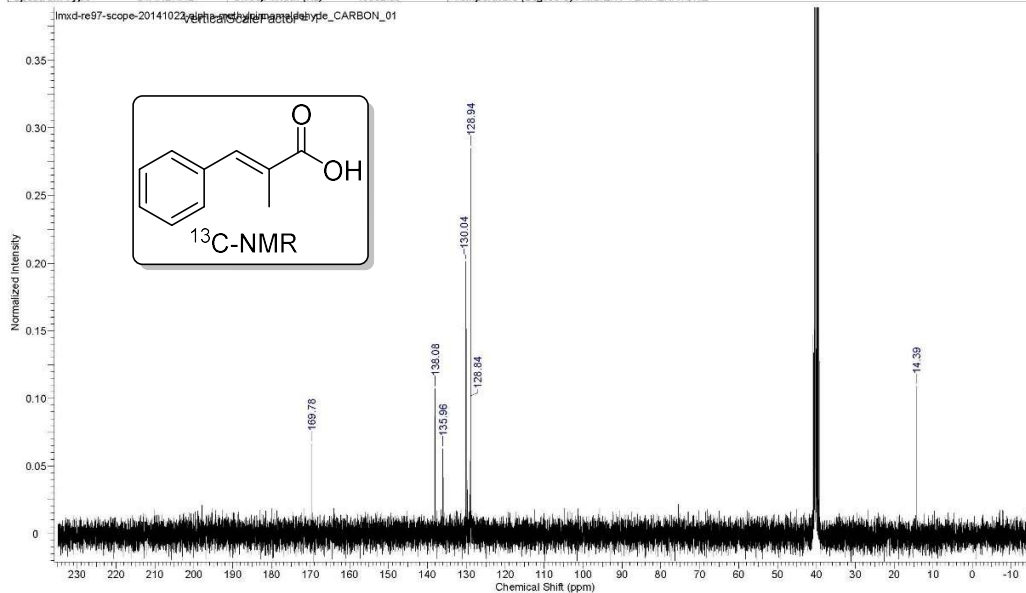
22/10/2014 10:10:12 PM

Acquisition Time (sec)	2.0480	Date	Oct 22 2014	Date Stamp	Oct 22 2014
File Name	G:\20140818-scope\additional\mxd-re97-scope-20141022-alpha-methylcinnamaldehyde_PROTON_01.fid	Frequency (MHz)	299.63		
Nucleus	¹ H	Number of Transients	8	Original Points Count	9818
Pulse Sequence	s2pul	Receiver Gain	39.00	Solvent	DMSO-d6
Spectrum Type	STANDARD	Sweep Width (Hz)	4793.88	Temperature (degree C)	AMBIENT TEMPERATURE
				Spectrum Offset (Hz)	1797.7788



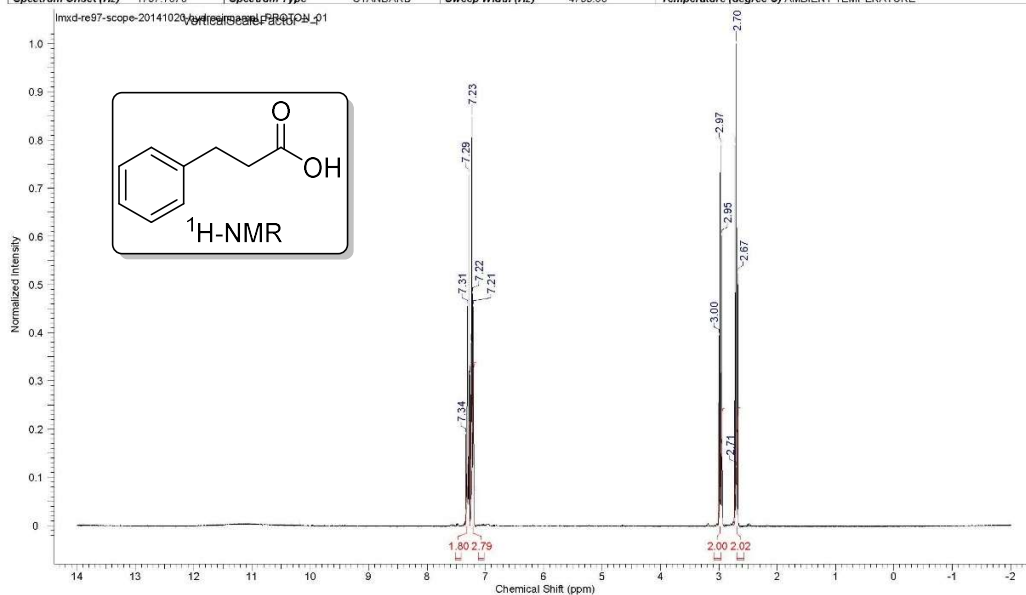
22/10/2014 10:12:21 PM

Acquisition Time (sec)	1.0420	Date	Oct 22 2014	Date Stamp	Oct 22 2014
File Name	G:\20140818-scope\additional\mxd-re97-scope-20141022-alpha-methylcinnamaldehyde_CARBON_01.fid	Frequency (MHz)	75.35		
Nucleus	¹³ C	Number of Transients	1750	Original Points Count	19624
Pulse Sequence	s2pul	Receiver Gain	30.00	Solvent	DMSO-d6
Spectrum Type	STANDARD	Sweep Width (Hz)	18832.39	Temperature (degree C)	AMBIENT TEMPERATURE
				Spectrum Offset (Hz)	8287.6016



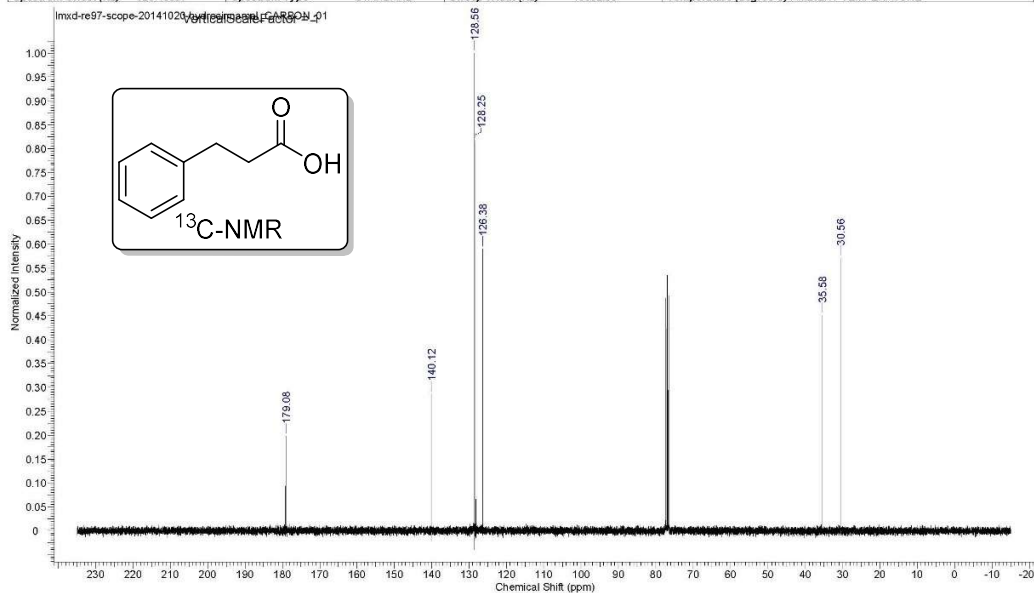
21/10/2014 8:18:29 AM

Acquisition Time (sec)	2.0480	Date	Oct 20 2014	Date Stamp	Oct 20 2014
File Name	G:\20140818-scope\additional\lmsd-re97-scope-20141020-hydrocinnamal_PROTON_01.fid	Frequency (MHz)	299.63		
Nucleus	¹ H	Number of Transients	8	Original Points Count	5818
Pulse Sequence	s2pul	Receiver Gain	30.00	Solvent	CHLOROFORM-d
Spectrum Offset (Hz)	1797.7676	Spectrum Type	STANDARD	Sweep Width (Hz)	4793.86
				Temperature (degree C)	AMBIENT TEMPERATURE



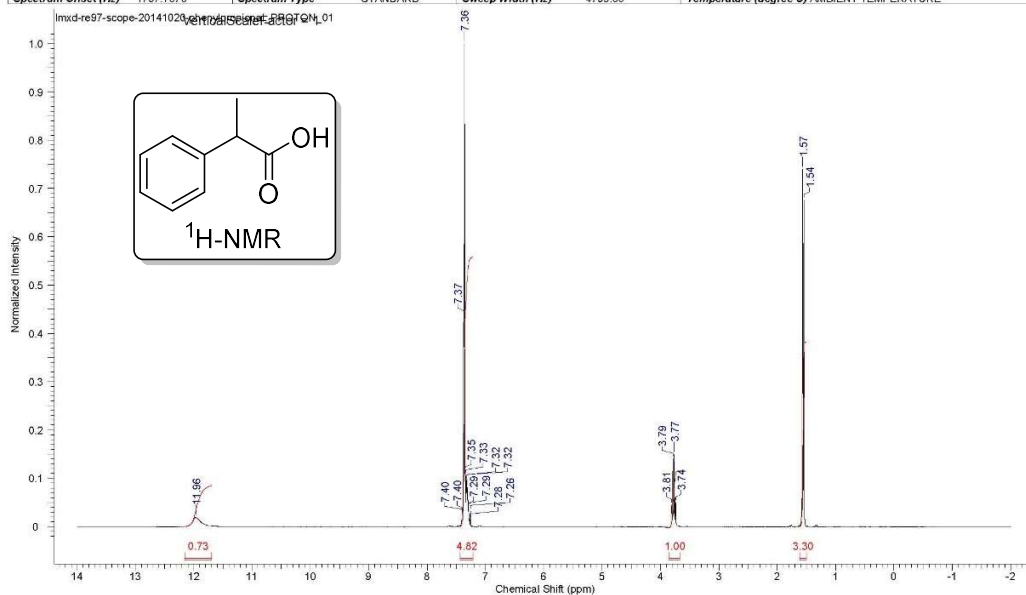
21/10/2014 8:19:04 AM

Acquisition Time (sec)	1.0420	Date	Oct 20 2014	Date Stamp	Oct 20 2014
File Name	G:\20140818-scope\additional\lmsd-re97-scope-20141020-hydrocinnamal_CARBON_01.fid	Frequency (MHz)	75.35		
Nucleus	¹³ C	Number of Transients	1700	Original Points Count	19624
Pulse Sequence	s2pul	Receiver Gain	30.00	Solvent	CHLOROFORM-d
Spectrum Offset (Hz)	6287.5557	Spectrum Type	STANDARD	Sweep Width (Hz)	18832.39
				Temperature (degree C)	AMBIENT TEMPERATURE



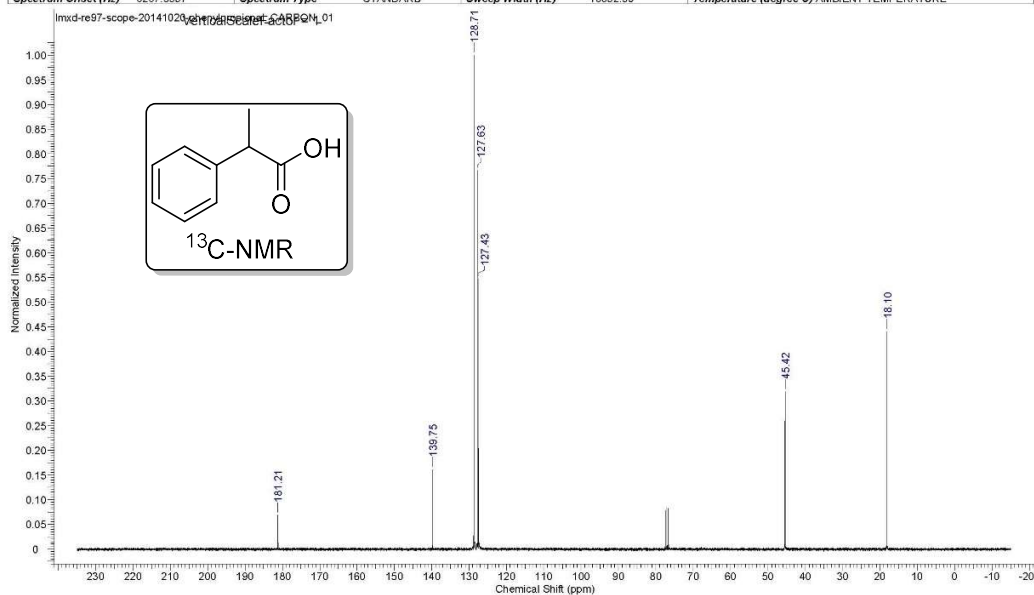
21/10/2014 8:22:27 AM

Acquisition Time (sec)	2.0480	Comment	STANDARD PROTON PARAMETERS	Date	Oct 20 2014
Date Stamp	Oct 20 2014	File Name	G:\20140818-scope\additional\mxd-re97-scope-20141020-phenylpropional_PROTON_01.fid		
Frequency (MHz)	299.63	Nucleus	¹ H	Number of Transients	8
Points Count	16384	Pulse Sequence	s2pul	Receiver Gain	18.00
Spectrum Offset (Hz)	1797.7676	Spectrum Type	STANDARD	Sweep Width (Hz)	4793.86
				Solvent	CHLOROFORM-d
				Temperature (degree C)	AMBIENT TEMPERATURE

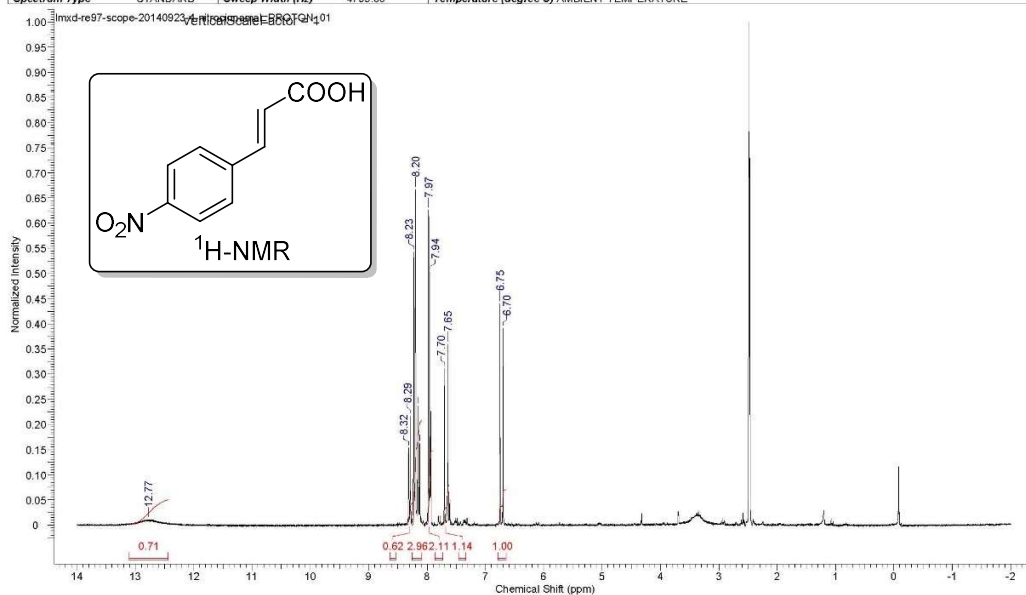


21/10/2014 8:23:25 AM

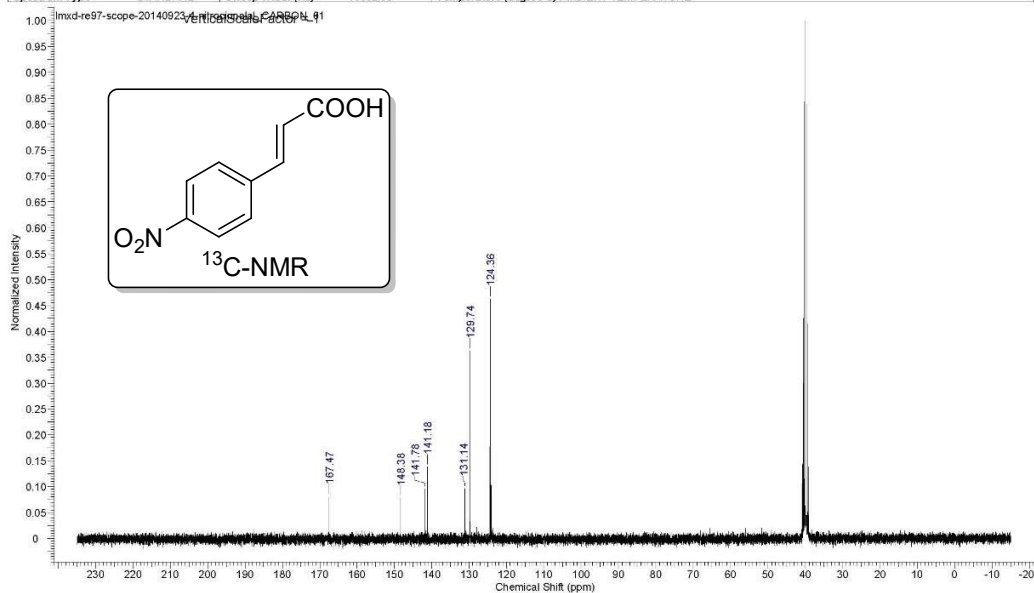
Acquisition Time (sec)	1.0420	Comment	STANDARD PROTON PARAMETERS	Date	Oct 20 2014
Date Stamp	Oct 20 2014	File Name	G:\20140818-scope\additional\mxd-re97-scope-20141020-phenylpropional_CARBON_01.fid		
Frequency (MHz)	75.35	Nucleus	¹³ C	Number of Transients	1700
Points Count	32768	Pulse Sequence	s2pul	Receiver Gain	30.00
Spectrum Offset (Hz)	6287.5557	Spectrum Type	STANDARD	Sweep Width (Hz)	18832.39
				Solvent	CHLOROFORM-d
				Temperature (degree C)	AMBIENT TEMPERATURE



Acquisition Time (sec)	2.0480	Date	Sep 24 2014	Date Stamp	Sep 24 2014
File Name	G:\20140818-scope\mxid-re97-scope-20140923-4-nitrocinamal_PROTON_01.fid\fid	Frequency (MHz)	299.63		
Nucleus	¹ H	Number of Transients	8	Original Points Count	9818
Pulse Sequence	s2pul	Receiver Gain	39.00	Solvent	DMSO-d6
Spectrum Type	STANDARD	Sweep Width (Hz)	4793.86	Temperature (degree C)	AMBIENT TEMPERATURE
				Spectrum Offset (Hz)	1797.7788

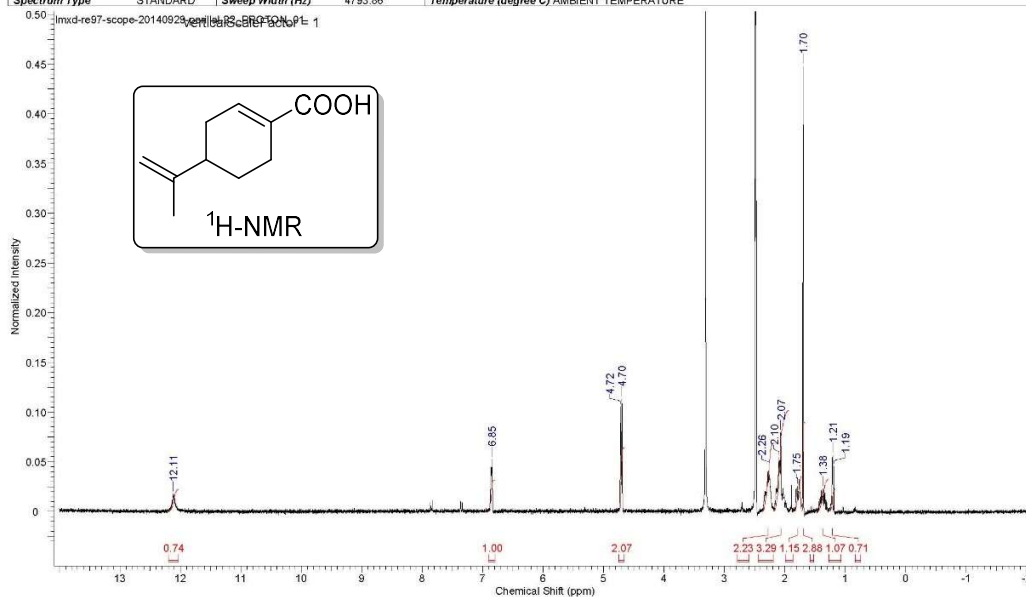


Acquisition Time (sec)	1.0420	Date	Sep 25 2014	Date Stamp	Sep 25 2014
File Name	G:\20140818-scope\mxid-re97-scope-20140923-4-nitrocinamal_CARBO_01.fid\fid	Frequency (MHz)	75.35		
Nucleus	¹³ C	Number of Transients	1700	Original Points Count	19624
Pulse Sequence	s2pul	Receiver Gain	30.00	Solvent	DMSO-d6
Spectrum Type	STANDARD	Sweep Width (Hz)	18832.39	Temperature (degree C)	AMBIENT TEMPERATURE
				Spectrum Offset (Hz)	6287.6016



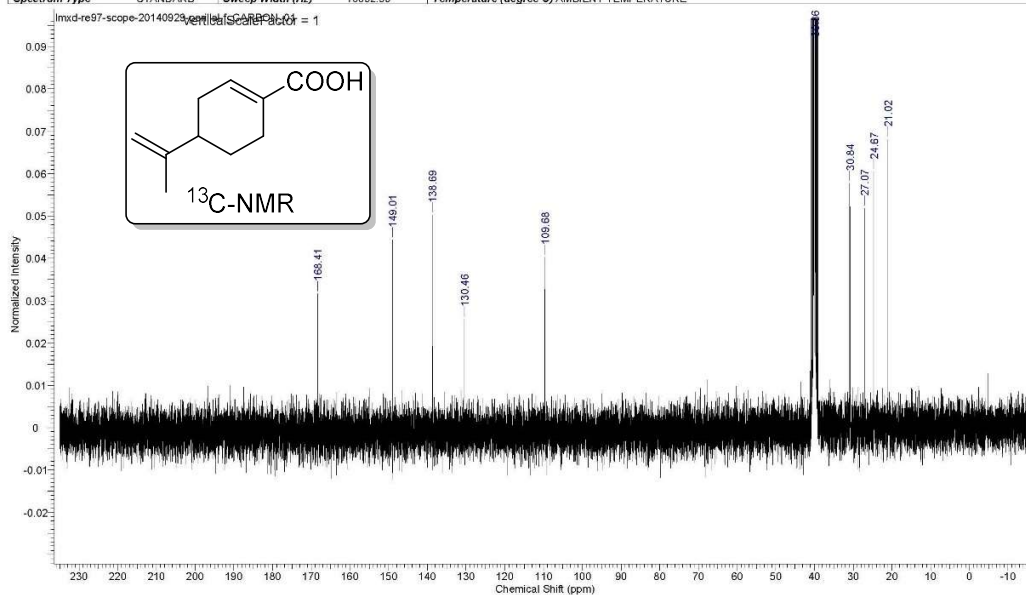
20/10/2014 10:09:27 PM

Acquisition Time (sec)	2.0480	Date	Sep 30 2014	Date Stamp	Sep 30 2014
File Name	G:\20140818-scope\lmd-re97-scope-20140929-perillal-22_PROTON_01.fid	Frequency (MHz)	299.63	Points Count	16384
Nucleus	¹ H	Number of Transients	8	Original Points Count	9818
Pulse Sequence	s2pul	Receiver Gain	39.00	Solvent	DMSO-d6
Spectrum Type	STANDARD	Sweep Width (Hz)	4793.86	Temperature (degree C)	AMBIENT TEMPERATURE
				Spectrum Offset (Hz)	1787.7768



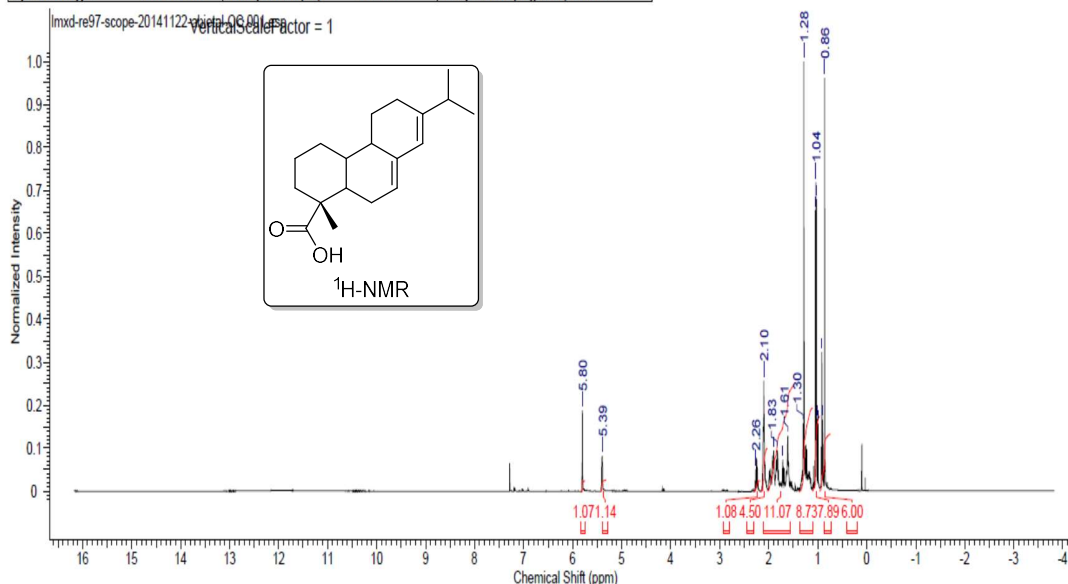
20/10/2014 10:12:34 PM

Acquisition Time (sec)	1.0420	Date	Sep 30 2014	Date Stamp	Sep 30 2014
File Name	G:\20140818-scope\lmd-re97-scope-20140929-perillal-f_CARBON_01.fid	Frequency (MHz)	75.35	Points Count	32768
Nucleus	¹³ C	Number of Transients	6800	Original Points Count	19624
Pulse Sequence	s2pul	Receiver Gain	30.00	Solvent	DMSO-d6
Spectrum Type	STANDARD	Sweep Width (Hz)	18632.39	Temperature (degree C)	AMBIENT TEMPERATURE
				Spectrum Offset (Hz)	8287.6016



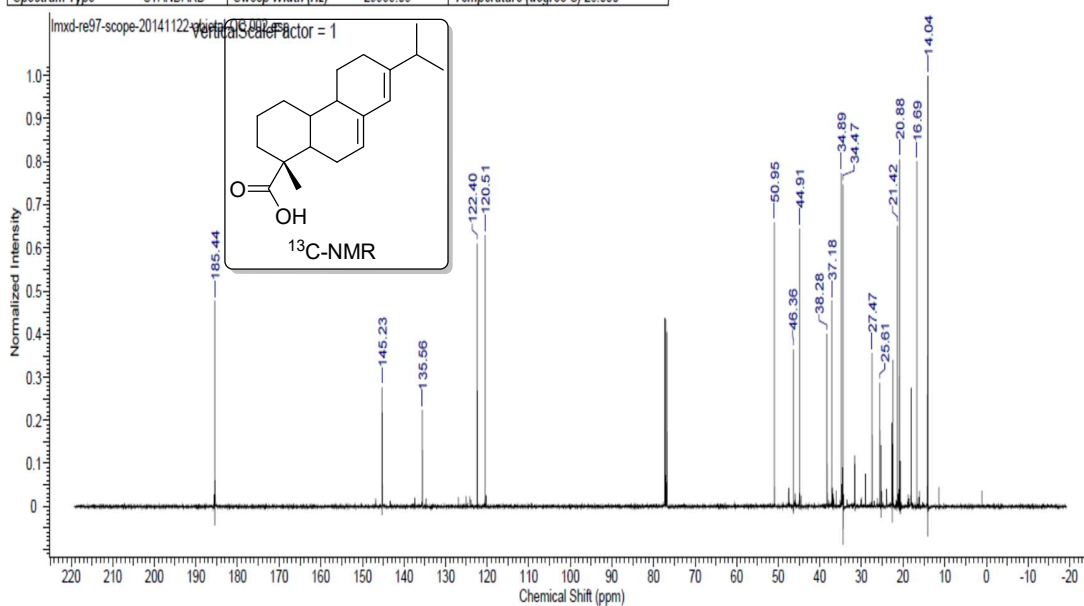
24/12/2014 12:27:32 AM

Acquisition Time (sec)	3.2768	Date	23 Dec 2014 12:29:36	Date Stamp	23 Dec 2014 12:29:36
File Name	C:\Users\IMLW\Desktop\lmd-re97-scope-20141122-abietal-CC1\fid	Frequency (MHz)	500.30	Original Points Count	32768
Nucleus	¹ H	Number of Transients	16	Origin	AVIII500HD
Owner	mcgillnmr	Points Count	32768	Pulse Sequence	zg30
SW(cyclical) (Hz)	10000.00	Solvent	CHLOROFORM-d	Receiver Gain	18.18
Spectrum Type	STANDARD	Sweep Width (Hz)	9999.70	Temperature (degree C)	26.013
				Spectrum Offset (Hz)	3089.5574



24/12/2014 12:25:56 AM

Acquisition Time (sec)	1.0923	Date	24 Dec 2014 00:17:52	Date Stamp	24 Dec 2014 00:17:52
File Name	C:\Users\IMLW\Desktop\lmd-re97-scope-20141122-abietal-CC2\fid	Frequency (MHz)	125.81	Original Points Count	32768
Nucleus	¹³ C	Number of Transients	3400	Origin	AVIII500HD
Owner	mcgillnmr	Points Count	32768	Pulse Sequence	zgpg30
SW(cyclical) (Hz)	30000.00	Solvent	CHLOROFORM-d	Receiver Gain	192.72
Spectrum Type	STANDARD	Sweep Width (Hz)	29999.08	Temperature (degree C)	26.000
				Spectrum Offset (Hz)	12578.9238

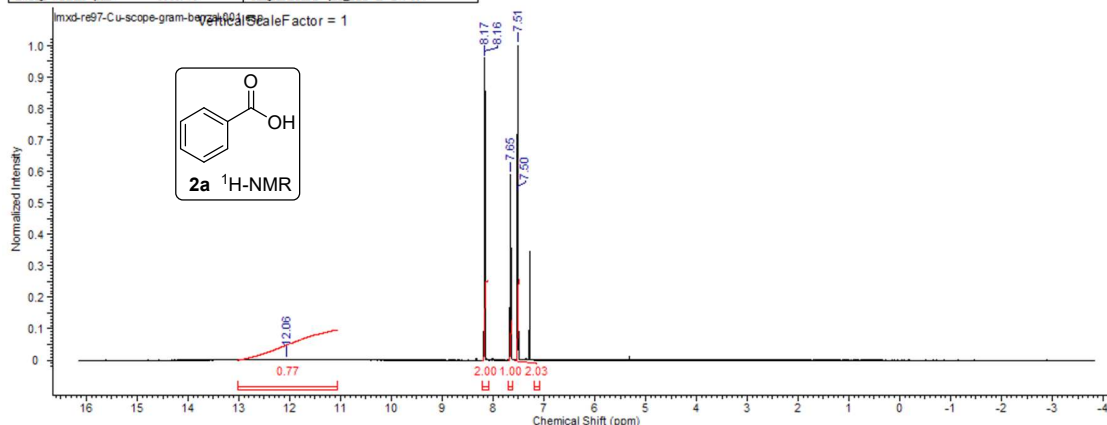


NMR spectra of products described in chapter 5

This report was created by ACD/NMR Processor Academic Edition. For more information go to www.acdlabs.com/nmrproc/

2015/10/28 21:19:11

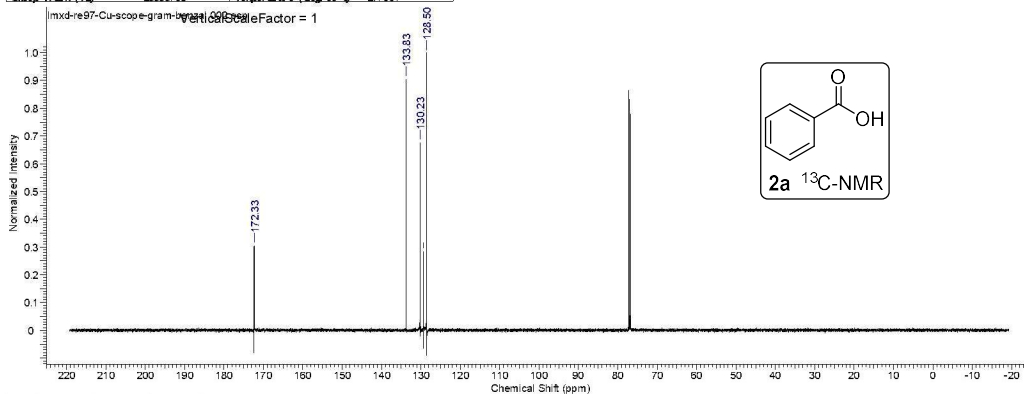
Acquisition Time (sec)	3.2768	Date	16 Sep 2015 18:15:28	Date Stamp	16 Sep 2015 18:15:28
File Name	C:\Users\MLMW\Desktop\新建文件夹\lmd-re97-Cu-scope-gram-benzal\1.fid	Origin	AVII500HD	Frequency (MHz)	500.130
Nucleus	¹ H	Number of Transients	16	Original Points Count	32768
Owner	mgjllnm	Pulse Count	32768	Pulse Sequence	zgpg30
SW (cyclical) (Hz)	10000.00	Solvent	CHLOROFORM-d	Receiver Gain	106.56
Sweep Width (Hz)	9999.70	Temperature (degree C)	27.007	Spectrum Offset (Hz)	3089.5574
				Spectrum Type	STANDARD



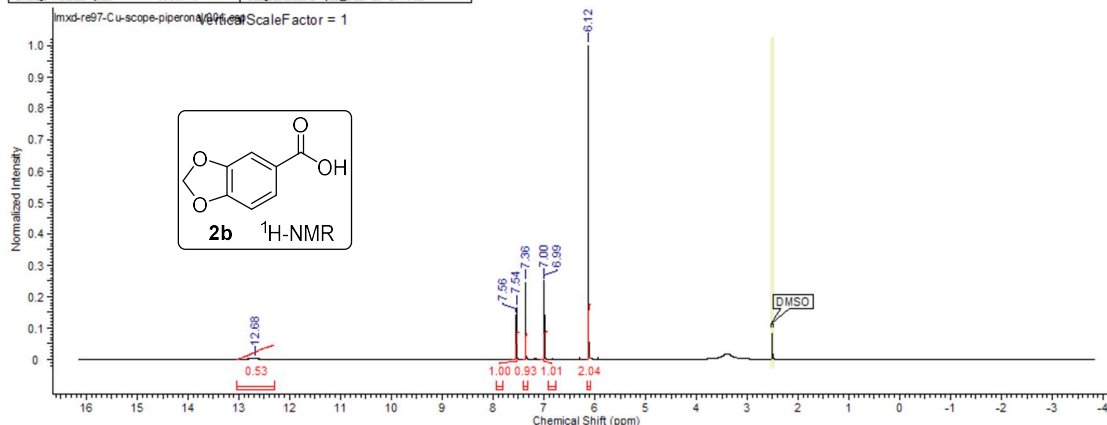
This report was created by ACD/NMR Processor Academic Edition. For more information go to www.acdlabs.com/nmrproc/

2015/9/16 22:54:50

Acquisition Time (sec)	1.0823	Date	16 Sep 2015 18:43:12	Date Stamp	16 Sep 2015 18:43:12
File Name	C:\Users\MLMW\Desktop\新建文件夹\lmd-re97-Cu-scope-gram-benzal\2.fid	Origin	AVII500HD	Frequency (MHz)	125.81
Nucleus	¹³ C	Number of Transients	512	Original Points Count	32768
Owner	mgjllnm	Pulse Count	32768	Pulse Sequence	zgpg30
SW (cyclical) (Hz)	30000.00	Solvent	CHLOROFORM-d	Receiver Gain	152.72
Sweep Width (Hz)	29999.08	Temperature (degree C)	27.001	Spectrum Offset (Hz)	12578.9238
				Spectrum Type	STANDARD



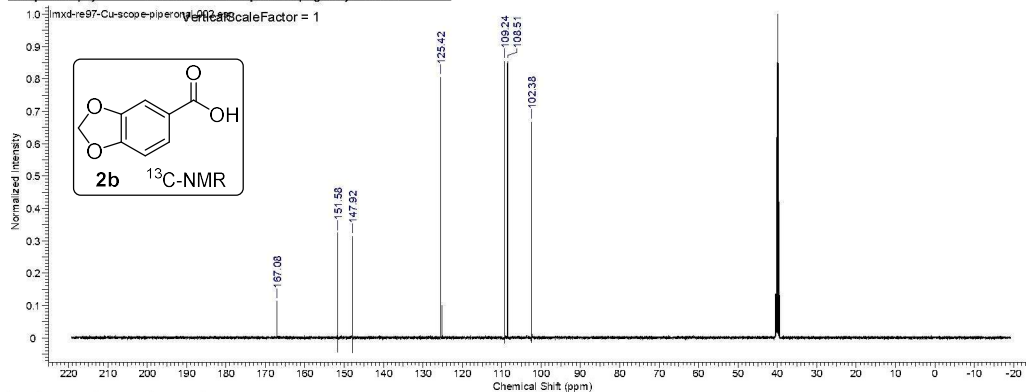
Acquisition Time (sec)	3.2768	Date	16 Sep 2015 18:47:28	Date Stamp	16 Sep 2015 18:47:28
File Name	C:\Users\MMLW\Desktop\新建文件夹\lmd-re97-Cu-scope-piperonal\1.fid	Frequency (MHz)	500.30	Original Points Count	32768
Nucleus	¹ H	Number of Transients	16	Origin	AVI1500HD
Owner	mcs11nmr	Points Count	32768	Pulse Sequence	zg30
SW (cyclical) (Hz)	10000.00	Solvent	DMSO-d6	Spectrum Offset (Hz)	3088.5574
Sweep Width (Hz)	9999.70	Temperature (degree C)	27.002	Spectrum Type	STANDARD



No.	(ppm)	Annotation	Layer No.	Created By	Created At	Modified By	Modified At
1	[2.49, 2.52]	DMSO	1	MMLWV	2015/10/28 21:20:07		

No.	(ppm)	Value	Absolute Value	Non-Negative Value	No.	(ppm)	Height
1	7.40	6.15203853536	2.01375355e+10	2.03853536	1	6.12	3061.0
2	7.185	7.06101398301	1.00165632e+10	1.01398301	2	6.99	3495.3
3	7.125	7.40093434620	9.22987622e+9	0.93434620	3	7.00	3503.5
4	7.814	7.60100033486	9.88174131e+9	1.00033486	4	7.36	3683.6
5	7.890	7.130052586061	5.19467878e+9	0.52586061	5	7.54	3772.1
					6	7.56	3781.8
					7	12.68	6346.2

Acquisition Time (sec)	1.0923	Date	16 Sep 2015 19:17:20	Date Stamp	16 Sep 2015 19:17:20
File Name	C:\Users\MMLW\Desktop\新建文件夹\lmd-re97-Cu-scope-piperonal\12.fid	Frequency (MHz)	125.81	Original Points Count	32768
Nucleus	¹³ C	Number of Transients	512	Origin	AVI1500-D
Owner	mcs11nmr	Points Count	32768	Pulse Sequence	zgpg30
SW (cyclical) (Hz)	30000.00	Solvent	DMSO-d6	Spectrum Offset (Hz)	12578.9238
Sweep Width (Hz)	28999.08	Temperature (degree C)	26.995	Spectrum Type	STANDARD

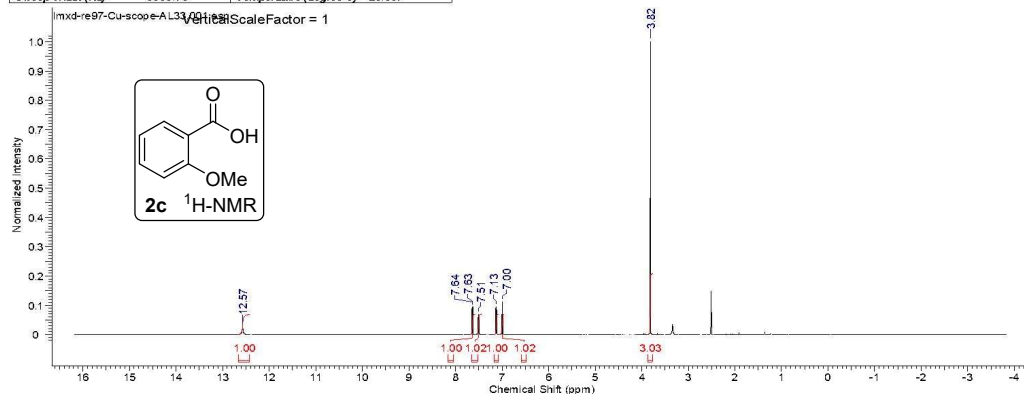


No.	(ppm)	(Hz)	Height
1	102.38	12880.6	0.8669
2	108.51	13651.5	0.8543
3	109.24	13743.9	0.8549
4	125.42	15779.1	0.8053
5	147.92	18610.0	0.3140
6	151.58	19070.5	0.3240
7	167.08	21021.5	0.1135

This report was created by ACD/NMR Processor Academic Edition. For more information go to www.acdlabs.com/nmrproc/

9/15/2015 10:50:47 AM

Acquisition Time (sec)	3.2768	Date	12 Jul 2015 20:32:00	Date Stamp	12 Jul 2015 20:32:00
File Name	C:\Users\Admin\CloudDrive\Revised_Fehling_Scope\imxd-re97-Cu-scope-AL3311f1d	Frequency (MHz)	500.30	Original Points Count	32768
Nucleus	¹ H	Number of Transients	18	Origin	AVIII500HD
Owner	mcgillnmr	Points Count	32768	Pulse Sequence	zgpg30
SW (cyclical) (Hz)	10000.00	Solvent	DMSO-d6	Spectrum Offset (Hz)	3089.5574
Sweep Width (Hz)	9999.70	Temperature (degree C)	26.007	Receiver Gain	106.56
				Spectrum Type	STANDARD

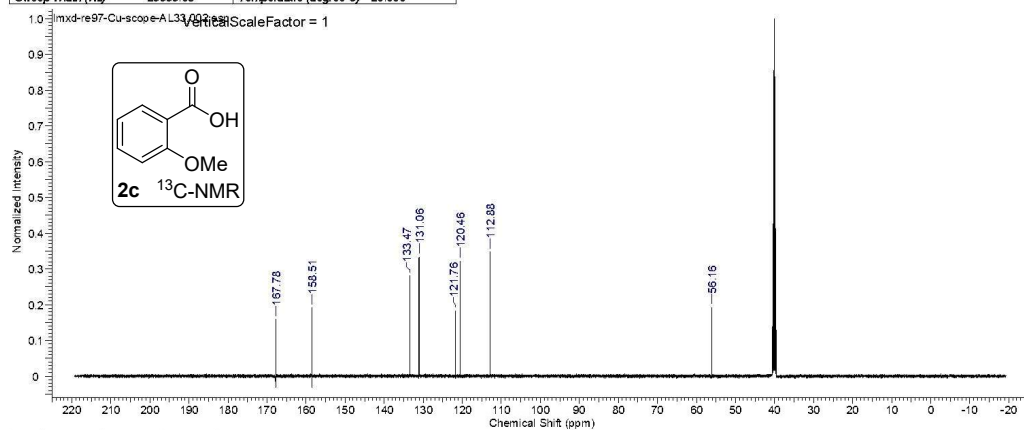


No.	(ppm)	Value	Absolute Value	Non-Negative Value	No.	(ppm)	(Hz)	Height
1	13.7696	3.875302564359	1.67259146e+10	3.02564359	1	3.82	1909.3	1.0000
2	7.6432	7.041015896653	5.61482291e+9	1.01569653	2	7.00	3500.5	0.1115
3	7.0787	7.18100280114	5.64243120e+9	1.00260115	3	7.13	3567.0	0.0941
4	7.4380	7.55102180207	5.64857498e+9	1.02180207	4	7.51	3755.6	0.0683
5	7.6745	7.63099070472	5.52941946e+9	0.99970472	5	7.63	3816.3	0.0952
6	7.2402	12.609983507	5.52713984e+9	0.9983507	6	7.64	3822.1	0.0915
7	12.57				7	12.57	6287.6	0.0248

This report was created by ACD/NMR Processor Academic Edition. For more information go to www.acdlabs.com/nmrproc/

9/15/2015 10:51:58 AM

Acquisition Time (sec)	1.0923	Date	12 Jul 2015 20:59:44	Date Stamp	12 Jul 2015 20:59:44
File Name	C:\Users\Admin\CloudDrive\Revised_Fehling_Scope\imxd-re97-Cu-scope-AL3312f1d	Frequency (MHz)	125.81	Original Points Count	32768
Nucleus	¹³ C	Number of Transients	512	Origin	AVIII500HD
Owner	mcgillnmr	Points Count	32768	Pulse Sequence	zgpg30
SW (cyclical) (Hz)	30000.00	Solvent	DMSO-d6	Spectrum Offset (Hz)	12578.9238
Sweep Width (Hz)	29999.08	Temperature (degree C)	26.000	Receiver Gain	192.72
				Spectrum Type	STANDARD

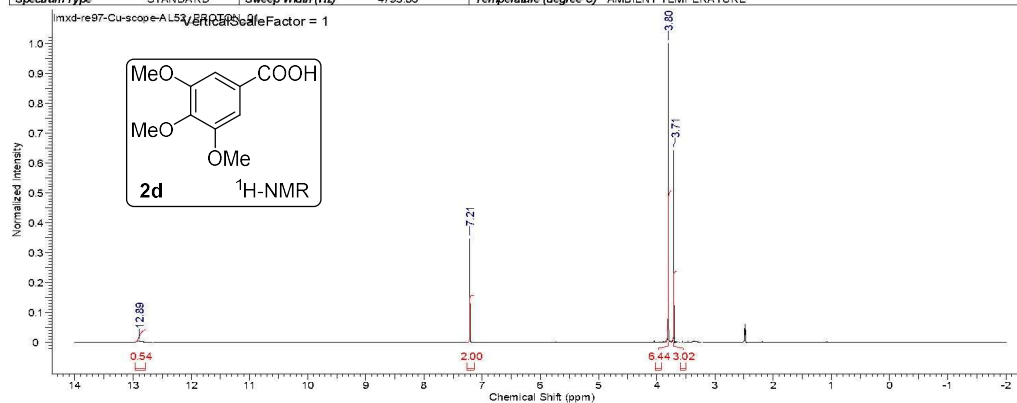


No.	(ppm)	(Hz)	Height
1	56.16	7065.2	0.1919
2	112.88	14201.7	0.3479
3	120.46	15155.7	0.3220
4	121.76	15319.6	0.1829
5	131.06	16489.6	0.3335
6	133.47	16792.6	0.2804
7	158.51	19942.1	0.1910
8	167.78	21108.3	0.1590

This report was created by ACD/NMR Processor Academic Edition. For more information go to www.acdlabs.com/nmrproof/

9/16/2015 3:36:42 PM

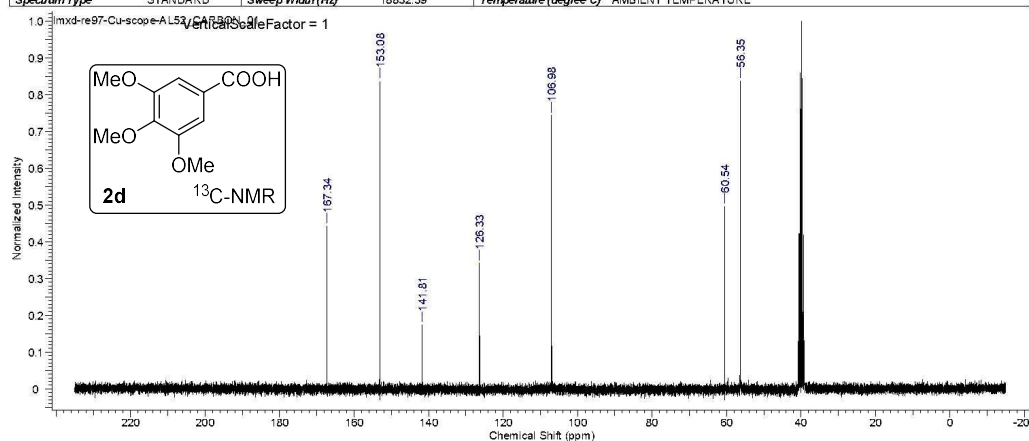
Acquisition Time (sec)	2.0480	Date	Jul 13 2015	Date Stamp	Jul 13 2015
File Name	C:\Users\Admin\CloudDrive\Revised_Fehling_Scope\lmsd-re97-Cu-scope-A152_PROTON_01.fid	Frequency (MHz)	299.63	Points Count	16384
Nucleus	¹ H	Number of Transients	8	Original Points Count	9818
Pulse Sequence	s2pul	Receiver Gain	30.00	Solvent	DMSO-d6
Spectrum Type	STANDARD	Sweep Width (Hz)	4793.86	Temperature (degree C)	AMBIENT TEMPERATURE



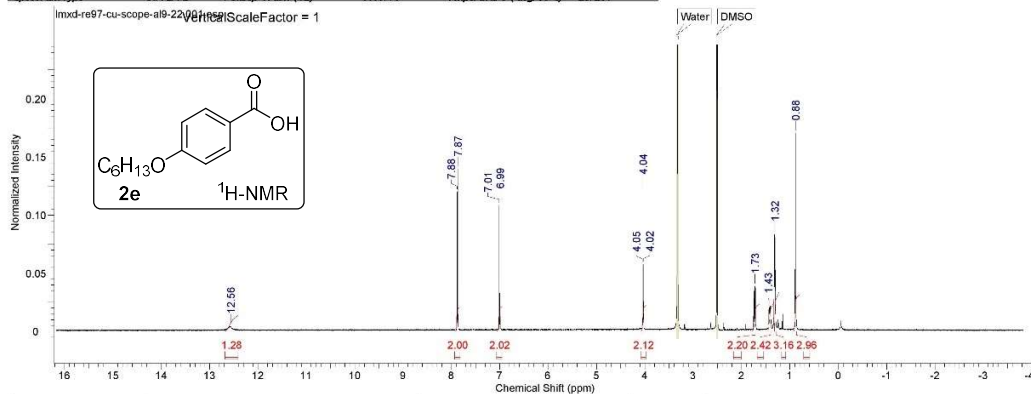
This report was created by ACD/NMR Processor Academic Edition. For more information go to www.acdlabs.com/nmrproof/

9/16/2015 3:38:30 PM

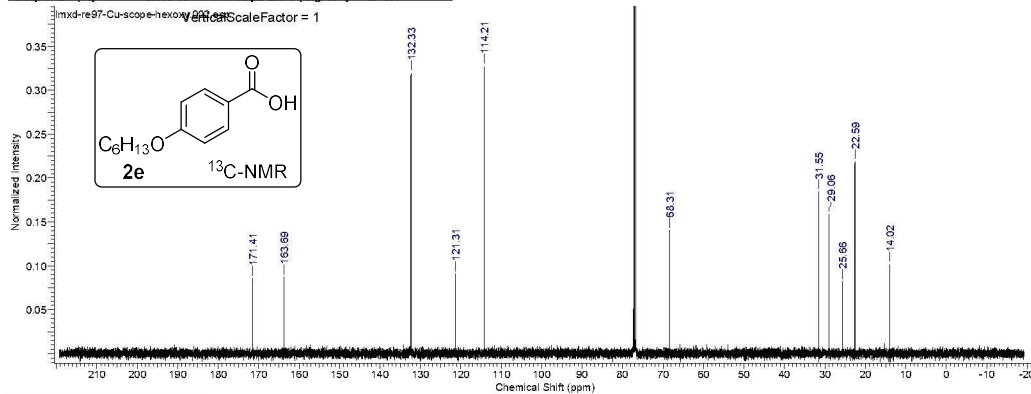
Acquisition Time (sec)	1.0420	Date	Jul 13 2015	Date Stamp	Jul 13 2015
File Name	C:\Users\Admin\CloudDrive\Revised_Fehling_Scope\lmsd-re97-Cu-scope-A152_CARBON_01.fid	Frequency (MHz)	75.35	Points Count	32768
Nucleus	¹³ C	Number of Transients	1700	Original Points Count	19624
Pulse Sequence	s2pul	Receiver Gain	30.00	Solvent	DMSO-d6
Spectrum Type	STANDARD	Sweep Width (Hz)	18832.39	Temperature (degree C)	AMBIENT TEMPERATURE



Acquisition Time (sec)	3.2768	Comment	Li_1d_FROTON DMSO/home.mingxi.n.1	Date	10 Apr 2016 19:23:44
Date Stamp	10 Apr 2016 19:23:44	File Name	C:\Users\MMLWW\Desktop\li1d-froton-cu-scope-al 9-22-11.fid	Frequency (MHz)	500.30
Original Points Count	32768	Nucleus	¹ H	Number of Transients	16
Receiver Gain	192.72	Order	mgill.nm	Points Count	32768
Spectrum Type	STANDARD	SF (cyclical) (Hz)	10000.00	Solvent	DMSO-d6
		Sweep Width (Hz)	9999.70	Temperature (degree C)	25.204
				Spectrum Offset (Hz)	3089.5574



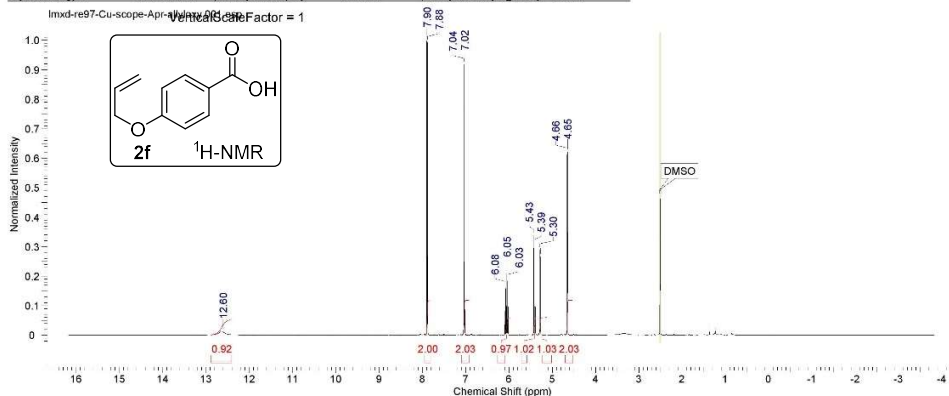
Acquisition Time (sec)	1.0923	Date	17 Sep 2015 03:21:36	Date Stamp	17 Sep 2015 03:21:36
File Name	C:\Users\MMLWW\Desktop\li1d-froton-cu-scope-al 9-22-11.fid	File Name	C:\Users\MMLWW\Desktop\li1d-froton-cu-scope-al 9-22-11.fid	Frequency (MHz)	125.81
Nucleus	¹³ C	Number of Transients	512	Origin	AM11500-D
Order	mgill.nm	Points Count	32768	Pulse Sequence	zgpg30
SF (cyclical) (Hz)	30000.00	Solvent	CDCl3	Receiver Gain	192.72
Sweep Width (Hz)	28999.08	Temperature (degree C)	27.000	Spectrum Offset (Hz)	12579.9208
				Spectrum Type	STANDARD



This report was created by ACD/NMR Processor Academic Edition. For more information go to www.acdlabs.com/nmrproc/

4/10/2016 10:27:30 PM

Acquisition Time (sec)	3.2768	Comment	Li 1d_PROTON DMSO /home mingxin 2	Date	08 Apr 2016 11:10:56
Date Stamp	08 Apr 2016 11:10:56	Nucleus	1H	File Name	C:\Users\Admin\Desktop\lmd-re97-Cu-scope-Apr-allyloxy\1\lmd
Frequency (MHz)	500.30	Owner	mgjllm	Number of Transients	16
Original Points Count	32768	SW (cycles)	10000.00	Points Count	32768
Receiver Gain	105.56	Sweep Width (Hz)	9999.70	Solvent	DMSO-d6
Spectrum Type	STANDARD			Temperature (degree C)	25.198
				Pulse Sequence	zg30
				Spectrum Offset (Hz)	3089.5574



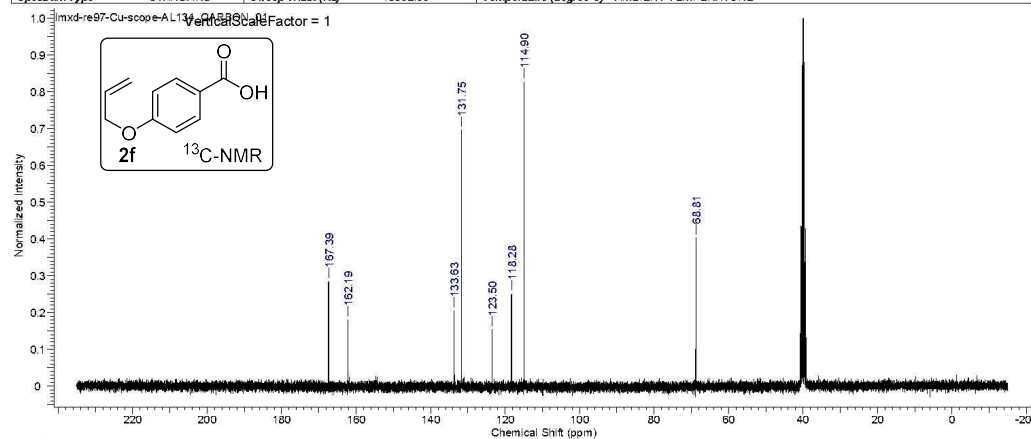
No.	(ppm)	Annotation	Layer No.	Created By	Created At	Modified By	Modified At
1	[2.49 .. 2.52]	DMSO	1	Admin	Sun 4/10/2016 10:26:59 PM		

No.	(ppm)	Value	Absolute Value	Non-Negative Value
1	4.5203 .. 4.702	0.03293276	9.06142003e+9	2.03293276
2	5.1346 .. 5.351	0.03081855	4.59379046e+9	1.03061855
3	5.3564 .. 5.471	0.02172697	4.55415808e+9	1.02172697
4	5.9706 .. 6.140	0.0249734	4.33472614e+9	0.97249734
5	6.9261 .. 7.082	0.03027868	9.04958976e+9	2.03027868
6	7.8134 .. 7.941	0.99954307	8.91259187e+9	1.99954307
7	12.4031 .. 12.80	0.91778070	4.09083699e+9	0.91778070

This report was created by ACD/NMR Processor Academic Edition. For more information go to www.acdlabs.com/nmrproc/

9/16/2015 4:22:51 PM

Acquisition Time (sec)	1.0420	Date	Jul 14 2015	Date Stamp	Jul 14 2015		
File Name	C:\Users\Admin\CloudDrive\Revised_Fehling_Scope\lmd-re97-Cu-scope-AL134_CARBON_01.fid.tifd				Frequency (MHz)	75.35	
Nucleus	¹³ C	Number of Transients	1700	Original Points Count	19524	Points Count	32768
Pulse Sequence	s2pul	Receiver Gain	30.00	Solvent	DMSO-d6	Spectrum Offset (Hz)	8287.6016
Spectrum Type	STANDARD	Sweep Width (Hz)	18832.39	Temperature (degree C)	AMBIENT TEMPERATURE		

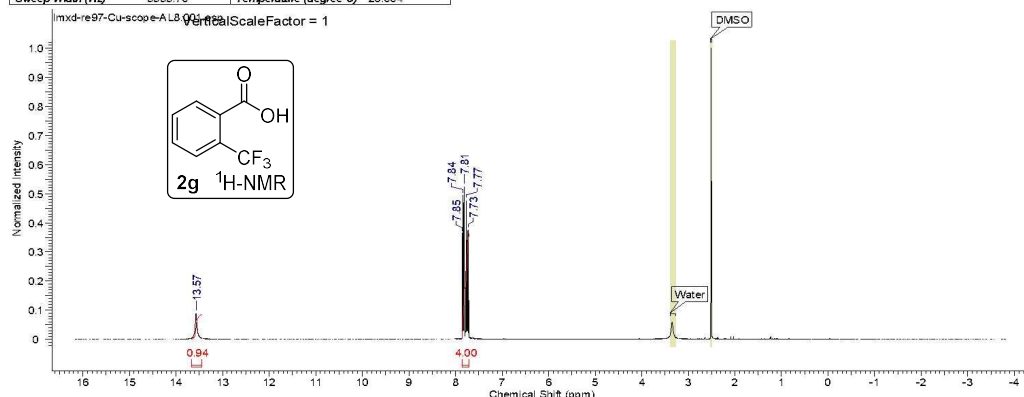


No.	(ppm)	(Hz)	Height
1	68.81	5184.9	0.4031
2	114.90	8657.4	0.8265
3	118.28	8912.1	0.2504
4	123.50	9305.7	0.1535
5	131.75	9927.6	0.6965
6	133.63	10069.0	0.2049
7	162.19	12220.8	0.1804
8	167.39	12612.8	0.2847

This report was created by ACD/NMR Processor Academic Edition. For more information go to www.acdlabs.com/nmrproc/

9/15/2015 10:20:34 AM

Acquisition Time (sec)	3.2768	Date	12 Jul 2015 19:25:52	Date Stamp	12 Jul 2015 19:25:52
File Name	C:\Users\Admin\CloudDrive\Revised_Fehling_Scope\mxid-re97-Cu-scope-AL8\1f1d	Frequency (MHz)	500.30	Original Points Count	32768
Nucleus	¹ H	Number of Transients	16	Origin	AVIII500H-D
Owner	mcgillnmr	Points Count	32768	Pulse Sequence	zg30
SW (cycles) (Hz)	10000.00	Solvent	DMSO-d6	Spectrum Offset (Hz)	3089.5574
Sweep Width (Hz)	9999.70	Temperature (degree C)	26.004	Spectrum Type	STANDARD

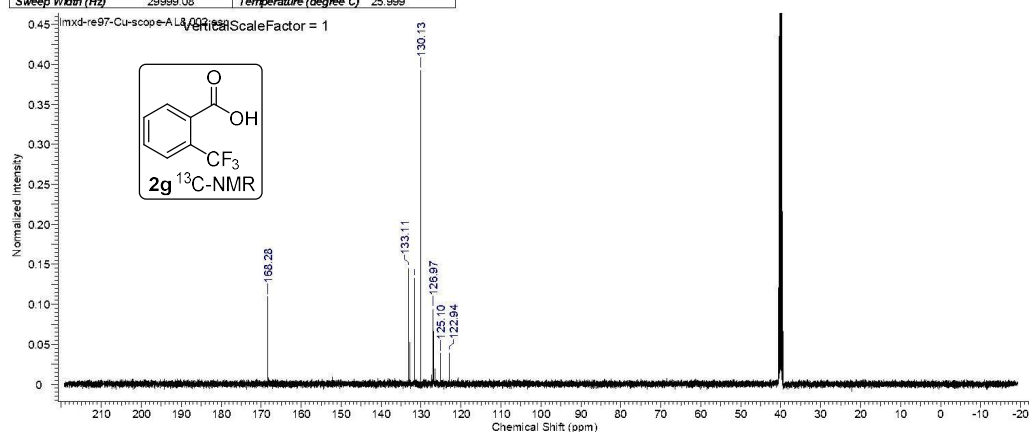


No.	(ppm)	Value	Absolute Value	Non-Negative Value	No.	(ppm)	(Hz)	Height
1	7.043	7.854000000	2.22094950e+10	4.00000000	1	7.73	3867.0	0.3747
2	7.439	13.609394554	5.21620787e+9	0.93945545	2	7.77	3887.1	0.4754
					3	7.81	3906.1	0.5240
					4	7.84	3920.1	0.4946
					5	7.85	3927.7	0.3634
					6	13.57	6788.4	0.0887

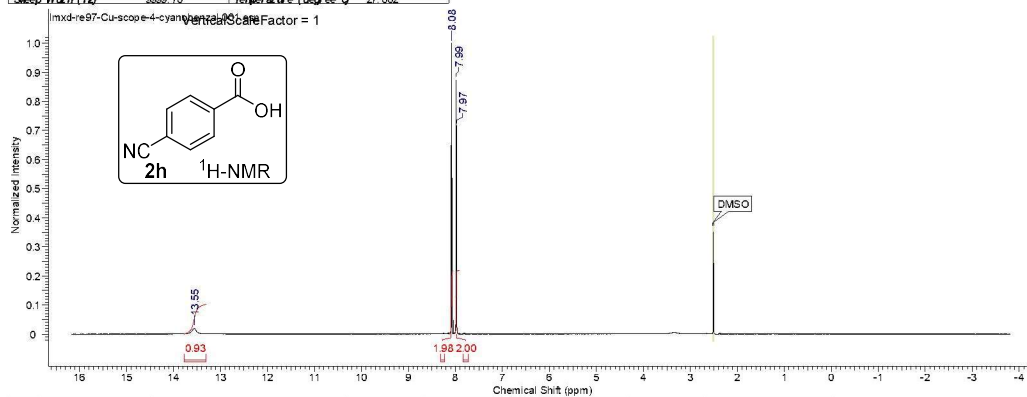
This report was created by ACD/NMR Processor Academic Edition. For more information go to www.acdlabs.com/nmrproc/

9/15/2015 10:23:39 AM

Acquisition Time (sec)	1.0923	Date	12 Jul 2015 19:53:36	Date Stamp	12 Jul 2015 19:53:36
File Name	C:\Users\Admin\CloudDrive\Revised_Fehling_Scope\mxid-re97-Cu-scope-AL8\2f1d	Frequency (MHz)	125.81	Original Points Count	32768
Nucleus	¹³ C	Number of Transients	512	Origin	AVIII500H-D
Owner	mcgillnmr	Points Count	32768	Pulse Sequence	zgpg30
SW (cycles) (Hz)	30000.00	Solvent	DMSO-d6	Spectrum Offset (Hz)	12578.9238
Sweep Width (Hz)	29999.08	Temperature (degree C)	25.999	Spectrum Type	STANDARD

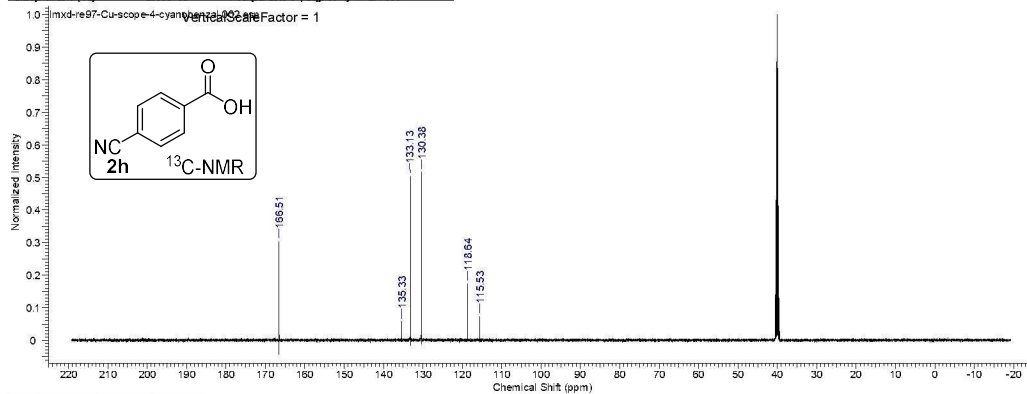


Acquisition Time (sec)	3.2768	Date	17 Sep 2015 13:55:12	Date Stamp	17 Sep 2015 13:55:12
File Name	C:\User\MLWW\Qoud\1\vel.Rev.sed_Feh\1\ng_Scope\1\mx-d-re697-Cu-scope-4-cyanobenzal\1\1.fid	Frequency (MHz)	500.30	Original Points Count	32768
Nucleus	¹ H	Number of Transients	16	Origin	AVI1500-D
Owner	mgj11nm	Points Count	32768	Pulse Sequence	zg30
Sweep Width (Hz)	10000.00	Solvent	DMSO-d6	Receiver Gain	106.56
Sweep Width (Hz)	9669.70	Temperature (degree C)	27.002	Spectrum Offset (Hz)	3089.5574
				Spectrum Type	STANDARD



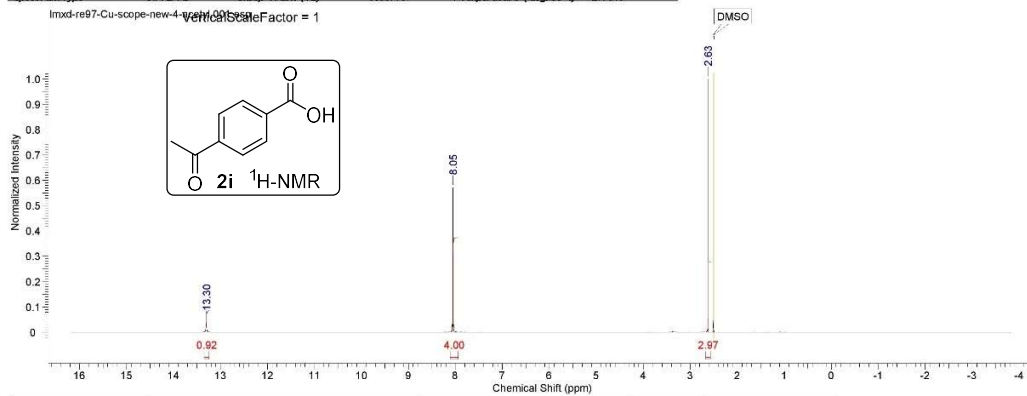
No.	(ppm)	Value	Absolute Value	Non-Negative Value	No.	(ppm)	(Hz)	Height
1	17.9205	8.03200000000	1.50756393e+10	2.00000000	1	7.97	3987.5	0.7159
2	18.9556	8.13198039293	1.49278444e+10	1.98039293	2	7.99	3996.4	0.8736
3	13.135	13.7093102527	7.01790054e+9	0.93102527	3	8.08	4040.0	1.0000
4					4	13.55	6780.2	0.0193

Acquisition Time (sec)	1.0923	Date	17 Sep 2015 14:22:56	Date Stamp	17 Sep 2015 14:22:56
File Name	C:\User\MLWW\Qoud\1\vel.Rev.sed_Feh\1\ng_Scope\1\mx-d-re697-Cu-scope-4-cyanobenzal\1\1.fid	Frequency (MHz)	125.81	Original Points Count	32768
Nucleus	¹³ C	Number of Transients	512	Origin	AVI1500-D
Owner	mgj11nm	Points Count	32768	Pulse Sequence	zgpg30
Sweep Width (Hz)	30000.00	Solvent	DMSO-d6	Receiver Gain	192.72
Sweep Width (Hz)	29999.08	Temperature (degree C)	27.003	Spectrum Offset (Hz)	12578.9238
				Spectrum Type	STANDARD

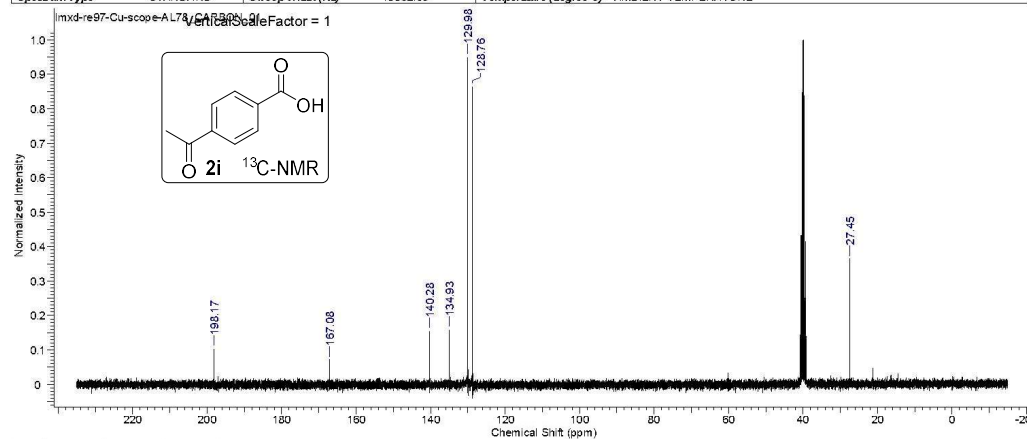


No.	(ppm)	(Hz)	Height
1	115.53	14534.9	0.0735
2	118.64	14926.8	0.1733
3	130.36	16403.5	0.5160
4	133.38	16749.6	0.5094
5	135.33	17025.1	0.0586
6	166.51	20949.1	0.3028

Acquisition Time (sec)	3.2788	Comment	Li_1d_FPCION.DMSO / home m1.npxl.n.56	Date	11 Mar 2016 13:28:20
Date Stamp	11 Mar 2016 13:28:20	File Name	C:\Users\MLWW\Desktop\NMR\results\1\1\mxid-re97-Cu-scope-new-4-acetyl\1\1.fid	Frequency (MHz)	500.30
Original Points Count	32768	Nucleus	1H	Number of Transients	16
Receiver Gain	106.96	Operator	mgl111nm	Points Count	32768
Spectrum Type	STANDARD	Shift (ppm) (Hz)	10000.00	Solvent	DMSO-d6
		Sweep Width (Hz)	9999.70	Temperature (degree C)	27.016
				Spectrum Offset (Hz)	3089.5574

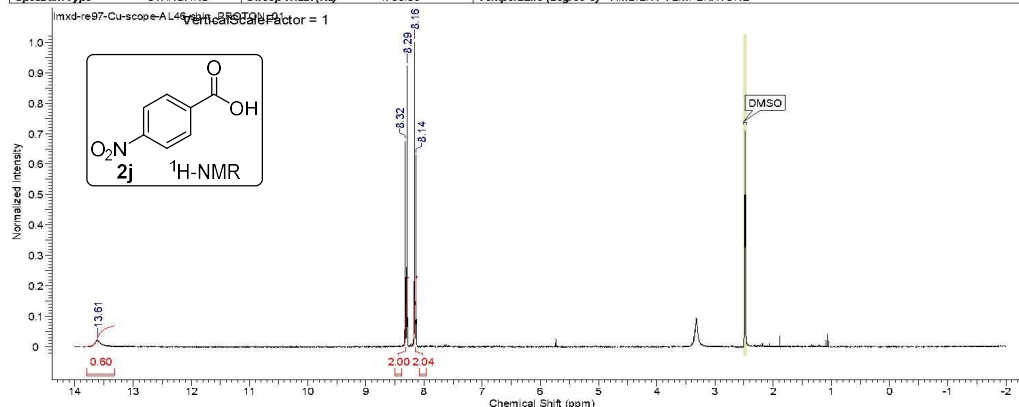


Acquisition Time (sec)	1.0420	Date	Jul 13 2015	Date Stamp	Jul 13 2015		
File Name	C:\Users\Administrator\CloudDrive\Revised_Fehling_Scope\mxid-re97-Cu-scope-AL78-CARBON_01.fid				Frequency (MHz)	75.35	
Nucleus	13C	Number of Transients	1700	Original Points Count	19524	Points Count	32768
Pulse Sequence	s2pul	Receiver Gain	30.00	Solvent	DMSO-d6	Spectrum Offset (Hz)	8287.6016
Spectrum Type	STANDARD	Sweep Width (Hz)	18832.39	Temperature (degree C)	AMBIENT TEMPERATURE		



9/16/2015 3:32:57 PM

Acquisition Time (sec)	2.0480	Date	Jul 13 2015	Date Stamp	Jul 13 2015		
File Name	C:\Users\Admin\CloudDrive\Revised_Fehling_Scope\mxid-re97-Cu-scope-AL48-shin_PROTON_01.fid.tif				Frequency (MHz)	299.63	
Nucleus	¹ H	Number of Transients	8	Original Points Count	9818	Points Count	16384
Pulse Sequence	s2pul	Receiver Gain	35.00	Solvent	DMSO-d6	Spectrum Offset (Hz)	1797.7788
Spectrum Type	STANDARD	Sweep Width (Hz)	4793.86	Temperature (degree C)	AMBIENT TEMPERATURE		

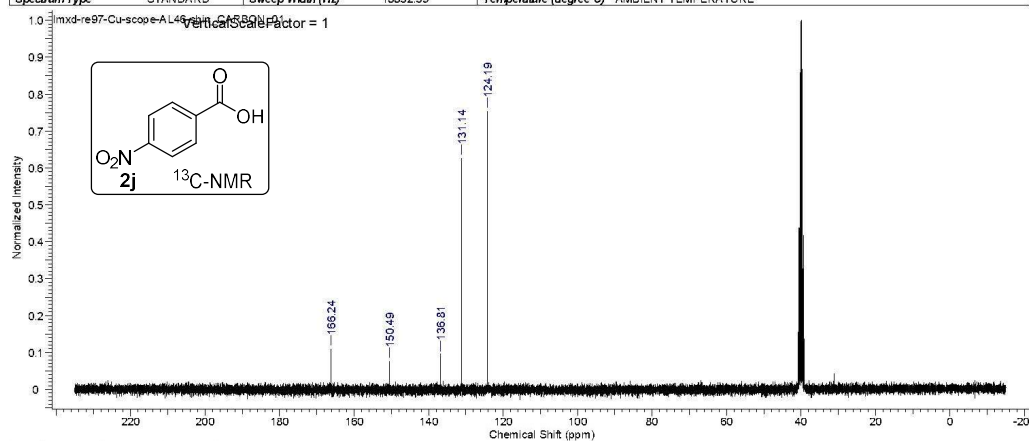


No.	(ppm)	Annotation	Layer No.	Created By	Created At	Modified By	Modified At
1	[2.46 - 2.51]	DMSO	1	Admin	Wed 9/16/2015 3:32:36 PM		

No.	(ppm)	Value	Absolute Value	Non-Negative Value	No.	(ppm)	(Hz)	Height
1	13.61	2.04063630	2.70860096e+8	2.04063630	1	8.14	2437.6	0.6300
2	8.32	8.37200006196	2.65474528e+8	2.00006199	2	8.16	2446.4	1.0000
3	8.29	13.7060130537	7.98131600e+7	0.60130537	3	8.29	2484.4	0.9221
					4	8.32	2493.5	0.6745
					5	13.61	4078.6	0.0206

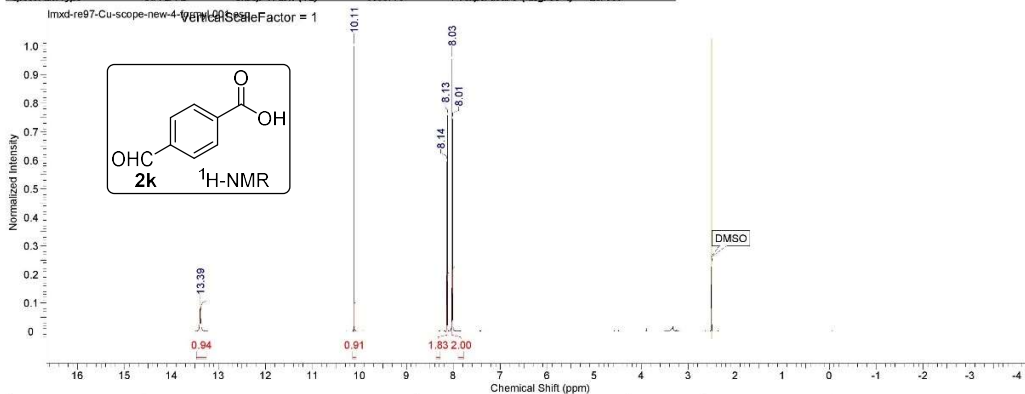
9/16/2015 3:33:54 PM

Acquisition Time (sec)	1.0420	Date	Jul 17 2015	Date Stamp	Jul 17 2015		
File Name	C:\Users\Admin\CloudDrive\Revised_Fehling_Scope\mxid-re97-Cu-scope-AL48-shin_CARBON_01.fid.tif				Frequency (MHz)	75.35	
Nucleus	¹³ C	Number of Transients	1700	Original Points Count	19624	Points Count	32768
Pulse Sequence	s2pul	Receiver Gain	30.00	Solvent	DMSO-d6	Spectrum Offset (Hz)	8287.6016
Spectrum Type	STANDARD	Sweep Width (Hz)	18832.39	Temperature (degree C)	AMBIENT TEMPERATURE		

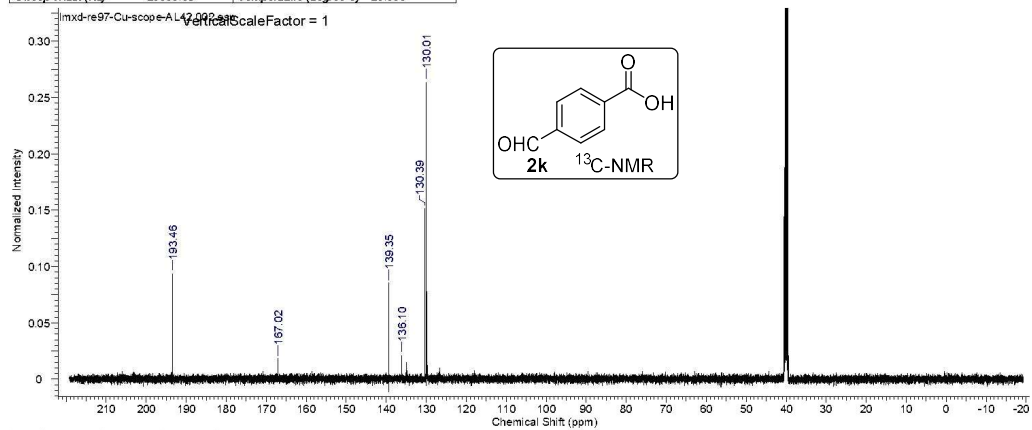


No.	(ppm)	(Hz)	Height
1	124.19	9357.5	0.7532
2	131.14	9881.6	0.6261
3	136.81	10308.7	0.0953
4	150.49	11339.7	0.0761
5	166.24	12526.0	0.1091

Acquisition Time (sec)	3.2788	Comment	Li_10_PFCION.DMSO / home.mingxi.n.57	Date	11 Mar 2016 14:31:12
Date Stamp	11 Mar 2016 14:31:12	File Name	C:\Users\MLWW\Desktop\NMR\result\Li10d-re97-Cu-scope-new-4-formp\11fid	Frequency (MHz)	500.30
Original Points Count	32768	Nucleus	1H	Number of Transients	16
Receiver Gain	106.96	Owner	mgjlll.nmr	Points Count	32768
Spectrum Type	STANDARD	SW (cyclic) (Hz)	10000.00	Solvent	DMSO-d6
		Sweep Width (Hz)	9999.70	Temperature (degree C)	26.956
				Spectrum Offset (Hz)	3089.5574

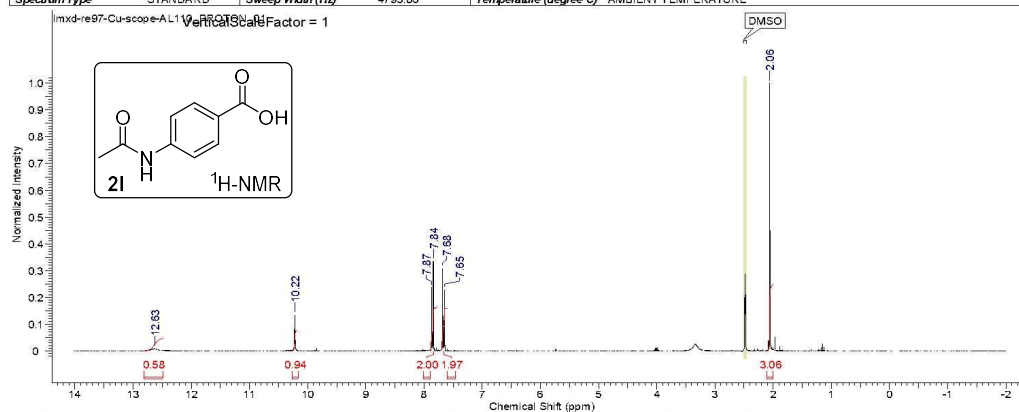


Acquisition Time (sec)	1.0923	Date	12 Jul 2015 22:08:00	Date Stamp	12 Jul 2015 22:08:00
File Name	C:\Users\Admin\CloudDrive\Revised_Fehling_Scope\1010-re97-Cu-scope-AL42\2fid			Frequency (MHz)	125.81
Nucleus	13C	Number of Transients	512	Origin	AVIII500HD
Owner	mcgillnmr	Points Count	32768	Pulse Sequence	zgpg30
SW(cyclical) (Hz)	30000.00	Solvent	DMSO-d6	Spectrum Offset (Hz)	12578.9238
Sweep Width (Hz)	29999.08	Temperature (degree C)	26.003	Spectrum Type	STANDARD



9/16/2015 4:03:05 PM

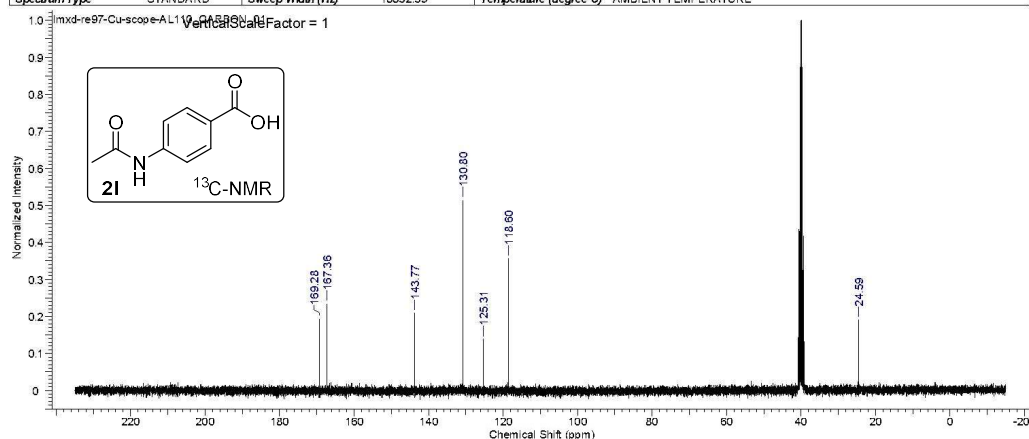
Acquisition Time (sec)	2.0480	Date	Jul 14 2015	Date Stamp	Jul 14 2015		
File Name	C:\Users\Admin\CloudDrive\Revised_Fehling_Scope\mxid-re97-Cu-scope-AL110_PROTON_01.fid.tif				Frequency (MHz)	299.63	
Nucleus	¹ H	Number of Transients	8	Original Points Count	9818	Points Count	16384
Pulse Sequence	s2pul	Receiver Gain	30.00	Solvent	DMSO-d6	Spectrum Offset (Hz)	1797.7788
Spectrum Type	STANDARD	Sweep Width (Hz)	4793.86	Temperature (degree C)	AMBIENT TEMPERATURE		



No.	(ppm)	Value	Absolute Value	Non-Negative Value	No.	(ppm)	(Hz)	Height
1	12.63	2.35231488e+8	2.35231488e+8	2.35231488e+8	1	2.06	616.4	1.0000
2	10.22	1.51078880e+8	1.51078880e+8	1.51078880e+8	2	7.65	2292.1	0.2271
3	7.84	1.53807648e+8	1.53807648e+8	1.53807648e+8	3	7.88	2300.9	0.3067
4	7.65	7.21323600e+7	7.21323600e+7	7.21323600e+7	4	7.84	2349.2	0.3343
5	7.87	4.42628200e+7	4.42628200e+7	4.42628200e+7	5	7.87	2358.0	0.2364
6	10.22	1.51078880e+8	1.51078880e+8	1.51078880e+8	6	10.22	3062.3	0.1341
7	12.63	2.35231488e+8	2.35231488e+8	2.35231488e+8	7	12.63	3783.0	0.0081

9/16/2015 4:03:53 PM

Acquisition Time (sec)	1.0420	Date	Jul 14 2015	Date Stamp	Jul 14 2015		
File Name	C:\Users\Admin\CloudDrive\Revised_Fehling_Scope\mxid-re97-Cu-scope-AL110_CARBON_01.fid.tif				Frequency (MHz)	75.35	
Nucleus	¹³ C	Number of Transients	1700	Original Points Count	19524	Points Count	32768
Pulse Sequence	s2pul	Receiver Gain	30.00	Solvent	DMSO-d6	Spectrum Offset (Hz)	8287.6016
Spectrum Type	STANDARD	Sweep Width (Hz)	18832.39	Temperature (degree C)	AMBIENT TEMPERATURE		

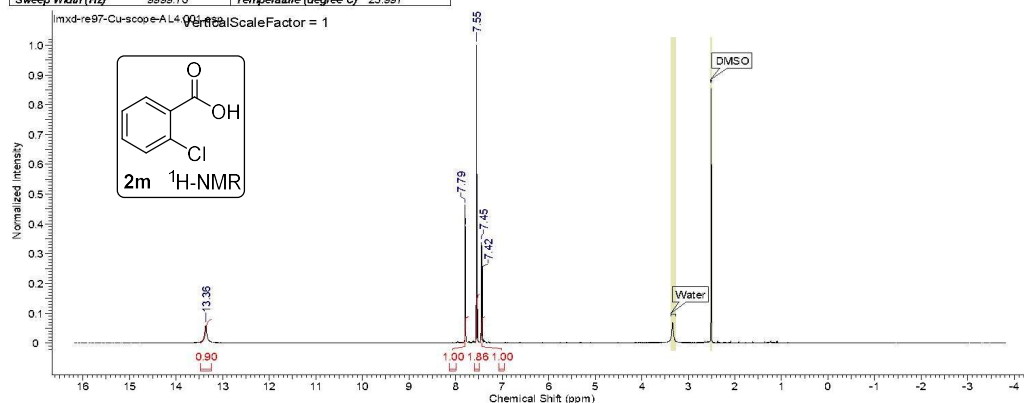


No.	(ppm)	(Hz)	Height
1	24.59	1853.1	0.1902
2	118.60	8936.2	0.3559
3	125.31	9442.0	0.1386
4	130.80	9855.8	0.5128
5	143.77	10833.4	0.2082
6	167.36	12610.5	0.2331
7	169.25	12755.3	0.1926

This report was created by ACD/NMR Processor Academic Edition. For more information go to www.acdlabs.com/nmrproc/

9/15/2015 10:16:56 AM

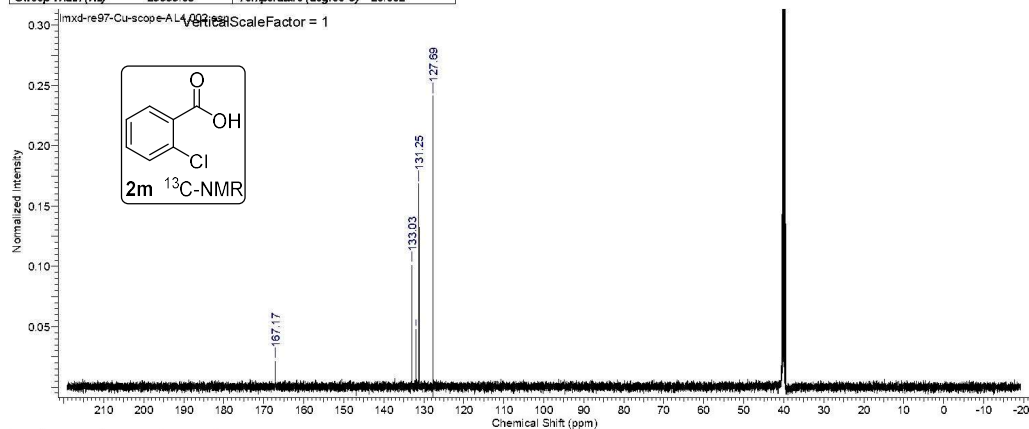
Acquisition Time (sec)	3.2768	Date	12 Jul 2015 18:51:44	Date Stamp	12 Jul 2015 18:51:44
File Name	C:\Users\Admin\CloudDrive\Revised_Fehling_Scope\mxid-re97-Cu-scope-AL411f1d	Frequency (MHz)	500.30	Original Points Count	32768
Nucleus	¹ H	Number of Transients	16	Origin	AVIII500-D
Owner	mcgillnmr	Points Count	32768	Pulse Sequence	zg30
SW (cyclical) (Hz)	10000.00	Solvent	DMSO-d6	Spectrum Offset (Hz)	3089.5574
Sweep Width (Hz)	9999.70	Temperature (degree C)	25.997	Spectrum Type	STANDARD



This report was created by ACD/NMR Processor Academic Edition. For more information go to www.acdlabs.com/nmrproc/

9/15/2015 10:18:38 AM

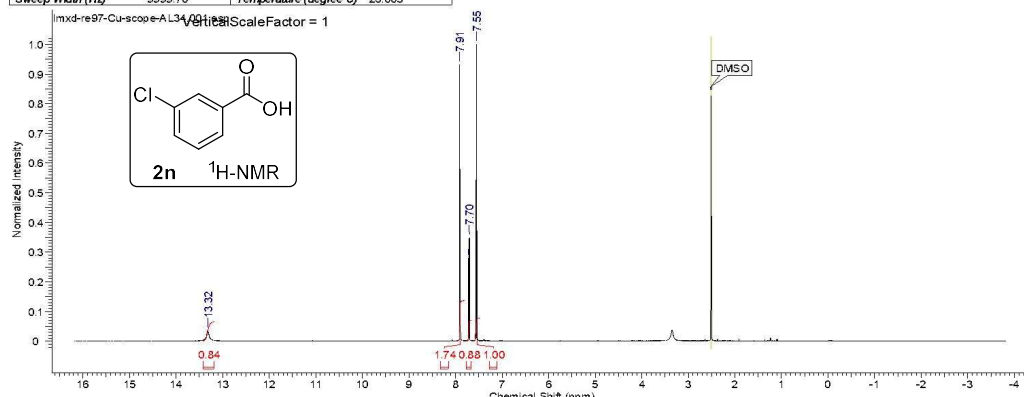
Acquisition Time (sec)	1.0923	Date	12 Jul 2015 19:19:28	Date Stamp	12 Jul 2015 19:19:28
File Name	C:\Users\Admin\CloudDrive\Revised_Fehling_Scope\mxid-re97-Cu-scope-AL412f1d	Frequency (MHz)	125.81	Original Points Count	32768
Nucleus	¹³ C	Number of Transients	512	Origin	AVIII500-D
Owner	mcgillnmr	Points Count	32768	Pulse Sequence	zgpg30
SW (cyclical) (Hz)	30000.00	Solvent	DMSO-d6	Spectrum Offset (Hz)	12578.9238
Sweep Width (Hz)	29999.08	Temperature (degree C)	26.002	Spectrum Type	STANDARD



This report was created by ACD/NMR Processor Academic Edition. For more information go to www.acdlabs.com/nmrproc/

9/15/2015 10:54:11 AM

Acquisition Time (sec)	3.2768	Date	12 Jul 2015 21:06:08	Date Stamp	12 Jul 2015 21:06:08
File Name	C:\Users\Administrator\CloudDrive\Revised_Fehling_Scope\mxd-re97-Cu-scope-AL34\1f1d	Frequency (MHz)	500.30	Original Points Count	32768
Nucleus	¹ H	Number of Transients	16	Origin	AVIII500H-D
Owner	mcgillnmr	Points Count	32768	Pulse Sequence	zg30
SW (cyclical) (Hz)	10000.00	Solvent	DMSO-d6	Spectrum Offset (Hz)	3089.5574
Sweep Width (Hz)	9999.70	Temperature (degree C)	26.003	Spectrum Type	STANDARD



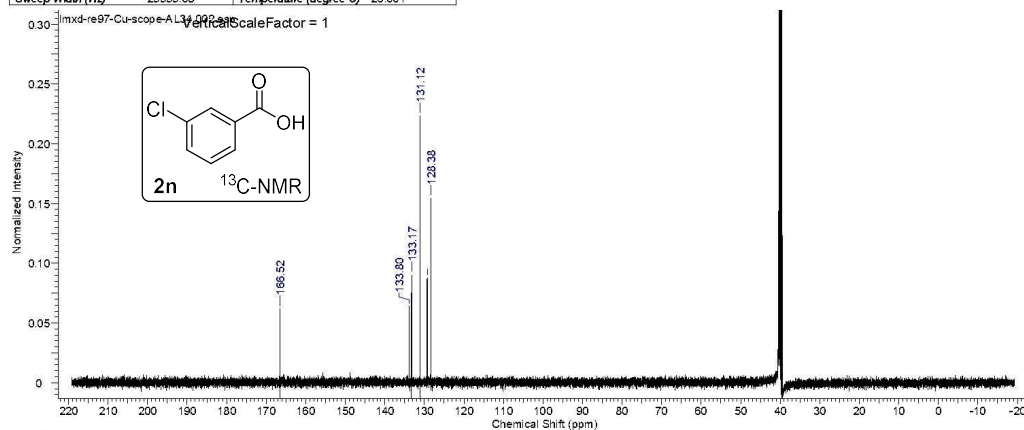
No.	(ppm)	Annotation	Layer No.	Created By	Created At	Modified By	Modified At
1	[2.49, 2.52]	DMSO	1	Admin	Tue 9/15/2015 10:53:47 AM		

No.	(ppm)	Value	Absolute Value	Non-Negative Value	No.	(ppm)	(Hz)	Height
1	7.55	1.0000000	6.81458432e+9	1.00000000	1	7.55	3778.2	1.0000
2	7.70	0.88319451	6.01860352e+9	0.88319451	2	7.70	3852.6	0.3487
3	7.81	1.74249649	1.18743890e+10	1.74249649	3	7.81	3861.8	0.2802
4	7.91	0.83838874	5.71327078e+9	0.83838874	4	7.91	3956.1	0.9318
5	13.32	0.0353			5	13.32	6662.7	0.0353

This report was created by ACD/NMR Processor Academic Edition. For more information go to www.acdlabs.com/nmrproc/

9/15/2015 11:25:04 AM

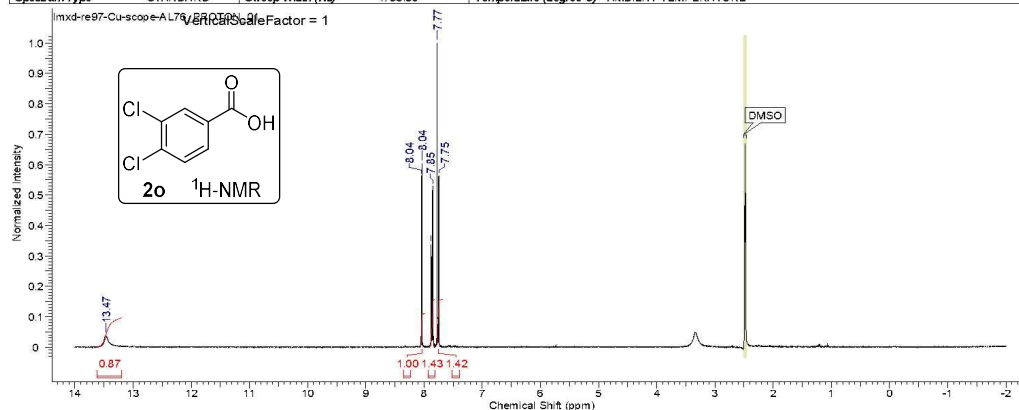
Acquisition Time (sec)	1.0923	Date	12 Jul 2015 21:33:52	Date Stamp	12 Jul 2015 21:33:52
File Name	C:\Users\Administrator\CloudDrive\Revised_Fehling_Scope\mxd-re97-Cu-scope-AL34\2f1d	Frequency (MHz)	125.81	Original Points Count	32768
Nucleus	¹³ C	Number of Transients	512	Origin	AVIII500H-D
Owner	mcgillnmr	Points Count	32768	Pulse Sequence	zgpg30
SW (cyclical) (Hz)	30000.00	Solvent	DMSO-d6	Spectrum Offset (Hz)	12578.9238
Sweep Width (Hz)	29999.08	Temperature (degree C)	26.001	Spectrum Type	STANDARD



No.	(ppm)	(Hz)	Height
1	128.38	16151.8	0.1542
2	129.28	16265.3	0.0874
3	131.12	16496.9	0.2231
4	133.17	16755.1	0.0900
5	133.80	16833.8	0.0640
6	166.52	20950.0	0.0619

9/18/2015 3:46:47 PM

Acquisition Time (sec)	2.0480	Date	Jul 13 2015	Date Stamp	Jul 13 2015
File Name	C:\Users\Admin\CloudDrive\Revised_Fehling_Scope\mxd-re97-Cu-scope-AL78	PROTON	01.fid	Frequency (MHz)	299.63
Nucleus	¹ H	Number of Transients	8	Original Points Count	9818
Pulse Sequence	s2pul	Receiver Gain	35.00	Solvent	DMSO-d6
Spectrum Type	STANDARD	Sweep Width (Hz)	4793.86	Temperature (degree C)	AMBIENT TEMPERATURE
				Spectrum Offset (Hz)	1797.7788

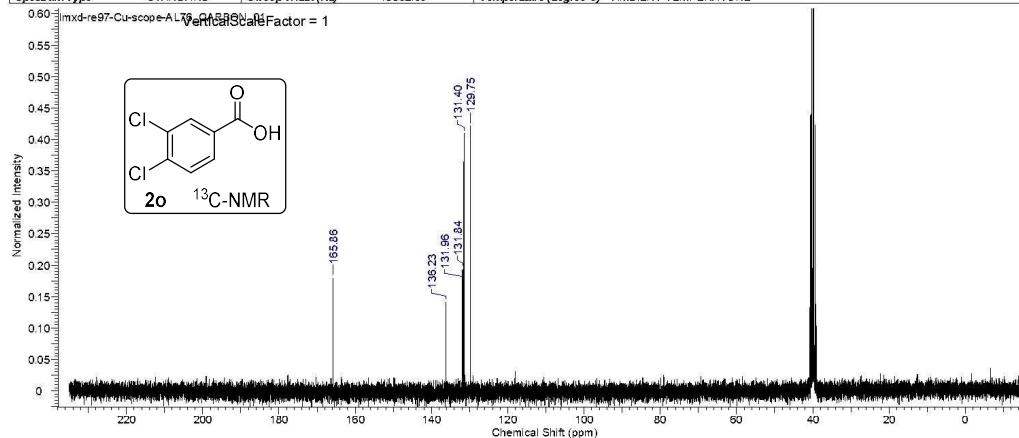


No.	(ppm)	Annotation	Layer No.	Created By	Created At	Modified By	Modified At
1	[2.46, 2.51]	DMSO	1	Admin	Wed 9/16/2015 3:46:25 PM		

No.	(ppm)	Value	Absolute Value	Non-Negative Value	No.	(ppm)	(Hz)	Height
1	7.799	7.81142338884	1.67815584e+8	1.42338884	1	7.75	2321.1	0.5629
2	7.8165	7.92142919215	1.68499792e+8	1.42919219	2	7.77	2329.3	1.0000
3	7.8804	8.08100024462	1.17927472e+8	1.00024462	3	7.85	2351.0	0.5296
4	7.977	13.6086823275	1.02363456e+8	0.86823279	4	7.88	2360.9	0.3371
					5	8.04	2408.3	0.6036
					6	8.04	2410.4	0.5628
					7	13.47	4035.5	0.0376

9/18/2015 3:48:10 PM

Acquisition Time (sec)	1.0420	Date	Jul 13 2015	Date Stamp	Jul 13 2015
File Name	C:\Users\Admin\CloudDrive\Revised_Fehling_Scope\mxd-re97-Cu-scope-AL78	CARBON	01.fid	Frequency (MHz)	75.35
Nucleus	¹³ C	Number of Transients	1700	Original Points Count	19524
Pulse Sequence	s2pul	Receiver Gain	30.00	Solvent	DMSO-d6
Spectrum Type	STANDARD	Sweep Width (Hz)	18832.39	Temperature (degree C)	AMBIENT TEMPERATURE
				Spectrum Offset (Hz)	8287.6016

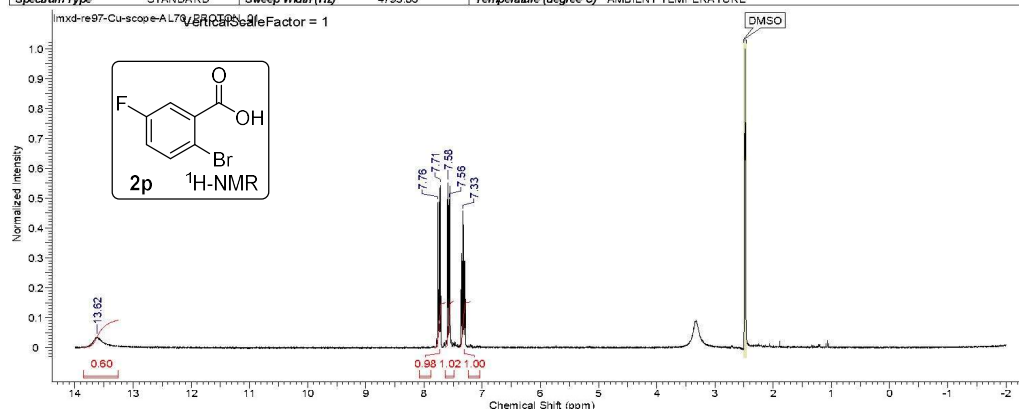


No.	(ppm)	(Hz)	Height
1	129.75	9777.0	0.4213
2	131.40	9901.2	0.4093
3	131.51	9909.2	0.3640
4	131.84	9933.9	0.1932
5	131.96	9943.1	0.1719
6	136.23	10265.0	0.1407
7	165.86	12497.3	0.1793

This report was created by ACD/NMR Processor Academic Edition. For more information go to www.acdlabs.com/nmrproc/

9/16/2015 3:43:48 PM

Acquisition Time (sec)	2.0480	Date	Jul 13 2015	Date Stamp	Jul 13 2015		
File Name	C:\Users\Admin\CloudDrive\Revised_Fehling_Scope\mxid-re97-Cu-scope-AL70-PROTON_01.fid.tif				Frequency (MHz)	299.63	
Nucleus	¹ H	Number of Transients	8	Original Points Count	9818	Points Count	16384
Pulse Sequence	s2pul	Receiver Gain	36.00	Solvent	DMSO-d6	Spectrum Offset (Hz)	1797.7788
Spectrum Type	STANDARD	Sweep Width (Hz)	4793.86	Temperature (degree C)	AMBIENT TEMPERATURE		



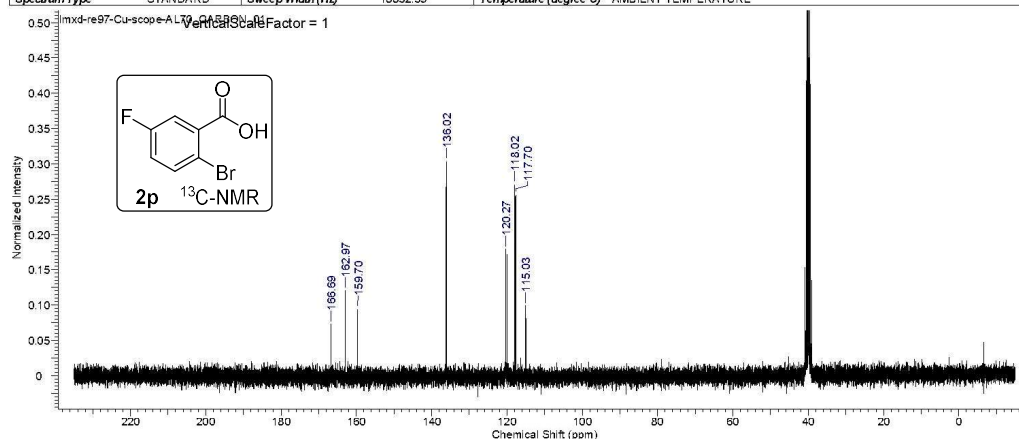
No.	(ppm)	Annotation	Layer No.	Created By	Created At	Modified By	Modified At
1	[2.46 - 2.51]	DMSO	1	Admin	Wed 9/16/2015 3:43:18 PM		

No.	(ppm)	Value	Absolute Value	Non-Negative Value	No.	(ppm)	(Hz)	Height
1	7.2019	7.40100000000	2.11924352e+8	1.00000000	1	7.33	2196.8	0.4568
2	7.4887	7.63101619279	2.15356000e+8	1.01619279	2	7.56	2266.4	0.4952
3	7.6389	7.83098054286	2.07800894e+8	0.98054266	3	7.58	2272.2	0.5508
4	7.7523	7.959879476	1.26899192e+8	0.59879476	4	7.71	2311.5	0.5430
					5	7.76	2325.5	0.4855
					6	13.62	4080.9	0.0357

This report was created by ACD/NMR Processor Academic Edition. For more information go to www.acdlabs.com/nmrproc/

9/16/2015 3:45:14 PM

Acquisition Time (sec)	1.0420	Date	Jul 13 2015	Date Stamp	Jul 13 2015		
File Name	C:\Users\Admin\CloudDrive\Revised_Fehling_Scope\mxid-re97-Cu-scope-AL70-CARBON_01.fid.tif				Frequency (MHz)	75.35	
Nucleus	¹³ C	Number of Transients	1700	Original Points Count	19624	Points Count	32768
Pulse Sequence	s2pul	Receiver Gain	30.00	Solvent	DMSO-d6	Spectrum Offset (Hz)	8287.6016
Spectrum Type	STANDARD		Sweep Width (Hz)	18832.39	Temperature (degree C)	AMBIENT TEMPERATURE	

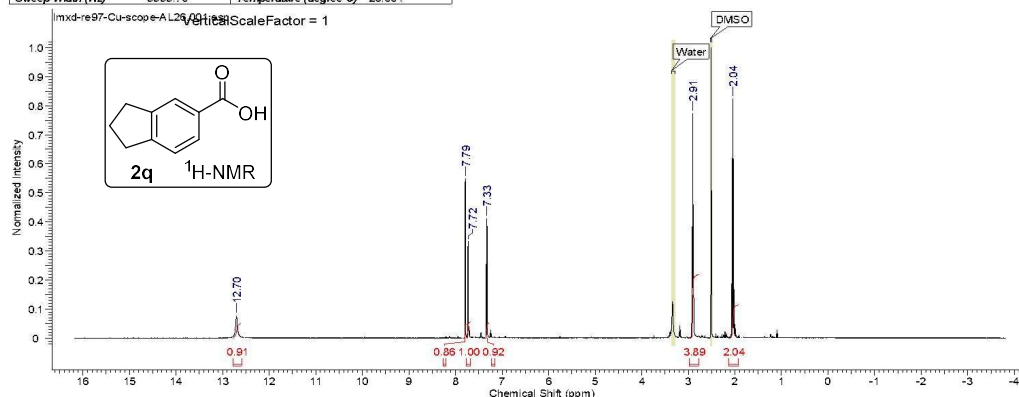


No.	(ppm)	(Hz)	Height
1	115.03	8667.2	0.0989
2	117.70	8868.4	0.2557
3	118.02	8893.1	0.2702
4	120.27	9062.1	0.1790
5	136.02	10249.5	0.3029
6	159.70	12033.4	0.0938
7	162.97	12280.0	0.1202
8	166.69	12559.9	0.0729

This report was created by ACD/NMR Processor Academic Edition. For more information go to www.acdlabs.com/nmrproc/

9/15/2015 10:39:59 AM

Acquisition Time (sec)	3.2768	Date	12 Jul 2015 20:00:00	Date Stamp	12 Jul 2015 20:00:00
File Name	C:\Users\Admin\CloudDrive\Revised_Fehling_Scope\mxid-re97-Cu-scope-AL28116d	Origin	AVIII500HD	Frequency (MHz)	500.30
Nucleus	¹ H	Number of Transients	16	Original Points Count	32768
Owner	mcgillnmr	Points Count	32768	Pulse Sequence	zg30
SW (cyclical) (Hz)	10000.00	Solvent	DMSO-d6	Receiver Gain	106.56
Sweep Width (Hz)	9999.70	Temperature (degree C)	26.004	Spectrum Offset (Hz)	3089.5574
				Spectrum Type	STANDARD



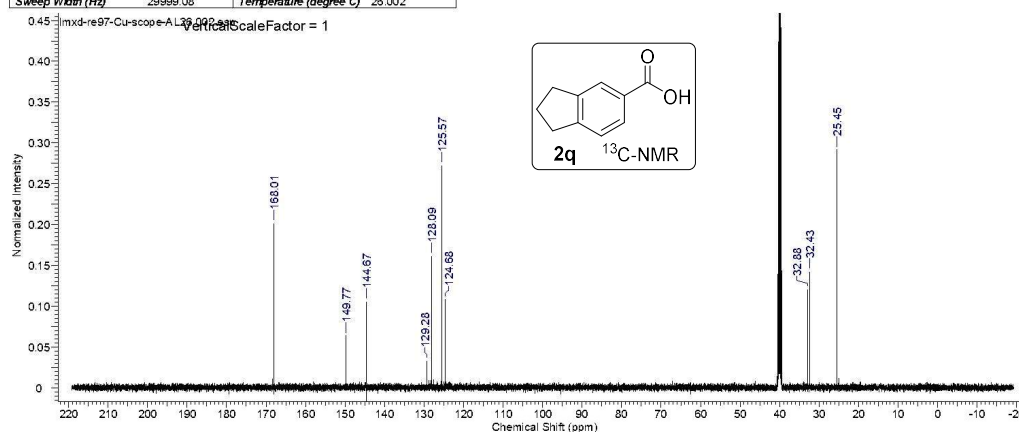
No.	(ppm)	Annotation	Layer No.	Created By	Created At	Modified By	Modified At
1	[2.49...2.52]	DMSO	1	Admin	Tue 9/15/2015 10:39:39 AM		
2	[3.29...3.35]	Water	1	Admin	Tue 9/15/2015 10:39:39 AM		

No.	(ppm)	Value	Absolute Value	Non-Negative Value	No.	(ppm)	(Hz)	Height
1	12.70	2.13203881240	9.05753702e+9	2.03881240	1	2.04	1022.8	0.8222
2	7.79	2.98389189410	1.72899553e+10	3.89189410	2	2.91	1454.6	0.7728
3	7.72	7.35092156684	4.09411174e+9	0.92156684	3	7.33	3668.9	0.4111
4	7.33	7.7909987531	4.44200141e+9	0.9987531	4	7.72	3862.4	0.3331
5	7.72	7.83085920805	3.81707930e+9	0.85920805	5	7.79	3895.7	0.5485
6	3.89	12.7091213864	4.05222659e+9	0.91213864	6	12.70	6354.5	0.0768

This report was created by ACD/NMR Processor Academic Edition. For more information go to www.acdlabs.com/nmrproc/

9/15/2015 10:41:24 AM

Acquisition Time (sec)	1.0923	Date	12 Jul 2015 20:27:44	Date Stamp	12 Jul 2015 20:27:44
File Name	C:\Users\Admin\CloudDrive\Revised_Fehling_Scope\mxid-re97-Cu-scope-AL28121d	Origin	AVIII500HD	Frequency (MHz)	125.81
Nucleus	¹³ C	Number of Transients	512	Original Points Count	32768
Owner	mcgillnmr	Points Count	32768	Pulse Sequence	zgpg30
SW (cyclical) (Hz)	30000.00	Solvent	DMSO-d6	Receiver Gain	192.72
Sweep Width (Hz)	29999.08	Temperature (degree C)	26.002	Spectrum Offset (Hz)	12578.9238
				Spectrum Type	STANDARD

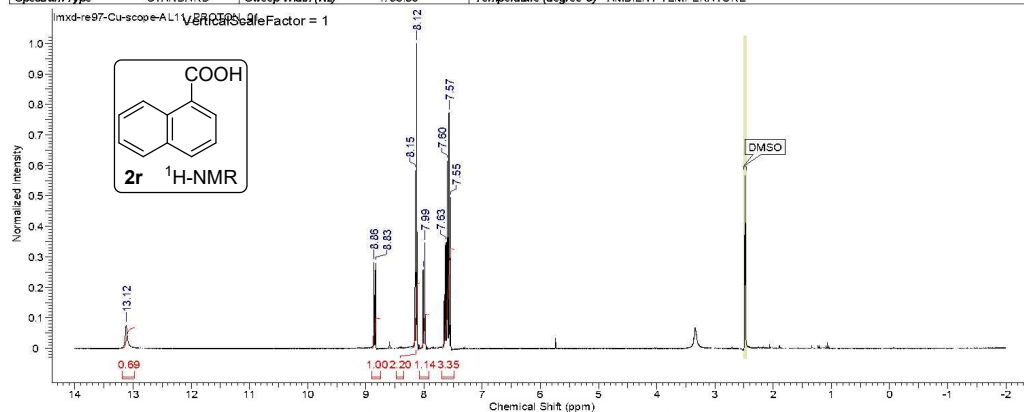


No.	(ppm)	(Hz)	Height
1	25.45	3202.6	0.2918
2	32.43	4080.5	0.1417
3	32.88	4136.4	0.1203
4	124.68	15686.7	0.1081
5	125.57	15798.4	0.2720
6	128.09	16115.1	0.1608
7	129.28	16265.3	0.0326
8	144.67	18201.6	0.1051
9	149.77	18842.5	0.0637
10	168.01	21137.7	0.2011

This report was created by ACD/NMR Processor Academic Edition. For more information go to www.acdlabs.com/nmrproc/

9/15/2015 10:36:33 AM

Acquisition Time (sec)	2.0480	Date	Jul 13 2015	Date Stamp	Jul 13 2015
File Name	C:\Users\Admin\CloudDrive\Revised_Fehling_Scope\lmsd-re97-Cu-scope-AL111.D	Frequency (MHz)	299.63	Points Count	16384
Nucleus	¹ H	Number of Transients	8	Original Points Count	9818
Pulse Sequence	zgpg30	Receiver Gain	30.00	Solvent	DMSO-d6
Spectrum Type	STANDARD	Sweep Width (Hz)	4793.86	Temperature (degree C)	AMBIENT TEMPERATURE
				Spectrum Offset (Hz)	1787.7788



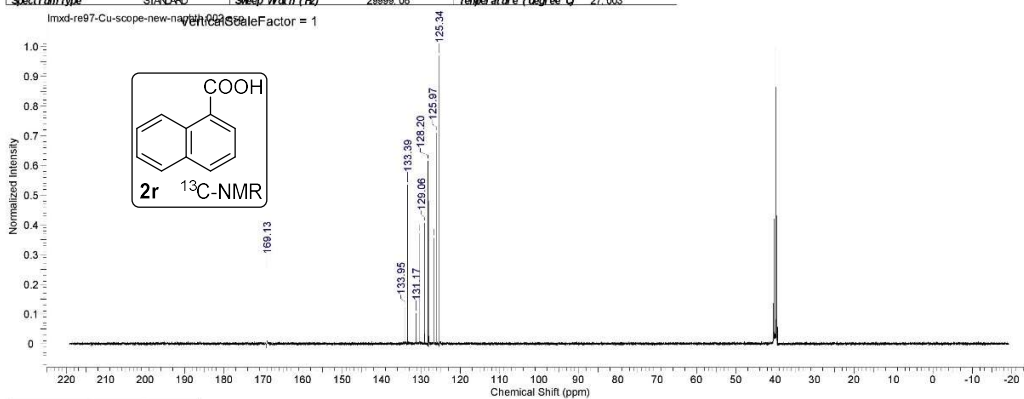
No.	(ppm)	Annotation	Layer No.	Created By	Created At	Modified By	Modified At
1	[2.46 - 2.51]	DMSO	1	Admin	Tue 9/15/2015 10:36:00 AM		

No.	(ppm)	Value	Absolute Value	Non-Negative Value
17	8.87	7.6833483994	3.82502432e+8	3.34838940
27	8.12	8.0711435183	1.30629136e+8	1.14351833
38	0.760	8.2122028191	2.51637744e+8	2.20281911
48	7.452	8.8810001157	1.14247832e+8	1.00011575
82	9.792	13.106947457	7.93838720e+7	0.69474578

This report was created by ACD/NMR Processor Academic Edition. For more information go to www.acdlabs.com/nmrproc/

2016/4/3 14:17:03

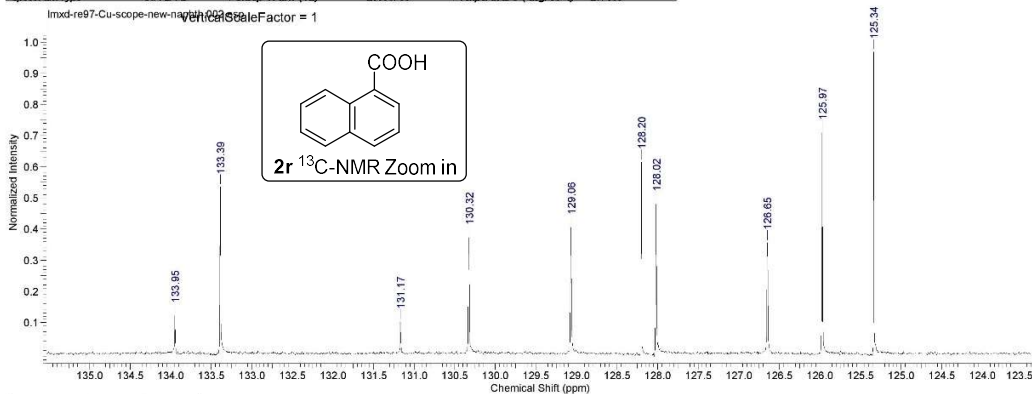
Acquisition Time (sec)	1.0923	Comment	Li_1d_C13_DMSO/home.nmrproj.n.58	Date	11 Mar 2016 21:29:20
Date Stamp	11 Mar 2016 21:29:20	Nucleus	¹³ C	File Name	C:\Users\MLW\Desktop\NMR\resubmit\lmsd-re97-Cu-scope-new.napht.hv2.fid
Frequency (MHz)	125.81	Owner	molli.nmr	Number of Transients	512
Original Points Count	32768	SW (Hz)	30000.00	Points Count	32768
Receiver Gain	192.72	Solvent	DMSO-d6	Pulse Sequence	zgpg30
Spectrum Type	STANDARD	Sweep Width (Hz)	26699.08	Temperature (degree C)	27.003
				Spectrum Offset (Hz)	12578.9238



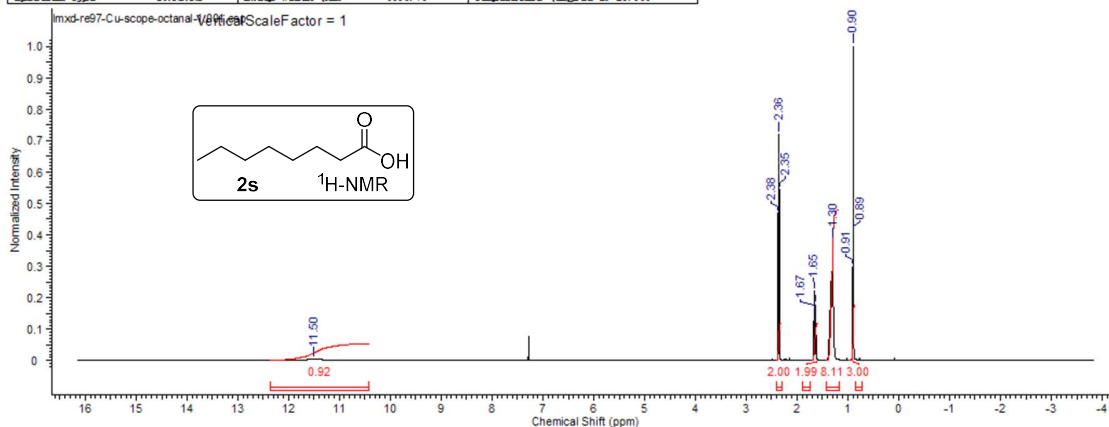
No.	(ppm)	(Hz)	Height
1	125.34	15769.1	0.9691
2	125.97	15848.7	0.7083
3	126.65	15933.9	0.3562
4	128.20	16128.9	0.6152
5	129.06	16237.8	0.4056
6	130.32	16396.2	0.3723
7	131.17	16502.4	0.1022
8	133.39	16781.7	0.5345
9	133.95	16852.1	0.1222
10	169.13	21278.7	0.2586

V

Acquisition Time (sec)	1.0923	Comment	Li_1d_C13_DMSO/home.mingxi.n.58	Date	11_Mar_2016_21:29:20
Date Stamp	11_Mar_2016_21:29:20	File Name	C:\Users\MLW\Desktop\NMR\result\11_mxd-re97-Cu-scope-new-naphthol-2.fid	Origin	AVI11500HD
Frequency (MHz)	125.81	Nucleus	13C	Number of Transients	512
Original Points Count	32768	Owner	mgill.mr	Points Count	32768
Receiver Gain	192.72	SW (cyclical) (Hz)	30000.00	Solvent	DMSO-d6
Spectrum Type	STANDARD	Sweep Width (Hz)	29999.08	Temperature (degree C)	27.003
				Spectrum Offset (Hz)	12578.9238

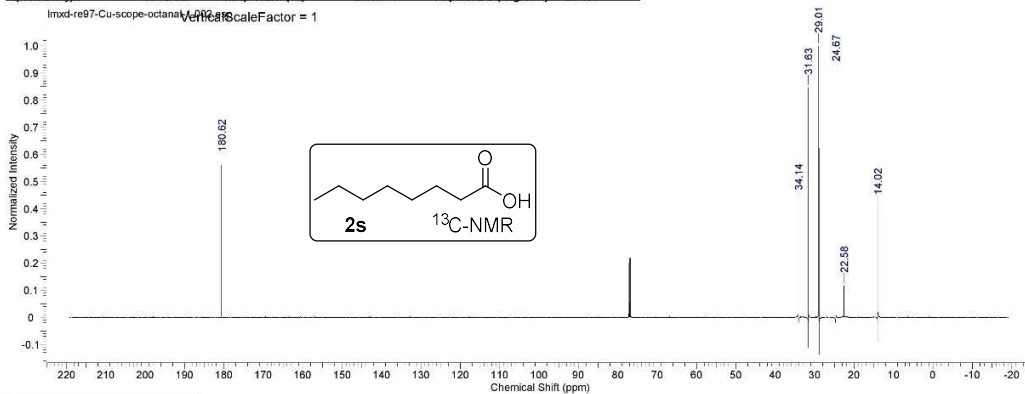


Acquisition Time (sec)	3.2768	Comment	1s	Date	27_Oct_2015_16:05:20
Date Stamp	27_Oct_2015_16:05:20	File Name	C:\Users\MLW\Desktop\新文件\1mxd-re97-Cu-scope-octanal-1.fid	Origin	AVI11500HD
Frequency (MHz)	300.30	Nucleus	1H	Number of Transients	16
Original Points Count	32768	Owner	mgill.mr	Points Count	32768
Receiver Gain	18.18	SW (cyclical) (Hz)	10000.00	Solvent	CHLOROFORM-d
Spectrum Type	STANDARD	Sweep Width (Hz)	9999.70	Temperature (degree C)	26.999
				Spectrum Offset (Hz)	3089.5574



2015/10/27 18:35:25

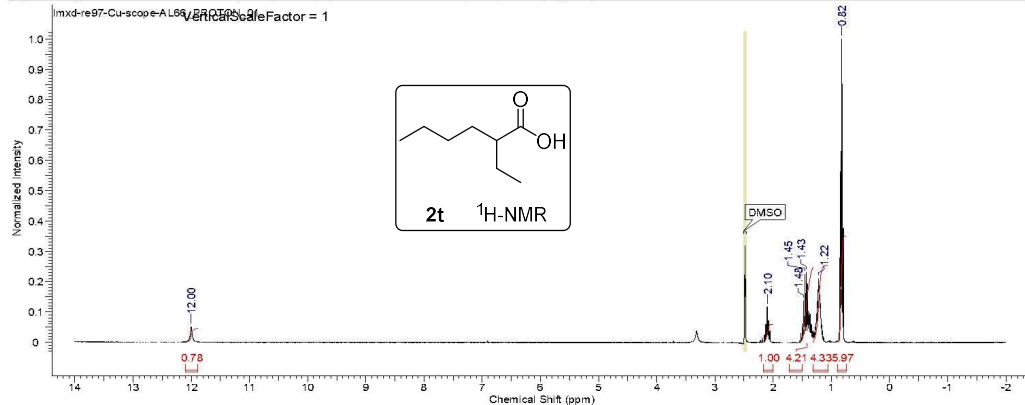
Acquisition Time (sec)	1.0923	Comment	Li	Date	27 Oct 2015 16:33:04
Date Stamp	27 Oct 2015 16:33:04	File Name	C:\Users\IML\W\Desktop\lmd-re97-Cu-scope-octanal-112.fid	Original Points Count	512
Frequency (MHz)	125.81	Nucleus	¹³ C	Number of Transients	32788
Original Points Count	32788	Owner	mtgill.nmt	Points Count	32788
Receiver Gain	192.72	SI (Focal) (Hz)	30000.00	Solvent	CHLOROFORM-d
Spectrum Type	STANDARD	Sweep Width (Hz)	29999.08	Temperature (degree C)	26.995
				Spectrum Offset (Hz)	12578.9238



No.	(ppm)	(Hz)	Height
1	14.02	1763.3	0.4043
2	22.58	2840.9	0.1165
3	24.67	3103.7	0.8957
4	29.01	3650.2	1.0000
5	31.63	3978.9	0.8466
6	34.14	4294.8	0.4211
7	180.62	22724.3	0.5626

9/16/2015 3:40:31 PM

Acquisition Time (sec)	2.0480	Date	Jul 20 2015	Date Stamp	Jul 20 2015
File Name	C:\Users\Admin\CloudDrive\Revised_Fehling_Scope\lmd-re97-Cu-scope-AL66_PROTON_01.fid	Frequency (MHz)	299.63	Original Points Count	9818
Nucleus	¹ H	Number of Transients	8	Points Count	16384
Pulse Sequence	s2pul	Receiver Gain	30.00	Solvent	DMSO-d6
Spectrum Type	STANDARD	Sweep Width (Hz)	4793.85	Temperature (degree C)	AMBIENT TEMPERATURE
				Spectrum Offset (Hz)	1797.7788



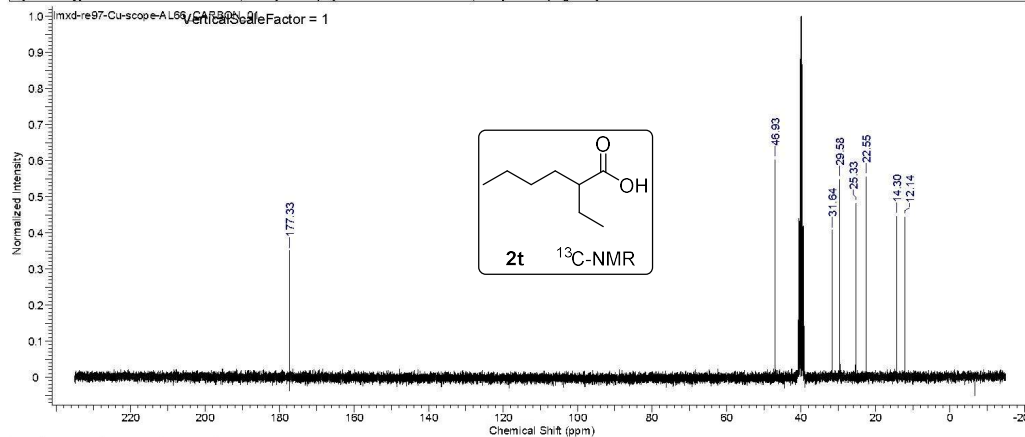
No.	(ppm)	Annotation	Layer No.	Created By	Created At	Modified By	Modified At
1	[2.46 - 2.51]	DMSO	1	Admin	Wed 9/16/2015 3:40:02 PM		

No.	(ppm)	Value	Absolute Value	Non-Negative Value	No.	(ppm)	(Hz)	Height
1	0.7417	0.8859718546	5.69174592e+8	5.97185469	1	0.82	245.0	1.0000
2	1.0558	1.31432917305	4.12611392e+8	4.32917309	2	1.22	366.8	0.2099
3	1.3153	1.53421133375	4.01380192e+8	4.21133375	3	1.40	420.6	0.1618
4	1.9982	2.16099952900	9.52646240e+7	0.99952900	4	1.43	427.6	0.2307
5	1.885	12.1077842957	7.41917440e+7	0.77842957	5	1.45	435.2	0.2244
					6	1.48	442.8	0.1368
					7	2.10	629.8	0.1165
					8	12.00	3596.3	0.0506

This report was created by ACD/NMR Processor Academic Edition. For more information go to www.acdlabs.com/nmrproc/

9/16/2015 3:41:27 PM

Acquisition Time (sec)	1.0420	Date	Jul 20 2015	Date Stamp	Jul 20 2015
File Name	C:\Users\Administrator\CloudDrive\Revised_Fehling_Scope\lmsd-re97-Cu-scope-AL66 CARBON_01.fid	Frequency (MHz)	75.35	Points Count	32768
Nucleus	¹³ C	Number of Transients	1700	Original Points Count	19624
Pulse Sequence	s2pul	Receiver Gain	30.00	Solvent	DMSO-d6
Spectrum Type	STANDARD	Sweep Width (Hz)	18832.39	Temperature (degree C)	AMBIENT TEMPERATURE

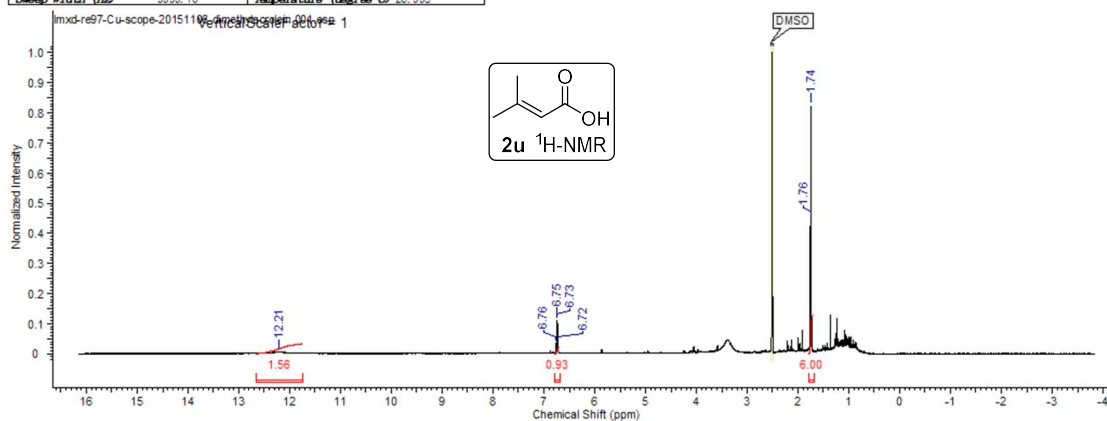


No.	(ppm)	(Hz)	Height
1	12.14	914.6	0.4443
2	14.30	1077.2	0.4459
3	22.55	1699.1	0.5553
4	25.33	1908.9	0.4817
5	29.58	2229.0	0.5483
6	31.64	2384.2	0.4072
7	46.93	3536.5	0.6028
8	177.33	13361.7	0.3508

This report was created by ACD/NMR Processor Academic Edition. For more information go to www.acdlabs.com/nmrproc/

2015/11/8 9:24:19

Acquisition Time (sec)	3.2768	Comment	1:1	Date	06 Nov 2015 12:57:20
Date Stamp	06 Nov 2015 12:57:20				
File Name	C:\Users\MMLW\Desktop\新建文件夹\新建文件夹\lmsd-re97-Cu-scope-20151106-dimethylacrolein\1.fid	Frequency (MHz)	500.30	Original Points Count	32768
Nucleus	¹ H	Number of Transients	16	Origin	AVII1500HD
Owner	mcgillinnr	Points Count	32768	Pulse Sequence	zg30
SW (cyclical) (Hz)	10000.00	Solvent	DMSO-d6	Receiver Gain	106.56
Sweep Width (Hz)	9999.70	Temperature (degree C)	26.985	Spectrum Offset (Hz)	3099.5574
				Spectrum Type	STANDARD

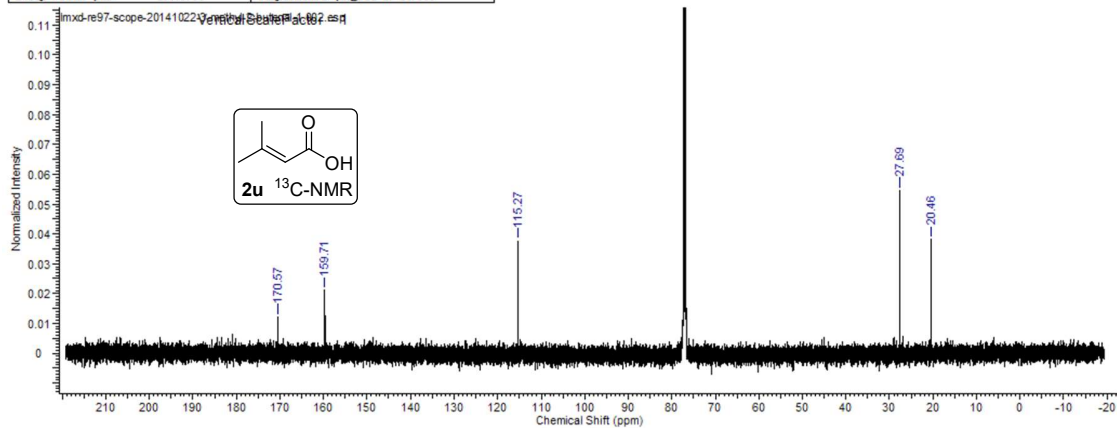


No.	(ppm)	Annotation	Layer No.	Created By	Created At	Modified By	Modified At
1	[2.49...2.52]	DMSO	1	MMLWV	2015/11/8 8:06:10		

No.	(ppm)	Value	Absolute Value	Non-Negative Value
1	8.31...	1.7950000000	1.08785132e+10	6.00000000
2	8.20...	6.79092587304	1.67868698e+9	0.92587304
3	7.373...	12.6156381214	2.83532518e+9	1.56381214

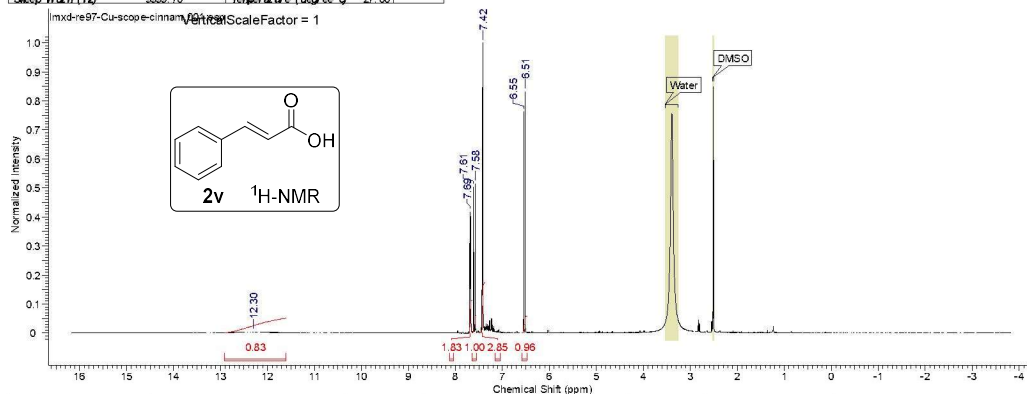
No.	(ppm)	(Hz)	Height
1	1.74	869.6	0.8218
2	1.76	879.0	0.4505
3	6.72	3361.9	0.0321
4	6.73	3368.9	0.1081
5	6.75	3376.0	0.1106
6	6.76	3381.8	0.0344
7	12.21	6108.5	0.0056

Acquisition Time (sec)	1.0923	Date	29 Oct 2015	Date Stamp	29 Oct 2015
File Name	C:\Users\MMLWW\Desktop\新建文件夹\lmdx-re97-Cu-scope-3-methyl-2-butenal-1.v2.fid	Frequency (MHz)	125.81	Original Points Count	32768
Nucleus	¹³ C	Number of Transients	3400	Pulse Sequence	zgpg30
Owner	mmlww	Points Count	32768	Receiver Gain	192.72
SW (cycles) (Hz)	30000.00	Solvent	CHLOROFORM-d	Spectrum Offset (Hz)	12575.9238
Sweep Width (Hz)	29999.08	Temperature (degree C)	24.955	Spectrum Type	STANDARD



No.	(ppm)	(Hz)	Height
1	20.46	2574.5	0.0381
2	27.69	3483.6	0.0546
3	115.27	14502.0	0.0377
4	159.71	20093.1	0.0212
5	170.57	21460.0	0.0122

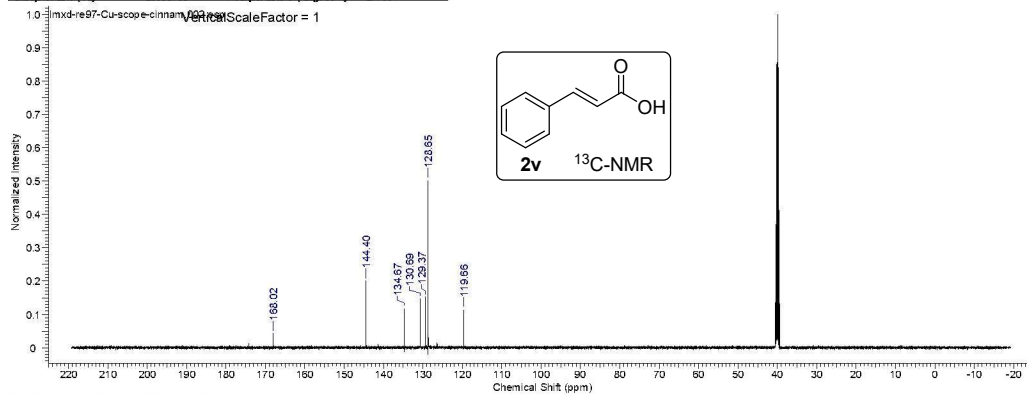
Acquisition Time (sec)	3.2768	Date	17 Sep 2015 04:59:44	Date Stamp	17 Sep 2015 04:59:44
File Name	C:\Users\MMLWW\Desktop\新建文件夹\lmdx-re97-Cu-scope-cinnamal-1.fid	Frequency (MHz)	500.30	Original Points Count	32768
Nucleus	¹ H	Number of Transients	16	Pulse Sequence	zg30
Owner	mmlww	Points Count	32768	Receiver Gain	77.88
SW (cycles) (Hz)	10000.00	Solvent	DMSO-d6	Spectrum Offset (Hz)	3088.5574
Sweep Width (Hz)	9999.70	Temperature (degree C)	27.001	Spectrum Type	STANDARD



No.	(ppm)	Value	Absolute Value	Non-Negative Value	No.	(ppm)	(Hz)	Height
1	6.51	3.10042112e+9	0.95609999	0.95609999	1	6.51	3259.4	0.8309
2	7.69	2.85231853	9.24943872e+9	2.85231853	2	6.55	3275.3	0.7619
3	7.42	0.99995567	3.24266778e+9	0.99995567	3	7.42	3709.8	1.0000
4	7.58	0.99995567	5.94876521e+9	1.83445538	4	7.58	3792.2	0.5142
5	7.61	0.99995567	5.94876521e+9	1.83445538	5	7.61	3808.4	0.5030
6	7.69	0.99995567	5.94876521e+9	1.83445538	6	7.69	3845.6	0.4171
7	12.30	0.0037	2.69692774e+9	0.83167171	7	12.30	6152.1	0.0037

2015/9/17 9:15:58

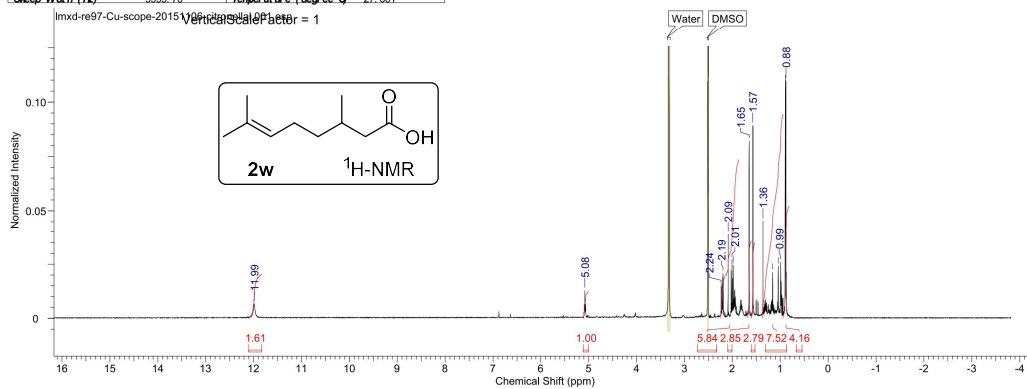
Acquisition Time (sec)	1.0823	Date	17 Sep 2015 05:27:28	Date Stamp	17 Sep 2015 05:27:28
File Name	C:\Users\MMLWW\Desktop\17md-re97-Cu-scope-clinnan\2\1.fid	Frequency (MHz)	125.81	Original Points Count	32768
Nucleus	¹³ C	Number of Transients	512	Origin	AM11500-D
Owner	regill.nmr	Points Count	32768	Pulse Sequence	zgpg30
Solvent	DMSO-d6	Receiver Gain	192.72	Spectrum Offset (Hz)	12578.9238
Sweep Width (Hz)	20000.00	Temperature (degree C)	27.001	Spectrum Type	STANDARD



No.	(ppm)	(Hz)	Height
1	119.66	15055.0	0.1127
2	128.65	16185.6	0.5010
3	129.37	16276.3	0.1521
4	130.69	16442.9	0.1469
5	134.67	16943.7	0.1174
6	144.40	18167.8	0.2000
7	168.02	21138.6	0.0426

2015/11/8 8:27:42

Acquisition Time (sec)	3.2788	Comment	Li	Date	06 Nov 2015 13:31:28
Date Stamp	06 Nov 2015 13:31:28	Frequency (MHz)	500.30	Original Points Count	32768
File Name	C:\Users\MMLWW\Desktop\17md-re97-Cu-scope-20151106-clinnan\1\1.fid	Origin	AM11500-D	Pulse Sequence	zgpg30
Nucleus	¹ H	Number of Transients	16	Receiver Gain	106.56
Owner	regill.nmr	Points Count	32768	Spectrum Offset (Hz)	3089.5574
Solvent	DMSO-d6	Temperature (degree C)	27.001	Spectrum Type	STANDARD
Sweep Width (Hz)	10000.00				



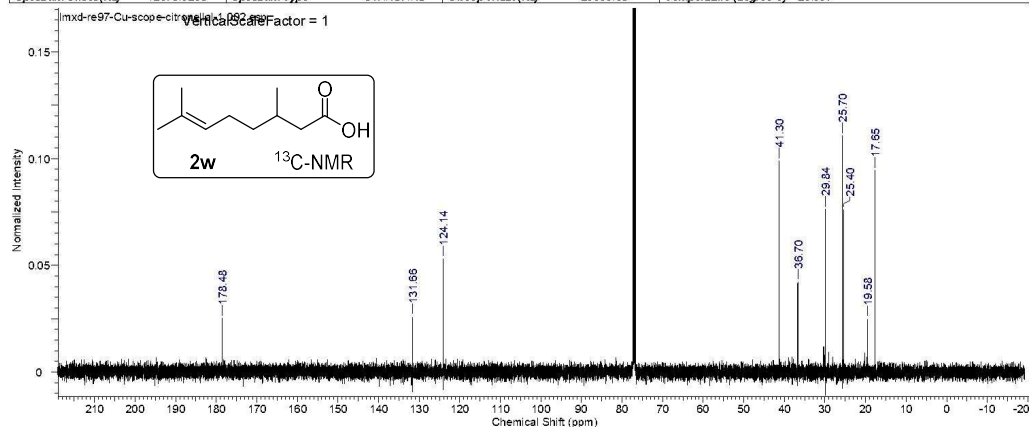
No.	(ppm)	Annotation	Layer No.	Created By	Created At	Modified By	Modified At
1	[2.49 .. 2.52]	DMSO	1	MMLWW	2015/11/8 8:09:52		
2	[3.30 .. 3.38]	Water	1	MMLWW	2015/11/8 8:09:52		

No.	(ppm)	Value	Absolute Value	Non-Negative Value
1	0.8179 .. 0.9441	16401482	3.38978534e+9	4.16401482
2	0.9404 .. 1.3775	52059031	6.12226099e+9	7.52059031
3	1.5306 .. 1.6027	79261613	2.27337549e+9	2.79261613
4	1.6086 .. 1.6928	85137415	2.32120832e+9	2.85137415
5	1.8647 .. 2.2658	84159184	4.75544474e+9	5.84159184
6	5.0052 .. 5.1109	99994230	8.14019584e+8	0.99994230
7	11.8320 .. 12.0161	374533	1.31369613e+9	1.61374533

This report was created by ACD/NMR Processor Academic Edition. For more information go to www.acdlabs.com/nmrproc/

10/27/2015 11:22:22 AM

Acquisition Time (sec)	1.0923	Comment	Li	Date	26 Oct 2015 23:29:04
Date Stamp	26 Oct 2015 23:29:04			File Name	C:\Users\Admin\Desktop\lmd-re97-cu-scope-citrone1121.fid
Frequency (MHz)	125.81	Nucleus	¹³ C	Number of Transients	1024
Original Points Count	32768	Owner	molllnmr	Points Count	32768
Receiver Gain	192.72	SW (cycles) (Hz)	30000.00	Solvent	CHLOROFORM-d
Spectrum Offset (Hz)	12578.9238	Spectrum Type	STANDARD	Sweep Width (Hz)	29999.08
				Temperature (degree C)	26.997

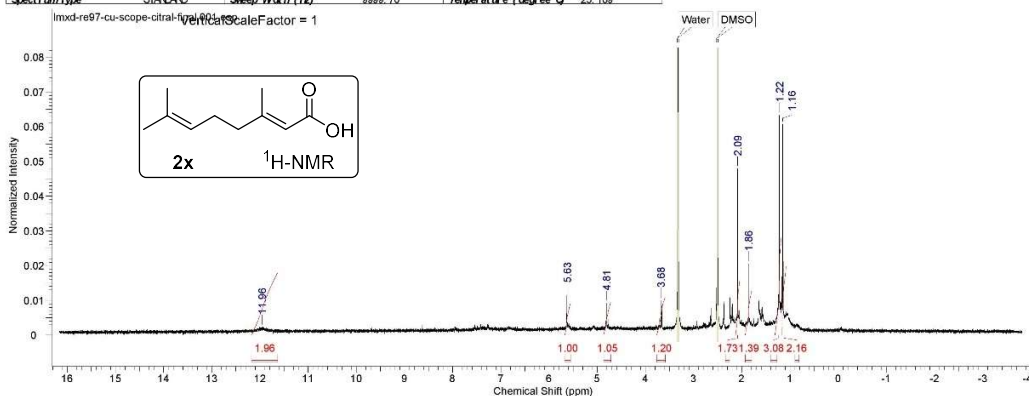


No.	(ppm)	(Hz)	Height
1	17.65	2220.2	0.0944
2	19.58	2462.8	0.0247
3	25.40	3196.1	0.0759
4	25.70	3233.7	0.1107
5	29.84	3754.6	0.0762
6	36.70	4617.0	0.0421
7	41.30	5196.6	0.0990
8	124.14	15618.9	0.0530
9	131.66	16564.7	0.0257
10	178.48	22455.2	0.0251

This report was created by ACD/NMR Processor Academic Edition. For more information go to www.acdlabs.com/nmrproc/

2016/4/15 22:52:09

Acquisition Time (sec)	3.2768	Comment	Li_1d_PROTON DMSO/home_mnpxl.n.2	Date	15 Apr 2016 22:37:52
Date Stamp	15 Apr 2016 22:37:52			File Name	C:\Users\MMLWW\Desktop\lmd-re97-cu-scope-citrone1121.fid
Frequency (MHz)	500.30	Nucleus	¹ H	Number of Transients	16
Original Points Count	32768	Owner	molllnmr	Points Count	32768
Receiver Gain	192.72	SW (cycles) (Hz)	10000.00	Solvent	DMSO-d6
Spectrum Type	STANDARD	Sweep Width (Hz)	9999.70	Temperature (degree C)	25.189
				Spectrum Offset (Hz)	3069.5574

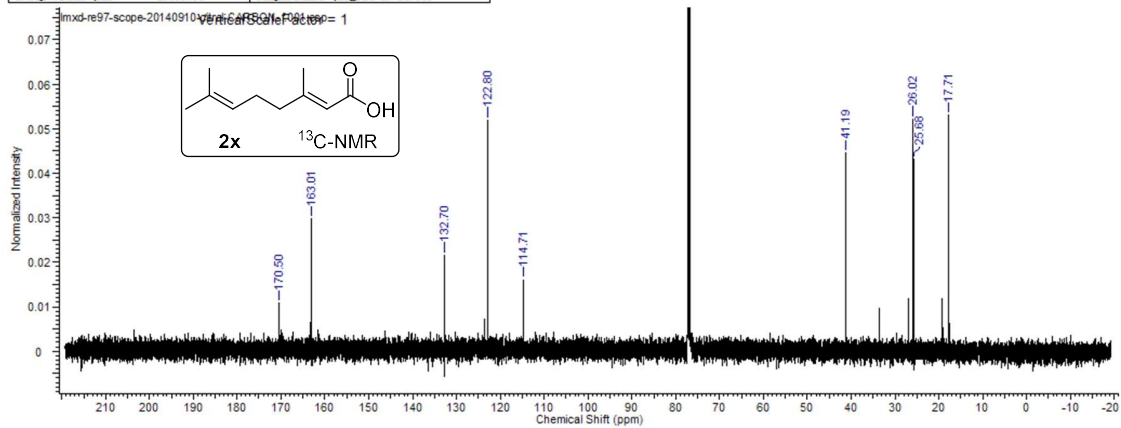


No.	(ppm)	Annotation	Layer No.	Created By	Created At	Modified By	Modified At
1	[2.49...2.52]	DMSO	1	MMLWW	2016/4/15 22:51:22		
2	[3.30...3.34]	Water	1	MMLWW	2016/4/15 22:51:22		

No.	(ppm)	Value	Absolute Value	Non-Negative Value	No.	(ppm)	Value	Absolute Value	Non-Negative Value
1	1.0804...	1.16215987538	1.00977600e+9	2.15987539	5	3.5890...	3.76119996274	5.61001600e+8	1.19996274
2	1.1799...	1.313107761955	1.43883597e+9	3.07761955	6	4.7161...	4.87104523216	4.88662624e+8	1.04523216
3	1.7987...	1.93139493787	6.52155584e+8	1.39493787	7	5.5560...	5.67099013086	4.66642016e+8	0.99013086
4	2.0418...	2.13173084044	8.09195328e+8	1.73084044	8	11.6339...	12.1195850002	9.15629824e+8	1.95850003

No.	(ppm)	(Hz)	Height	No.	(ppm)	(Hz)	Height	No.	(ppm)	(Hz)	Height
1	1.16	578.1	0.0608	3	1.86	932.4	0.0205	5	3.68	1840.9	0.0100
2	1.22	610.8	0.0634	4	2.09	1043.8	0.0478	6	4.81	2407.6	0.0081
								7	5.63	2816.0	0.0113
								8	11.96	5981.3	0.0022

Acquisition Time (sec)	1.0923	Date	10 Sep 2015 09:19:18	Date Stamp	10 Sep 2015 09:19:18
File Name	C:\Users\MLM\OneDrive\Desktop\新建文件夹\lmd-re97-Cy-scope-citrai-CARBON\1.fid	Frequency (MHz)	125.81	Original Points Count	32768
Nucleus	¹³ C	Number of Transients	3300	Origin	AV1130QHD
Owner	mcgillnmr	Points Count	32768	Pulse Sequence	zgpg30
SW (cyclical) (Hz)	30000.00	Solvent	CHLOROFORM-d	Receiver Gain	192.72
Sweep Width (Hz)	29998.08	Temperature (degree C)	25.000	Spectrum Offset (Hz)	12578.9238
				Spectrum Type	STANDARD

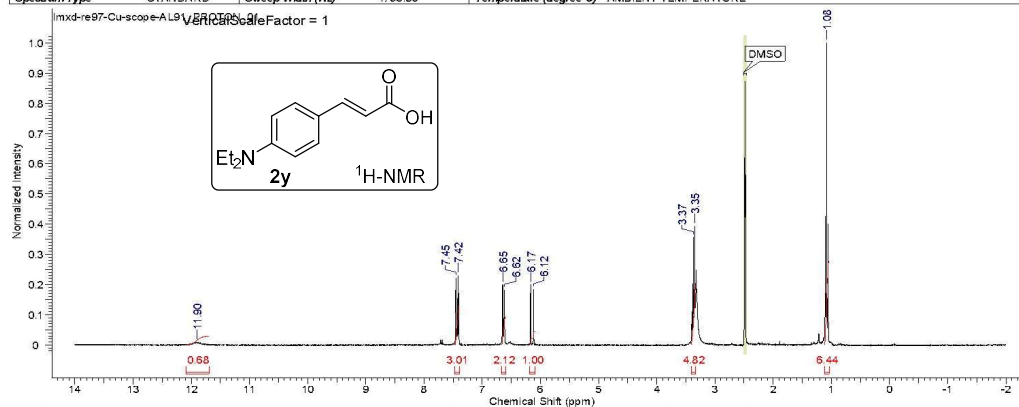


No.	(ppm)	(Hz)	Height
1	17.71	2228.4	0.0530
2	25.68	3230.9	0.0432
3	26.02	3273.0	0.0522
4	41.19	5181.9	0.0445
5	114.71	14431.5	0.0161
6	122.80	15449.6	0.0519
7	132.70	16695.6	0.0216
8	163.01	20508.8	0.0297
9	170.50	21451.8	0.0108

This report was created by ACD/NMR Processor Academic Edition. For more information go to www.acdlabs.com/nmrproc/

9/16/2015 3:57:48 PM

Acquisition Time (sec)	2.0480	Date	Jul 20 2015	Date Stamp	Jul 20 2015
File Name	C:\Users\Admin\CloudDrive\Revised_Fehling_Scope\lmsd-re97-Cu-scope-AL91	PROTON_01.fid	Frequency (MHz)	299.83	
Nucleus	¹ H	Number of Transients	8	Original Points Count	9818
Pulse Sequence	s2pul	Receiver Gain	36.00	Solvent	DMSO-d6
Spectrum Type	STANDARD	Sweep Width (Hz)	4793.86	Temperature (degree C)	AMBIENT TEMPERATURE
				Spectrum Offset (Hz)	1797.7788



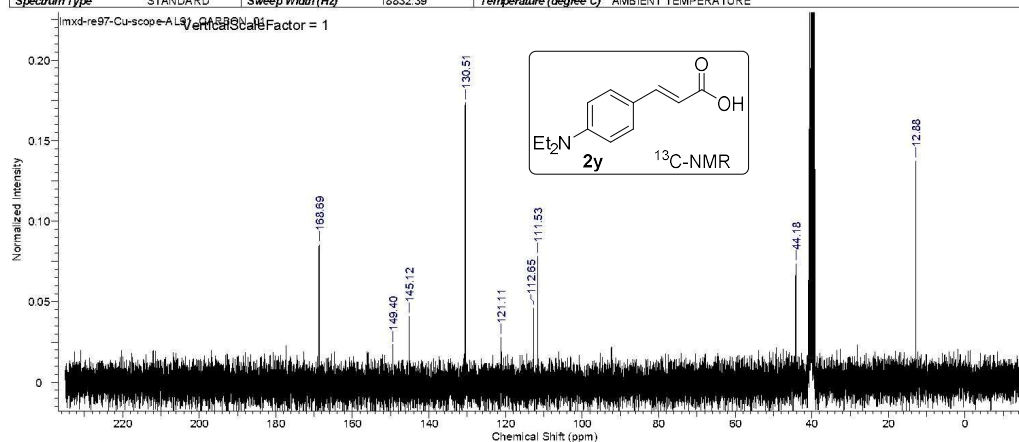
No.	(ppm)	Annotation	Layer No.	Created By	Created At	Modified By	Modified At
1	[2.46 - 2.51]	DMSO	1	Admin	Wed 9/16/2015 3:55:57 PM		

No.	(ppm)	Value	Absolute Value	Non-Negative Value
11	11.90379	1.11644441032	3.03145408e+8	6.44441032
23	7.45111	3.41631745052	2.26813136e+8	4.81745052
318	6.650890	6.18099568617	4.68371320e+7	0.99568617
418	6.655	6.66212280107	9.98566720e+7	2.12280107
517	6.000	7.47301118636	1.41646388e+8	3.01118636
611	6.953	12.0068278217	3.21181100e+7	0.68278217

This report was created by ACD/NMR Processor Academic Edition. For more information go to www.acdlabs.com/nmrproc/

9/16/2015 4:00:33 PM

Acquisition Time (sec)	1.0420	Date	Jul 20 2015	Date Stamp	Jul 20 2015
File Name	C:\Users\Admin\CloudDrive\Revised_Fehling_Scope\lmsd-re97-Cu-scope-AL91	CARBON_01.fid	Frequency (MHz)	75.35	
Nucleus	¹³ C	Number of Transients	1700	Original Points Count	19624
Pulse Sequence	s2pul	Receiver Gain	30.00	Solvent	DMSO-d6
Spectrum Type	STANDARD	Sweep Width (Hz)	18832.39	Temperature (degree C)	AMBIENT TEMPERATURE
				Spectrum Offset (Hz)	8287.6016

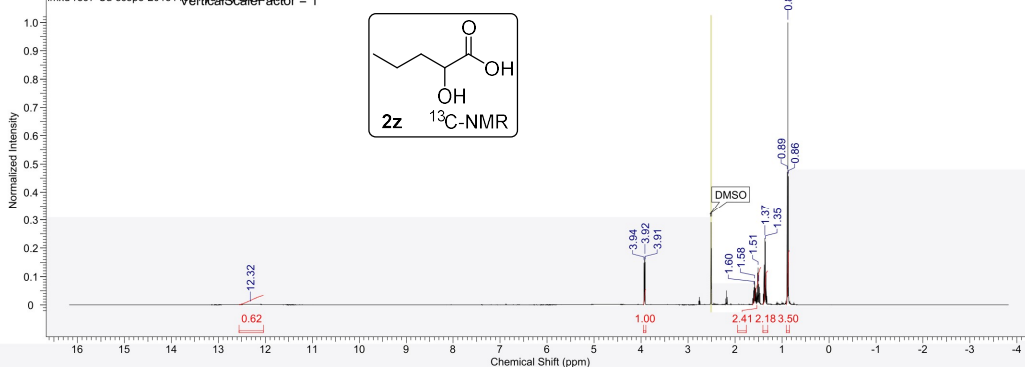


No.	(ppm)	(Hz)	Height
1	12.88	970.3	0.1373
2	44.18	3329.1	0.0735
3	111.53	8404.0	0.0793
4	112.65	8487.9	0.0481
5	121.11	9125.9	0.0279
6	130.51	9833.9	0.1736
7	145.12	10935.1	0.0411
8	149.40	11257.6	0.0234
9	168.69	12711.1	0.0354

Acquisition Time (sec)	3.2788	Comment	Li	Date	07 Nov 2015 18:57:52
Date Stamp	07 Nov 2015 18:57:52				
File Name	C:\Users\MMLWW\Desktop\1\lmd-re97-Cu-scope-20151107-hydroxy-2,1.fid	Frequency (MHz)	500.30		
Nucleus	¹ H	Number of Transients	16	Origin	AM11500HD
Owner	mgj11nmr	Points Count	32768	Pulse Sequence	zg30
SW (cyclical) (Hz)	10000.00	Solvent	DMSO-d6	Receiver Gain	106.56
Sweep Width (Hz)	9999.70	Temperature (degree C)	27.005	Spectrum Offset (Hz)	3089.5574
				Spectrum Type	STANDARD

lmd-re97-Cu-scope-20151107-hydroxy-2,1.fid

Vertical Scale Factor = 1

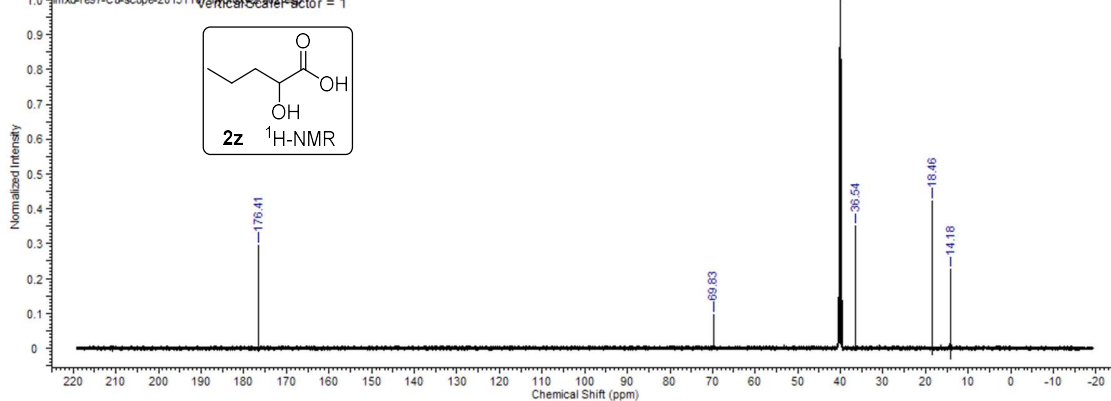


No.	(ppm)	Annotation	Layer No.	Created By	Created At	Modified By	Modified At
1	[2.49 .. 2.52]	DMSO	1	MMLWW	2015/11/8 7:58:55		
No.	(ppm)	Value	Absolute Value	Non-Negative Value			
1(0.8442 .. 0.90350216508			1.92036782e+10	3.50216508			
2(1.8045 .. 1.40216367219			1.19738900e+10	2.16367219			
3(1.8455 .. 1.63240971994			1.32133939e+10	2.40971994			
4(3.8982 .. 3.98099948967			5.48057498e+9	0.99948967			
5(2.4413 .. 12.40161682671			3.38229094e+9	0.61682671			

Acquisition Time (sec)	1.0923	Comment	Li	Date	07 Nov 2015 18:40:32
Date Stamp	07 Nov 2015 18:40:32				
File Name	C:\Users\MMLWW\Desktop\新建文件夹\新建文件夹\lmd-re97-Cu-scope-20151107-hydroxy-2,1.fid	Frequency (MHz)	125.81		
Nucleus	¹³ C	Number of Transients	512	Origin	AV11500HD
Owner	mgj11nmr	Points Count	32768	Pulse Sequence	zgpg30
SW (cyclical) (Hz)	30000.00	Solvent	DMSO-d6	Receiver Gain	192.72
Sweep Width (Hz)	28998.08	Temperature (degree C)	27.021	Spectrum Offset (Hz)	12578.9238
				Spectrum Type	STANDARD

lmd-re97-Cu-scope-20151107-hydroxy-2,1.fid

Vertical Scale Factor = 1

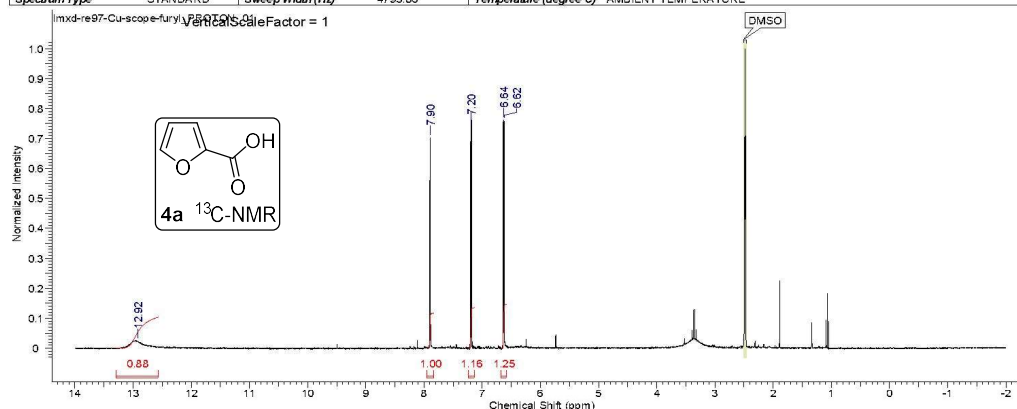


No.	(ppm)	(Hz)	Height
1	14.18	1784.4	0.2260
2	18.46	2322.7	0.4224
3	36.54	4596.9	0.3497
4	69.83	8785.4	0.0959
5	176.41	22194.2	0.2954

This report was created by ACD/NMR Processor Academic Edition. For more information go to www.acdlabs.com/nmrproc/

9/16/2015 4:28:04 PM

Acquisition Time (sec)	2.0480	Date	Jul 13 2015	Date Stamp	Jul 13 2015		
File Name	C:\Users\Admin\CloudDrive\Revised_Fehling_Scope\mxid-re97-Cu-scope-furyl_PROTON_01.fid				Frequency (MHz)	299.63	
Nucleus	¹ H	Number of Transients	8	Original Points Count	9818	Points Count	16384
Pulse Sequence	s2pul	Receiver Gain	39.00	Solvent	DMSO-d6	Spectrum Offset (Hz)	1797.7788
Spectrum Type	STANDARD	Sweep Width (Hz)	4793.86	Temperature (degree C)	AMBIENT TEMPERATURE		



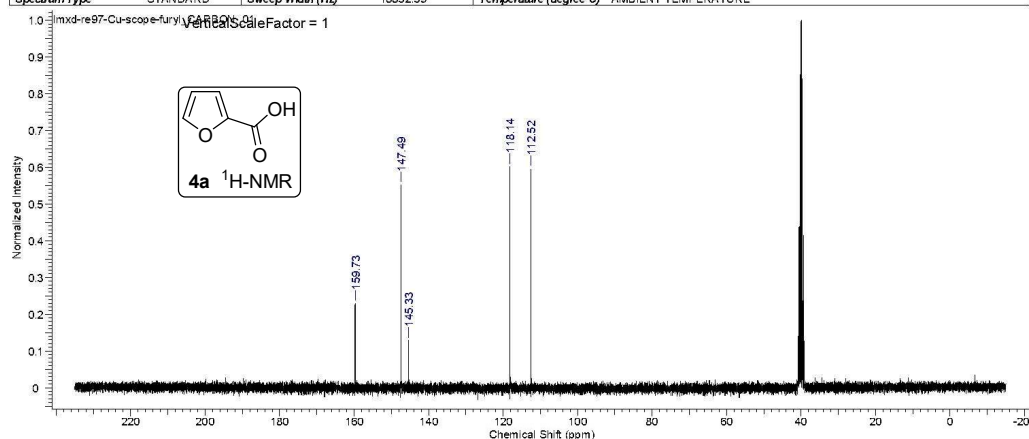
No.	(ppm)	Annotation	Layer No.	Created By	Created At	Modified By	Modified At
1	[2.46 - 2.51]	DMSO	1	Admin	Wed 9/16/2015 4:27:43 PM		

No.	(ppm)	Value	Absolute Value	Non-Negative Value	No.	(ppm)	(Hz)	Height
1/6	6.62	25392854	2.67382656e+8	1.25392854	1	6.62	1984.9	0.7582
2/7	13.36	7.24115573204	2.46443632e+8	1.15573204	2	6.64	1988.4	0.7615
3/7	3.01	7.95100028288	2.13296288e+8	1.00028288	3	7.20	2156.1	0.7368
4/2	6.64	13.3088215148	1.88106416e+8	0.88215148	4	7.90	2365.9	0.7015
					5	12.92	3870.8	0.0232

This report was created by ACD/NMR Processor Academic Edition. For more information go to www.acdlabs.com/nmrproc/

9/16/2015 4:28:39 PM

Acquisition Time (sec)	1.0420	Date	Jul 13 2015	Date Stamp	Jul 13 2015		
File Name	C:\Users\Admin\CloudDrive\Revised_Fehling_Scope\mxid-re97-Cu-scope-furyl_CARBON_01.fid				Frequency (MHz)	75.35	
Nucleus	¹³ C	Number of Transients	1700	Original Points Count	19624	Points Count	32768
Pulse Sequence	s2pul	Receiver Gain	30.00	Solvent	DMSO-d6	Spectrum Offset (Hz)	8287.6016
Spectrum Type	STANDARD	Sweep Width (Hz)	18832.39	Temperature (degree C)	AMBIENT TEMPERATURE		

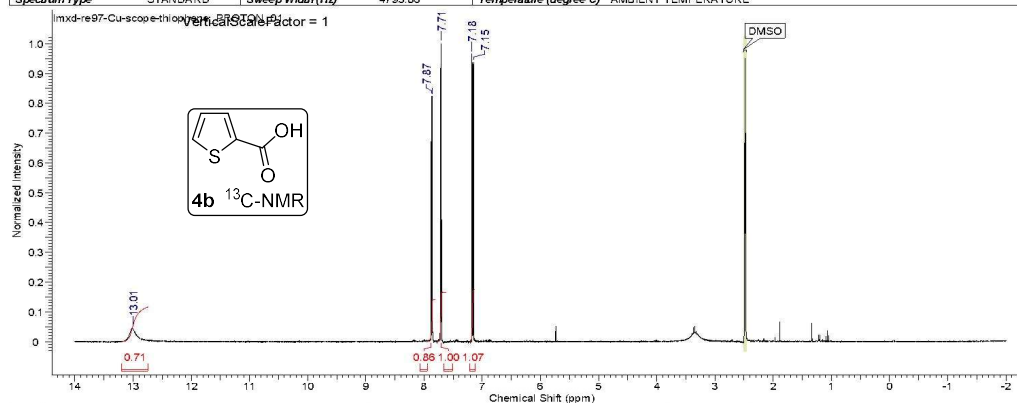


No.	(ppm)	(Hz)	Height
1	112.52	8478.7	0.5951
2	118.14	8901.7	0.6015
3	145.33	10950.6	0.1285
4	147.49	11113.3	0.5508
5	159.73	12035.7	0.2291

This report was created by ACD/NMR Processor Academic Edition. For more information go to www.acdlabs.com/nmrproc/

9/16/2015 4:30:00 PM

Acquisition Time (sec)	2.0480	Date	Jul 13 2015	Date Stamp	Jul 13 2015		
File Name	C:\Users\Admin\CloudDrive\Revised_Fehling_Scope\imxd-re97-Cu-scope-thiophene_PROTON_01.fid.fid				Frequency (MHz)	299.63	
Nucleus	¹ H	Number of Transients	8	Original Points Count	9818	Points Count	16324
Pulse Sequence	s2pul	Receiver Gain	35.00	Solvent	DMSO-d6	Spectrum Offset (Hz)	1797.7788
Spectrum Type	STANDARD	Sweep Width (Hz)	4793.86	Temperature (degree C)	AMBIENT TEMPERATURE		



This report was created by ACD/NMR Processor Academic Edition. For more information go to www.acdlabs.com/nmrproc/

9/16/2015 4:30:41 PM

Acquisition Time (sec)	1.0420	Date	Jul 13 2015	Date Stamp	Jul 13 2015		
File Name	C:\Users\Admin\CloudDrive\Revised_Fehling_Scope\imxd-re97-Cu-scope-thiophene_CARBON_01.fid.fid				Frequency (MHz)	75.35	
Nucleus	¹³ C	Number of Transients	1700	Original Points Count	19524	Points Count	32768
Pulse Sequence	s2pul	Receiver Gain	30.00	Solvent	DMSO-d6	Spectrum Offset (Hz)	8287.6016
Spectrum Type	STANDARD	Sweep Width (Hz)	18832.39	Temperature (degree C)	AMBIENT TEMPERATURE		

